MODIFIED GRAPHENE-POLYMER NANOCOMPOSITES AND THEIR UTILIZATION IN VARIOUS APPLICATIONS

MODİFİYE GRAFEN - POLİMER NANOKOMPOZİTLER VE ÇEŞİTLİ UYGULAMALARDA KULLANILMASI

HIBA SALIH HUSSEIN SALIH

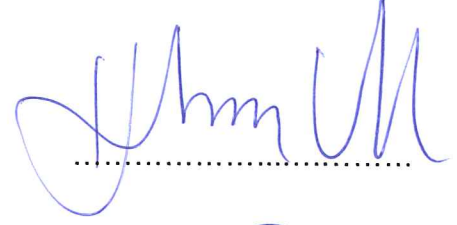**Prof. Dr. NURSEL PEKEL BAYRAMGİL**

Supervisor

Submitted to Graduate School of Science and Engineering of Hacettepe University
as a Partial Fulfillment to the Requirements
for the Award of the Degree of Doctor of Philosophy
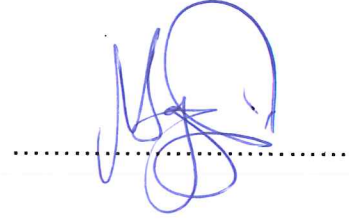Chemistry

2018

This work named "**Modified Graphene – Polymer Nanocomposites and their Utilization in various Applications**" by **HIBA SALIH HUSSEIN SALIH** has been approved as a thesis for the Degree of **DOCTOR OF PHILOSOPHY** in **CHEMISTRY** by the below mentioned Examining Committee Members.
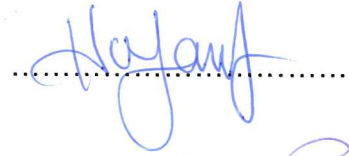
Prof. Dr. İbrahim USLU
Head

Prof. Dr. Nursel PEKEL BAYRAMGIL
Supervisor

Prof. Dr. Handan YAVUZ ALAGÖZ
Member

Assist. Prof. Dr. Hale BERBER
Member

Assist. Prof. Dr. Cengiz UZUN
Member

This thesis has been approved as a thesis for the Degree of **DOCTOR OF PHILOSOPHY in CHEMISTRY** by Board of Directors of the institute for Graduate School of Science and Engineering.

Prof. Dr. Menemşe GÜMÜŞDERELİOĞLU
Director of the Institute of
Graduate School of Science and Engineering

To my family

YAYINLAMA VE FİKRİ MÜLKİYET HAKLARI BEYANI

Enstitü tarafından onaylanan lisansüstü tezimin/raporumun tamamını veya herhangi bir kısmını, basılı (kağıt) ve elektronik formatta arşivleme ve aşağıda verilen koşullarla kullanıma açma iznini Hacettepe üniversitesine verdiğimi bildiririm. Bu izinle Üniversiteye verilen kullanım hakları dışındaki tüm fikri mülkiyet haklarım bende kalacak, tezimin tamamının ya da bir bölümünün gelecekteki çalışmalarda (makale, kitap, lisans ve patent vb.) kullanım hakları bana ait olacaktır.

Tezin kendi orijinal çalışmam olduğunu, başkalarının haklarını ihlal etmediğimi ve tezimin tek yetkili sahibi olduğumu beyan ve taahhüt ederim. Tezimde yer alan telif hakkı bulunan ve sahiplerinden yazılı izin alınarak kullanması zorunlu metinlerin yazılı izin alarak kullandığımı ve istenildiğinde suretlerini Üniversiteye teslim etmeyi taahhüt ederim.

☐ **Tezimin/Raporumun tamamı dünya çapında erişime açılabilir ve bir kısmı veya tamamının fotokopisi alınabilir.**
(Bu seçenekle teziniz arama motorlarında indekslenebilecek, daha sonra tezinizin erişim statüsünün değiştirilmesini talep etseniz ve kütüphane bu talebinizi yerine getirse bile, tezinin arama motorlarının önbelleklerinde kalmaya devam edebilecektir.)

☐ **Tezimin/Raporumun ………….. tarihine kadar erişime açılmasını ve fotokopi alınmasını (İç Kapak, Özet, İçindekiler ve Kaynakça hariç) istemiyorum.**
(Bu sürenin sonunda uzatma için başvuruda bulunmadığım taktirde, tezimin/raporumun tamamı her yerden erişime açılabilir, kaynak gösterilmek şartıyla bir kısmı ve ya tamamının fotokopisi alınabilir)

☒ **Tezimin/Raporumun 07.02.2023 tarihine kadar erişime açılmasını istemiyorum, ancak kaynak gösterilmek şartıyla bir kısmı veya tamamının fotokopisinin alınmasını onaylıyorum.**

☐ **Serbest Seçenek/Yazarın Seçimi**

07 / 02 / 2018

(İmza)

Öğrencinin Adı Soyadı
Hiba Salih Hussein

ETHICS

In this thesis study, prepared in accordance with the spelling rules of Institute of Graduate Studies in Science of Hacettepe University,

I declare that

- all the information and documents have been obtained in the base of the academic rules
- all audio-visual and written information and results have been presented according to the rules of scientific ethics
- in case of using others works, related studies have been cited in accordance with the scientific standards
- all cited studies have been fully referenced
- I did not do any distortion in the data set
- and any part of this thesis has not been presented as another thesis study at this or any other university.

12/01/2018

HIBA SALIH HUSSEIN SALIH

ABSTRACT

MODIFIED GRAPHENE-POLYMER NANOCOMPOSITES AND THEIR UTILIZATION IN VARIOUS APPLICATIONS

HIBA SALIH HUSSEIN SALIH

Doctor of Philosophy, Department of Chemistry

Supervisor: Prof. Dr. NURSEL PEKEL BAYRAMGİL

January 2018, 162 pages

Graphene is a rising material in the field of materials science and condensed-matter physics. It indicates a two-dimensional material having high electronic and crystal property and has its own applications in new physics, which will be discussed briefly in this study, Graphene does not need any evidence highlighting its important in fundamental physics, unlike the case in the recognition of applications only when their material commercial products come into being. Generally, graphene, in terms of concept, is a new set of materials that is in the thickness of one atom that opens roads into physics that is low-dimensional. This new material, graphene, in the field of materials science, has, in the studies available, proved to be magnificent and amazing in providing a ground fertile for applications in different domains of sciences, such as (pharmaceutics, medicine, nanotechnology, and others).

For this study, modification of graphene was started with by some acids and bases to obtain acid- and amine-modified graphenes. Secondly, composites were prepared with acid- and amine-modified graphenes, and then their characterizations were made using different instrumental analysis methods such as FT-IR, XRD, SEM, Elemental analysis, TEM, Raman Spectroscopy, Mechanical test and DSC analysis.

Thirdly, modified-graphene nanocomposite film with 2-hydroxyethylcellulose (2-HEC) with and without *doxorubicine (*DOXO*)* (which is used for cancer therapy) was prepared for the purpose of drug delivery. Furthermore, to search the electrical properties of modified-graphene / 2-HEC nanocomposite films, with 4-point probe conductivity measurements were used.

Key words: Graphene, modification, 2-Hydroxyethylcellulose, Elemental mapping.

ÖZET

MODİFİYE GRAFEN - POLİMER NANOKOMPOZİTLER VE ÇEŞİTLİ UYGULAMALARDA KULLANILMASI

HIBA SALIH HUSSEIN SALIH

Doktora, Kimya Bölümü

Tez Danışmanı: Prof. Dr. NURSEL PEKEL BAYRAMGİL
Ocak 2018, 162 Sayfa

Grafen; malzeme, malzeme bilimi ve yoğun madde fiziğinin ufukta hızla yükselen bir yıldızıdır. Kısa geçmişinde, fizik ve potansiyel uygulama çeşitliliği göstermekle birlikte, iki boyutlu bu malzeme olağanüstü yüksek kristal ve elektronik özellikler sergilemektedir. Ortaya konan ticarî ürünler, uygulamaların gerçekliği konusunda su götürmez iken, artık temel fizik açısından grafenin ne kadar önemli olduğuna dair başka bir kanıta gerek yoktur. Genel olarak, grafen sadece bir atom kalınlığına sahip, kavramsal olarak yeni bir materyal sınıfını temsil eder ve bu temelde, sürprizleri elden bırakmayan ve uygulamalara elverişli zemin sağlamaya devam eden düşük boyutlu fiziğe yeni fırsatlar sunar.

Bu tez çalışmasına, grafenin asit ve bazlarla modifiye edilmesiyle başlanmış ve asit ve amin ile modifiye edilmiş grafenler elde edilmiştir. İkinci olarak, asit ve amin ile modifiye edilmiş grafenlerle kompozitler hazırlanmış ve FTIR, XRD, SEM, Elementel analiz, TEM, Raman Spektroskopisi, Mekanik Test ve DSC analizi gibi farklı enstrümantal analiz yöntemleri kullanılarak karakterizasyonları yapılmıştır Üçüncü olarak, ilaç salımı amacıyla doksorubisin (DOXO) (kanser tedavisi için kullanılan) içeren ve içermeyen 2-hidroksietilselülozlu (2-HEC) modifiye grafen nanokompozit filmleri hazırlanmıştır. Ayrıca, modifiye grafen / 2-HEC nanokompozit filmlerin elektriksel özelliklerini araştırmak için bu filmlerin 4 nokta prob iletkenlik ölçüm sistemi kullanılarak iletkenlikleri ölçülmüştür.

Anahtar kelimeler: Grafen, modifikasyon, 2-Hidroksietilselüloz, Elemental haritalama.

ACKNOWLEDGMENT

TABLE OF CONTENTS

LIST OF TABLES

LIST OF FIGURES

ABBREVIATION

CAN   Ceric ammonium nitrate

DEA   Diethylamine

EDA   Ethylenediamine

G   Graphene

GL   Graphene-perchloric acid

GN   Graphene-nitric acid

GP   Graphene-phosphoric acid

GS   Graphene-sulphuric acid

2-HEC   2-Hydroxyethylcellulose

PEI   Polyethylenimine

VIM   N-vinylimidazole

DSC   Differential Scanning Calorimetry

FT-IR   Fourier Transform Infrared

SEM   Scanning Electron Microscopy

TEM   Transmission Electron Microscopy

XRD   X-Ray Diffraction

1. Introduction

The science of materials is a point of focus nowadays, especially with regard to new materials progress. Polymer nanocomposite results from dispersing nano fillers within the polymer matrix with the 1-100 nm range dimension. Polymer nanocomposites have improving electrical, thermal, antibacterial, mechanical, barrier, etc. properties with a little amount of filler, without the material density being disturbed [1,2]. Nanoscience gave way to future medicines [3], especially with the breakthrough of graphene in the science of materials in 2004 by Novoselov *et al.* from University of Manchester. Graphene is a 2D (two dimensional) carbon nanomaterial which is a thick monolayer graphite sheet in a hexagonal shape; the stacking arrangement in graphene makes it the strongest material. Graphene is characterized by a high specific surface area (2630 m^2 g^{-1}), electrical conductivity (200,000 cm^2 V^{-1} S^{-1}), and outstanding thermal conductivity (5000 W m^{-1} K^{-1}) [1]. Graphene, having hydrophobic nature, is compatible with almost all exciting organic polymers and cannot be dispersed repeatedly. The only way to stabilize suspension and dispersion is to modify chemically or functionalize graphene. GO (graphene oxide) and rGO (reduced graphene oxide), which are graphene-based materials, are smart alternative selections. The GO (graphene oxide) form of graphene is synthesized from an existing graphite of a low cost, containing a great number of oxygen (like carbonyl, epoxy hydroxyl, and carboxyl). The rGO (reduced graphene oxide) form of graphene results from simple reduction of GO by chemical, thermal, hydrothermal etc. methods. Unlike GO, rGO has less number of oxygen. 2006 was the year when polymer nanocomposite by using polystyrene and graphene was published. Then, polymer was used widely to synthesis graphene-polymer nanocomposites in modern technologies [1].

Cellulose is one of the most abundant and sustainable natural polymers in the world. Apart from being biocompatible, biodegradable and low in cost, cellulose possesses many other unique features, such as light weight, high water-retaining capacity, high strength and ease for chemical modification [4,5]. It is a kind of solid polymer which colorless, odorless, nontoxic, light weight, and eco-friendly [2]. Cellulose is highly hydrophilic in nature. It is mechanically robust and also non-

soluble in water owing to the high crystallinity coupled with massive inter- and intra- molecular hydrogen bonds [5].

To our study, we started by the modification of graphene by some acids and bases to obtain graphene that are modified by both acid and amine. Secondly, we prepared composites with acid-modified graphene and amine-modified graphene. Thirdly, graphene/cellulose nanocomposite films were obtained by mixing graphene and modified graphenes with 2-hydroxyethylcellulose (2-HEC). The characterization of the systems in these three stages was made using different instrumental analysis methods such as FTIR, XRD, SEM, elemental mapping, TEM, Raman Spectroscopy, mechanical tests for films and DSC. For the practical part of the work, we prepared graphene (and modified graphenes) nanocomposite films with 2-hydroxyethylcellulose including *doxorubicine (DOXO)*, which is used for cancer therapy, and applied them in the measurement of drug release rates, which can bring future revolution as drug delivery. In addition, the electrical conductivities of the 2-HEC films prepared with graphene and modified graphenes were measured so that the contribution of the modification to the electrical properties was revealed.

2. Literature Review

2.1. Carbon

Carbon, which is origin of organic chemistry, is an element that is greatly studied. [4]. It is a six-electron tetravalent, with four electrons and a chemical bond that is covalent [6]. After hydrogen, helium, and oxygen, carbon is the fourth world element. However, carbon is not the most prevalent element in Earth's crust, as elements such as iron, silicon, or even titanium are found in higher quantities. Nevertheless, carbon constitutes the very fundamental building block of life [6]. It is also widely applied in most technologies, since it is often found in its pure elemental forms (i.e., coal, graphite, and diamond) in large deposits and requires only minimal processing for subsequent applications. Specifically in electrochemical applications, carbon materials are of enormous industrial importance for already more than 100 years. Due to carbon materials properties (high exact surface area, high conductivity, and good electrochemical stability) they have been largely employed as capacitive materials of a low cost [7,8]. Carbon electrodes are frequently utilized on a manufacturing scale for metallurgy; fabrication of silicon, yellow phosphorus, and calcium carbide; or in batteries (the zinc−carbon battery is the most popular low-cost battery available). These applications are largely made possible by the excellent chemical and physical properties of carbon-based materials. These include the ability to carry a large amount of electrical current, withstand very high temperatures, exhibit fast heterogeneous electron transfer (in the case of amorphous carbon and graphite), and exhibit good mechanical properties, even under the aforementioned extreme conditions [9].

2.1.1. Graphite and Diamond

Carbon is classified as a non-metal. Carbon, in its diamond form, is transparent and its opaque in its black form as graphite. There for it is both hard in its diamond form and soft in its graphite form. Diamonds are hardly electrically conductive, while graphite is an excellent conductor [10]. Under usual conditions, diamond, carbon nanotubes, and graphene have the highest thermal conductivities of all known materials [11].

Graphite is sp^2 hybridized, while diamond is sp^3 hybridized. Amorphous carbon materials are other forms of carbon that is sp^3 hybridized [11,12].

The layers in graphite, every one of which is called graphene. Each graphene layer has carbon atoms in a honeycomb lattice form with a 0.142 nm separation and a 0.335 nm distance between planes [11,13,14].

Carbon materials impacted many domains of science being used in chemistry and catalysis. Carbon has a two-fold function: a catalyst or a catalyst support owing to its prominent properties (excellent electron conductivity, high porosity, relative chemical inertness and large specific surface area). It is used to improve catalytic activity when functionalizing or being decorated with metallic nano particles and enzymes [15]. Carbon physical and chemical properties, its applications in nanomaterials (carbon nanotubes (CNTs), nano or micro diamonds and graphene) are still fields of study (Figure 2.1) [16].

Such nanomaterials are able to modify other functional groups surfaces. Graphene, owing to its properties and structure, is among the materials that are carbon based to be studied [16].
Material science developments gave way to progress in electrochemical filed applications [17].
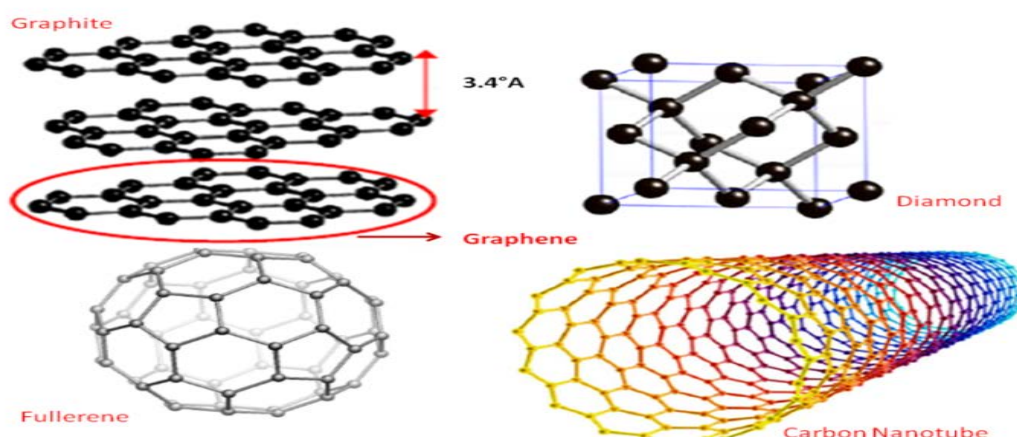
Figure 2.1. Carbon different allotropes [18].

2.1.2. Carbon nanotube

Carbon nanotubes structures have magnificent properties (mechanical, electronic and magnetic). Carbon nanotubes conduct electricity and heat in a better way than copper. CNT improve or control conductivity in polymers [16,19].

CNT are distinct because of the tough bond between the atoms and the tubes ratios. CNT have many properties (length, structures, number of layers and differing in thickness) and consist of 3 various types:

(1) single-walled CNT (SWCNT), (2) double-walled CNT (DWCNT) and (3) multi-walled CNT (MWCNT) [20,21]. Nanotubes characteristics differ according to the sheet of graphene rolling up for the tube formation leading it to acting as either a semiconductor or metallic (Figure 2.2).
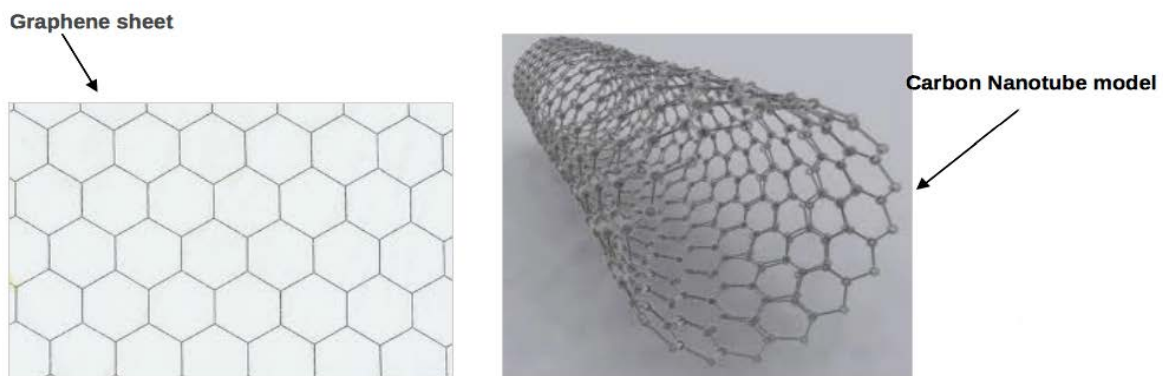
Figure 2.2. Scheme for carbon nanotube made from rolled graphene sheet

The nanotubes of carbon are structurally strong and flexible, which makes them easy to join other materials to concrete. Carbon nanotubes can be power extractors from sunlight and hence a source of heats. Also, they are conductive thermally but not in the tube itself. They are also electrically conductive which promotes them to be replaceable to metal wires [21,22]. Pharmaceutically, Carbon nanotubes are applied as chemical carriers, in a way where the drug is attached to the carbon nanotube that will attack the cells containing cancer, for instance [21,23].

2.1.3. Fullerenes

They are carbon allotropes consisting of tubes of carbon atoms and balls, 'cages' [24], and used for delivery drug in the body, and as in catalysts and lubricants [25].

Fullerenes are like graphite in structure (i.e. hexagonal) but can also be pentagonal or heptagonal [24].

2.1.4. Graphene family nanomaterials (GFNs)

The nanomaterial's of graphene family are categorized according to the chemical modifications of layers or their number in the sheet. Hence, there are mono layer graphene, bi-layer graphene, multilayer graphene, GO and rGO (Figure 2.3), each one of which will be detailed in this study. The layers differ in the number of layers, purity, surface chemistry, lateral dimensions, defect composition and density [25].
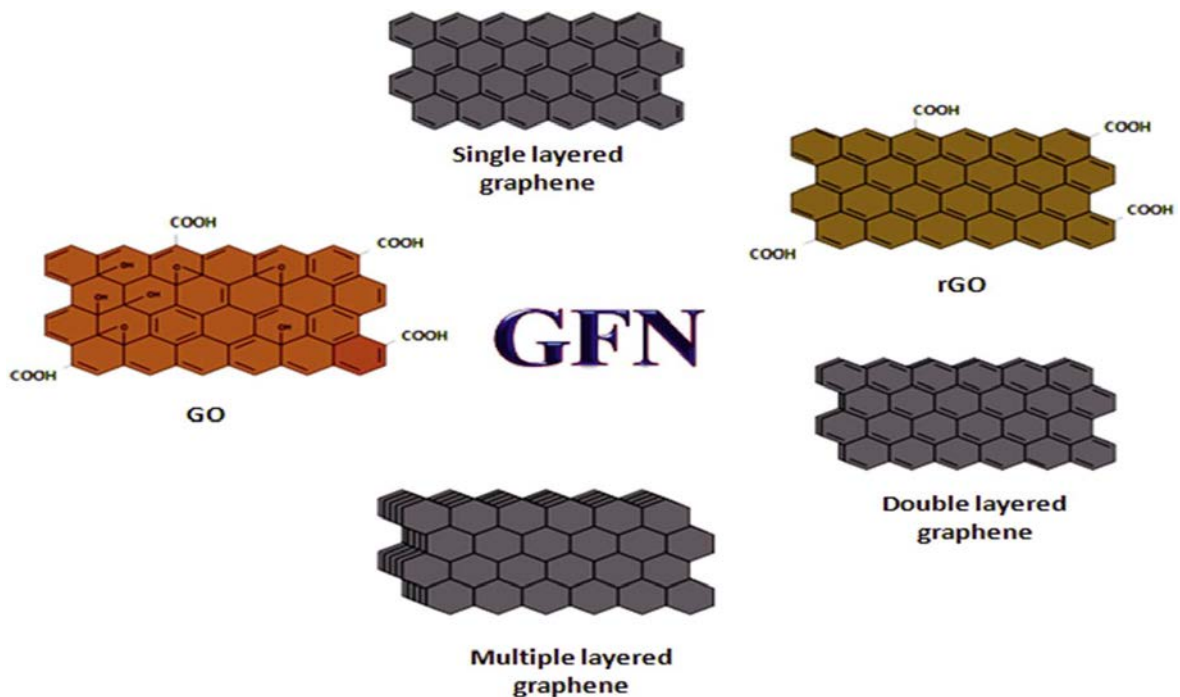
Figure 2.3. Graphene family-nanomaterials [25,26].

2.1.5. Graphene

Graphene has been the subject of a wealth of scientific researcher [27]. Graphene is a pure carbon substance. It has hexagonal pattern like graphite with a 0.34 nm of sp^2 hybridized carbon atoms thickness [28]. What made graphite crystal is the

6

millions of graphene [29]. Graphene has been the subject of a wealth of scientific research and received much media's attention since the early papers of Geim and Novoselov in 2004 [30]. Graphene is considered to be the 'wonder material' because of many unique and fascinating properties [31]. Graphene is a 2D nanomaterial having an sp^2-bonded of carbon atoms with distinct chemical and physical properties (conductivity, electronic, optical, mechanical and thermal) properties [32].

Graphene has been a point of interest being the last of allotropes of carbon discovered [33,34] and because of its properties, an amazing 2D carbon nanomaterial [35], its atomic crystal structure in a hexagonal lattice [36-40], and being all nanostructures mother (3D graphite, 0D fullerenes and 1D carbon nanotube) (Figure 2.4) [41], where only hexagons are there. It also has properties that have exceeded its predecessor (CNTs); it is, therefore, used in biosensors, energy conversion and storage, optoelectronic, photocatalysis/photovoltaic, bacteria killing, switching and information storage, and other technological applications in the imminent carbon age. The use of graphene with carbon catalysis within a framework is considered to be a new area of research in the introduction of green and sustainable, materiel and organic chemistry [40]. Graphene molecular behavior and its derivatives enable them to be modified for the purpose of improving their properties and functions extending [42].
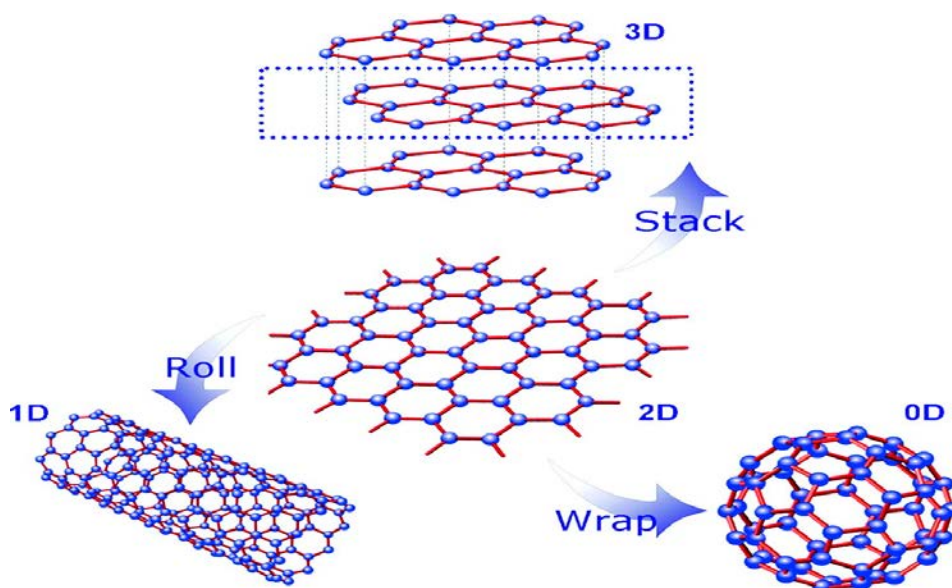
Figure 2.4. Graphene as a basic building block [43].

7

2.1.5.1. Properties of graphene

Graphene is distinguished through its exceptional physical and chemical properties from other nanomaterial. Each carbon atom, in the two dimensional plain, forms three sigma bonds with each of its neighbors. For each atom, a fourth electron is delocalized over the whole graphene layer, which allows high conductivity. The graphene generally stable due to the carbon atoms being intensely packed and because of an sp^2 hybridization. The energy bands that non-conductive can either full or empty with energy gaps, while the conductive one, like metals, are filled in part. The energy momentum graph of graphene shows energy bands as two circular cones, connected at their extremities, known as „Dirac Cones". This results in the unusual behavior of the graphene electrons i.e. they all have same velocity and almost zero inertia.

When the graphene is exposed to molecules with carbon (like hydrocarbons and organic compounds), it has the ability to heal itself. When there is an array of carbon atoms, they formulate into hexagons perfectly. Graphene is a carbon form where every atoms, they reacts from two lateral sides. The atoms at the graphene sheet also have special chemical reactivity. graphene oxide (GO) can be obtained from the modification of graphene easily resulting from oxygen and other functional groups. The precise graphene oxide structure has been deliberated over the years.

Graphene possess various novel properties of interest such as intrinsically superior electrical conductivity (10^6 Ω^{-1} cm^{-1}), nearly transparent in visible light (97.7%), intrinsic carrier mobility being high (2.5×10^5 cm^2 $V^{-1}s^{-1}$), high specific surface area also being high (2630 m^2 g^{-1}), excellent mechanical strength (Young's modulus > 1 TPa), and high thermal conductivity (above 3000 W mK^{-1}) [2]. These properties make graphene as one of the most promising upcoming material which has potential possibility of applications in electronics, photonics and several other fields [2,44,45].

The mechanical, electrical, and optical properties of graphene are excellent [46,47]. Due to these properties of the graphene, it is potential to be highly applied to many fields. The graphene, having the aforementioned properties, is considered

mechanically as very strong and flexible. Graphene is 100 times greater than steel in terms of breaking strength. Graphene crystal is unchangeable in nature. Electrically, the carrier mobility of graphene is 100% time more than silicon at room temperature. When The stretched up to 20%, the crystal of graphene structure keeps its nature. Electrically, the carrier mobility of graphene is 100 time more than silicon at room temperature. When graphene interacts with optical materials of an ultra-wide-band, the interaction is strong, and a broad range of wavelengths of light is given out. 2.3% of light id absorbed by graphene in the visible - infrared range. Graphene absorption coefficient is higher than the materials of semi-conductivity with a magnitude of one to three orders. The above features of graphene makes it potential to be used in a variety of fields, as in photo detectors and photonics devices. In general, the possible fields of applications are too many and can be : capacitors, interconnects, sensors, gas barriers, memory devices, solar cells, heat dissipaters, hydrogen storage, transparent conductive films, ultra-capacitors, environment, nanocomposites, drug delivery, photo thermal treatment and membranes and so on (Figure 2.5). In order to get graphene in a high quality, it can be mechanically exfoliated from graphite [48-50].
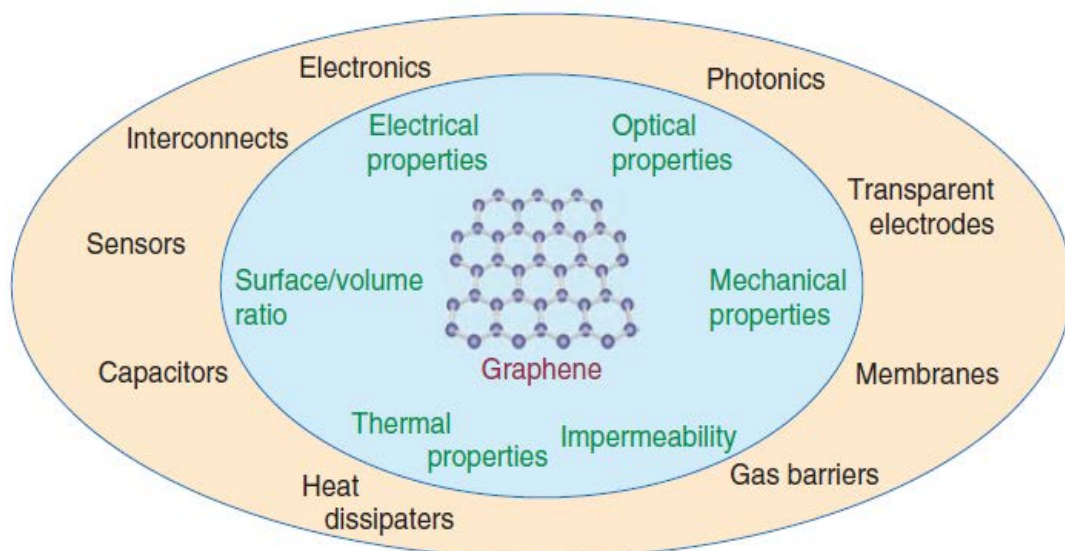
Figure 2.5. Structure of graphene and its potential applications [51].

2.1.5.1.1. Physicochemical properties

The 2D sp^2 hybridized carbon atoms (where each carbon atom has a free π electron) that are linked together by a sigma bond, which all lead to forming an

electron network, are what the graphene consist of. As a result, this shows that the electrophilic substitution is to be chosen rather than the nucleophilic substitution. What augments the chemical reactivity of graphene is its defects in its planar structure. To add, the aforementioned properties of graphene and the large surface area make graphene important in applications of drug delivery [52].

2.1.5.1.2. Thermal and electrical properties

Graphene is highly conductive thermally and electrically due to the strong bonding of carbon-carbon. The high thermal conductivity of the graphene is owing to its single layered defect free structure. Graphene electrical conductivity is reduced due to the defects that appeared during the chemical modification. The distinct properties of graphene - thermal and electrical – make it useful and applicable in developing of biomedical and electronic devices [52].

2.1.5.1.3. Optical properties

Every graphite layer is graphene; the atoms of carbon are in a honeycomb lattice shape, where every one of which is separated for 0.142 nm, and 0.335 nm as the distance between planes where the atoms are covalently bonded. The layers of graphite are bonded weakly by van der Waals. This allows graphite layers to separate easily or slip over one another electron network leading to photoluminescence, which is of a great importance in cellular imaging. Graphene, in addition to being photoluminescent and high light transmittant, is applicable in magnetic resonance imaging and biomedical imaging due to the property of charge mobility [52].

2.1.5.1.4. Mechanical properties

Mechanically, graphene is the strongest of all materials (about 1100 GPa), including GO. Conjugation of graphene with polymers augments the stiffness and modulus for use in biological applications [52].

2.1.5.1.5. Biological properties

The graphene nanomaterials family can be used in delivering and detecting of RNA and DNA, due to adsorption property. Positive charging of the graphene

makes it interact with the negatively charged nucleotides, which leads to protecting them from nuclease enzymes [52].

2.1.5.2. Synthesis of graphene

Graphene is the novel two-dimensional (2D) material in the carbon family [53]. Various synthesizing methods for graphene have been developed (Figure 2.6), including epitaxial growth, thermal exfoliation of graphite oxide, gas phase synthesis, chemical reduction from graphene oxide, and the exfoliation of graphite in the liquid phase. Nevertheless, the collective production of highly functional, fully exfoliated graphene sheets still remains as a formidable challenge.
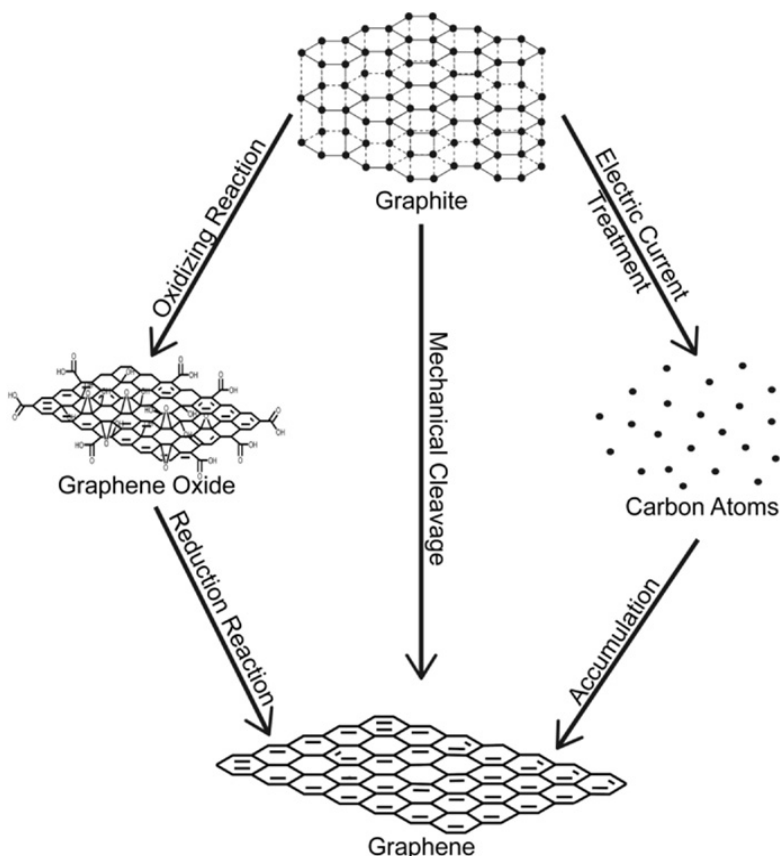
Figure 2.6. Synthesis of graphene [54]

2.1.5.3. Modifications of graphene

Insolubility and intractability are properties of pristine graphene, which, before melting, decomposes. This makes it not shapeable by into desired structures by any conventional material processing techniques. Solid supports are what graphene layers stand on physically. The layers of graphene that are free standing can either be together through π-π and hydrophobic interactions or form wrinkles.

In order for graphene to be applied in fields such as electronics or optoelectronics, the zero band gap material must be opened. When pristine graphene interacts with molecules of a small size or polymers, Catalytically, this limits its performance in composites, sensors, and catalysis. For the purpose of tackling these issues, many chemical reaction have been employed and developed to modify the surface area of graphene sheets and electronic structures. By chemical functionalization, the structure of graphene and its properties can be modified. The chemical groups attached covalently transmit the state of hybridization from sp^2 to sp^3, perhaps to create a graphene band gap [55].

Covalent bonds and non-covalent interactions as well as the functional molecules decoration of the graphene can modify and expand its properties [7]. (Figure 2.7).
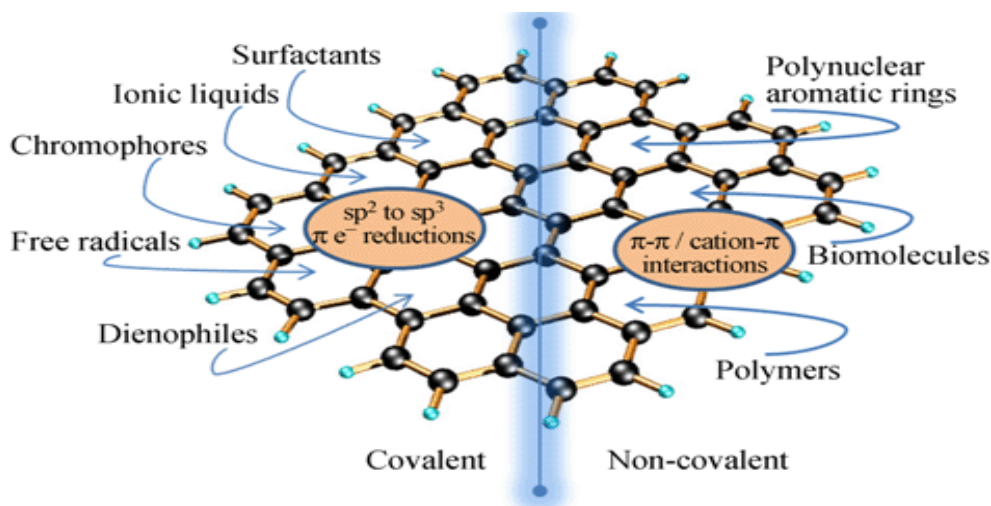
Figure 2.7. Covalent and non-covalent interactions [56].

2.1.5.3.1. Covalent modifications

The units of reactive olefin, which can act as either a diene or dienophile through cycloaddition reaction, are important for the covalent modifications. Furthermore, hydroxyls, carbonyls and carboxylic acids groups that are added to the surface are important for bringing about different chemical reaction. As for the electrochemical, photochemical and chemical methods, they stabilize the covalent bonds. Different wet chemistry techniques and click chemistry, they add many modifications [7].

Surface modification of graphene (GNSs) by nitric acid treatment (to give H-GNSs), was expected to increase the number of sites being active for the surface; for this, reactions of an electrochemical nature are effected, and to allow the aqueous electrolyte penetrations , improving the super capacitive performance is done [57].

2.1.5.3.2. Non-covalent modifications

Non-covalent interactions are highly important in up to date research in chemistry and is basic in chemistry of supramolecular, biochemistry and materials science.

Revision was done on graphene non-covalent functionalization, hydrophobic surfactant and graphene and hydrogen bonding interactions attraction, and π-π interactions. Moreover. The point of graphene and organic molecules non-covalent interactions is important because such methods modify the surface of graphene without minimizing the properties of the 2D sp^2 network. To disperse the sheets of individual graphene in a stable manner without affecting graphene integrity, macromolecules, ionic liquids or surfactants were widely used to achieve non-covalent modification of graphene surface [58].

To modify the graphene which employs electrostatic interaction, van der Waals force, hydrogen bonding, π-π stacking interactions or coordination bonds (Table 2.1), non-covalent methods are used. The π-π stacking interactions are mostly frequently employed to prepare graphene based composites, because in this way the structural nature of graphene is not affected. Furthermore, in some cases non-covalent modifications over all of the graphene surface can be achieved and reversible in some cases, when super intrinsic graphene properties are required, modifications of such kinds are important [59].

13

Table 2.1. Non-covalent interactions modifications and their basic applications[60].

Interaction type	Basic applications
Electrostatic interaction	Self-assembly composite materials
Van der Waals force	Improved imaging techniques
Hydrogen bonding	Strength of enhanced materials
π-π Stacking interaction	Smart materials
Coordination bonds	transition metals / Graphene composite

2.1.5.3.3. Acid modification

For the purpose of increasing the surface active sites of electrochemical reactions and promoting the wettability through the graphene aqueous electrolyte, the graphene was treated by a nitric acid for the chemical modification of the surface, which gave off more nitrogen and oxygen that contain functional groups on the graphene surface and obviously augmented the hydrophilicity. The electrode performance improved greatly due to modification of graphene by nitric-acid (H-GNS), with a maximum specific capacitance.

The above modification process (to give H-GNS), (Figure 2.8), which was expected to increase the number of active sites like –OH group and other groups, the -OH group, may significantly change the properties of graphene [61] for electrochemical reactions occurring on the surface and lead to the aqueous electrolyte penetration, which improves the supercapacitive performance [62].
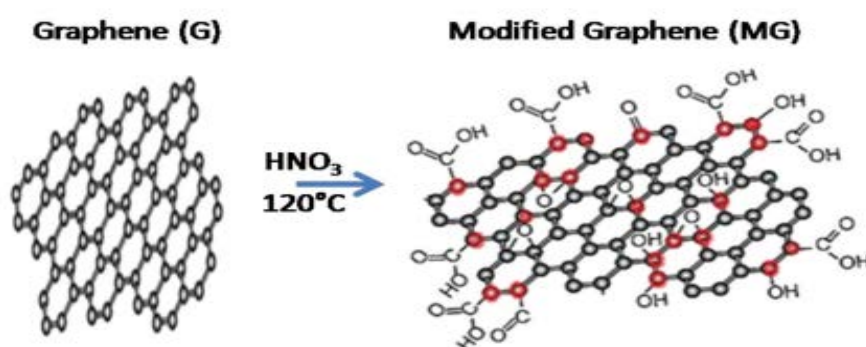
Figure 2.8. Modification of graphene by nitric acid [63].

2.1.5.3.4. Base modification

The electrical properties of graphene oxide affected by adding some amine compounds lead to the production of graphene oxide that contains the amino compound (possibly classified as nanocarbon compounds that contain nitrogen (Nitrogen-doped carbon nanomaterials). The amines served as spacers between graphene layers, in addition to augmenting electrical graphene oxide properties [64,65].

For the purpose of transferring the positive charge to the platform of graphene and then complexing with the molecules of DNA or RNA that are negatively charged for gene transfer aims, polyethylenimine (PEI) was used. The complex PEI-graphene-nucleic acid proved to be enzymes protective (e.g., nucleases) [66].

The modification of graphene by ethylenediamine (EDA), has been a point of focus due to the fact of graphene solubility improvement and being beneficial for more functionalization. Many ways are used for EDA-functionalized graphene preparation (Figure 2.9), such as the substitution reaction of fluorinated graphene and the nucleophilic ring opening reaction of graphene oxide [62].
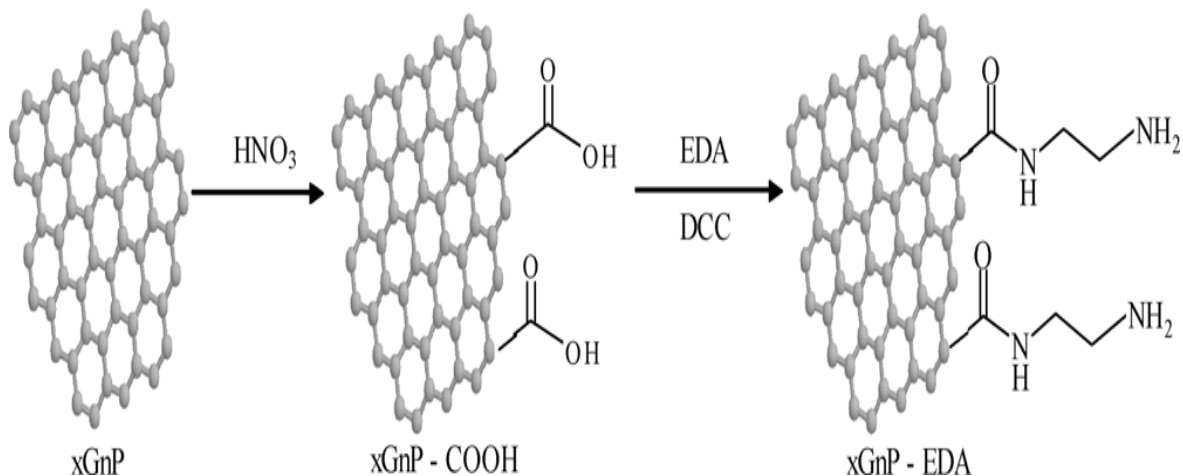
Figure 2.9. Modification of graphene by nitric acid followed by ethylenediamine

2.1.5.4. Graphene derivatives

Two oxidation states are there for graphene: reduced graphene oxide (rGO) and graphene oxide (GO), (Figure 2.10 and 2.11). GO can be solved with water with low electronic conductivity. On the other hand rGO shows a good conductive property and low water solubility.

The reason that GO has good solubility level because of being rich with oxygen-containing groups and hydrophilic groups, as in carbonyl, hydroxyl and carboxylic groups. The oxygen-containing groups- hydroxyl, and carboxyl, for example – will be removed after reduction. In this way, GO turns into a graphene rich with be π-conjugation, symbolized as rGO.
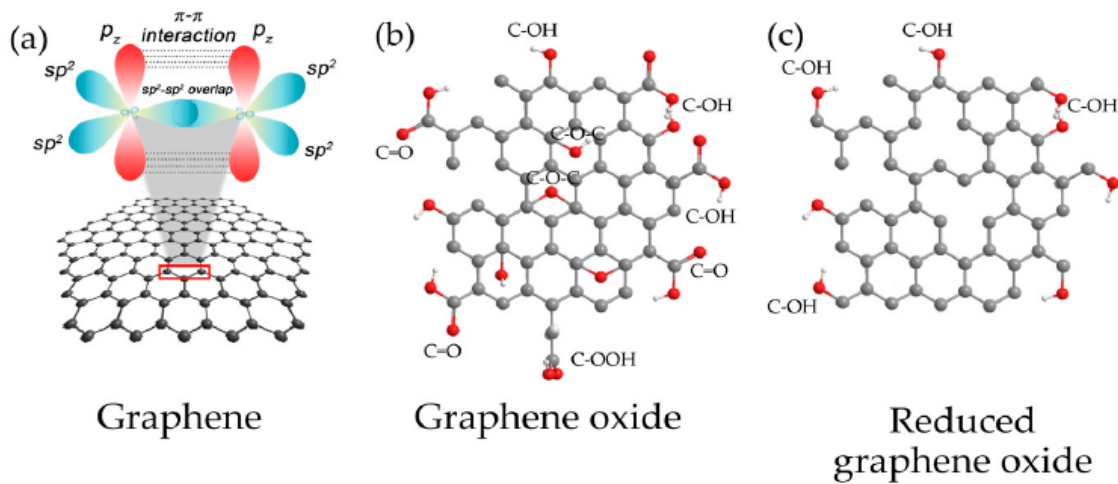
Figure 2.10. Structures of graphene-derivatives [67].

16
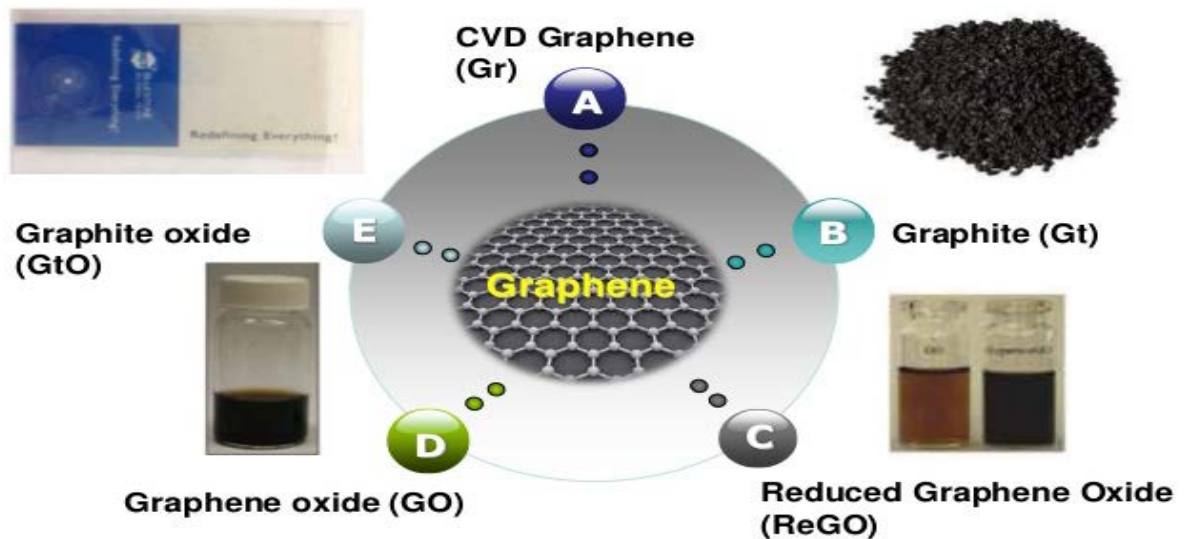
Figure 2.11. Graphene and its derivatives [68]**.**

The π-conjugation in the sheet of graphene has the ability to make a graphene conductive again and reduce the solubility in other organic solvents and water. The reduction decreases graphene processability and limits its applications [69].

2.1.5.4.1. Graphene Oxide

The GO, as a single carbon monolayer in aromatic regions randomly distributed (sp^2 carbon atoms) and domains of oxygenated aliphatic (sp^3 carbon atoms)and the functional groups containing oxygen -, carbonyl, epoxy and hydroxyl groups on the basal plane, with the groups of carboxyl on the edges - are created when oxidation happens by oxidative exfoliation of graphite or by using oxidation through strong chemical oxidants [70]. The functional groups attached to GO surface work effectively as anchoring sites to immobilize various active species [71]. GO is hydrophilic because of the aforementioned oxygen- containing functionalities and by this, the dispersion of water could be accomplished by ultrasonication processes. In other words, GO is miscible in water and can be merged with many hydrophilic polymers [72]. In order for dispersion to occur in organic solvents, there must be an adjustment of graphene oxide with compounds transforming the edge and surface groups (carboxyl and hydroxyl groups) into groups of carbamate and amide. This chemical treatment changed exfoliation nature, rendering all of graphene oxide exfoliation to single sheets easily dispersed in to organic solvents.

Graphene oxide does not settle in water and in solvents of a polar organic nature. As in N-methyl-2-pyrrolidone, N,N-dimethylformamide, tetrahydrofuran, and ethylene glycol whereby the exfoliated graphene oxide nanosheets tended to gather through the stacking π-π and gave off big graphite oxide particles. On the other hand, the functional groups of oxygen connected to graphene oxide led to mixing with different ceramic or polymeric materials to augment desirable properties for biomedical applications [73].

2.1.5.5. Applications of graphene

In order to use graphene or its modified form materials, there must usually be exploitation of its features as in the high electrical conductivity or large surface area. At present, many of the functionalized graphene applications concentrate on electronic devices and clean energy, in addition to sensors, medical devices and catalysis [74].

2.1.5.5.1. Nanotechnology

Nano is now a famous word used in modern science and has recently appeared in dictionaries, in words such as nanometer, nanoscale, nanoscience, nanotechnology, nanoelectronics, nanocrystal, nanofibers, nanoporous, etc. [75]. Nanotechnology is a science of technology and engineering on the nanoscale (from 1 to 100 nanometers) studying minute things applications and employed in fields of other sciences, as in biology, physics, chemistry, engineering and materials science [76,77].

Furthermore, this science of nanotechnology is useful in devices designing and new materials creation on the nanoscale to be applied widely; nanotechnology importance goes high in computing and materials science [78,79].

On the other hand, nanotechnology is also concerned with issues such as toxicity and environmental impact of nanomaterials [80].

The field of this technology is also used in developing technical disciplines (technology and polymer science) and research [81]. With regard to other domains of applications, nanoparticle drug delivery, polymer-based biomaterials, fuel cell electrode polymer bound catalysts, nanofibers, layer-by-layer self-

assembled polymer films,   polymer blends and nanocomposites. In the nanocomposites field there are a variety of issues, such as bactericidal properties, cosmetic applications, composite reinforcement, flame resistance, barrier properties, electro-optical properties, [82].

2.1.5.5.2. Composites

Composites are composed of two or more kinds of materials [83], combined in a way that reveals the materials as distinguishable. The components of the composite make up for the weakness in the individual components and they add strength[84].

Composites are basically designed with the purpose of adding strength, efficiency or durability [85].

In General, a polymer matrix is a natural fiber (such as carbon, glass or aramid) made by man or engineered to obtain composites. The function of the fiber is to protect from any external damage and from the environment [85].

Furthermore, fibers strengthen the matrix and are against fractures and cracks. Fibers are mainly asbestos, glass, carbon or silicon carbide, while metal, plastic or ceramic materials usually make the matrix [86].

The following kinds of matrix determine three sorts of composites:

- Polymer matrix composites (PMCs), of which Glass-fiber reinforced plastic is a famous example.
- Metal-matrix composites (MMCs**)** exactly use silicon carbide fibers embedded in a matrix made from an alloy of magnesium and aluminum , but iron, titanium and copper (other matrix materials) are used increasingly.
- Ceramic-matrix composites (CMCs): Such type of composites have the fiber of silicon carbide fastened in matrix of borosilicate glass. This kind of composite fit to be used in as parts for airplane jet engines, lightweight, high-temperature components [87- 89].

Composites are replaceable with metals for machine parts, but they are lighter and stronger than metals, with a better performance when there are high temperatures. they also do not lead to fractures, which are points of weakness [90].

2.1.5.5.2.1. Nanocomposites

The nanomaterials-graphene combination (resulting in a graphene−nanoparticle hybrid structure) has distinct physicochemical properties that are beneficial for bio applications because it reveals the properties of both the graphene and the nano particle, in addition to other more useful synergistic properties [91,92].

Generally, this combination (graphene−nanoparticle) can be classified into (1) graphene−nanoparticle composites, where nanoparticles are the decoration grown on the sheet of graphene. (2) graphene-encapsulated nanoparticles, where the graphene coats or wraps the nanoparticle surface [92].

2.1.5.5.2.1.1. Graphene Nanocomposites

Graphene with its high properties is an excellent nanofiller in the matrices of polymer for developing materials of high performance [23]. Incorporation of nano-fillers (as in carbon nanotubes and clay nano-sheets) augmented both the thermal and mechanical properties of the resulting nanocomposites with a small load [93].

 Recently, nanofillers, like graphene sheets, graphite nano-platelets, and graphene oxide, to obtain distinct thermal and mechanical properties [93].

Graphene oxide can be prepared in a variety of ways, having the spacing property, together with different oxygen functional groups (e.g., hydroxyl and carbonyl groups) on the edges and basal planes. These structures make it easy for graphene oxide to exfoliate in water and organic solvents at lower concentrations into single layers. The graphene oxide reduction to obtain graphene nano-filler to be used in polymer nanocomposites is a famous method [94]. (Figure 2.12).
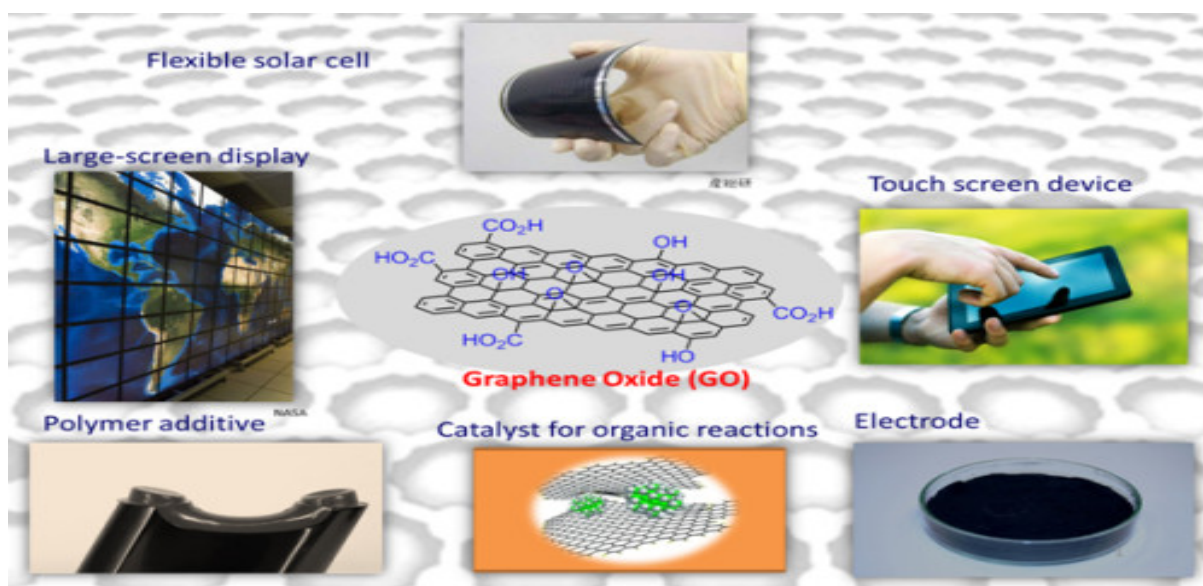
Figure 2.12. Uses of graphene oxide [95].

The exfoliation and reduction of graphene oxide can be done chemically and thermally to produce structures that are loosely stacked with a large area of specific surface [96]. Graphene-polymer studies investigated development in polymer properties through the graphene oxide incorporation (Figure 2.13).
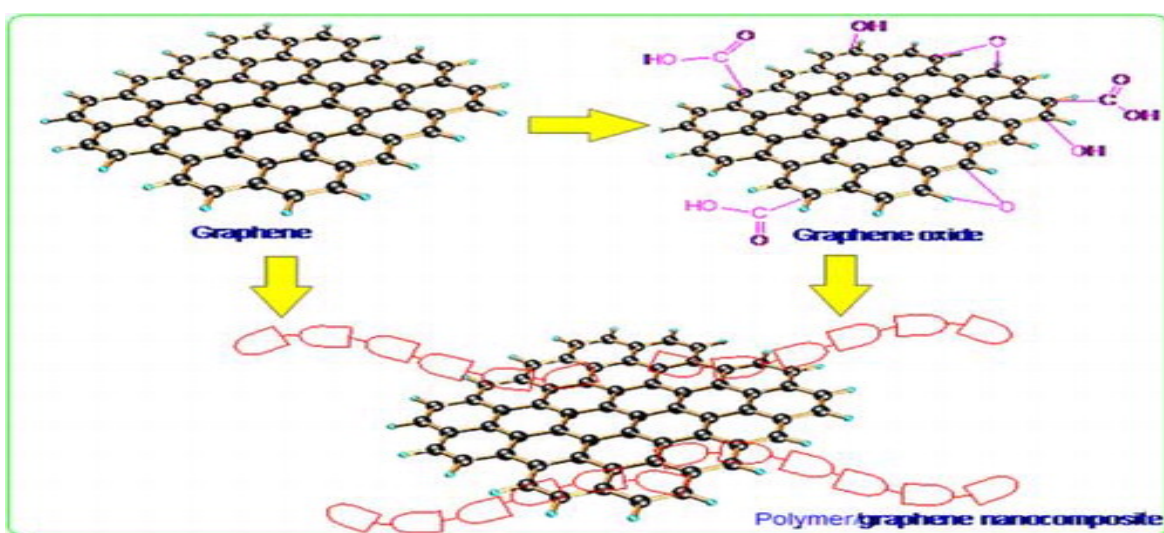
Figure 2.13. Preparation of graphene-polymer nanocomposite [23].

2.1.5.5.3. Cellulose

Cellulose, a polymer found in nature - paper, wood and cotton, is -best-known polymer of glucose, consisting of units of glucose held together by linkages of 1,4-β-glucosidic [97]. Cellulose is a fiber of an excellent nature. The monomer glucose in repeated units is what makes the cellulose [98]. Cellulose is a useful, biocompatible and safe biopolymer used in modern applications of medicine [99]. Cytotoxicity of cellulose is low. Cellulose is water soluble and nonionic, which makes it fit for applications of tissue engineering [100].

2.1.5.5.3.1. 2-Hydroxyethylcellulose (2-HEC)

2-Hydroxyethylcellulose (2-HEC), is a prominent derivative of cellulose, which copies its properties (low cytotoxicity, excellent biocompatibility, water solubility and high mechanical properties) and is employed in many fields, like, textile manufacturing, pharmaceutical industries, food industry, building materials and paints. When 2-HEC is cross-linked, more desirable characteristics are obtained [98].

To get a high quality performance of hydroxyethyl cellulose, sheet of graphene oxide are used as a filler in the film of 2-HEC composite. The film was exposed to a benign physical environment. In addition, water was used as only solvent to avoid obstacles [101].

Figure 2.14 shows the structures of cellulose and 2-hydroxyethylcellulose.
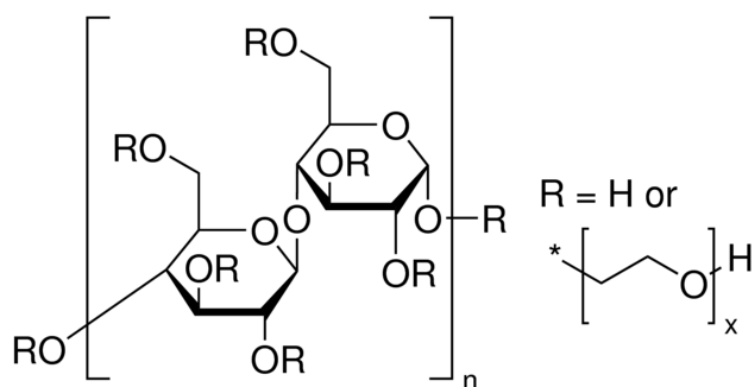
Figure 2.14. Structure of cellulose (R = H) and 2-hydroxyethylcellulose (some of R is replaced by -CH$_2$CH$_2$OH groups, and the others are H.)

2.1.5.5.4. Bio-medical applications

By applying biology principles to nanotechnology, this gives way to more miniaturizing and improving of artificial devices performance. The synergy of nanographene and biotechnology makes bio-medical applications more applicable in such fields as tissue engineering, gene and drug delivery, and cancer therapy. the following Figure displays how the materials of the family of graphene apply more medically than non-medically.
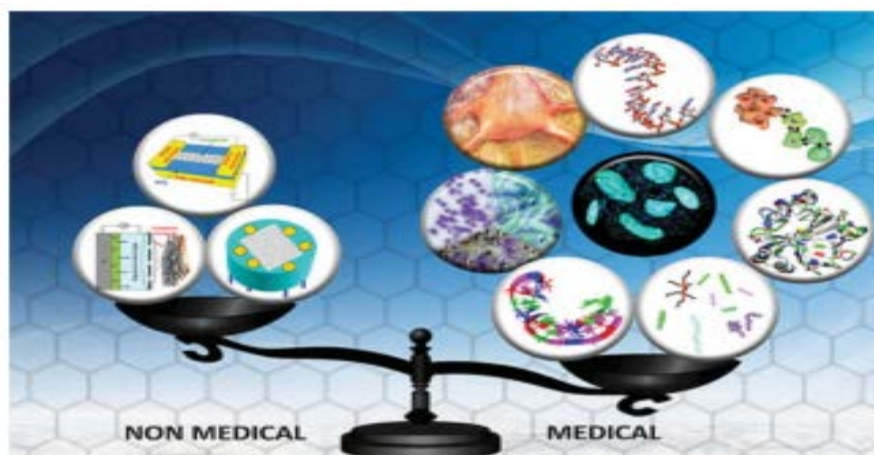
Figure 2.15. Tipping the scales of medical to the non-medical [102].

2.1.5.5.4.1. Gene delivery

Recently, gene therapy has been used to treat diseases related to genetic disorders, such as cystic fibrosis, cancer and Parkinson's disease [103]. Safe and efficient gene vectors are required for a successful gene therapy this to protect the DNA from nuclease degradation and to make it easy and more effective for the DNA uptake in transfection. literature has shown graphene as very effective in applications in the fields of protein delivery, gene delivery and gene–drug co-delivery. Graphene is used in gene delivery because of its functional property with cationic polymer, such as polyethylenimine (PEI), which is a gene vector that is non-viral because of its electrostatic interactions with negatively charged phosphates of RNA and DNA, where the interactions proved to be strong. Further properties of polyethylenimine (PEI) are that they offer a chemically easy modification leading to an efficient increasing transfection efficiency, reduced cytotoxicity and cell selectivity; however, the high toxicity and low biocompatibility of PEI hinder its applications in biomedicine [49].

2.1.5.5.4.2. Drug delivery

What makes graphene and effective carrier of drug is the ultra-high surface area (2630 m^2 g^{-1}) and the area of sp^2 hybridized carbon [104], and sp^2 hybridized carbon area. Graphene has a high therapeutic molecule loading capacity on both size of layer sheet of the single atoms [105]. Many drugs like *doxorubicine* (DOXO) complexed with the surfaces of graphene (Figure 2.16).
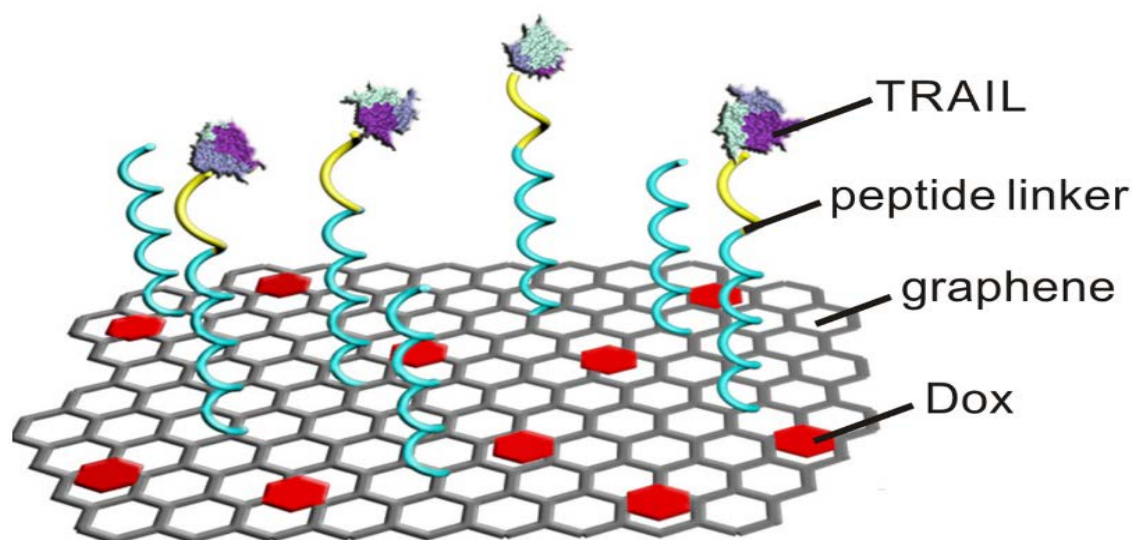
Figure 2.16. TRAIL and *doxorubicine* (DOXO) – onto graphene strip [106].

Graphene is one atom thick, which is originally a sheet of carbon that is two-dimensional. TRAIL is carried to the cancer cell membrane while DOXO is delivered to the nucleus. Researchers delivered the two drugs sequentially to cause the most damage to the cancer cell. due to molecular structure of the drug and the graphene similarities, DOXO is bound physically to the graphene. A chain of amino acids, peptides, binds the TRAIL to the graphene surface. "The graphene strips rich with the drug are introduced into the blood stream and they travel like nanoscale flying carpets," which, Once in the bloodstream, penetrate into the tumor through leaks of some blood cells, which the cancer tumor caused [107]. The stability of complex, which avoid chemical conjugation, is due to the $\pi - \pi$ stacking between the aromatic rings and the graphene carbon surface [66].

Due to the fact that graphenes are carriers of hydrophobic drugs, solubility problems are overcome. DOXO solubility property releases it from the nanocarrier in the acidic environment of tumor, when a comparison with the normal

physiological pH is done. *Rituxan* antibody which targets cancer releases the drug and causes destruction of the tumor [26].

Recently, due to the strong bonds and interactions among the aromatic regions of the sheets of graphene and hydrophobic drugs, developing graphene for loading and delivering of drugs has been of a great importance and interest (Figure 2.17). Graphene and carbon nanotube (CNT) properties have proved efficacy as excellent therapeutic agents in biomedical application. This makes them beneficial in such sciences as pharmacodynamics, pharmacokinetics and bio recognisation, for they decrease the degradation of drug and rise its efficiency.
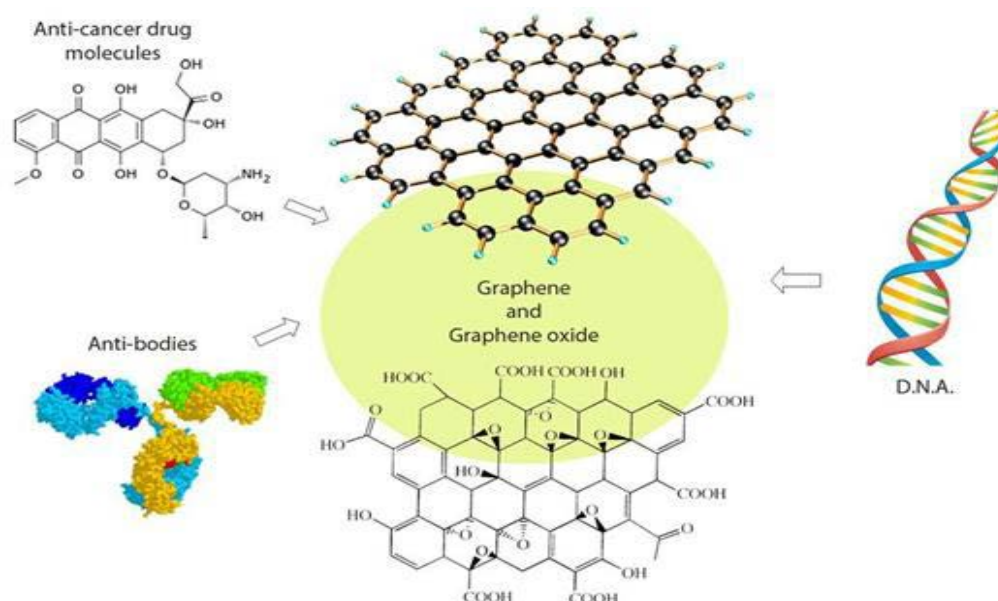
Figure 2.17. Diagram of graphene and graphene oxide as nano-therapeutic drug carriers (Platforms to deliver various therapeutics from antibodies, small drug molecules and DNA) [108]**.**

2.1.5.5.4.2.1. *Doxorubicine* (DOXO)

Doxorubicine (DOXO) is a chemotherapeutic agents used widely for being an efficient anti-tumor. However, DOXO has a limited use for it can be harmful to healthy cells, like myelosuppression, the dose-dependent cardio toxicity, multidrug resistance and nephrotoxicity [109].

2.1.5.5.4.3. Tissue Engineering

The materials related to graphene are promising in the field of tissue engineering [66]. Tissue engineering try to be a biological substitute to regain, keep, or develop

the tissue function or that of an organ. Lately, the materials that are based on graphene have been investigated and proved to be good in wound healing, regenerative medicine, stem cell engineering, and tissue engineering. The weak properties of hydrogels reduce their applicability in tissue engineering, even though they are viscoelastic and transport properties mimicking natural tissues. Graphene has excellent mechanical properties (strength, high elasticity, flexibility) and ability to have different functionalities on the surfaces that are flat. In fact, Graphene oxide incorporation into PVA-based hydrogels greatly augmented compressive strength (36%) and tensile strength (132%) of composite hydrogel without effect on their cytocompatibility [110]. Moreover, the film of graphene-reinforced chitosan with augmented mechanical features did not show toxicity when examined on murine fibrosarcoma L929 cell culture [111].

2.1.5.5.4.4. Cancer Therapy

Because of the distinct properties of graphene and its derivatives it has been applied in pharmacology and biomedical applications.

Doxorubicine, an anthracycline antibiotic, has been used greatly in chemotherapy as an anti-cancer drug through intravenous administration. The drug distribution to tumor sites by this method is limited due cellular barriers of the tissues, which can be prevented using nano-carriers such as graphene and GO. With the aid of sonication, which gives a high drug concentration on the surface of the graphene, DOXO is loaded on graphene oxide. Radiotherapy and chemotherapy have many disadvantages due to their restricted specificity to the cells of cancer, which may result in side effects on normal organs and tissues. DOXO, as anti-cancer drug delivery, has the advantage of, when compared with conventional cancer therapies, exceptional selecting cancer cells on tumor site and killing them with no inadvertent site effect [108].

2.1.5.5.5. Graphene as Antimicrobials

The toxicity of graphene based nanomaterial and their antibacterial function have been studied and shown their effect on bacteria, which appeared to be contradictory [66]. There with a membrane damage in gram-positive bacteria, which was unnoticed in gram-negative bacteria [66].

Through the direct interaction between the extremely sharp edges of graphene sheets and the cell wall membrane of bacteria, graphene and graphene derivatives showed significant bacterial inhibition of growth [112].

2.1.5.5.6. Graphene as Sensors of Biomolecules

Nanotechnology is a field of science engaged in searching for materials for bio sensing purposes - that is, sensitive, accurate, and selective detection of biomarkers. Lately, the biosensors that are graphene based are widely divers. The biosensors of graphene for caspase-3 and thrombin are good tools for monitoring acute and chronic pathological conditions. Also, genetic disorders, such as Alzheimer's or cystic fibrosis, are traced by single nucleotide polymorphisms.

Electronic determination of bioanalytes with field-effect transistor (FET) biosensors by using carbon nanomaterials like CNTs and graphene could achieve in very high sensitivity because the nanomaterials are very sensitive to the electronic effect after binding biomolecules onto the material surface. Previously, FET biosensors based on 2D graphene sheets were prepared for the quantitative detection of protein, DNA, antigen, and the analysis of protein-antibody interaction [113].

There are two alternative technologies for graphene nanomaterial's by a bio sensing uses. One is molecule- probed on the sheet of graphene interacting with the analyte and the other is label-free depending on the changes of the electrical properties of the platform of graphene interacting with an analyte Figure 2.18.
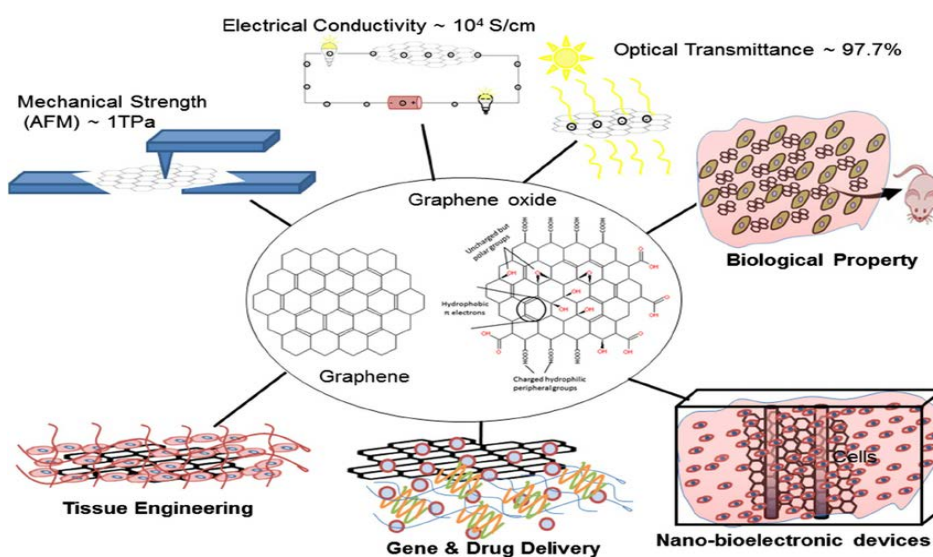
Figure 2.18. A preview of various applications of graphene [114]

2.1.5.5.7. Significance of graphene for electrochemical biosensing

The graphene basal and edge carbon atoms play a different role in electrochemistry [115]. The combination of graphene and sensors is natural, because of graphene's large surface-to-volume ratio, high carrier mobility, unique optical properties, high thermal conductivity, excellent electrical conductivity, and density, many other attributes can be greatly beneficial for sensor functions. The superior advantages offered by graphene for electrochemical biosensing are as follows:

- Capability of automation and miniaturization
- High electron transfer rate
- Biocompatibility
- Easier operation
- Extraordinary carrier mobility and capacitance
- Excellent transparency
- Exceptionally large surface-to volume ratio
- Single atom thickness
- Lower cost
- Flexibility and robustness
- Excellent conductivity

The above properties have been focused on for the development of electrochemical biosensors that are graphene-based. for the detection of a range of analytes like cholesterol, glucose, hemoglobin, glutamate and more, graphene has been employed as electrode material in different electrochemical biosensors [50].

2.1.5.5.8. Applications of graphene in electrical fields and others

Nanopore devices set where control and electronic sensing are done immediately at the pore was introduced with the graphene use as a membrane device [116]. Graphene then became has become promising for electronic material generation. The properties of graphene that are material (thermal conductivity, atomically thin dimension, unparalleled room-temperature, mobility and current carrying capacity) are more superior than silicon, but the two-dimensionality property (2D) is naturally

suitable to the Standard Complementary Metal-Oxide Semiconductor (CMOS) based technologies. However, it should be noticed that graphene, being a gapless semiconductor, cannot directly be applied in standard digital electronic circuitry [117].

Graphene is applied in other sciences - electrical engineering, mechanical engineering, and micro-electronics – and is considered of great importance in engineering and electronics.

2.1.5.5.8.1. Low-cost, thinner display screens for mobile devices

In organic light emitting diodes (OLED), Graphene can be replaceable with electrodes that are indium-based. The electronic device screens requiring consumption of a low power use diodes. This material is thinner and cheap and electrically conductive critically. That makes the materials good for displays that are with a flat-screen employed in smart phones requiring electricity to operate optical elements, and to react to the touch of the user. Graphene use instead of indium decreases the expenditure and eliminates metals use in (OLED), a property which makes devices easy to recycle [55].

2.1.5.5.8.2. Lithium-ion batteries that recharge faster

Lithium-ion batteries have graphene on the anode surface use graphene. The lithium ions have the chance to attached to anode substrate time to be recharge when there are defect in the sheet of graphene [55,118]. Lithium-ion batteries required longer time to be recharge than batteries with the graphene anode the graphene [55,118] because a one-gram graphene has a 2600 – square - meter surface area equal to almost ten tennis courts, which signifies that a reaction has more opportunities to happen in the battery [55].

2.1.5.5.8.3. Ultra-capacitors with better performance than batteries

Electrons are stored on the sheets of graphene in ultra-capacitors, where the large graphene surface increases the electrical power in the capacitor, which makes the recharging time shorter – in minutes rather than hours [55,118].

2.1.5.5.8.4. Low cost water desalination

Thin membranes prepared using graphene allows the water to flow through but, blocks the harmful particles and gases. Graphene–based membrane can be employed to desalinate the water of the sea with no high costs than the use of the techniques of reverse osmosis used recently [55,118].

2.1.5.5.8.5. Integrated circuits with graphene transistors

Using graphene with transistors is an achievement because of the graphene semi-conductivity. Transistors of such a kind operate twice the speed of silicon transistors. To process signals at a range of frequencies in radio applications, a mixer of a broad band radio frequency has been used. The transistors that use graphene are more effective in complex radio systems [55,118].

2.1.5.5.8.6. Transistors that operate at higher frequency

Transistors with graphene have a higher frequency due to the fact that graphene electrons movements, being higher than those in silicon. The improvement of the techniques of lithography that can be used to produce circuits that are integrated and graphene based [55,118].

2.1.5.5.8.7. Corrosion-resistant coating

Graphene used as a very important metallurgical tool. Corrosion-resistive coatings can be made from graphene which could protect important building and machinery elements from corrosion. It can help in doing so by conducting the charges responsible for corrosion of a material [55,118].

2.1.5.5.9. Environmental applications of graphene

Pollution of the environment is worldwide concern because of toxic pollutant that dissolve in water. Purification of water requires a variety of ways, filtration,

desalination, osmosis, disinfection, adsorption, and sedimentation. Materials based on carbon, like carbon nanotubes and activated carbon were employed for the purification of water. Use of functionalized graphene with a low cost resulted in many adsorbents in the purification of water. Because of the properties the graphene has (large surface area, the two-dimensional layer structure, pore volume and presence of surface functional groups in these materials. The wide surface area of graphene is due to the inorganic nanoparticles in the nanocomposite of 2D graphene which prevent the aggregation of graphene [119]. Graphene based materials also good in adsorbing heavy metals and organic pollutants (polycyclic aromatic hydrocarbons, dyes, and gasoline) (Figure 2.19) [20,21,119]. Graphene-based materials are used in environmental application, but they are limited in the adsorption of metal ions in aqueous medium due hydrophobicity [57].
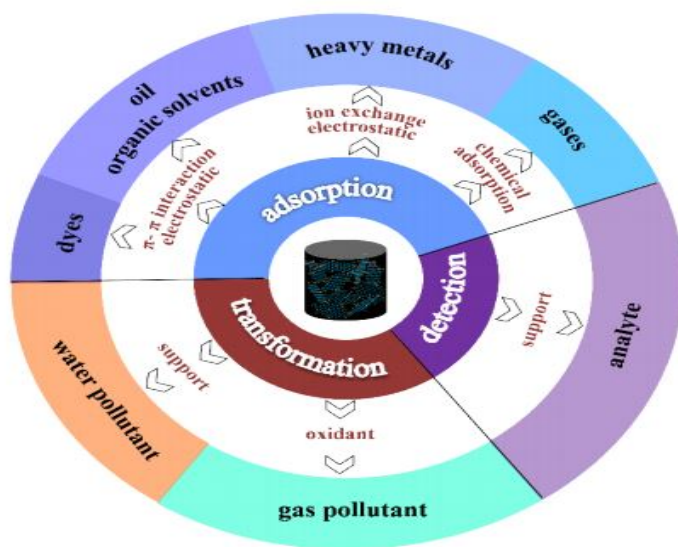
Figure 2.19. The environmental applications corresponding mechanisms for different types of pollutants [120].

2.1.5.5.10. Catalytical applications

Graphene properties (the stable structure, electrical and thermo-conductivities) made it applicable in catalysis because it affects the surface bound metal catalyst electronic properties leading to tune catalyst properties. Immobilizing the metal catalyst on graphene is a challenge [74].

2.1.5.6. Toxicity and Biocompatibility of Graphene Materials

In order to use graphene greatly in industries and applications, a toxicological assessment in vivo and in vitro are required [66].

Graphene and its nanocomposites have also been found involved in higher reactive oxygen species production, DNA damage, cell cycle changes, interference with metabolic routes and apoptosis. Lately, graphene oxide has shown toxic effects in several in-*vitro* and in-*vivo*. The cytotoxicity pertains to the physical damage of the membrane of cell plasma [121,122]. In order for the graphene oxide to be successful in nano-medicine, its influence on the stability of cells and its reduction of toxicity, which is still unsolved, must be tackled. The flakes of graphene pose a risk if inhaled by the lungs or penetrated the area around the lungs [99].

2.2. Instrumental Methods Commonly Used to Characterize Graphene and its Nanocomposites

2.2.1. Fourier Transform Infrared (FT- IR) Spectroscopy

Some of the infrared radiation that the sample is exposed to is taken by the sample (i.e. absorbed) and the other goes through it (i.e. transmitted). The detector signals spectrum, which is the sample molecular 'fingerprint.' Since molecules (i.e. different chemical structures) lead to different spectral finger prints, this makes infrared spectroscopy useful [123].

In the literature, for the investigation of the bonding interactions in graphene before and after the process of oxidation, infrared technique was employed [124].

2.2.2. X- Ray Diffraction (XRD)

In order to characterize general crystalline material, the XRD (X-ray Diffraction) is the most known employed technique. This technique functions so as to determine the orientation of a single crystal or grain and measure the average spacing's between layers or rows of atoms, [124].

To investigate the structural changes of graphene after acid modification, the XRD pattern of graphene modified by acid was obtained. The XRD patterns of the graphene (GNSs), and acid modified graphene ((H-GNSs) both exhibit a sharp diffraction peak from the (002) plane, which shows their high crystallinity. There are no obvious changes in intensity and position of the (002) diffraction peak for the H-GNSs compared to the GNSs, indicating that the primary structure is not changed after acid-modification. However, the slight shift to low angle of the (002) peak suggests that the interplanar spacing has expanded because of incorporation of oxygen/nitrogen-containing groups [125].

2.2.3. Scanning Electron Microscopy (SEM)

The scanning of electron microscopy (SEM) is a tool that is powerful and used in characterizing sample morphology such as particle size, grain size, and surface structure. Electron microscopy replaces the light source in traditional microscopy with a high energy electron beam source. However, the resolution is restricted to source wavelength. The formation of SEM image is dependent on the amount of signals produced due to the interaction occurring between the specimen and the

electron beam. The interaction can be categories into two class : elastic and inelastic interactions. Elastic interaction results from deflecting electrons without loss of energy.

The scanning of electron microscopy (SEM) has the function of determining the structure and morphology (form) of nanomaterial's and is a very beneficial instruments used for examining the characterizations of one of the most useful instruments available for the examination of the chemical composition and microstructure morphology [126].

The scanning of electron microscope (SEM) is similar to the TEM in that it uses a focused beam of electrons, possessing a much smaller wavelength than light waves, to irradiate a sample and scan its surface. The interaction of the electrons in the beams with the sample's atomic constituents provides reconstructed images of the material topology, which can be visualized as actual images of the sample. The resolution of an SEM is extremely high, due to small wavelength of the electron beam, and because there are no lenses involved (because there is no light source), highly tunable electromagnets are used to control the resolution at a level of very fine detail, as well as from a larger working distance to image a larger portion of the sample than can be managed by a TEM [127].

2.2.4. Elemental Mapping

In order to show the distribution of elements in the textural context, element maps are employed for this purpose; they display the compositional zonation through a Wavelength-Dispersive X-Ray Spectroscopy (WDS) system or an Energy-Dispersive X-Ray Spectroscopy (EDS) [128].

The detector of EDS (i.e. Energy-Dispersive X-ray Spectroscopy) is availed of to isolate the X-ray characteristics of different elements into a spectrum of energy. The software of EDS system is employed for the purpose of analyzing the spectrum of energy to specify the abundance of certain elements. EDS can exactly highlight the composition of materials chemically, even down to the size of a few microns, and make elemental maps over a broader area [129].

2.2.5 Transmission Electron Microscopy (TEM)

TEM (Transmission Electron Microscopy) is a tool of microscopy in which electron beam is transmitted across a sample of a thin nature and experiences interference due the scattering of some of the electrons from the atoms within the material. In an optical microscope, a light source is used to image a sample material, whereas in a TEM, the electron beam acts as the light source. While the electrons are passing through the sample, the beam stays fixed on the sample and some of the electrons are scattered in random directions, whereas the unscattered electrons are collected on a screen, thus creating a shadow image of the sample. Optical microscopes have lower resolution than TEMs do. Consequently, a TEM may examine the fine atomic structure of materials, down to single rows of atoms. Although TEM can provide fairly clear images of atomic structure, it is not well suited for making determinations for particle layer counts because of the small number of sample particles that can be examined within a reasonable period of time. TEMs can also output the scattering patterns directly, and these can give accurate ideas of layer number at particular points within the sample. According to literature [127], TEM images of graphene show single-layer, bilayer, tri layer, and multi-layer graphene nanoparticles. Single-layer graphene displays the hexagonal packing structure of the graphene honeycomb, with a single white dot indicating the placement of the atoms on the hexagon. Bilayer graphene displays two white dots at each hexagonal position, owing to the displacement of the carbon atoms between the layers; i.e., the carbon atoms in one layer are stacked above the holes on the layer below it. Tri layer graphene will exhibit several dots, whereas multi-layer graphene will display many points, which ultimately become of sufficient number to make continuous rings for bulk graphite [127].

By TEM, which is a 2-D microscopy device, It is difficult to delve into 3-D. To measure the thickness of the layers of graphene cross-sectional TEM is used [129].

2.2.6. Raman Spectroscopy

The noticeable variations in the structure that happen through the graphene and the derivatives of graphene chemical processing have also been characterized by Raman spectroscopy [130]. The device of Raman Spectroscopy is a commonly employed technique for determining the characteristic of the products of carbon,

taking into account that conjugated and double carbon- carbon bonds result in high Raman intensities [21].

Material properties can be characterized by using Raman spectroscopy without damaging the sample (Raman spectroscopy provides valuable information such as atomic structure, number of layers, type of disorder, and functional groups.).

The graphene layers numbers can be determined from 2D band position and broadness. The shape of the 2D band is different in graphite compared to graphene. The 2D band in graphite consists of two peaks, while 2D band in graphene shows only one sharp peak. This is due to the smaller number of layers in graphene. The presence of D band indicates a defect in the graphene sheet. The appearance of 2D in Raman spectra is clear evidence of graphene existence. The intensity ratio of D band G band provides information related to structural defect in a graphene sheet. For example, the ratio of I_D/I_G increases after annealing due to loss of carbon atoms [131].

The device of Raman Spectroscopy provides information about the reliability of the outline of carbon. D band intensity rise is owing to consecutive introducing of either sp^3 centers or holes due to the covalent binding of the addend. However, the challenge that Raman Spectroscopy device faces is that it cannot tell the difference between holes and sp^3 defects by Raman Spectroscopy [132].

Raman device is used to study the rotational, vibrational, and other modes of low frequencies. Every material has a distinct wavelength, known as the fingerprint of material. Raman effect is related to electromagnetic field of incident beam and sample material interaction. Raman effect lies in dealing with the dispersed beam [133].

2.2.7. Differential Scanning Calorimetry (DSC)

The thermal stability of the material is determined by DSC device [134]; this device can be employed in a variety of industries (polymer and pharmaceuticals, nanomaterial's and food products, etc.). Such a device provides information that helps to understand the behavior of crystalline and amorphous, eutectic transitions, polymorph curing and degree of cure, and the properties of other materials employed to test, design, manufacture product [135].

For the examination of the thermal properties of the composite prepared, some measurements of DSC have applied. In each example, two unique cooling and heating cycles were performed in a 25° C - 400° C range [136].

2.2.8. Mechanical Test Method

A crystalline solid are controlled by characteristics of its pristine crystal lattice and structural defects like dislocations and grain boundaries by the studying of mechanical properties.

For example, lattice geometry, defect-free crystal lattice and atom-atom interactions in the ideal cause elastic properties of a solid, whereas plastic flow stress and strength also suffer from the defects characteristic. The defects that already exist significantly minimize the real solids strength in the mechanical load, whereas the ideal strength in their counterparts are free from defect. Since structural defects always exist in conventional macroscale solids, this influences their mechanical properties, which is inevitable. However, in nanoscale solids defect may be absent in the initial state which is non-deformed; consequently, such solids may display a higher strength closer to the ideal highest value [137].

The general properties of mechanical test of graphene are:

1. Stiffness: Graphene is of a great importance as a material and a reinforcing agent in composite due to its unique properties, which are exceptional for they are significant and efficient for the stability of the sp^2 bond that compose the hexagonal lattice and detain the in-plane deformations.

2. Strength: The graphene which is Defect-free, monolayer is said to be the strongest material ever tested.

3. Toughness: Fracture toughness is a very significant mechanical property of graphene because of being related to the applications of engineering [138].

2.2.9. Electrical Conductivity

Measuring the electrical current amount of a material or its ability to carry it is known as electrical conductivity, which is also identified as specific conductance. It

is symbolized as σ and has SI units of Siemens per meter (S/m) [139]. (σ) is the reciprocal of the electrical resistivity (ρ):

$$\sigma = 1/\rho$$

The transport of electrons in grapheme has been a point of examination theoretically and experimentally lately. The Bloch–Grüneisen (BG) temperature is a new energy scale, different from Debye temperature, of purely electronic origin. In the 2D electron gas in semiconductor hetero structure or in graphene, electron density varies according to the magnitude of voltage. Graphene DC resistivity has been investigated and distinguished from the AC (a finite frequency regime), where BG (the new frequency and the study of the behaviour of AC conductivity) has been introduced.

Graphite and graphene, as carbon materials, display high electrical conductivity. The electrical conductivity of the graphene that is natural and synthetic was compared with other graphite materials of a different nature and carbon nanotubes under the 0.3 to 60 MPa compression. Synthetic graphene displayed a noticeable increment in electrical conductivity in comparison with natural graphene. Electrical conductivity was bigger in denser graphite, unlike the case in nanocarbon materials, like carbon nanotube and graphene, owing to, probably, the difference in layer arrangements of materials that are nanocarbon.

3. Experimental

3.1. Materials

Graphene nanosheet (6-8 nm, Skys nanometarials); nitric acid 68%, phosphoric acid 85% perchloric acid 60%, and sulphuric acid 95-98%, (all supplied from Merck, Darmstadt, Germany); ethylenediamine, diethylamine (Sigma-Aldrich); polyethylenimine (branched, M_n ~600, Aldrich); N-vinylimidazole (Sigma-Aldrich); 2-hydroxyethylcellulose (Sigma-Aldrich), *Doxorubicine* (Oncology Hospital) (Figure 3.1).

The other commercially available chemicals that were used without further purification were analytical grade reagents. Laboratory glassware was washed with a 5% nitric acid solution overnight. Before using the glassware, it was rinsed with deionized water and put in an environment free from dust to be dried.

A Thermo Scientific Barnstead *Smart2Pure* Water Purification System was used to purify the water used in all of the experiments.

Polyethylenimine

N-vinylimidazole

2- Hydroxyethylcellulose

Doxorubicine
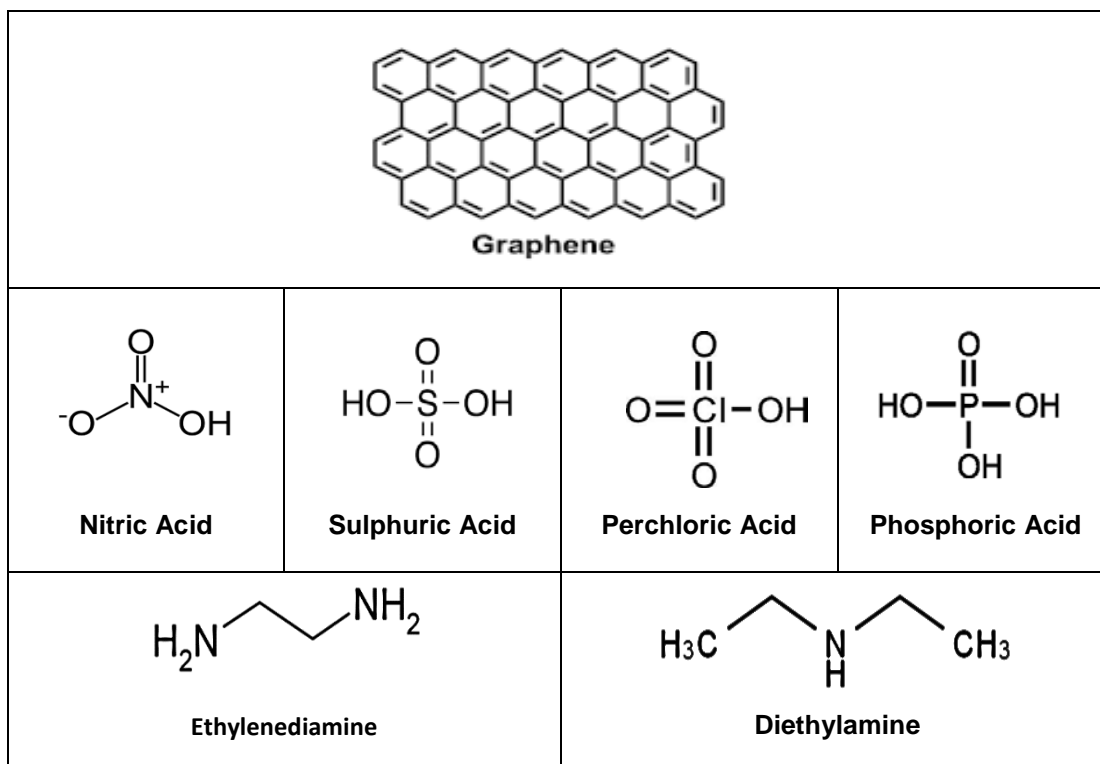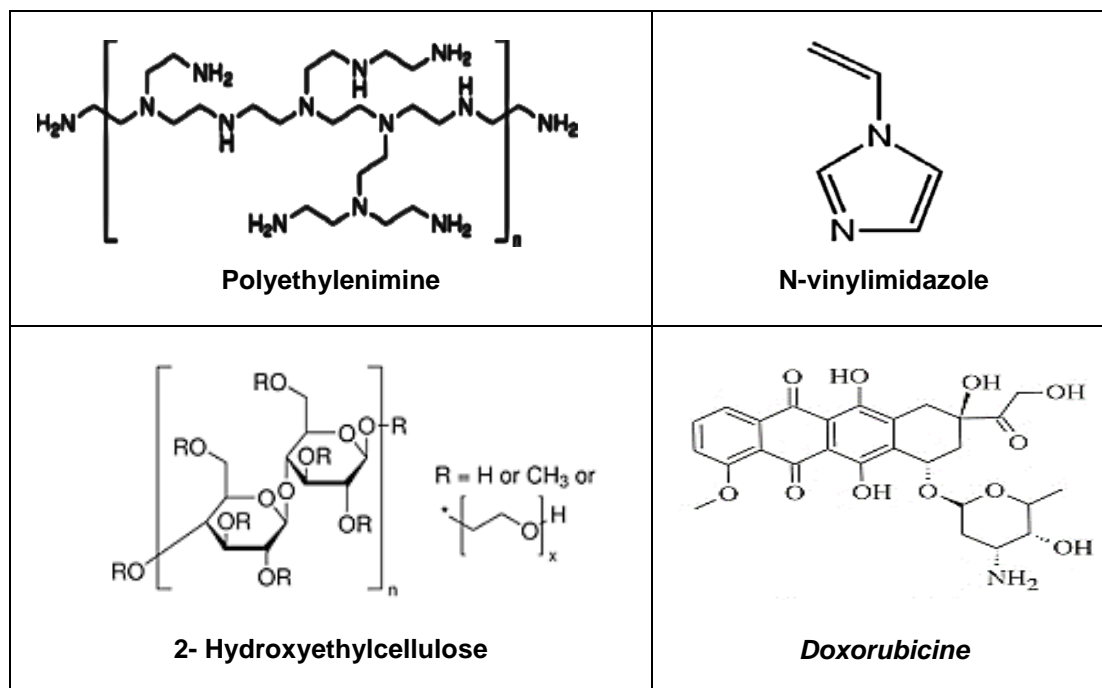
Figure 3.1. Chemicals formula used for this thesis study

3.2. Methods

3.2.1. Chemical modification of graphene

3.2.1.1. Acid modification

Graphene were chemically modified using different acid solutions. Briefly, 0.75 g of graphene were dispersed in 60 ml of acid solution at different conditions (concentration, time of stirring) at 60 °C, shown in the following Figure 3.2, Table 3.1, and stirred, The product was put for one day (24 h.) at 45°C in order for the reaction to be completed; after that, cooling the mixture was done to be like the room temperature; it was also filtered and washed with deionized water. At the end, the product was put in a 45°C oven for another one day (24 h.) to be dried, and then in the dry vacuum.
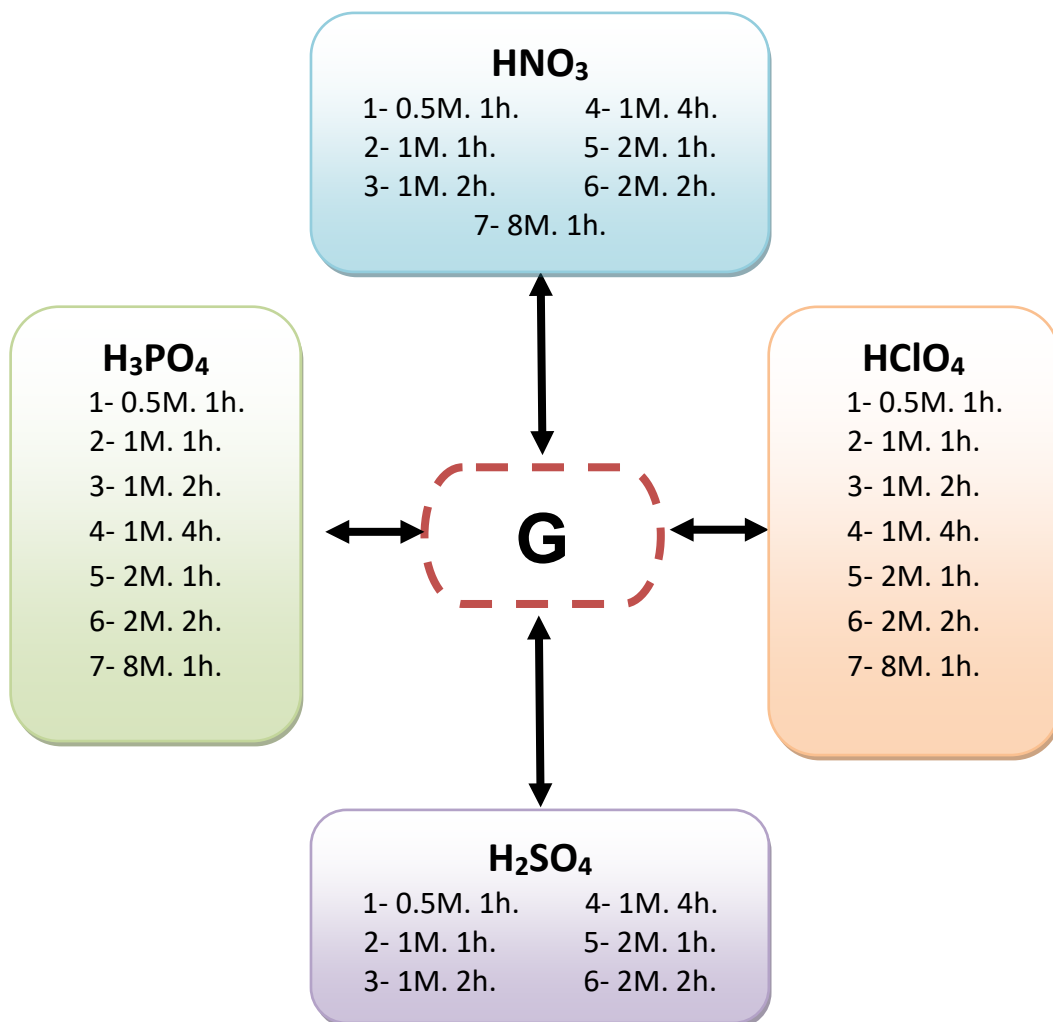
Figure 3.2. Modification of graphene by different acids at different conditions

Table 3.1. The reaction conditions for acid modified graphene

	Modifying agent	Acid concentration	Stirring time	Code of sample
Graphene	HNO_3	0.5 M	1 h	GN 01
		1 M	1 h	GN 11
		1 M	2 h	GN 12
		1 M	4 h	GN 14
		2 M	1 h	GN 21
		2 M	2 h	GN 22
		8 M	1 h	GN 81
	$HClO_4$	0.5 M	1 h	GL 01
		1 M	1 h	GL 11
		1 M	2 h	GL 12
		1 M	4 h	GL 14
		2 M	1 h	GL 21
		2 M	2 h	GL 22
		8 M	1 h	GL 81
	H_3PO_4	0.5 M	1 h	GP 01
		1 M	1 h	GP 11
		1 M	2 h	GP 12
		1 M	4 h	GP 14
		2 M	1 h	GP 21
		2 M	2 h	GP 22
		8 M	1 h	GP 81
	H_2SO_4	0.5 M	1 h	GS 01
		1 M	1 h	GS 11
		1 M	2 h	GS 12
		1 M	4 h	GS 14
		2 M	1 h	GS 21
		2 M	2 h	GS 22

3.2.1.2. Base modification

Graphene were chemically modified using different base solutions (Ethylene diamine (EDA), diethylamine (DEA), N-vinylimidazole (VIM), and polyethylenimine (PEI)). Briefly, 0.75 g of graphene were dispersed in 60 mL amine solution at different conditions (concentration, time of stirring) at 60°C, shown in the following Figure 3.3, Table 3.2, and stirred; The product was put for one day (24 h.) at 45°C in order for the reaction to be completed; after that, cooling the mixture was done

to be like the room temperature; it was also filtered and washed with deionized water. At the end, the product was put in a 45°C oven for another one day (24 h.) to be dried, and then in the dry vacuum.

```
                    ┌─────────────┐
                    │     PEI     │
                    │  1- 2M, 1H  │
                    │  2- 2M, 2H  │
                    └─────────────┘
                           ↕
┌─────────────┐     ┌ ─ ─ ─ ─ ─ ┐     ┌─────────────┐
│     VIM     │     │           │     │     DEA     │
│  1- 2M, 1H  │ ↔   │     G     │  ↔  │             │
│  2- 2M, 2H  │     │           │     │  1- 2M, 2H  │
└─────────────┘     └ ─ ─ ─ ─ ─ ┘     └─────────────┘
                           ↕
                    ┌─────────────┐
                    │     EDA     │
                    │             │
                    │  1- 2M, 2H  │
                    └─────────────┘
```
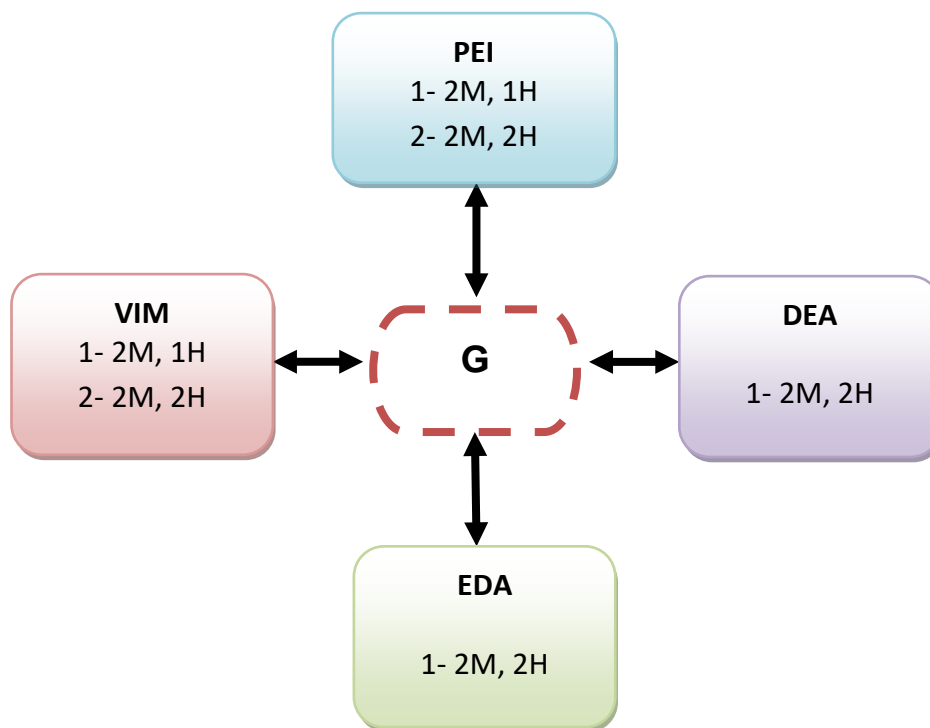
Figure 3.3. Modification of graphene by different bases

Table 3.2. The reaction conditions for base modified graphene

	Modifying agent	Base concentration	Stirring time	Code of sample
Graphene	PEI	2 M	1 h	GPEI 21
		2 M	2 h	GPEI 22
	VIm	2 M	1 h	GVIM 21
		2 M	2 h	GVIM 22
	EDA	2 M	2 h	GEDA 22
	DEA	2 M	2 h	GDEA 22

3.2.2. Preparation of composites

The modified graphene (prepared by using some acids and bases) was again subjected to modification in the presence of N-vinylimidazole and polyethylenimine, separately. Briefly, 0.75 g of modified graphene were dispersed in 60 mL N-vinylimidazole (or polyethylenimine) solution at different conditions (concentration, time of stirring) at 60°C, shown in the following Figure 3.4 and Table 3.3, and then stirred, The product was put for one day (24 h.) at 45°C in order for the reaction to be completed; after that, cooling the mixture was done to be like the room temperature; it was also filtered and washed with deionized water. At the end, the product was put in a 45°C oven for another one day (24 h.) to be dried, and then in the dry vacuum.
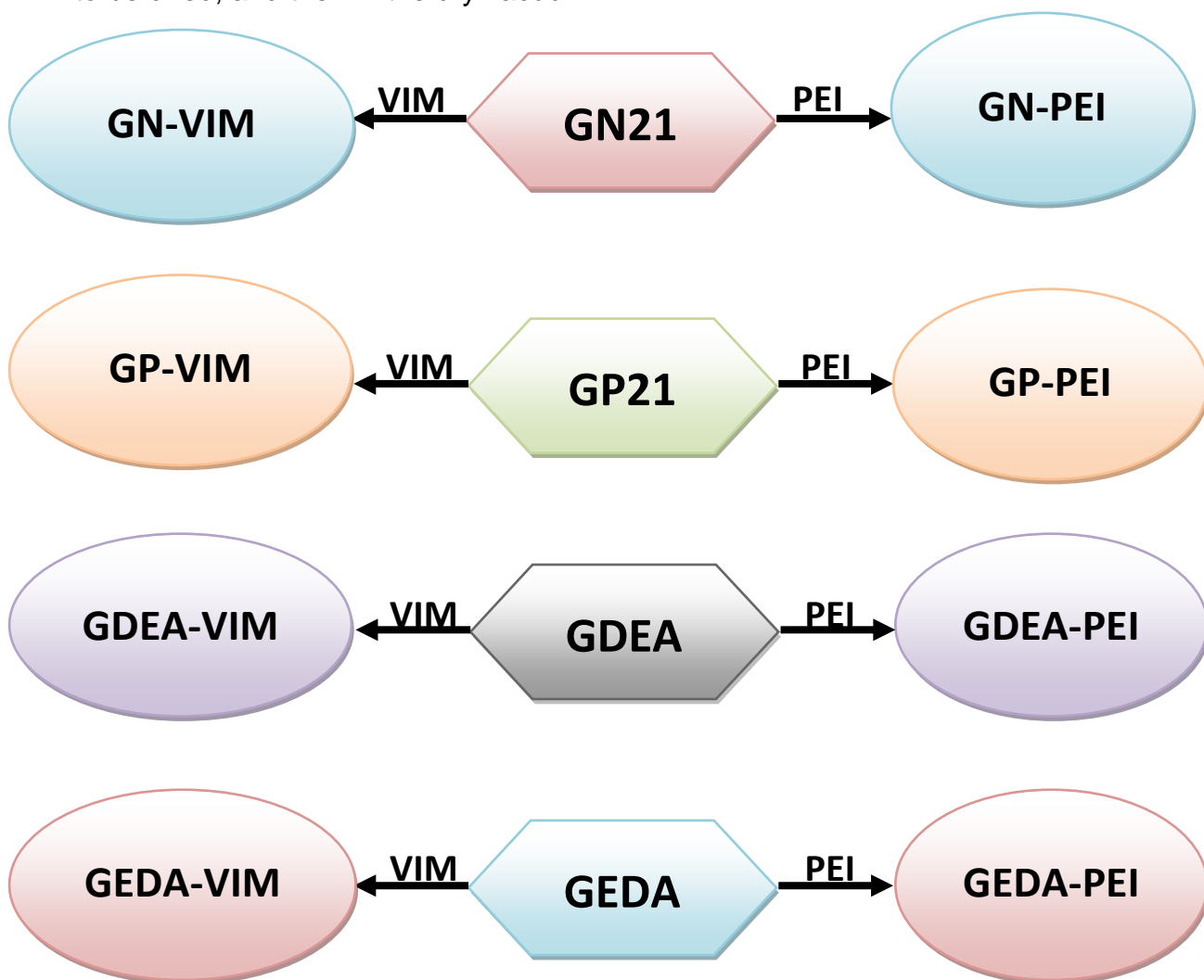
Figure 3.4. The reactions for preparation of graphene composites.

Table 3.3. The reaction conditions for preparation of graphene composites

Starting material	Composite material	Composite material concentration	Stirring time	Code of sample
GN 21	PEI	2 M	2 h	GN - PEI
	VIM	2 M	2 h	GN - VIM
GP 21	PEI	2 M	2 h	GP - PEI
	VIM	2 M	2 h	GP - VIM
GDEA 22	PEI	2 M	2 h	GDEA - PEI
	VIM	2 M	2 h	GDEA - VIM
GEDA 22	PEI	2 M	2 h	GEDA - PEI
	VIM	2 M	2 h	GEDA - VIM

3.2.3. Preparation of nanocomposite films

We prepared 2-hydroxyethylcellulose (2-HEC) solution with the concentration of 10% in water and left to stand for 12 hours. To 5 mL of this solution 0.0025 g of graphene and 0.08 g of cross-linking agent (ceric ammonium nitrate (CAN)) were added. The film solutions were stirred in an ultrasonic bath at 60°C for 15 minutes. After that, pouring the solutions into small petri dishes (5 cm in a diameter) was applied to be dried at room temperature for a week. The same test route was repeated for modified graphenes. 2-HEC / graphene nanocomposite films containing DOXO were prepared in the same manner (Figures 3.5 - 3.6 and Table 3.4).
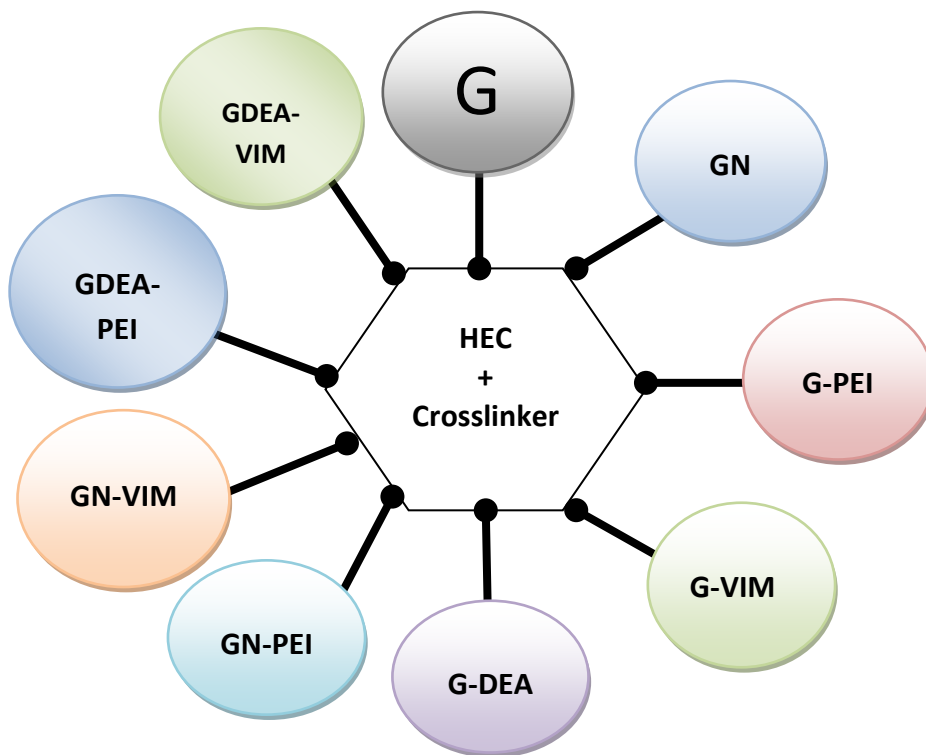
Figure 3.5. Preparation of nanocomposites with 2-hydroxyethylcellulose (2-HEC).
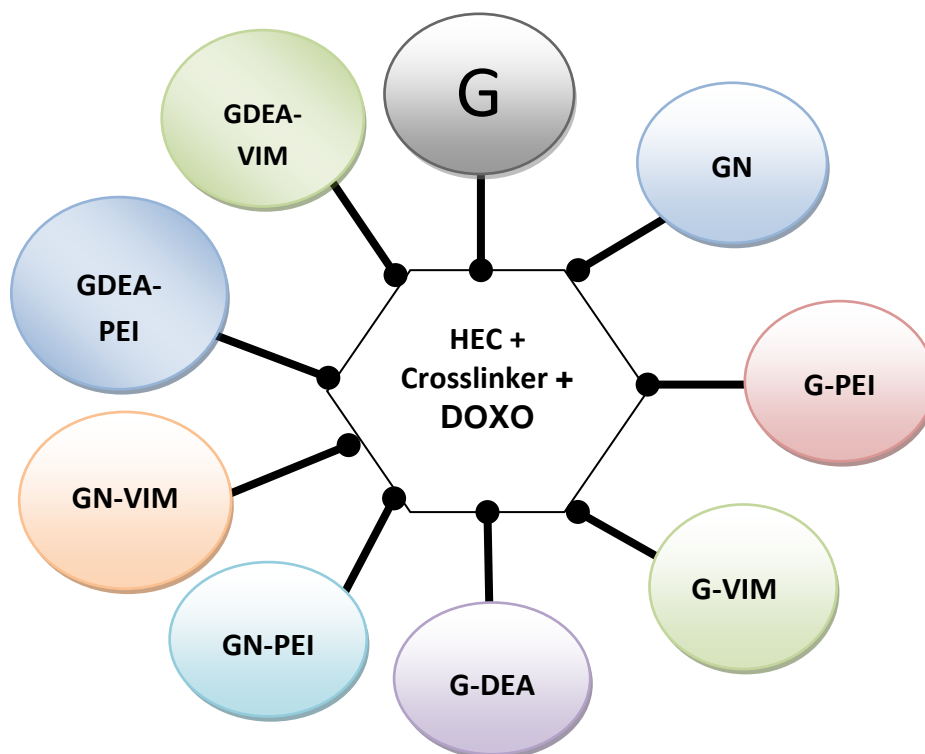
Figure 3.6. Preparation of nanocomposites with 2-hydroxyethylcellulose (2-HEC) and DOXO.

Table 3.4. 2-HEC nanocomposite films containing graphene and modified graphenes

No	Graphene and graphene derivatives	Matrix	Drug
1	Graphene	10% 2-HEC	-
2	GN 21		
3	GPEI		
4	GVIM		
5	GDEA		
6	GNPEI		
7	GNVIM		
8	GDEA with PEI		
9	GDEA with VIM		
10	Graphene	10% 2-HEC	DOXO
11	GN 21		
12	GPEI		
13	GVIM		
14	GDEA		
15	GNPEI		
16	GNVIM		
17	GDEA with PEI		
18	GDEA with VIM		

3.2.4. DOXO release from 2-HEC/graphene nanocomposite films

Drug release assays from the obtained nanocomposites were performed with a Perkin Elmer brand Lambda 25 model UV-Vis device. Drug release from selected 2-HEC / graphene nanocomposite films was studied at pH 4.5 and 7.4 by taking *doxorubicine*, a commonly used drug in cancer treatments. The maximum wavelength for *doxorubicine* was measured as 254 nm. The concentration of drug released into the buffer medium for different periods was calculated from the calibration and the amount of released drug - time plots were drawn.

3.3. Instrumental Methods

3.3.1. Fourier Transform Infrared (FT- IR) Spectroscopy

The covalent and non-covalent functionalization were characterized by FT-IR spectra tool which is useful for this purpose. FT-IR spectra were recorded using Perkin Elmer instrument, model 100 spectrum, ATR mode in a 400-4000 cm^{-1} frequency range.

3.3.2. X- Ray Diffraction (XRD)

The pure substance x-ray diffraction pattern is what characterizes it; it is like a fingerprint. Polycrystalline phases are suitably characterized and identified by the powder diffraction method. The XRD – related data were collected with a Empyrean X-ray diffractometer in the 2 θ angle with the range of 10 - 60°.

3.3.3. Scanning Electron Microscopy (SEM)

The SEM tool is concerned with high resolution imaging and analyzing the elements (elemental analysis), and recently, the crystals (crystallographic analysis). In addition to that, SEM is employed to identify the micro-appearance of the fracture surface and decide on the nature of the kind of fracture process (cleavage, dimple rupture, intergranular which is brought about by the environment, etc.). SEM (Carl Zeiss, Model Supra 40 VP) was used to observe the edge as well as the top surfaces of the graphenes/ composites/films.

3.3.4. Elemental Mapping

The elemental content of a surface, what is near the surface, the bulk as a whole, or interior of a product can be determined by the elemental mapping method. In this study, elemental composition in graphenes / composites/films were determined by applying the mapping method with the Bruker EDX detector.

3.3.5. Transmission Electron Microscopy (TEM)

In order to image the nanomaterials with an aim to determining the quantity of the particles, grain size and its distribution, as well as the morphology, TEM is a very important tool for this purpose. High Contrast TEM evaluations were performed on

the FEI microscope, under the condition that it operates at 120 kV. accelerating voltage.

3.3.6. Raman Spectroscopy

Raman spectroscopy shows itself to be a powerful tool to identify the carbonaceous materials e.g. graphene, carbon nanotube and nanodiamond because of the high Raman intensities yielding. A Renishaw in Via spectrometer. (A 532 nm laser used as the excitation source) was used to specify The Raman spectra taken at room temperature.

3.3.7. Differential Scanning Calorimetry (DSC)

For the measurement of temperature at the melting point, latent melting heat, fusion heat, the energy of reaction and its temperature, transition temperature of the glass, the temperature transition of the crystalline phase and its energy, the energy of precipitation and its temperature, temperatures of denaturation, the induction times of oxidation, and heat capacity, DSC is employed. DSC functions in a way to determine the energy amount released or absorbed by a sample when the sample is cooled or heated. In this way, it provides data relevant to the quantity and quality of the sample on the endothermic (heat absorption) and exothermic (heat evolution) processes. Differential Scanning Calorimetry (DSC) using a Rigaku, Thermoplus Evo DSC model 8230 (Japan) was used to determine the thermal transitions of the samples. In a N_2 atmosphere, the experiments were implemented using about a 5 mg of the sample which ,is sealed in aluminium pans. The temperature of the samples were raised starting from the room temperature to 500°C over it. For all the cases, the rate of heating was 10°C per minute.

3.3.8. Mechanical tests

One of the most common mechanical test methods is the tensile test. The tensile test increases a tensile load in one direction, usually until fracture occurs. The load can be applied in tension, compression or shear.

The experiments of Stress-strain were implemented in a room temperature by Baehr (Germany) with a testing machine that had a load of 10 kN. maximally. The initial distance between jaws is 40 mm. Three samples were cut from each cellulose film and thickness measurements were made with three different locations of each sample with a digital micrometer. The mean values obtained from the specimens subjected to the stress and elongation calculations were taken into account. The samples were cut with a cutting device conforming to ASTM 638 standard Type V. The results of stress and elongation were obtained by the calculation method according to EN ISO 527-1:

All stress values (σ), in MPa, based on the initial cross-sectional area of the test specimens were calculated from below formula

$$\sigma = F, \text{ Force (or load, Newton) } / A, \text{ Area (mm}^2)$$

and elongation values (ε) from

$$\varepsilon \ (\%) = 100^*(\Delta L/L_0)$$

was calculated as a percentage based on the jaw separation distance. Where L_0 is the initial distance between the jaws in mm of the test sample and ΔL is the extension value in relation to the beginning of the test sample between the jaws.

3.3.9. Electrical Conductivity Measurements

In order to measure the Direct Current (DC) conductivity of the nanocomposite films by four point probe method, The samples were cut into an oblong shape with a 1 x 2 cm dimension to measure conductivity. Impedance measurements were made with the Agilent 4294 A at a frequency range of 40 Hz-110 MHz.

4. Results and Discussion

In this work there are four main sections. The materials obtained in each section were analyzed in instrumental analysis methods and presented in a certain order. The results obtained for each section are also used in the next section. Analysis methods include FT-IR, XRD, SEM; Elemental Mapping (using EDS), TEM, Raman, Mechanical Test and DSC. These four main sections are listed below:

Modification of pristine graphene by acids and bases.

Preparation of composites based on acid and base modified graphene treated by N-vinylimidazole and polyethylenimine.

Preparation of polymer/graphene nanocomposite films (graphene and modified graphene doped 2- hydroxyethylcellulose (2-HEC)).

Applications of nanocomposite films in biomedical and electrical fields.

4.1. Results of graphene modifications

4.1.1. Fourier Transform Infrared (FT- IR) analysis of pristine graphene and modified graphene

FT-IR spectra were taken to investigate the bonding interactions in pristine graphene before and after the modification process, and measurements were performed in order to obtain the bending and stretching vibrations of functional group present in the samples.

4.1.1.1. FT-IR analysis of pristine graphene and acid modified graphene

The changes in pristine graphene modified by acids (HNO_3, H_3PO_4, $HClO_4$ and H_2SO_4) at different conditions and pristine graphene were detected by FT-IR; results are given in Figure 4.1 – Figure 4.4.

Figure 4.1 shows the changes in pristine graphene after treatment by HNO_3 at different conditions.
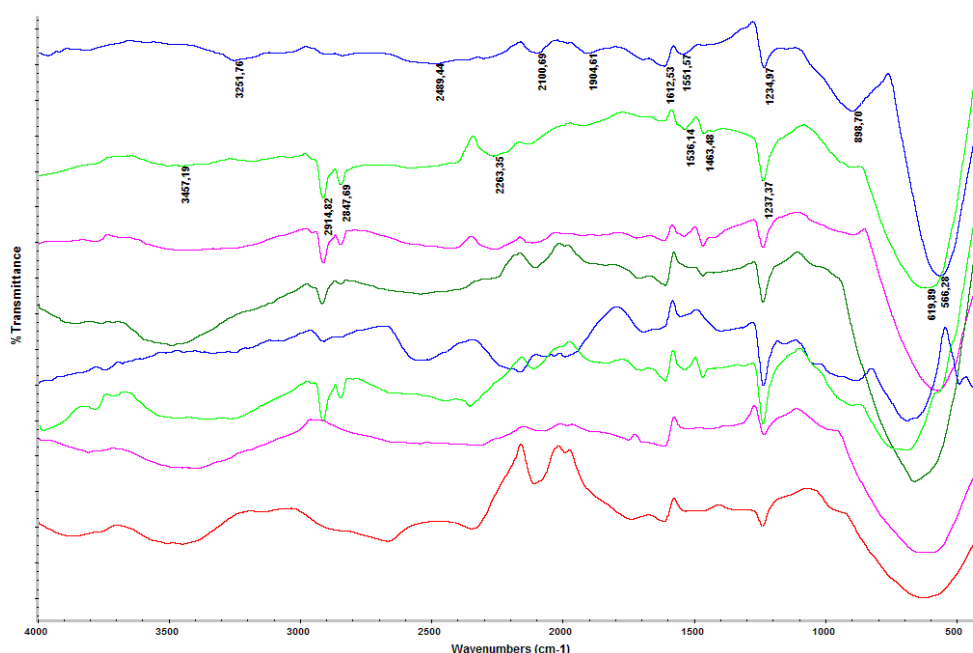
Figure 4.1. FT-IR spectra of pristine graphene and modified graphene by HNO_3 at different conditions (from top to bottom: G, GN01, GN11, GN12, GN14, GN21, GN22, and GN81).

From these FT-IR spectra it is obvious that pristine graphene gives a typical band at the range between 800 - 900 cm^{-1} is ascribable to C–H out-of-plane bending in aromatic ring; also FT-IR spectrum of pristine graphene showed the band of -C=C-bond around at 1612 cm^{-1} due to aryl group. The spectra of the graphenes modified by HNO_3 are characterized by the presence of the band at 1237 cm^{-1} indicating to C-O stretching in acids group. A band at 1463 cm^{-1} can be ascribed to C-OH bending of hydroxyl groups, the band at 2847 cm^{-1} is attributed to C-H stretching vibrations and band at 2914 cm^{-1} belongs to aliphatic C-H adjacent to the aromatic ring. When graphene reacted with HNO_3 having concentrations ranging from 0.5 M to 8 M, only high concentration may lead to oxidation product forming C=O. Also the C-H absorption band observed at 2920 cm^{-1} gradually disappear with high concentration of HNO_3 means that the reaction produced more C-OH group than C-H. In other words the oxidation state proportional with acid concentration and reaction time, especially in GN22 and GN81, lead to the broadened band in the range from 2900 to 3500 cm^{-1} belonging to stretching vibration of O-H group [140].

Figure 4.2 shows the new groups that have attached to graphene after treatment by H_3PO_4 at different conditions.
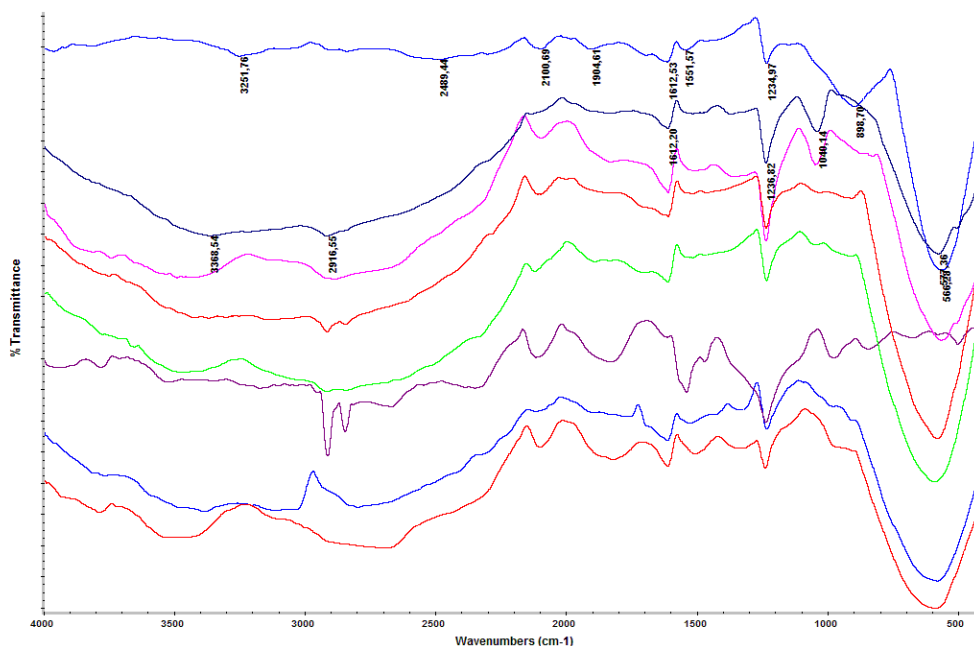
Figure 4.2. FT-IR spectra of graphene modified by H_3PO_4 at different conditions (from top to bottom: G, GP01, GP11, GP12, GP14, GP21, GP22, and GP81)

There are many new peaks in the FT-IR spectra of H_3PO_4 modified graphene compared to that of pristine graphene. The band at 1040 cm^{-1} due to P-C stretching vibration which is not observed in graphene's spectrum proves the phosphoric acid reaction with pristine graphene. Also, the increase in P-C band depending on higher reaction time and concentration is the evidence that this reaction is time- and concentration- dependent. The bands at 3368 cm^{-1} and around at 1820 cm^{-1} belong to –OH and C=O groups, and the C=C stretching vibration was observed at 1612 cm^{-1} [141].

Graphene was treated by HClO₄ at different conditions (G, GL01, GL11, GL12, GL14, GL21, GL22, and GL81), and the new groups that have formed on graphene are shown in Figure 4.3.
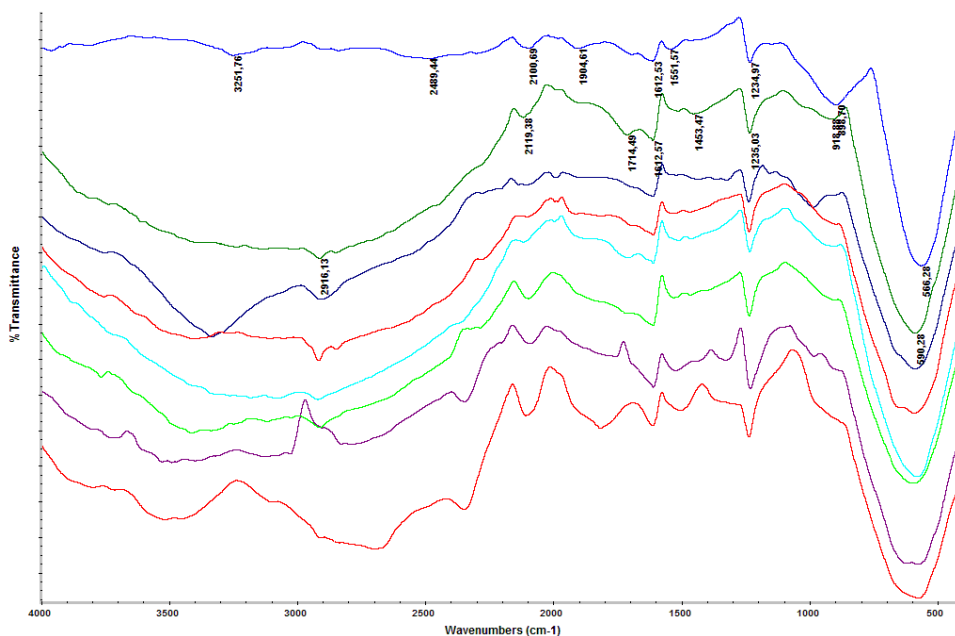
Figure 4.3. FT-IR spectra of graphene modified by HClO₄ at different conditions (from top to bottom: G, GL01, GL11, GL12, GL14, GL21, GL22, and GL81)

When pristine graphene is treated with HClO₄, in Figure 4.3, at the range of 3500 - 3300 cm^{-1} O-H group was appeared; a band around 1715-1800 cm^{-1} indicated C=O stretching vibration that was appeared by weak absorption, the strong absorption was observed only at higher concentration and long reaction time. Also, C-OH bending at 1453 cm^{-1} indicated the oxidation of pristine graphene and stronger absorption was realized out only at high concentration and long reaction time [142].

The FT-IR spectra taken after the reaction of graphene with H_2SO_4 at different conditions are presented in Figure 4.4.
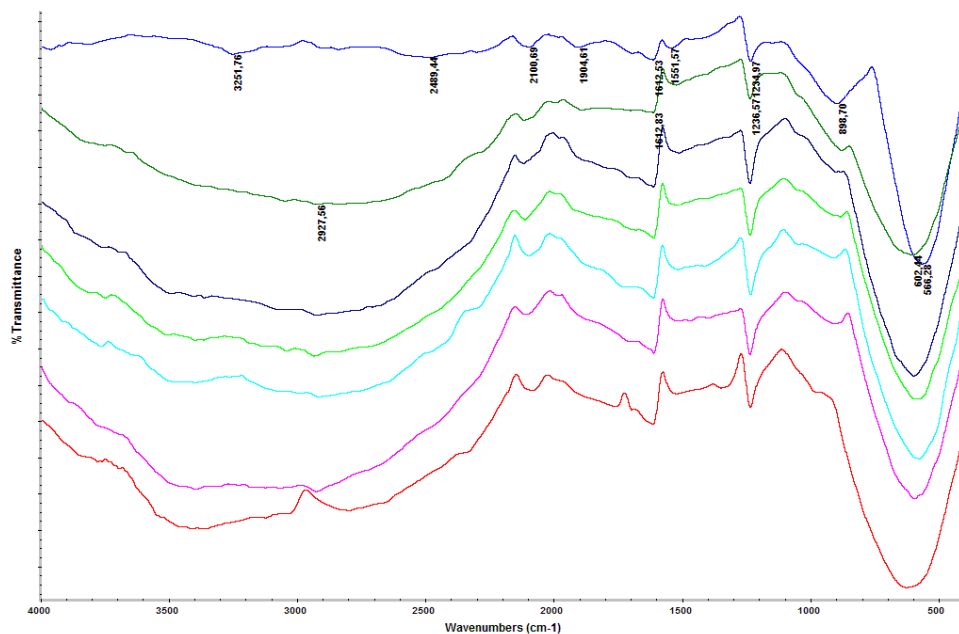
Figure 4.4. FT-IR spectra of graphene and modified graphene by H_2SO_4 at different conditions (from top to bottom: G, GS01, GS11, GS12, GS14, GS21, and GS22)

After pristine graphene has been treated with H_2SO_4, a weak C=O band was appeared around at 1700 cm^{-1}, and its intensity was increased by a small amount at higher concentration and longer reaction time.

The general evaluation for these FT-IR spectra can be made as follows: FT-IR spectra of pristine graphene and modified graphene by different acids show that there is absorption band between 3600 - 3350 cm^{-1} due to stretching vibration of –OH, a deformation peak observed between 1240 cm^{-1} and 1210 cm^{-1} is usually attributed to C–O stretching vibrations. The bands at 2930 cm^{-1} and 2850 cm^{-1} belong to the symmetric and anti-symmetric stretching vibrations of CH_2, while the presence of two absorption peaks observed in the medium frequency area, at 1630 cm^{-1} can be attributed to the stretching vibration of C=C [143].

As first tool that used to detect modifications what happened, results of FT-IR characterizations showed that there is many oxygen containing groups added to graphene after treating by different acids at different concentration, also, the amount of oxidation varied depending on the concentration of acids [144]; these changes in FT-IR showed the graphene structure was successfully modified after acid treatment.

4.1.1.2. FT-IR analysis of base modified graphene

The changes in graphene modified by different bases (EDA, DEA, VIM, and PEI) were detected by FT-IR, results are shown in Figure 4.5 – Figure 4.7.

Figure 4.5 shows the changes in graphene after treatment of 2 M, 2 h by EDA and DEA.
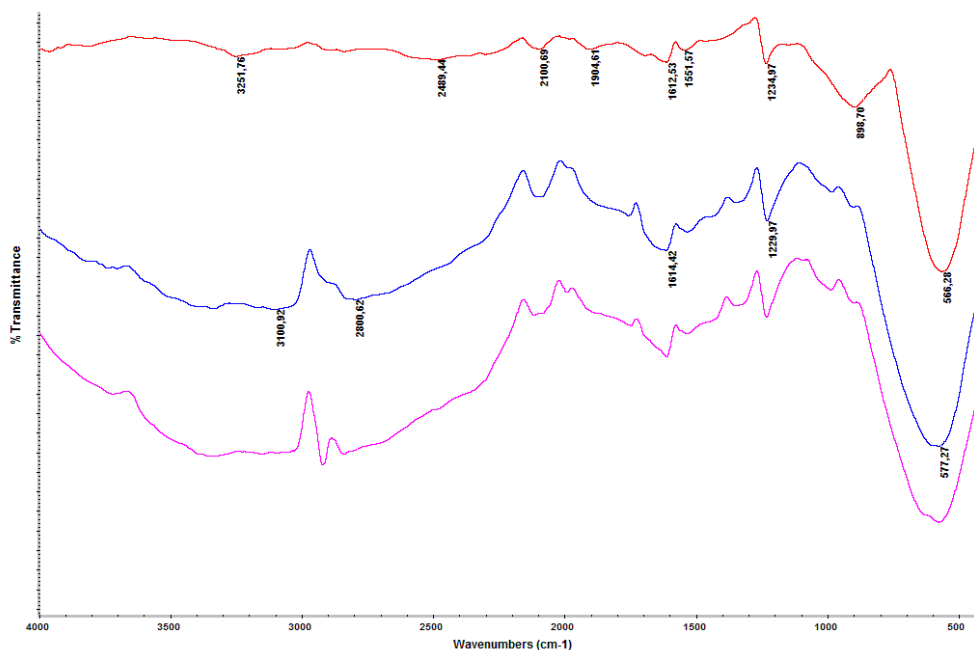
Figure 4.5. FT-IR spectra of graphene modified by EDA and DEA (from top to bottom: G, GEDA22, GDEA22)

FT-IR spectra of GEDA and GDEA showed an absorption around 1615 cm^{-1}, due to the C=C stretching. The band at 1230 cm^{-1} corresponding to the C−N characteristic stretching vibrations. The presence of N−H stretching and bending vibrations at 3340 and 1640 cm^{-1}, −CH_2 stretching bands (2920 and 2830 cm^{-1}) of graphene-DEA and the two stretching bands at 2900 - 2800 cm^{-1} of graphene-EDA demonstrated the successful addition of DEA and EDA to graphene [145].

The FT-IR spectra taken after the reaction of graphene with VIM at different conditions are given in Figure 4.6.
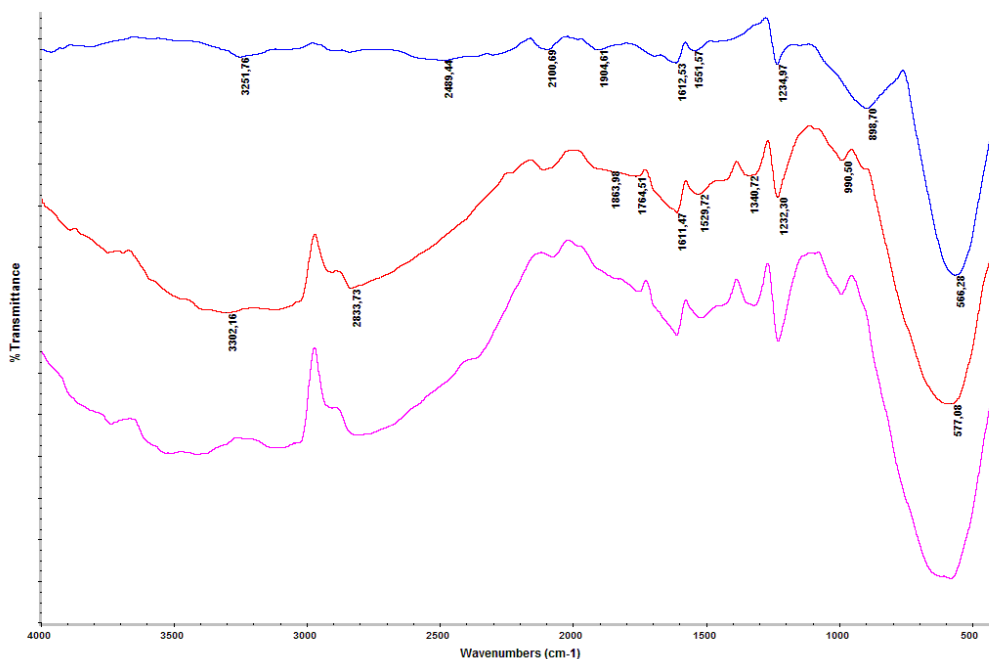
Figure 4.6. FT-IR spectra of graphene modified by VIM at different conditions (from top to bottom : G, GVIM 21, GVIM 22)

In the FT-IR spectra of graphene modified by VIM, new peaks were appeared at around 3300 cm^{-1} corresponding to -NH- groups; absorption at around 1612 due to aryl C=C group the band at 1340 cm^{-1} is associated with the C-N stretching vibration of the imidazole ring [146].

The FT-IR spectra taken after the reaction of graphene with PEI at different conditions are given in Figure 4.7.
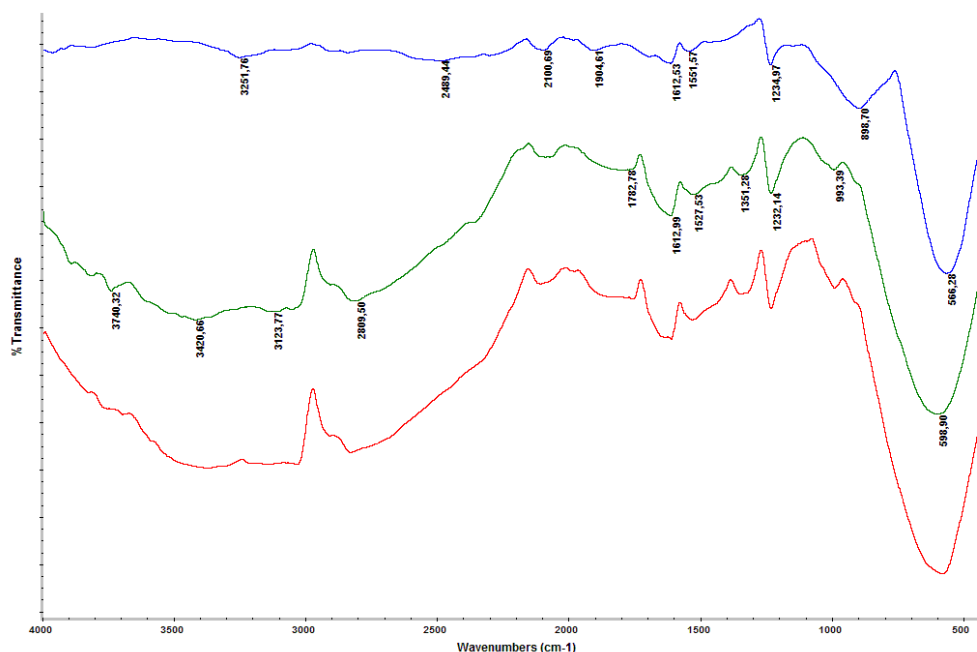
Figure 4.7. FTIR spectra of graphene modified by PEI at different conditions (from top to bottom: G, GPEI 21, GPEI 22)

The small difference in intensity of the strong absorption N−H stretching vibrations ranging from 3200 to 3740 cm^{-1} for graphene-PEI showed that when the reaction run for 2 h compared to the results from 1 h reaction has an important role in the amination of graphene. The small difference in the shape of –OH stretching vibration at 3320 - 3420 cm^{-1} gave the same result similar to that of N-H absorption. Also, strong and broad C-H stretching vibrations at 2809 cm^{-1} and at 2833 cm^{-1} for graphene-PEI and graphene-VIM, respectively, indicated 2 h reaction has more effect on amination. It is possible to make the same interpretations about the strong absorption band of C-N at 1351 cm^{-1} .

As a result, we observed from these FT-IR spectra that the amines participate in the graphene structure, but the changes that the amines cause in the graphene structure are not as effective as the effects of the acids [147].

58

4.1.2. X-Ray Diffraction (XRD) analysis of graphene and modified graphene

XRD analysis is a good tool to estimate the interlayer spacing between the graphitic layers and the crystalline properties, as well as to determine the completion of reaction [148].

4.1.2.1. XRD analysis of graphene

The XRD results of the pristine graphene are given in the Table 4.1.

Table 4.1. XRD results of pristine graphene.

Starting material (Graphene)	XRD information		
	Pos. [°2 Th.] θ	**Height [cts]**	**D-spacing [Å]**
	26.5877	14327.12	3.35270

Several bands were observed in the XRD spectrum of the pristine graphene, however, their intensity is very low, such as 2θ: 44.44 ; 54.6992 ; 77.6046; 83.6980 ; 87.2124°. The highest and sharp peak of the graphene crystal (002) plane was recorded at 2θ : 26.5877° with *d- spacing* 3.3527 Å, which shows the high crystallinity.

4.1.2.2. XRD analysis of acid modified graphene

The changes in the graphene structure after the modification with different acids were observed with XRD, and the results of the modification with HNO_3 are presented in Table 4.2. Generally speaking, no obvious changes in position of diffraction peak for acid modified graphene have been observed [149]. This indicates that the basic formula of graphene has not changed. Details are given below.

Table 4.2. XRD results for graphene modified by HNO_3

Concentration of acid	Stirring time	XRD information		
		Pos. [°2 Th.] Θ	Height [cts]	D-spacing [Å]
0.5 M	1 h	26.5343	9179.26	3.35932
1 M	1 h	26.5417	5091.77	3.35840
1 M	2 h	26.5288	8933.22	3.36000
1 M	4 h	26.5083	9049.48	3.36256
2 M	1 h	26.5558	3341.72	3.35665
2 M	2 h	26.5969	10212.70	3.35156
8 M	1 h	26.5302	33466.03	3.35983
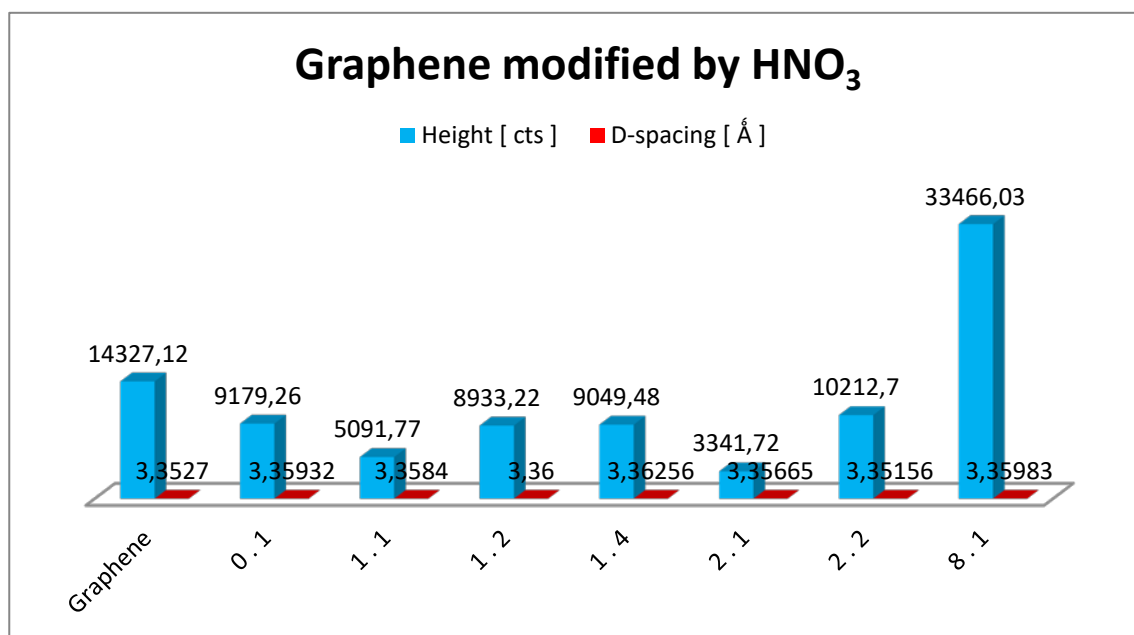
Figure 4.8. 3D column display of XRD results of modified graphene with HNO_3

Table 4.2 and Figure 4.8 show the XRD patterns of graphene modified by HNO_3 for different period of time [149], and concentration of acids. There is no difference in the position of 2θ appeared between 26.5 - 26.6°, and *d- spacing* between 3.35 - 3.36 Å, compared with graphene has $2\theta = 26.6°$ and *d-spacing* of 3.35 Å. Also, when time is established with concentrations (1M.1h and 2M.1h) it was observed that the intensity of 2θ peak was decreased due to the interactions of -OH groups

between the layers of graphene. But in the case of high concentration and the time of stirring (1M.2h, 1M.4h, 2M.2h, and 8M.1h)   the intensity gradually increased due to the occurrence of high oxidation and carboxylic groups bonded to surface area of graphene, especially in 8M, 1h. The other peaks that was mentioned above in appeared in pristine graphene by low intensity it also arise in modification graphene by with a little high concentration than pristine graphene [150].

Table 4.3. XRD results for graphene modified by H_3PO_4

Concentration of acid	Stirring time	XRD information		
		Pos. [°2 Th.] θ	Height [cts]	D-spacing [Å]
0.5 M	1 h	26.5520	7288.27	3.35712
1 M	1 h	26.5095	3506.85	3.36240
1 M	2 h	26.5141	5251.87	3.36184
1 M	4 h	26.5281	8102.79	3.36009
2 M	1 h	26.5089	3941.21	3.36248
2 M	2 h	26.5625	7222.53	3.35582
8 M	1 h	26.5723	30218.49	3.35461
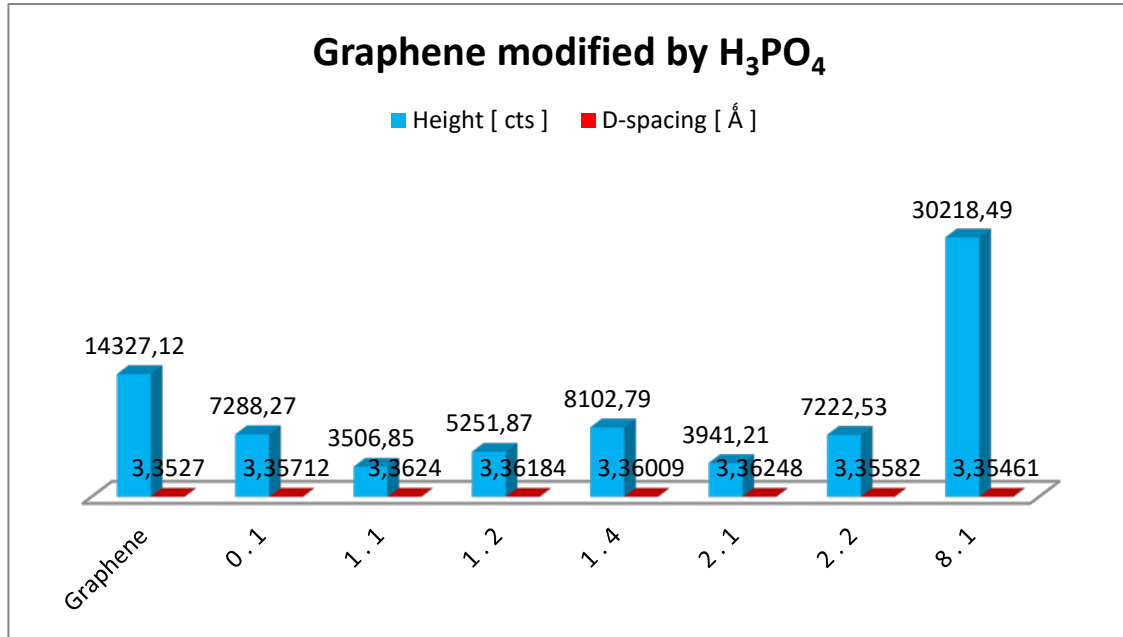
Figure 4.9. 3D column display of XRD results of modified graphene with H_3PO_4

Table 4.3 and Figure 4.9 show the XRD results of modified graphene with H_3PO_4. The diffraction peaks corresponding to graphene modified by H_3PO_4 were observed in the samples sintered at around 26, 44, 54, 83 and 87° respectively. Also, a peak corresponding to main structure of graphene crystal (002) plane was observed around at 26.5-26.6° by *d-spacing* 3.36 Å for all graphene and H_3PO_4 modified graphene. Different scattering is arised from different degree of oxidation based on concentration of acid and time of stirring. The intensity of some H_3PO_4 modified graphene (1M.1h, and 2M.1h) compared to that of pristine graphene was lowest in the same position due to same crystal of graphene with new functional group. But when time of stirring and the concentration were increased (1M.2h, 1M.4h, 2M.2h, and 8M.1h), the intensity of peak gradually increased that indicates oxidation of more in surface area of graphene by functional group having same hybridization like in carbonyl group. The other peaks that was mentioned above appeared in graphene by low intensity it also showed in modification graphene, differential by concentration of acid [151].

Table 4.4. XRD results for graphene modified by $HClO_4$

Concentration of acid	Stirring time	XRD information		
		Pos. [°2 Th.] θ	Height [cts]	D-spacing [Å]
0.5 M	1 h	26.5408	6858.61	3.35852
1 M	1 h	26.5427	5376.10	3.35828
1 M	2 h	26.5363	7749.79	3.35907
1 M	4 h	26.4839	2009.35	3.36560
2 M	1 h	26.5172	5826.87	3.36145
2 M	2 h	26.6050	12899.62	3.35055
8 M	1 h	26.5826	26034.37	3.35333
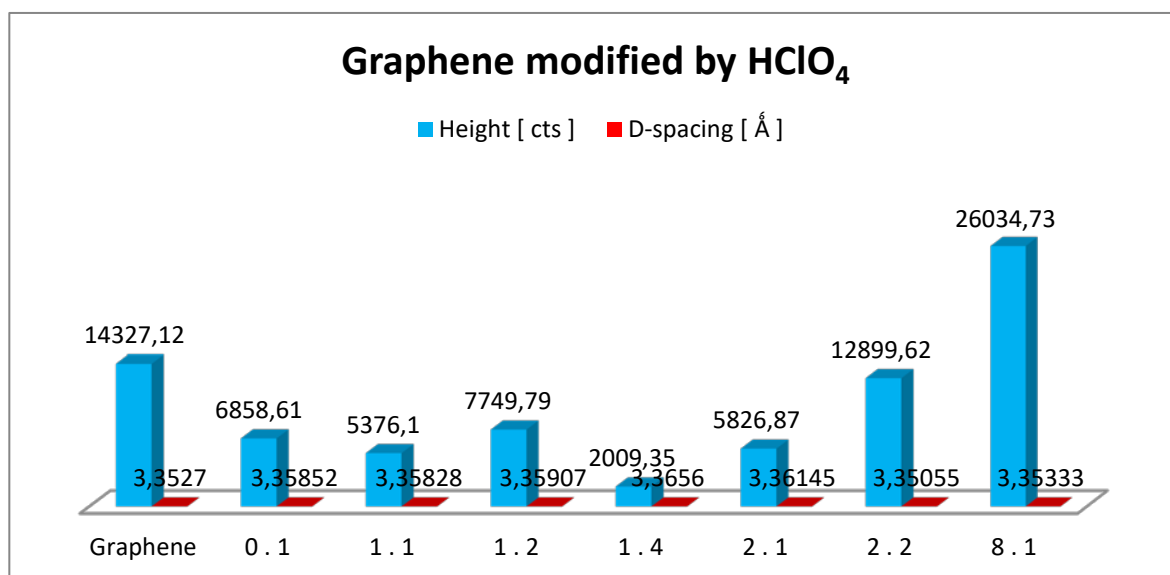
Figure 4.10. 3D column display of XRD results of modified graphene with $HClO_4$

Table 4.4 and Figure 4.10 shows the XRD results of modified graphene with $HClO_4$. It was observed that same things were happened compared to other acid modifications. Also the functional group changed the scattered wavelength due to Bragg's law. The increase in stirring time and concentration produce an increase in oxidation forming more carbonyl group and lead to rise the intensity of main structure around at 26.5° - 26-6°. But this acid specially showed peak with very low intensity for the reaction lasted for 4 hours (1M.4h). This means that more functional group has single bond that pervade molecules and surface

area [151].

Table 4.5. XRD results for graphene modified by H_2SO_4

Concentration of acid	Stirring time	XRD information		
		Pos. [°2 Th.] θ	Height [cts]	D-spacing [Å]
0.5 M	1 h	26.4928	4323.46	3.36449
1 M	1 h	26.5363	4524.41	3.35908
1 M	2 h	26.5467	9388.80	3.35778
1 M	4 h	26.5281	15219.08	3.36010
2 M	1 h	26.5311	3330.90	3.35972
2 M	2 h	26.6097	9384.80	3.34998
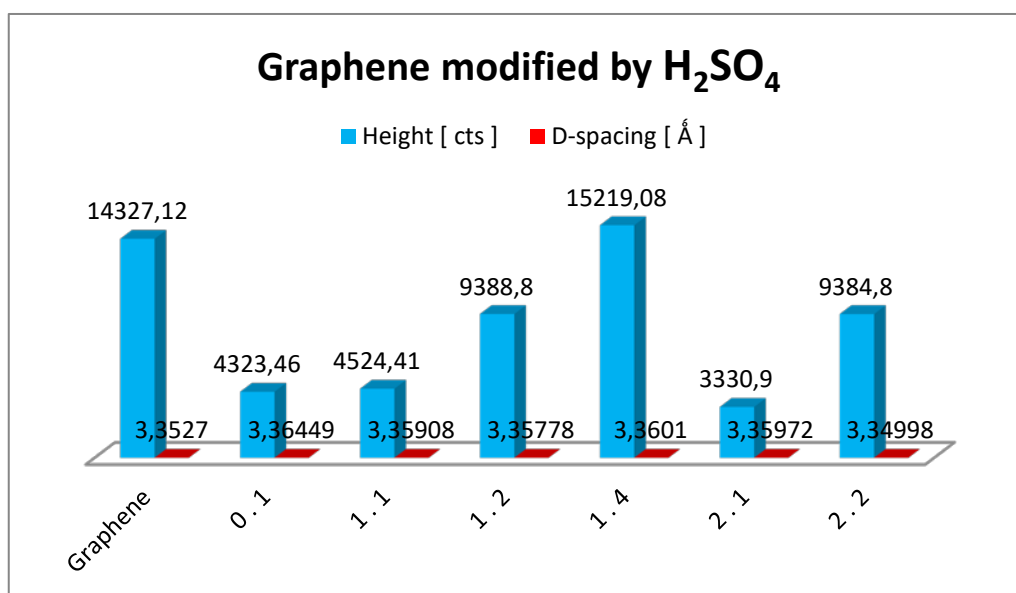
Figure 4.11. 3D column display of XRD results of modified graphene with H_2SO_4

Table 4.5 and Figure 4.11 show the XRD results of modified graphene with H_2SO_4. In use, a beam of X-rays irradiates a sample, causing the incident X-rays to diffract in various specific directions due to the organizational structure and atomic patterning of the substance. The differences in the angle of diffraction that happened in incident beam affects in the height intensities corresponding to different group exist in molecule. Therefore, new groups added to graphene by different concentration and time has an important factor the change in intensity

measured relating to the density of electrons within the crystalline material, from which the positions of the constituent atoms, and chemical bonds between them [152].

4.1.2.3. XRD analysis of base modified graphene

The changes in the graphene structure after the modification with different amines were observed with XRD, and the results for EDA, DEA, VIM and PEI are presented in Table 4.6 – Table 4.8, respectively. All information has been presented in Figure 4.12.

Table 4.6. XRD results for graphene modified by EDA and DEA

Concentration of acid	Stirring time	XRD information		
		Pos. [°2 Th.] Θ	Height [cts]	D-spacing [Å]
2 M	2 h	26.6021	11642.89	3.35092
2 M	2 h	26.5348	4446.72	3.35927

Table 4.7. XRD results for graphene modified by VIM

Concentration of acid	Stirring time	XRD information		
		Pos. [°2 Th.] Θ	Height [cts]	D-spacing [Å]
2 M	1 h	26.5479	7047.97	3.35763
2 M	2 h	26.5360	6984.26	3.353911

Table 4.8. XRD results for graphene modified by PEI

Concentration of acid	Stirring time	XRD information		
		Pos. [°2 Th.] Θ	Height [cts]	D-spacing [Å]
2 M	1 h	26.5501	5635.34	3.35736
2 M	2 h	26.5804	9878.97	3.35360

Graphene modified by bases

■ Height [cts] ■ D-spacing [Å]

	Graphene	2 . 1 PEI	2 . 2 PEI	2 . 1 VIm	2 . 2 VIm	2 . 2 EDA	2 . 2 DEA
Height	14327,12	5635,34	9878,97	7047,97	6984,26	11642,89	4446,72
D-spacing	3,3527	3,35736	3,3536	3,35763	3,353911	3,35092	3,35927
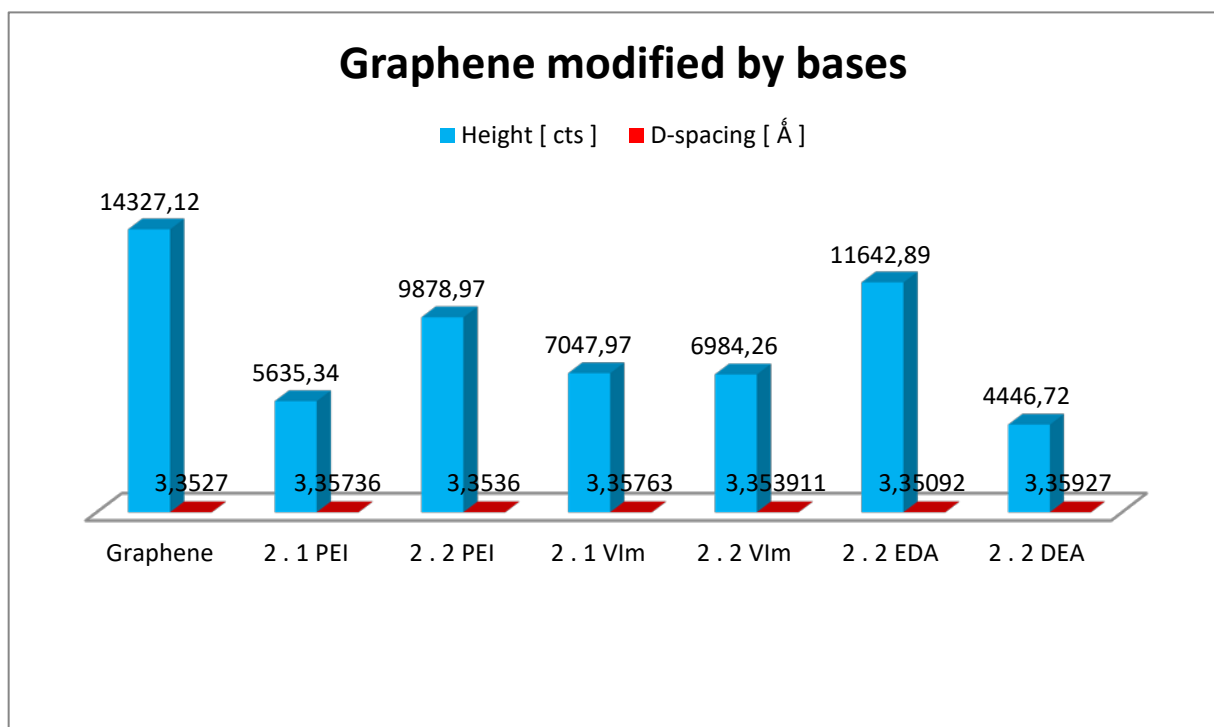
Figure 4.12. 3D column display of XRD results of modified graphene with EDA, DEA, VIM and PEI.

From Figure 4.12 and Table 4.6 – Table 4.8, we observed that the XRD analysis was used to further confirm and compare the crystallinity of pristine structure and composition of base modified graphene. XRD patterns of graphene and base modified graphene show a diffraction peak at around $2\theta = 26.5°$ which corresponds to *d-spacing* of 3.36 Å with (002) crystal plane. Meanwhile, graphene exhibits typical diffraction indicate to keep the same crystal, by different intensity corresponding to interlayer group linked. It has been clearly seen from Figure 4.12 that PEI was attached to graphene by different ratio because of the difference in the stirring time (2M.1h , 2M.2h). Modification with VIM gave close results in 2M.1h and 2M.2h. EDA and DEA provided the same theta position ($2\theta = 26.5°$, 26.6°) with different peak intensities due to different diffraction and scattered beams caused by several functional groups attached to the surface of the graphene with some defects associated with different interactions [153].

As can be seen from the XRD results given above the differences between the height of peak intensity after modified graphene by different acids and amines are the evidence of the entry of different groups to graphene.

The XRD patterns of acid- and amine- modified graphene compared to that of pristine graphene show that the primary structure is not changed after acid- and amine- modification. However, the slight shift to low angle and the decrease of height suggests that the interplanar spacing has expanded because of incorporation of hydroxyl, carboxyl, and amine- containing groups. Also, we saw that the primary structure of graphene is still exist: the changes found in the height of peaks and also in the d-spacing indicate some functional groups was interred between the layers of graphene.

4.1.3. SEM analysis of graphene and modified graphene

In order to facilitate the morphological analysis, SEM images of the pristine graphene and modified graphenes obtained in this study are shown in Figure 4.13 – Figure 4.20. It can be obviously seen that graphene has a flat and smooth surface area, depicting a dark color [154].
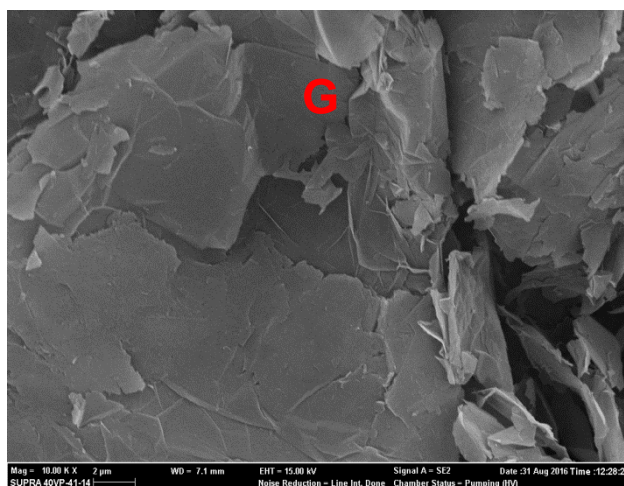
Figure 4.13. SEM analysis of pristine graphene

4.1.3.1. SEM analysis of acid modified graphene

When we compared the SEM images of the acid modified graphene with the pristine graphene, some changes were appeared in the surface.
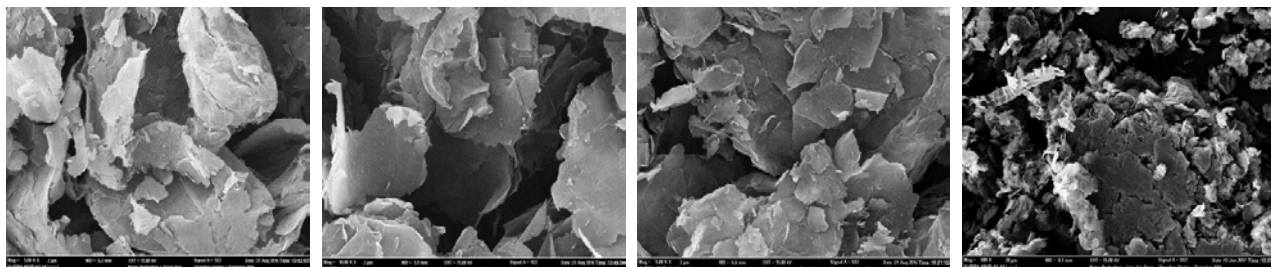
Figure 4.14. SEM images of HNO$_3$ modified graphene

The SEM images of HNO$_3$ modified graphene by different concentrations, given in Figure 4.14, displayed that there are more gaps in GN 11, GN 21, and GN 22, and bright colors compared with pristine graphene due to functionalization of graphene after modification. When we modified graphene by high concentration of HNO$_3$, i.e. GN 81, the shape was crumpled and wrinkled, which may be indicate to oxidation in the surface of graphene.
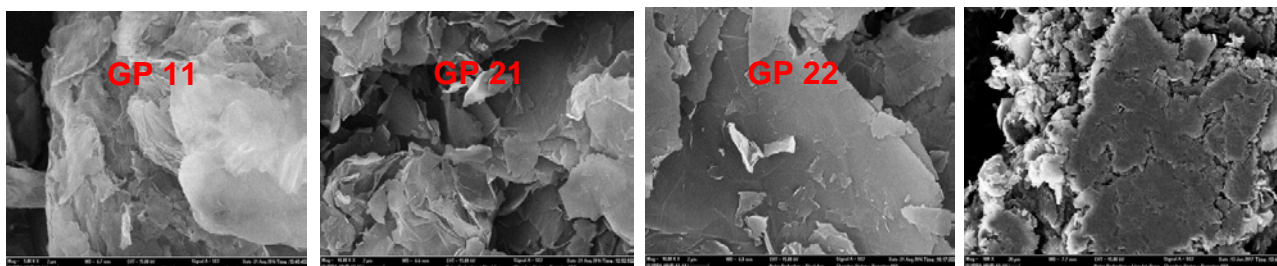
Figure 4.15. SEM images of H$_3$PO$_4$ modified graphene

The SEM image of H$_3$PO$_4$ modified graphene in Figure 4.15 shows the remarkable aggregated particles in various sizes due to the incorporation of oxygenated groups.
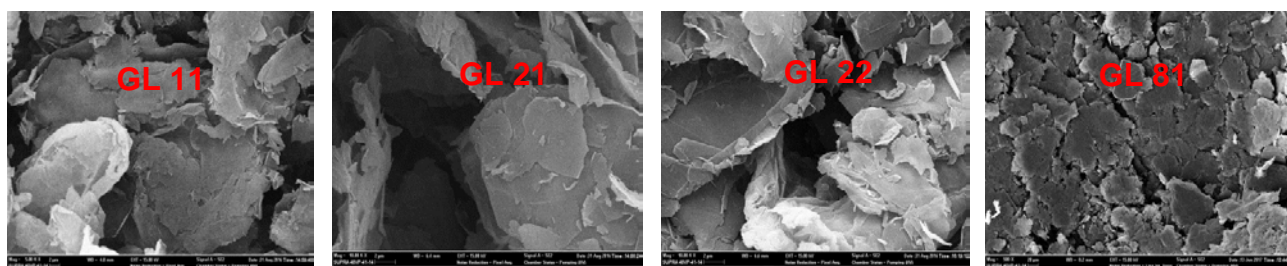
Figure 4.16. SEM images of HClO₄ modified graphene

Figure 4.16 shows morphological change happened after modification of graphene by HClO₄ in different concentrations and times. The SEM image showed roughness of the fractured surface due from successful reaction compared to the surface of pristine graphene.
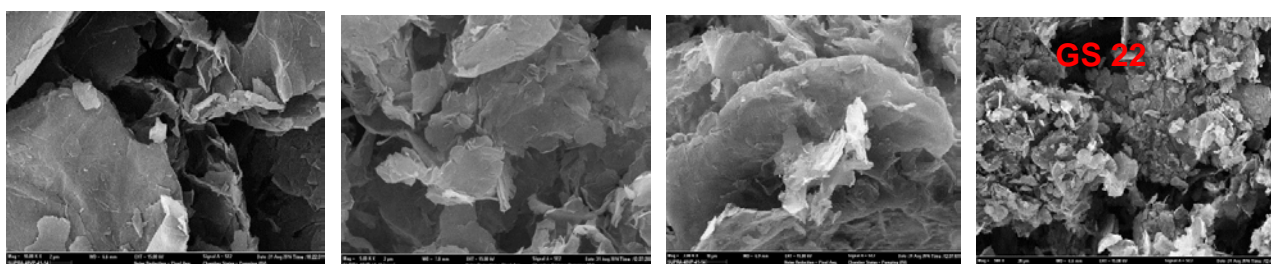
Figure 4.17. SEM images of H₂SO₄ modified graphene

The surface of graphene was more cracked after modification with H₂SO₄, Figure 4.17. Comparing the SEM micrographs of the pristine graphene given in Figure 4.13 and H₂SO₄ modified graphene presented above, it was seen that the graphene modified by H₂SO₄, by different time and concentration, exhibited a flower-like morphology which is differ from the pristine graphene with flake-like morphology [155].

4.1.3.2. SEM analysis of base modified graphene

Figure 4.18 – 4.20 illustrate the change in appearance of graphene compared with amine modified graphene.
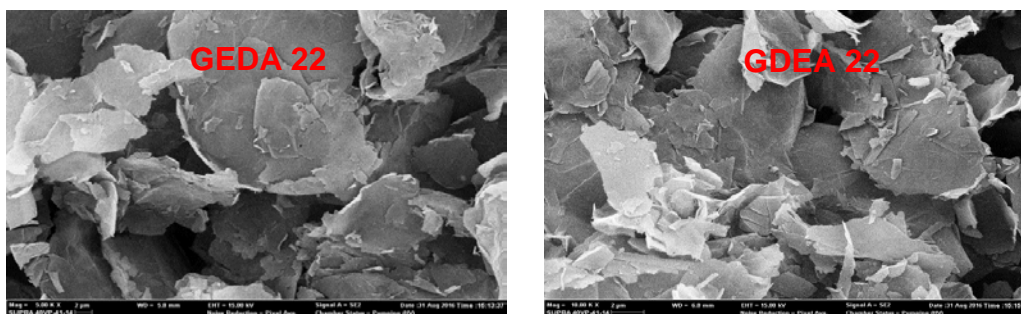
Figure 4.18. SEM images of EDA and DEA modified graphene

SEM images of EDA and DEA modified graphene given in Figure 4.18 demonstrate that the amines were in adhesive character in the surface of graphene that was clearly appeared from the lamella surface.
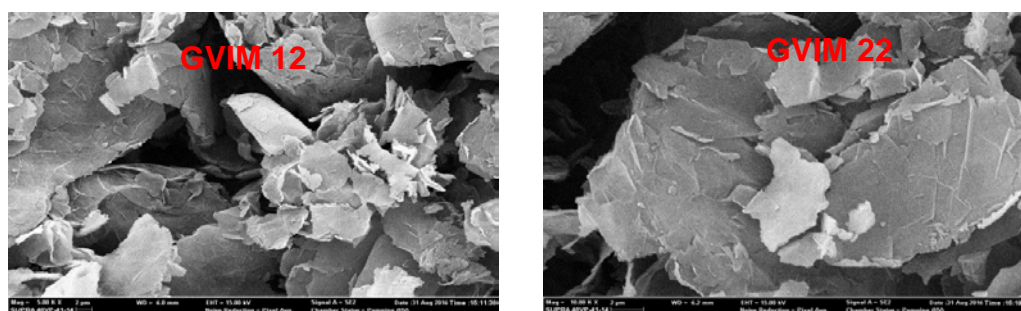
Figure 4.19. SEM images of VIM modified graphene

SEM images of VIM modified graphene given in Figure 4.19 illustrate that the crumpled and wrinkled surface was appeared depend on VIM linked to graphene backbone.
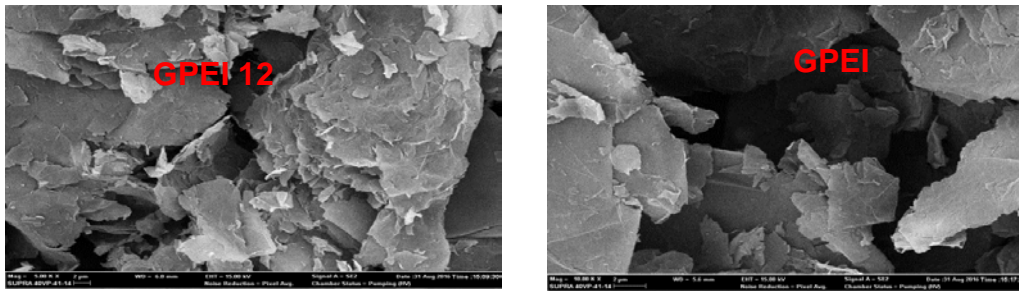
Figure 4.20. SEM images of PEI modified graphene

Clearly different feature with more gaps and coarse structure from other amine-modified graphene was observed in the SEM image of PEI-modified graphene shown in Figure 4.20.

As mentioned above, SEM determines image contrast via topology and relative conductivity, among other factors. Therefore, we can deduce that the brighter, lighter areas in the images represent areas dominated by acids and bases, and the darker, more conductive areas represent areas consisting mainly of graphene [156].

4.1.4. Results of Elemental mapping analysis of graphene and modified graphene

High resolution images from a Scanning Electron Microscope (SEM) and elemental spectral data gained using Energy Dispersive X-ray Spectroscopy (EDX) can be combined to allow for an extremely detailed analysis of materials and multi-phase samples [157]. The basic physics of Energy Dispersive X-ray Spectroscopy is based on the detection of characteristic X-rays emitted of an element as a result of the de-excitation of core electron holes created by a high energy electron beam. An electron from a higher binding energy electron level falls into the core hole and an X-ray with the energy of the difference of the electron level binding energies is emitted. Due to the quantization of electron energy levels, the emitted characteristic X-ray energies for elements will generally be different from element to element with only a few spectral peaks overlapping. If the identification of one peak is ambiguous, other peaks or limited knowledge of

the sample history will often allow a reasonable elemental identification of the peak [158].

The elemental mapping analysis results for graphene and modified graphene were presented in tables (4.9 – 4.13) and figures (4.21 - 4.38). The results show that all elements are homogeneously distributed throughout the graphene [159].

4.1.4.1. Elemental Mapping results of pristine graphene

C and O contents (%) of the graphene were measured by elemental analysis. The qualitative elemental compositions of the graphene were confirmed by X- ray microanalysis coupled with energy dispersive spectrometer (EDS). The results in Table 4.8 and Figure 4.21 were obtained as percentage of elements in the pristine graphene structure.
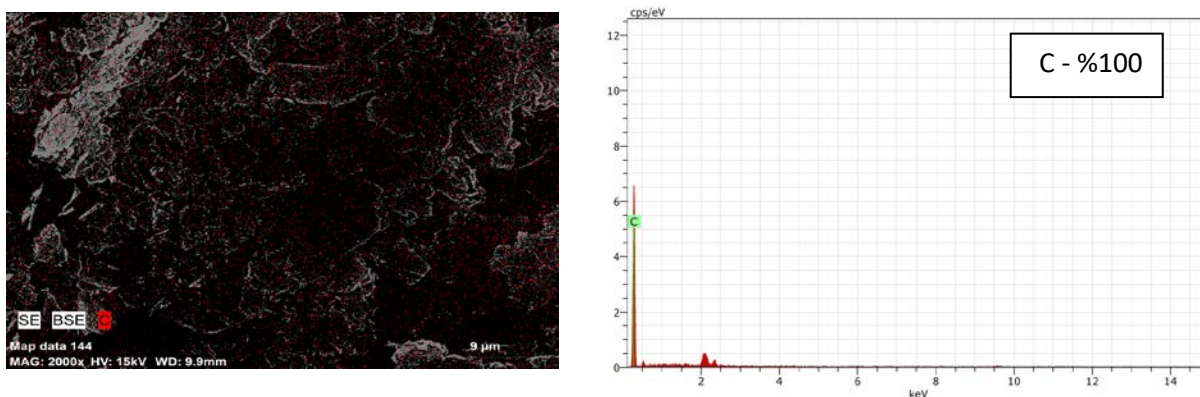
Figure. 4.21. The elemental mapping image taken with EDS for pristine graphene

4.1.4.2. Elemental Mapping results for acid modified graphene

Table 4.8 shows the percentage of the elements that are contained in pristine graphene and also in modified graphene with HNO_3 in different conditions.

Table 4.9. The percentage of the elements in pristine graphene and in modified graphene with HNO_3.

Sample	C%	O%	N%
G	100	0	0
GN01	89.88	8.54	1.58
GN11	86.48	8.77	4.75
GN14	87.68	8.84	3.48
GN21	86.36	9.62	4.02
GN22	85.07	10.57	4.36
GN81	83.19	12.46	4.35

Table 4.9 and figures (4.21 - 4.27) illustrate the percentage of the elements (C, O, N) in pristine graphene and in modified graphene by HNO_3 in different conditions. From these data, the C content of graphene was decreased in high concentration of acid within long times comparing with pristine graphene, while the percentage of new elements (like O from OH, and other oxygenated groups, and N from HNO_3) depending on modification was increased.
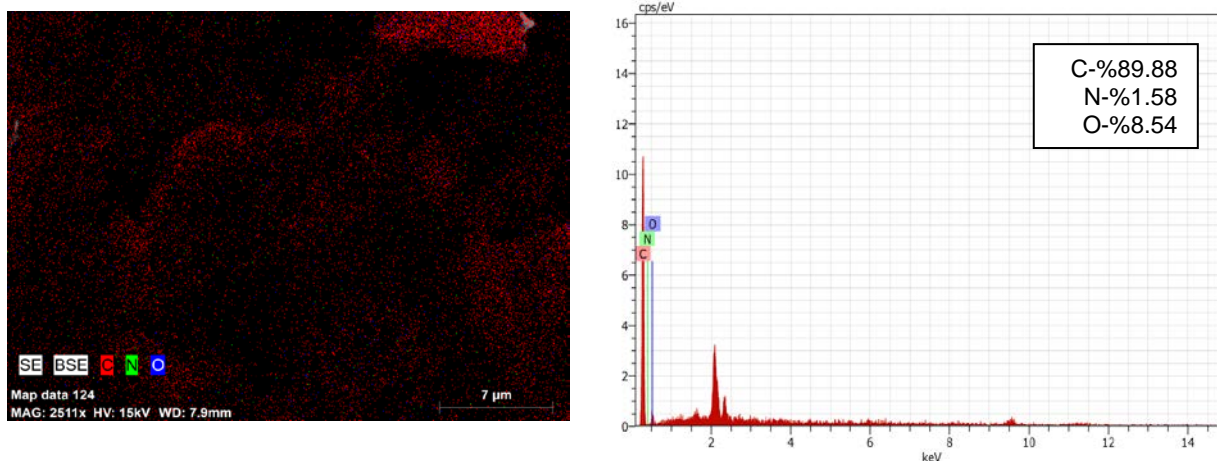
Figure 4.22. The elemental mapping image taken with EDS for graphene modified by HNO_3 (0.5 M, 1 h)
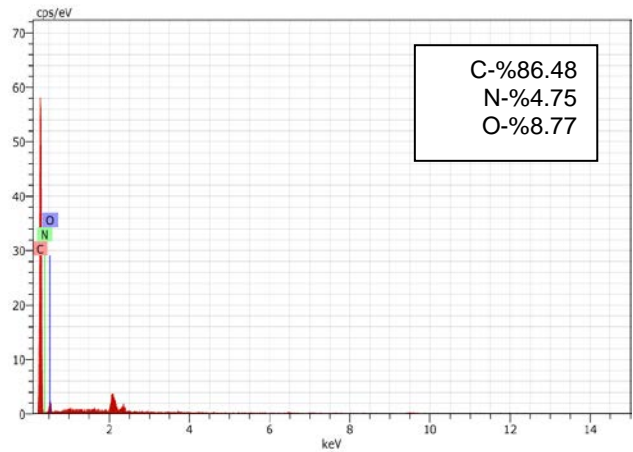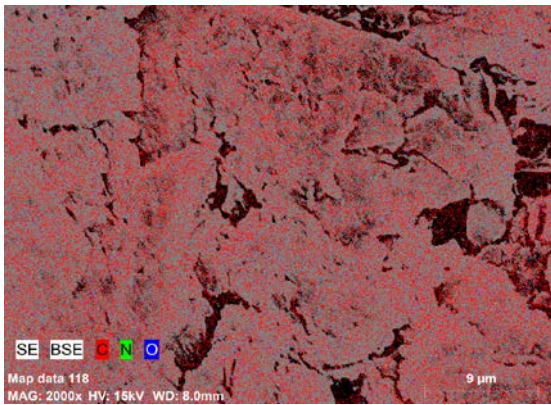
Figure 4.23. The elemental mapping image taken with EDS for graphene modified by HNO_3 (1 M, 1 h)
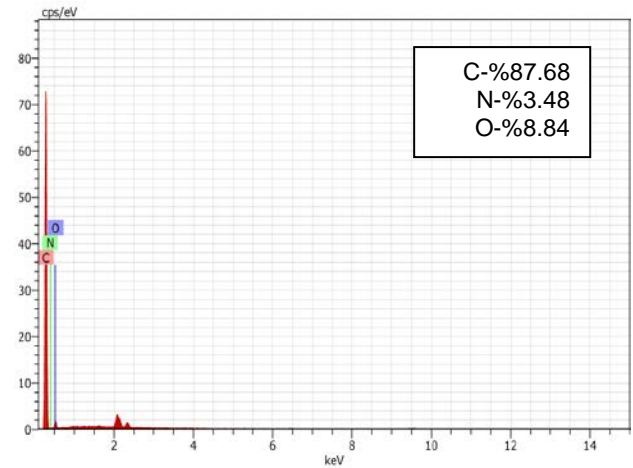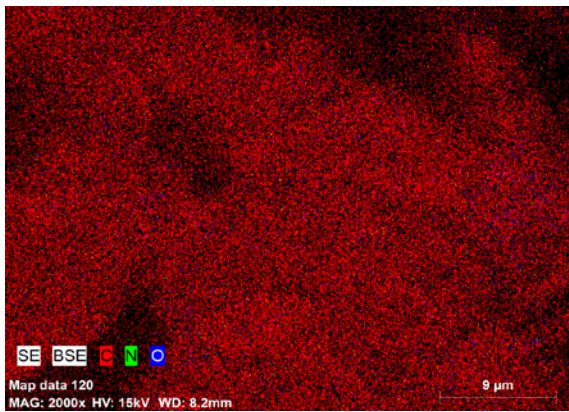
Figure 4.24. The elemental mapping image taken with EDS for graphene modified by HNO_3 (1 M, 4 h)
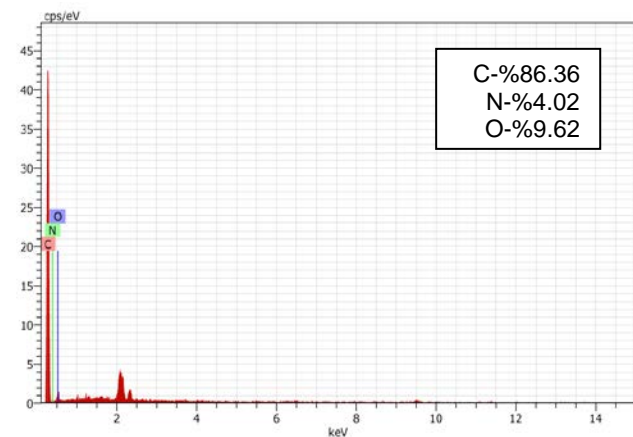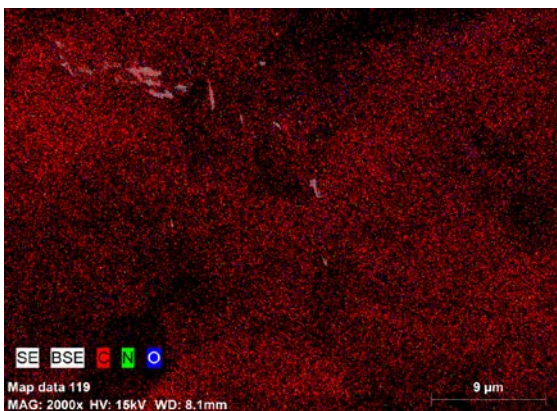
Figure 4.25. The elemental mapping image taken with EDS for graphene modified by HNO_3 (2 M, 1 h)
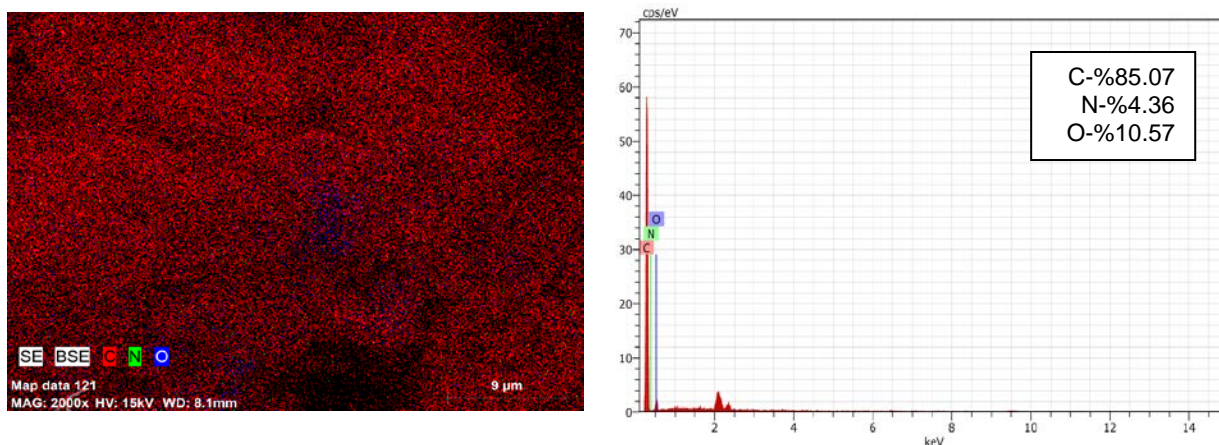
Figure 4.26. The elemental mapping image taken with EDS for graphene modified by HNO_3 (2 M, 2 h)
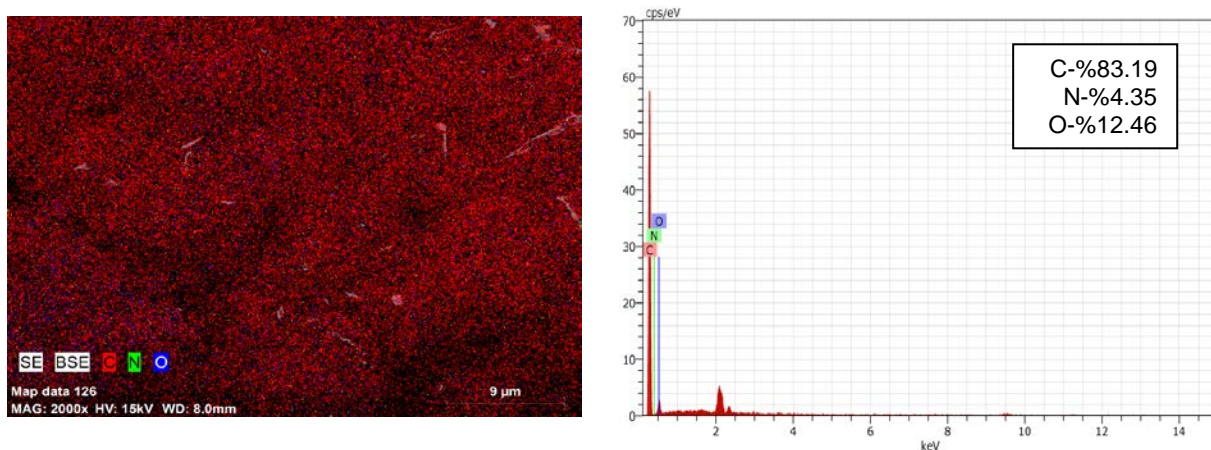
Figure 4.27. The elemental mapping image taken with EDS for graphene modified by HNO_3 (8 M, 1 h)

Table 4.10 lists the percentage of the elements that contained in pristine graphene and also in modified graphene by H_3PO_4 in different conditions.

Table 4.10. The percentage of the elements in pristine graphene and in modified graphene by H_3PO_4

Sample	C%	O%	P%
G	100	0	0
GP21	89.65	8.26	2.09
GP22	88.92	6.87	4.21
GP81	89.08	9.06	1.86

Table 4.10 and figures (4.28 - 4.30) illustrate the percentage of the elements (C, O, P) in pristine graphene and in modified graphene by H_3PO_4 in different conditions. From these data, the C content of graphene was decreased in high concentration of acid within long times comparing with pristine graphene, while the percentage of new elements (like O from OH, and other oxygenated groups, and P from H_3PO_4) depending on modification was increased.
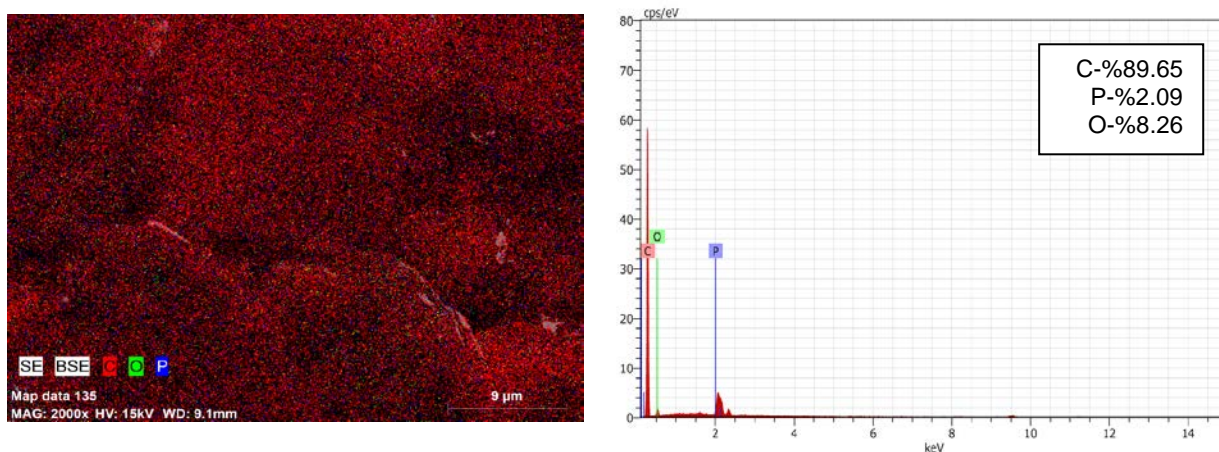
Figure 4.28. The elemental mapping image taken with EDS for graphene modified by H_3PO_4 (2 M, 1 h)
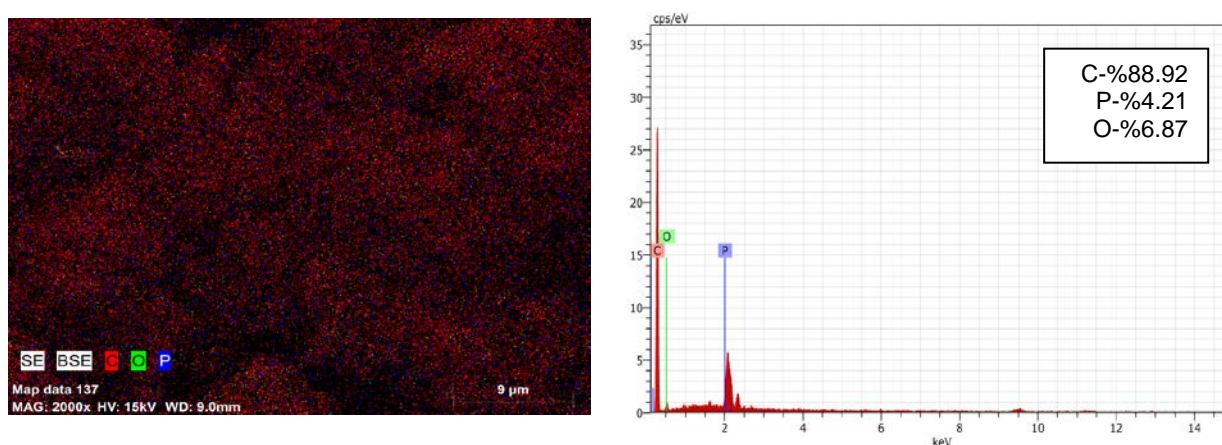
Figure 4.29. The elemental mapping image taken with EDS for graphene modified by H_3PO_4 (2 M, 2 h)

C-%89.08
P-%1.86
O-%9.06
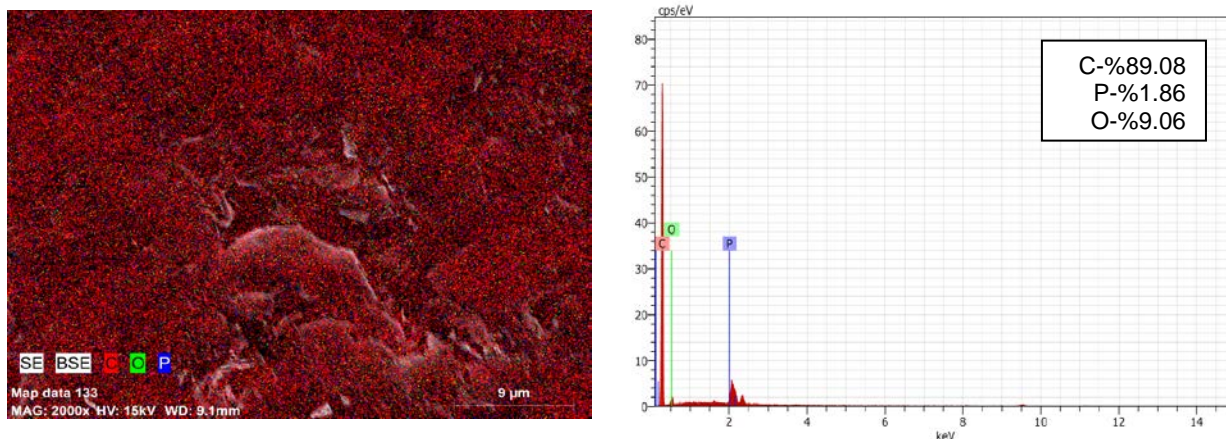
Figure 4.30. The elemental mapping image taken with EDS for graphene modified by H_3PO_4 (8 M, 1 h)

Table 4.11 lists the percentage of the elements that contained in pristine graphene and also in modified graphene by $HClO_4$ in different conditions.

Table 4.11. The percentage of the elements in pristine graphene and in modified graphene by $HClO_4$

Sample	C %	O %	Cl %
G	100	0	0
GL21	91.23	8.76	0.01
GL22	89.74	10.18	0.08
GL81	91.24	8.76	0.00

Table 4.11 and figures (4.31- 4.33) illustrate the percentage of the elements (C, O, Cl) in pristine graphene and in modified graphene by $HClO_4$ in different conditions. From these data, the C content of graphene was decreased in high concentration of acid within long times comparing with pristine graphene, while the percentage of new elements (like O from OH, and other oxygenated groups, and Cl from $HClO_4$) depending on modification was increased. Remarkably, the percentage of other atoms except C and O is lower in the case of $HClO_4$ than the others. According to

this result, we can say that the effect of HClO₄ on graphene is lower than the other acids.
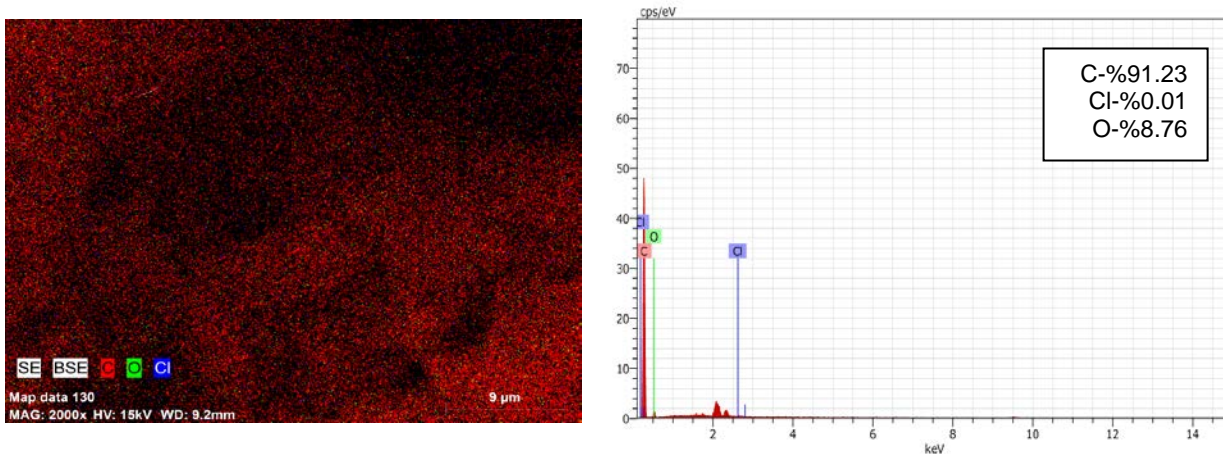
Figure 4.31. The elemental mapping image taken with EDS for graphene modified by HClO₄ (2 M, 1 h)
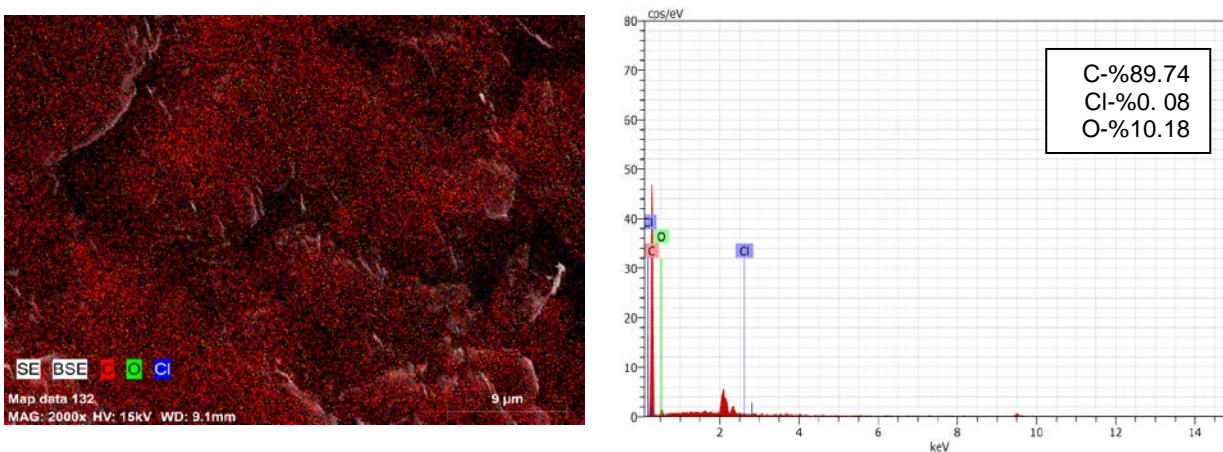
Figure 4.32. The elemental mapping image taken with EDS for graphene modified by HClO₄ (2 M, 2 h)
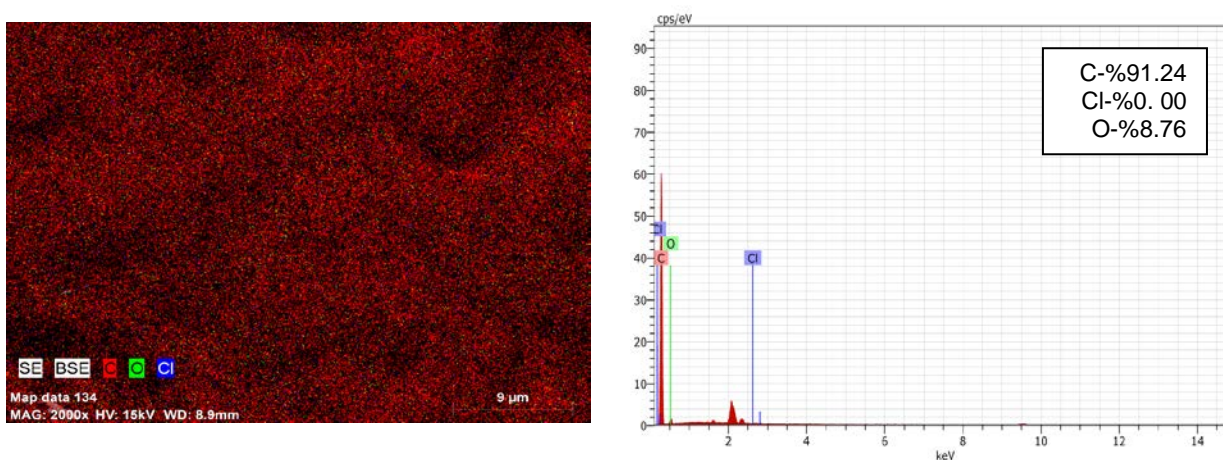
Figure 4.33. The elemental mapping image taken with EDS for graphene modified by HClO₄ (8 M, 1 h)

Table 4.12 lists the percentage of the elements that contained in pristine graphene and also in modified graphene by H_2SO_4 in different conditions.

Table 4.12. The percentage of the elements in pristine graphene and in modified graphene by H_2SO_4

Sample	C%	O%	S%
G	100	0	0
GS11	91.48	6.11	2.40
GS21	90.39	8.45	1.16
GS22	90.41	8.46	1.13

Table 4.12 and figures (4.34 - 4.36) illustrate the percentage of the elements (C, O, S) in pristine graphene and in modified graphene by H_2SO_4 in different conditions. From these data, the C content of graphene was decreased in high concentration of acid within long times comparing with pristine graphene, while the percentage of new elements (like O from OH, and other oxygenated groups, and S from H_2SO_4) depending on modification was increased.
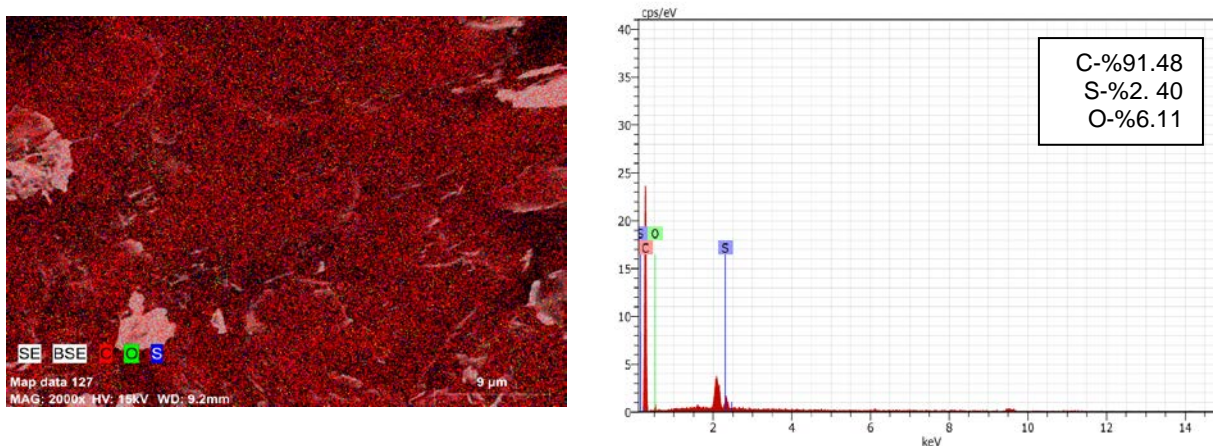
Figure 4.34. The elemental mapping image taken with EDS for graphene modified by H_2SO_4 (1 M, 1 h)
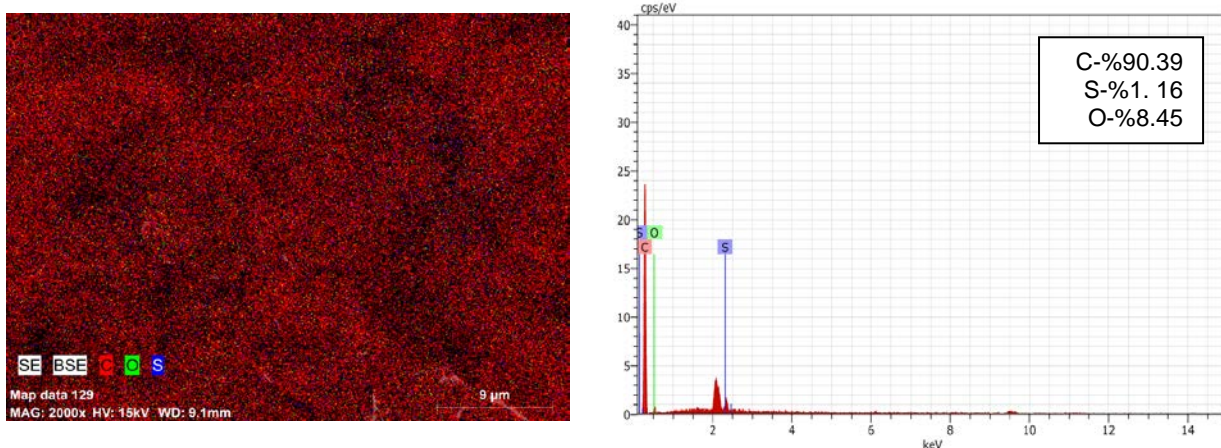
Figure 4.35. The elemental mapping image taken with EDS for graphene modified by H_2SO_4 (2 M, 1 h)
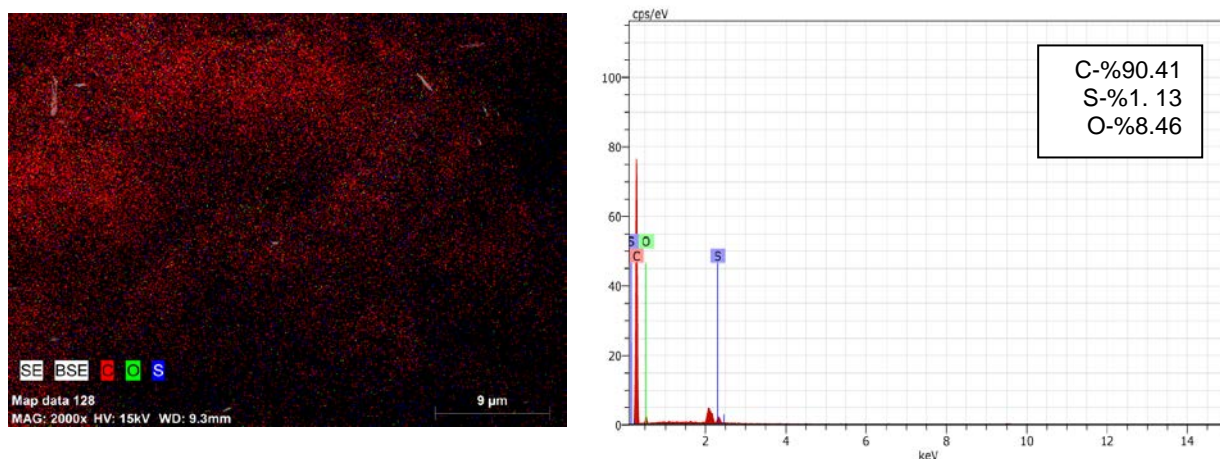
Figure 4.36. The elemental mapping image taken with EDS for graphene modified by H_2SO_4 (2 M, 2 h)

4.1.4.3. Elemental Mapping results for base modified graphene

The elemental mapping results confirm the uniform distribution of the elements (C, O and N) throughout graphene by different amines.

Table 4.13 lists the percentage of the elements that contained in pristine graphene and also in modified graphene by amines in different conditions.

Table 4.13. The percentage of the elements in pristine graphene and modified graphene by bases

Sample	C %	O %	N %
G	100	0	0
GVIM	88.38	7.08	4.54
GPEI	85.56	9.50	4.94

Table 4.13 and Figures 4.37 and 4.38 illustrate the percentage of the elements (C, O, N) in pristine graphene and in modified graphene by N-vinylimidazole and polyethylenimine respectively. From these data, the C content of graphene was decreased after modification with amines comparing with pristine graphene, while the percentage of N was increased.
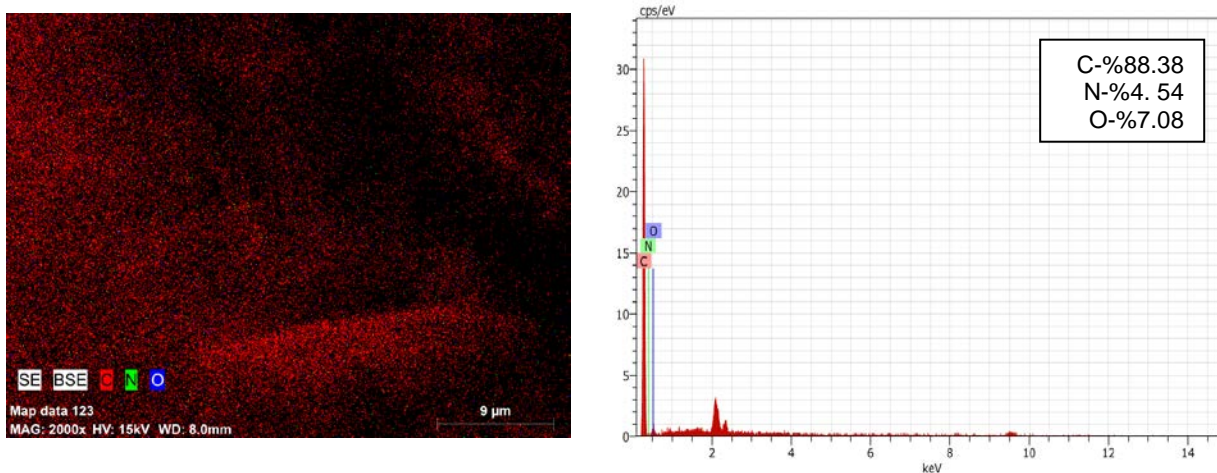
Figure 4.37. The elemental mapping image taken with EDS for graphene modified by VIM
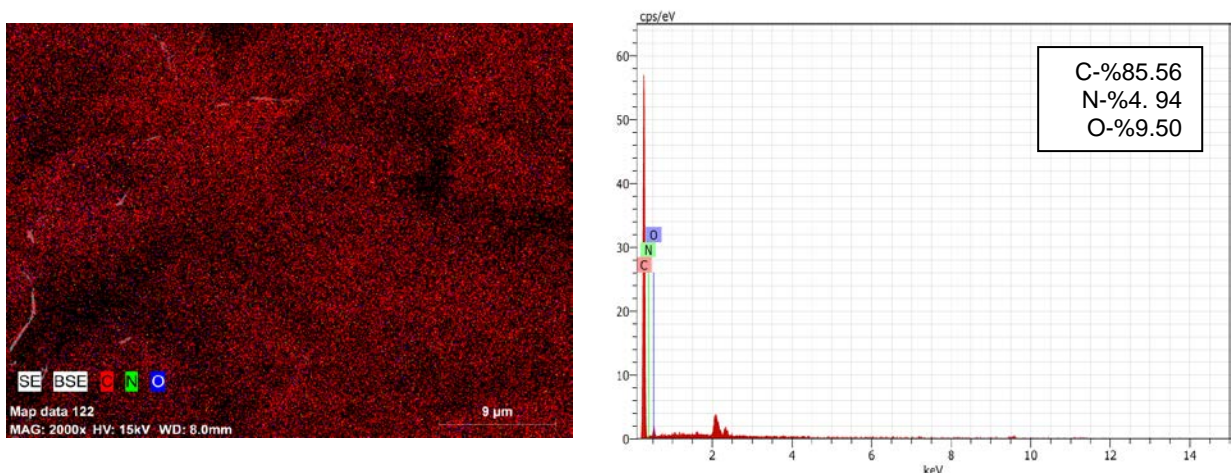
Figure 4.38. The elemental mapping image taken with EDS for graphene modified by PEI

Elemental Mapping analysis results obtained for pristine graphene and also modified graphene with acids or bases confirm the presence of O and N or P or S or Cl atoms other than C atoms, so we can say that oxidation and amination of graphene structures were successfully realized.

4.1.5. Transmission electron microscopy (TEM) analysis of graphene and HNO$_3$ modified graphene

Figures 4.39 and 4.40 illustrate the morphology of graphene and HNO$_3$ modified graphene structures.
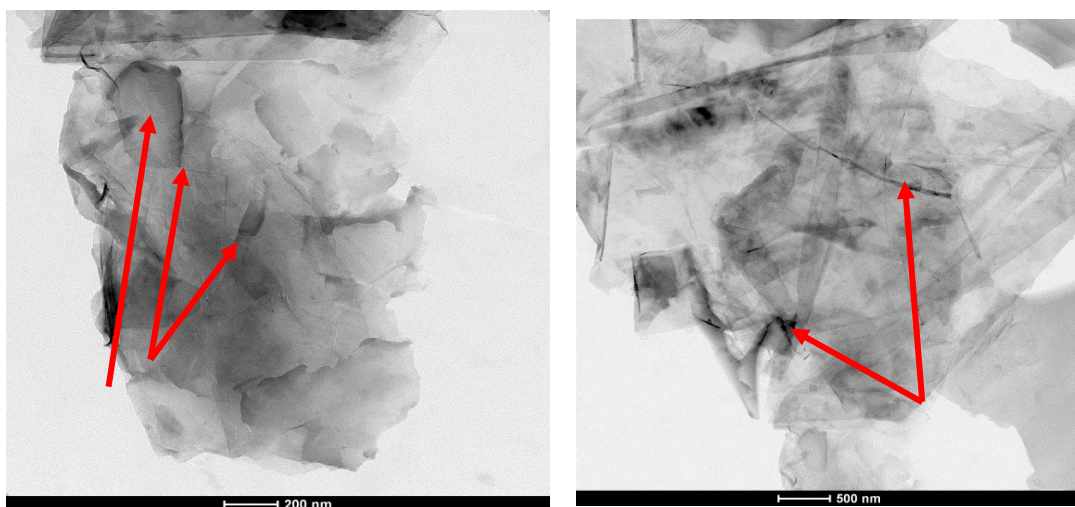
Figure 4.39. TEM image for pristine graphene

From the TEM images of pristine graphene, we can clearly see that the graphene resembles transparent and rippled silk waves and some graphene are inclined to overlap owing to their hydrophobic nature and the van der Waals interaction [160].
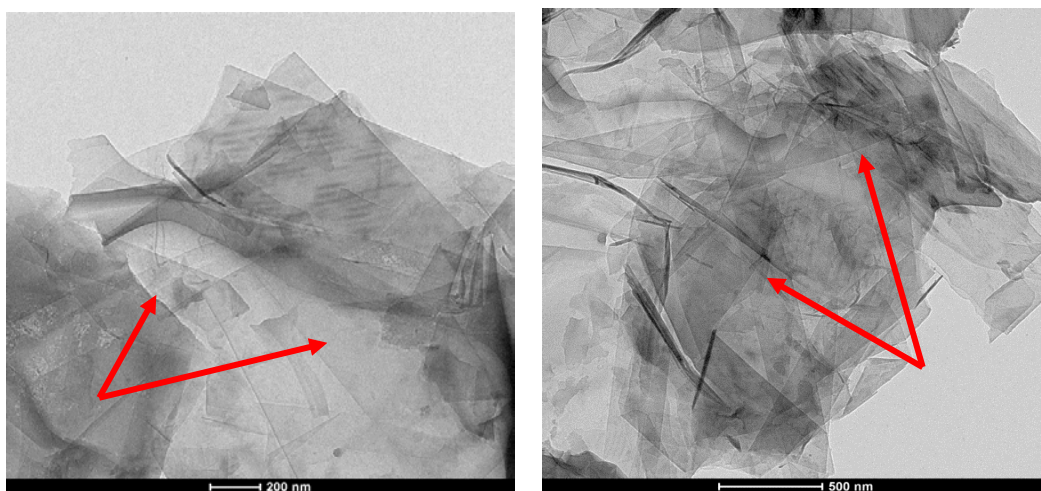
Figure 4.40. TEM image for HNO_3 modified graphene

After HNO_3 is grafted onto the graphene, we find the surfaces become rough with some particles immobilized on it as shown in Figure 4.40, quite different from the transparent and smooth surface features of graphene nanosheets, which implies the successful attachment of hydroxyl groups to graphene [161].

4.1.6. Raman spectroscopic analysis results for graphene and modified graphene

Since Raman spectroscopy is an important tool to deduce the structure in particularly defects and disorder nature of graphene-based materials, we took Raman spectra of some samples of graphene modified by acids and base and compared with that of pristine graphene. These spectra are presented in Figure 4.41 – Figure 4.46. Experimentally the 2D band can be used to determine the number of graphene layers [162].
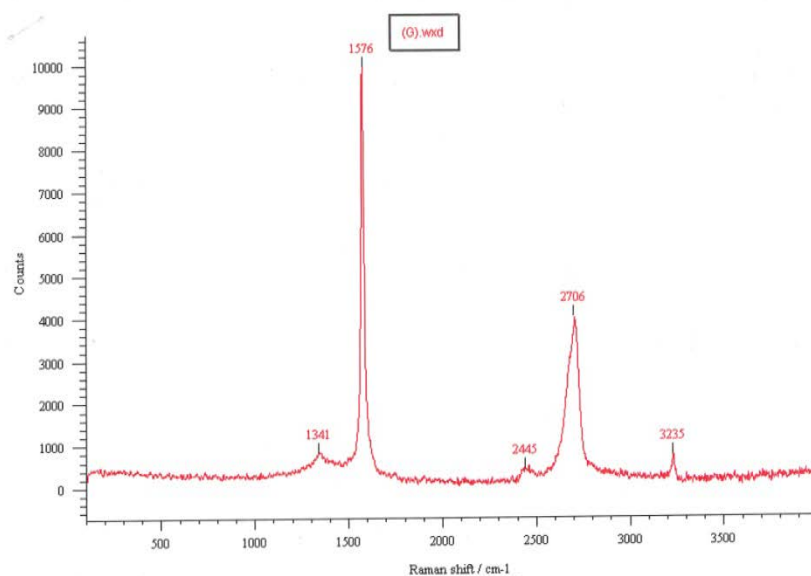
Figure 4.41. Raman spectrum of pristine graphene

The Raman spectrum of pristine graphene exhibits two remarkable peaks at around 1341 cm^{-1} and 1576 cm^{-1} corresponding to the well-defined D band and G band, respectively. The graphene peak (G band) at 1576 cm^{-1} is due to the vibrational mode of the C-C bond (refer to sp^2 vibrations) stretching and the disorder peak (D-band) at 1341 cm^{-1} by very low intensity that is due to the vibrational mode for sp^3 bond. The intensity ratio of the D and G bands (I_D/I_G ratio) helps to estimate the defects of graphene-based samples where a higher ratio ensures more defects on graphene [163].

Table 4.14. Raman analysis results for graphene and acid modified graphene

Sample	D Position (cm^{-1})	G Position (cm^{-1})	2D Position (cm^{-1})	I_D/I_G	I_{2D}/I_G
G	1341	1576	2706	0.08	0.40
GN14	1358	1581	2717	0.12	0.46
GN21	1352	1583	2714	0.21	0.45
GP21	1353	1578	2703	0.32	0.50
GL21	1350	1581	2711	0.15	0.42
GS21	1349	1580	2709	0.21	0.39

4.1.6.1. Raman spectral analysis of graphene and acid modified graphene

Table 4.14 shows the net difference in D and G band of acid modified graphene through Raman spectroscopy. The change in I_D/I_G ratio indicates some defects in graphene structure due from some functional group inserted to graphene.   Figure 4.42 – Figure 4.46 clarify this datum.
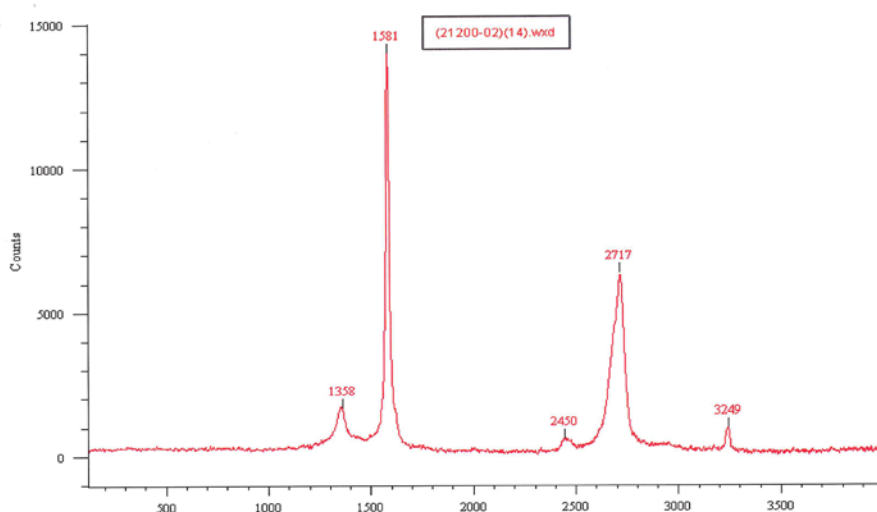
Figure 4.42. Raman spectrum of HNO_3 modified graphene (1M, 4 h)

Figure 4.42 shows the Raman spectrum of graphene modified with HNO_3 (1M, 4h). The D band seen for pristine graphene at 1341 cm^{-1} clearly shifts to 1358 cm^{-1} and G band at 2706 cm^{-1} shifts to 2717 cm^{-1}, due to the interaction between acid group and graphene. See more information in Table 4.14.
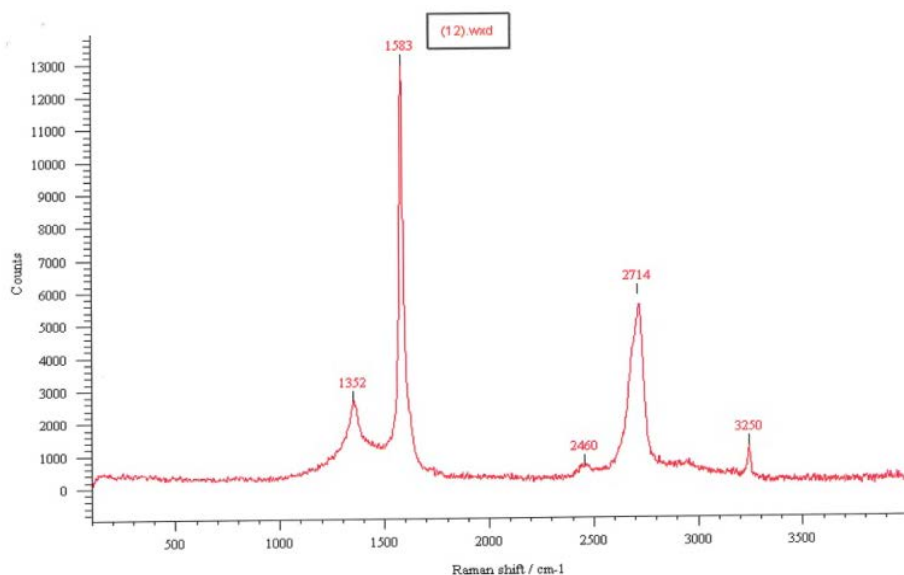
Figure 4.43. Raman spectrum of HNO₃ modified graphene (2M, 1h)

In Figure 4.43, two prominent peaks in HNO₃ modified graphene (2M,1h) are visible, corresponding to the so-called D and G bands at 1352 cm^{-1} and 1583 cm^{-1}, respectively. The D band arises from the activation in the first order scattering process of sp^3 carbons in modified graphene sheets, and the intensity ratio of D and G bands expresses the sp^2/sp^3 carbon ratio, a measure of the extent of disorder. See the information in Table 4.14
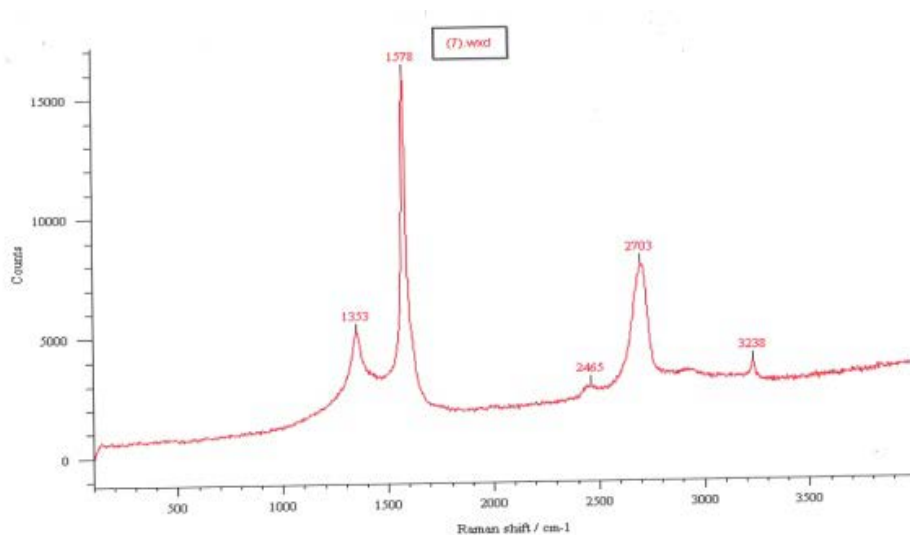
Figure 4.44. Raman spectrum of H₃PO₄ modified graphene (2M, 1h)

86

Figure 4.44 shows the Raman spectrum for graphene modified with H_3PO_4 (2 M, 1h). The samples after oxidation show D and G bands in 1353, 1578 cm^{-1}, respectively. The D-band is quite intense in H_3PO_4 modified graphene compared with pristine graphene. (All information is available in Table 4.14.)
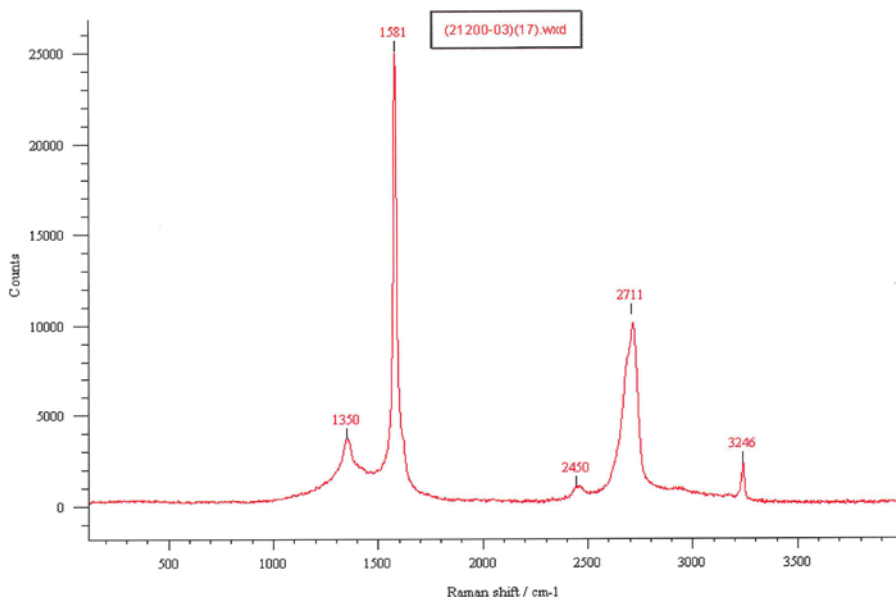
Figure 4.45. Raman spectrum of $HClO_4$ modified graphene (2M, 1h)

Figure 4.45 indicates the change happened when graphene was modified with $HClO_4$ (2M,1h) which were identify through D and G bands observed in 1350, 1581 cm^{-1} ; the I_D/I_G ratio also prove that there is new group bonded with graphene (see Table 4.14).
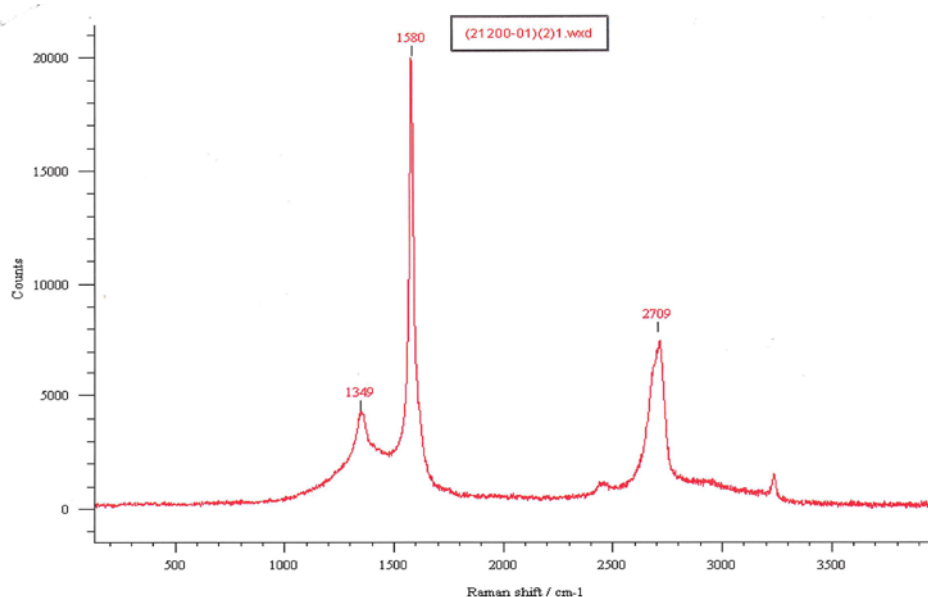
Figure 4.46. Raman spectrum of H_2SO_4 modified graphene (2M, 1h)

Figure 4.46 explains the shifts in D band at 1349 cm^{-1} and in G band at 1580 cm^{-1} and intensities of these bands attributed to addition of some functional groups with H_2SO_4 (2M,1h) to graphene crystal.

Finally, it was shown that there are changes in D, G, 2D positions when the Raman spectra analysis results of graphene modified by acid were evaluated, and there is slightly defect in structure caused from new bonds formed in graphene.

4.1.6.2. Raman spectral analysis of base modified graphene

From the information tabulated in Table 4.15, we can see that there are some peak changes and also shifts observed at D, G, and 2D positions for base modified graphene; these are given in Figure 4.47 – Figure 4.50.

Table 4.15. Raman analysis results for graphene and base modified graphene

Sample	D Position (cm^{-1})	G Position (cm^{-1})	2D Position (cm^{-1})	I_D/I_G	I_{2D}/I_G
G	1341	1576	2706	0.08	0.40
GPEI	1351	1580	2707	0.37	0.35
GVIM	1346	1575	2699	0.05	0.33
GDEA	1336	1574	2700	0.09	0.39
GEDA	1359	1569	2688	0.06	0.33
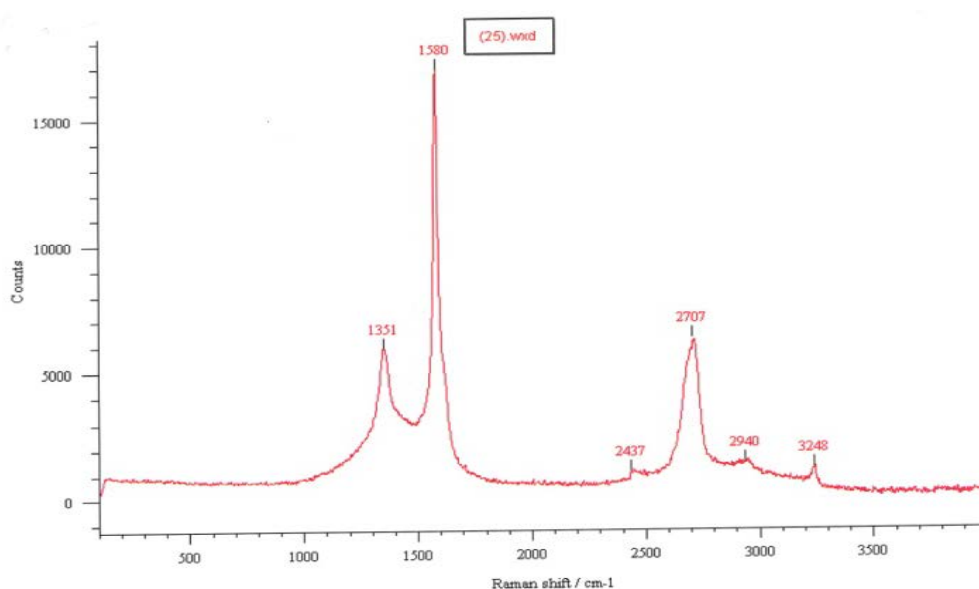
Figure 4.47. Raman spectrum of PEI modified graphene

The Raman spectrum of PEI modified graphene given in Figure 4.47 reveals that the intensity of D band at 1341 cm^{-1} in pristine graphene is lower than that of D band at 1351cm^{-1}. We believe that this may be due to the formation of more sp^3 bonds in graphene flakes modified with PEI with an I_D/I_G ratio of 0.37 which show more defects than graphene having I_D/I_G ratio of 0.08. See Table 4.15.
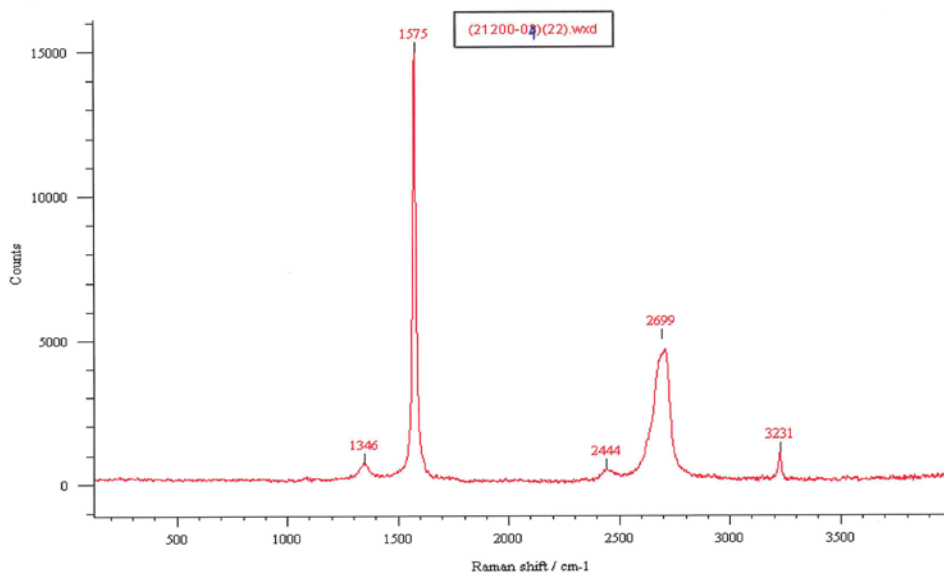
Figure 4.48 Raman spectrum of VIM modified graphene

Figure 4.48 shows the Raman spectrum of VIM modified graphene. The D band at 1341 cm^{-1} in pristine graphene shifted to 1346 cm^{-1} depending on VIM modification of graphene, but the intensity is lower than that in graphene and G band was shown in 1575 cm^{-1}. These findings led to obtain lower I_D/I_G ratio (as 0.05) due to binding of N-vinylimidazole into graphene structure.

As we shall see in the future, although the defects are small, the VIM modified graphene is at the foreground in practice, and we believe that this is due to π-π stacking interactions between the VIM ring and the graphene ring.
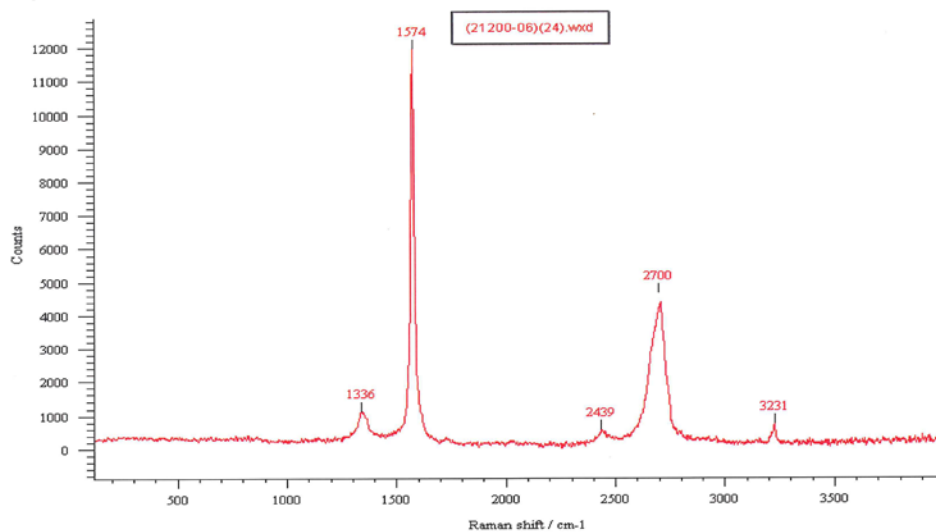
Figure 4.49. Raman spectrum of DEA modified graphene

Figure 4.49 shows the Raman spectrum of DEA modified graphene. Here, D and G bands were observed at 1336cm^{-1}, 1574cm^{-1} by the ratio of I_D/I_G = 0.09, that means nearly same feature for graphene that has the ratio of I_D/I_G 0.08. This result says that there are few defects in the graphene structure. See Table 4.15.
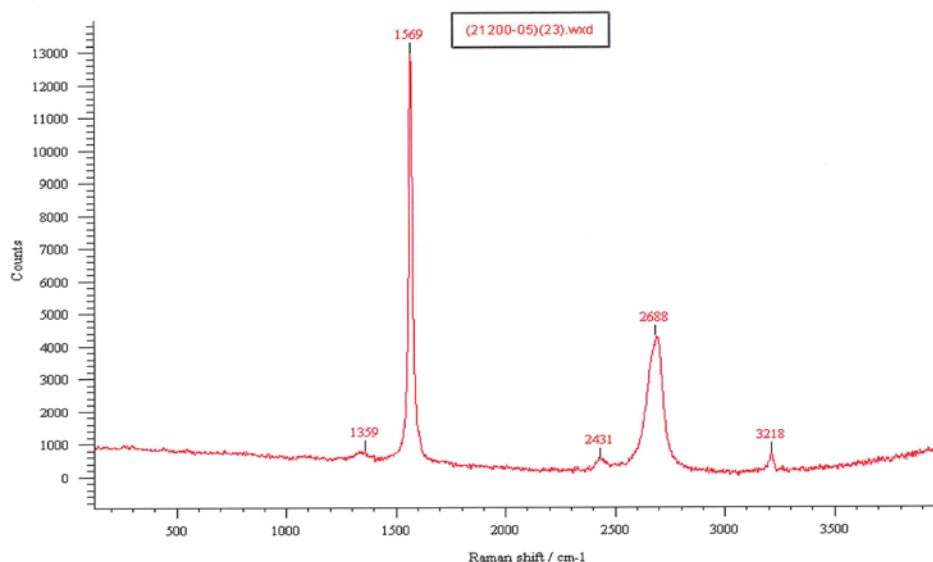
Figure 4.50. Raman spectrum of EDA modified graphene

Figure 4.50 shows the Raman spectrum of EDA modified graphene. Here, D and G bands were observed at 1359 cm^{-1}, 1569 cm^{-1} by the ratio of I_D/I_G 0.06. This result suggests that EDA is less effective than DEA in producing defects on the graphene. See Table 4.15.

4.1.7. Differential Scanning Calorimetry (DSC) analysis of graphene and modified graphene

DSC measurements have been further performed to examine the thermal properties of the graphene depending on modification. A heating process has been performed in the temperature range of 25 - 400°C.

4.1.7.1. DSC analysis of graphene and acid modified graphene
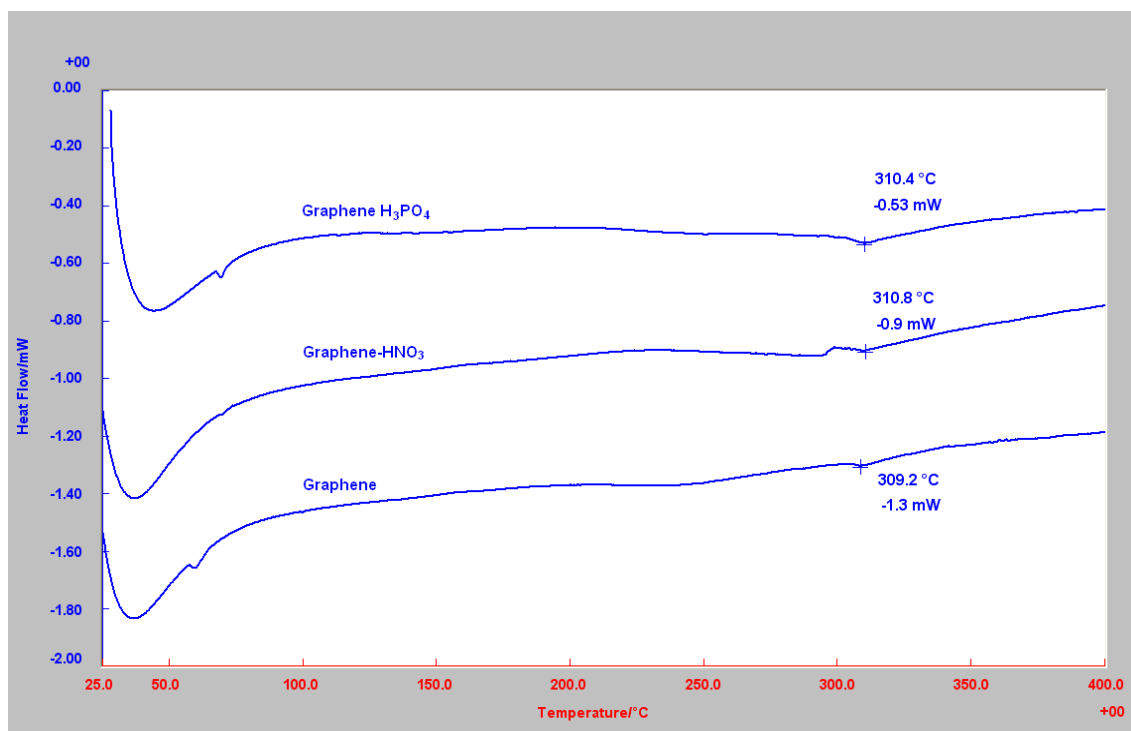
Figure 4.51. DSC thermograms of graphene and acid modified graphene

Figure 4.51 show the DSC thermograms and corresponding T value of the pristine graphene, GN and GP. The endothermic minima were seen at ~39, 41 and 44°C for G, GN, and GP, respectively. GN shows an increase in T value of 310.8°C when compared with GP 310.4°C and pristine graphene 309.2°C. The increase

92

in T value in GN and GP is due to oxidation by incorporation of HNO_3 and H_3PO_4 and –OH groups to graphene and this constrains the motion by H-bonds and electrostatic attraction. The change in T value from 309.2°C to 310.8°C in GN and to 310.4°C in GP (1.6°C and 1.2°C differences) means that no significant change in crystallization in graphene.

4.1.7.2. DSC analysis of graphene and base modified graphene
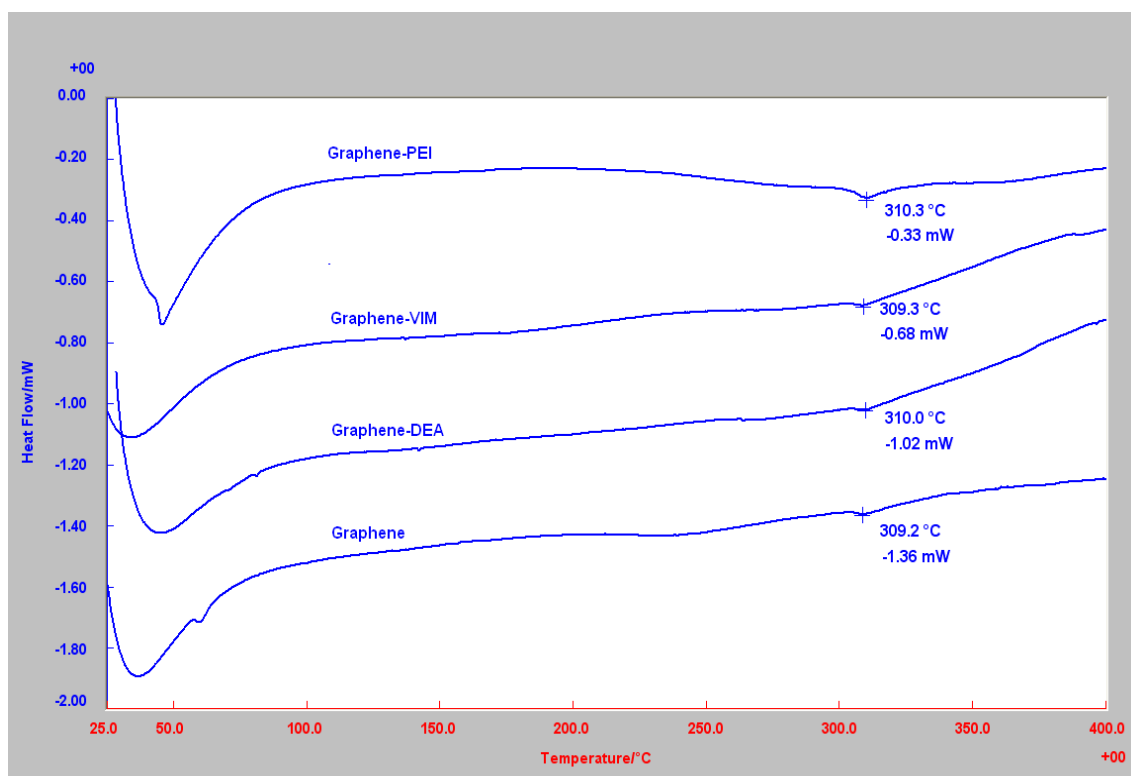
Figure 4.52. DSC analysis of graphene and base modified graphene

Figure 4.52 show the DSC thermograms and corresponding T value of the pristine graphene, GDEA, GVIM and GPEI. The endothermic minima were seen at ~30, 41 and 44°C for G, GDEA, GVIM and GPEI, respectively. GDEA shows an increase in T value of 310.0°C when compared to GVIM with 309.3°C. (This value is very close to that of pristine graphene (309.2°C) may be due from imidazole ring.)

The increase in T value in GDEA and GPEI may be due from bonding between graphene and N-H group of amine and this constrains the motion by H-bonds and electrostatic attraction. The change in T value from 309.2°C to 310.0°C in GDEA and 310.3°C in GPEI (1.1°C and 0.8°C differences)   means that no significant change in crystallization in graphene [164].

4.2. Results for modified graphene composites

4.2.1. FT-IR analysis of acid and base modified graphene composites

4.2.1.1. FT-IR analysis of HNO₃ modified graphene-VIM and HNO₃ modified graphene-PEI composites

The FT-IR spectra of G, GN, GN-PEI and GN-VIM composites are shown in Figure 4.53.
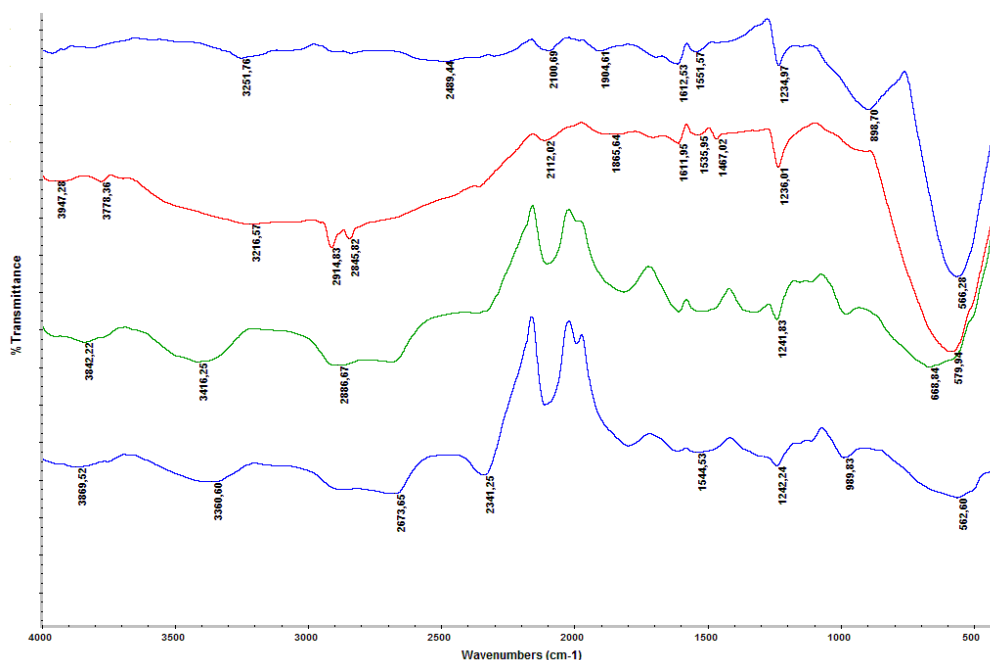
Figure 4.53. FT-IR spectra of the composites (from top to bottom: G, GN, GN-PEI, GN-VIM)

As can be seen from figure, broad absorption bands around at 3840 cm^{-1} for graphene-HNO₃-PEI and at 3869 cm^{-1} for graphene-HNO₃-VIM are assigned for N-H stretching vibrations. The absorption band at around 3416 and 3360 cm^{-1} due to the –OH stretching vibrations. Two sharp absorption peaks at 2914 and 2886 cm^{-1} is due to the C-H stretching vibrations. The C-H stretching vibration was not observed for graphene. This may due to more   C-H groups formed depending on modification. The main absorption band at around 1860 cm^{-1} is characteristic band for C=O group which observed by weak band in HNO₃ modified graphene and sharp absorption in graphene-HNO₃-VIM and graphene-HNO₃-PEI. From the FT-IR spectra evaluations, the absorptions (3840 and 1860 cm^{-1}) may due to the formation of amide which is aroused from oxidation of graphene by HNO₃ followed by amines. The broad and weak band at 1535-1470 cm^{-1} may be due to

95

symmetrical stretching vibration of –NO$_2$ in graphene-HNO$_3$, graphene-HNO$_3$-VIM and graphene-HNO$_3$-PEI, while that is not observed in graphene spectrum. Strong absorptions were observed at 2350 and 2150 cm^{-1} due to O=C=O, N=C=N respectively; this is an evidence of composite formation.

The absorption of C=C stretching vibration was observed clearly at around 1612 cm^{-1} in graphene and graphene-HNO$_3$, and its composites. The C-O stretching vibration was observed for graphene-HNO$_3$-PEI and for graphene-HNO$_3$-VIM around 1240 cm^{-1}, and O-H bending at 1467 cm^{-1} [141,165,166].

4.2.1.2. FT-IR analysis of H$_3$PO$_4$ modified graphene-VIM and H$_3$PO$_4$ modified graphene-PEI composites
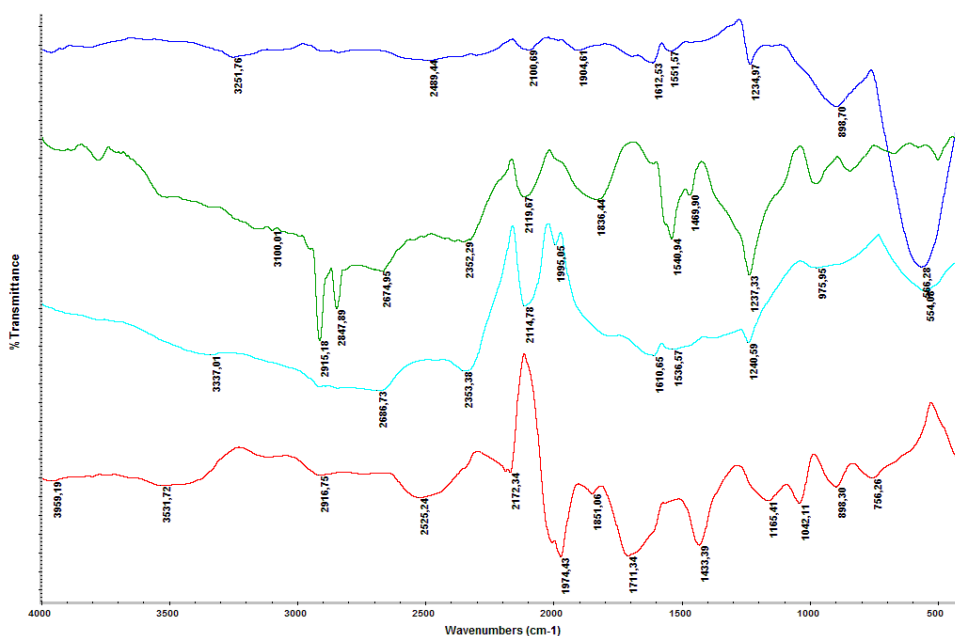
Figure 4.54. FT-IR spectra of the composites (from top to bottom: G, GP, GP-PEI, GP-VIM)

Figure 4.54 shows the FT-IR spectra of H$_3$PO$_4$ modified graphene and its composites. The stronger and sharp bands of C-H stretching vibration for graphene-H$_3$PO$_4$ assigned at 2850 and 2916 cm^{-1}, while these bands were observed as moderate and broad at around 2900 cm^{-1} in graphene-H$_3$PO$_4$-PEI. This situation may be due to more absorption of C-H stretching vibration when PEI was added to graphene-H$_3$PO$_4$. The aromatic C-H stretching vibration of graphene-

96

H_3PO_4-VIM was observed at around 3100 cm^{-1}. While the absorption of C=O stretching was not observed in graphene, strong and broad absorption of C=O stretching can be seen at 1700 and 1850 cm^{-1} of graphene-H_3PO_4 and graphene-H_3PO_4-VIM, respectively. At 1980 cm^{-1}, there is a strong absorption of C=N stretching vibration indicating imidazole moiety in reaction of graphene-H_3PO_4-VIM.

The FT-IR spectrum of graphene-H_3PO_4-VIM also showed C-N absorption at 1410 cm^{-1} that was not observed in graphene and graphene modified with H_3PO_4. This indicates that the imine group introduced to the graphene structure. [167].

4.2.1.3. FT-IR analysis of DEA modified graphene-VIM and DEA modified graphene-PEI composites

Figure 4.55 indicates the FT-IR spectra of G, GDEA, GDEA-PEI and GDEA-VIM composites.
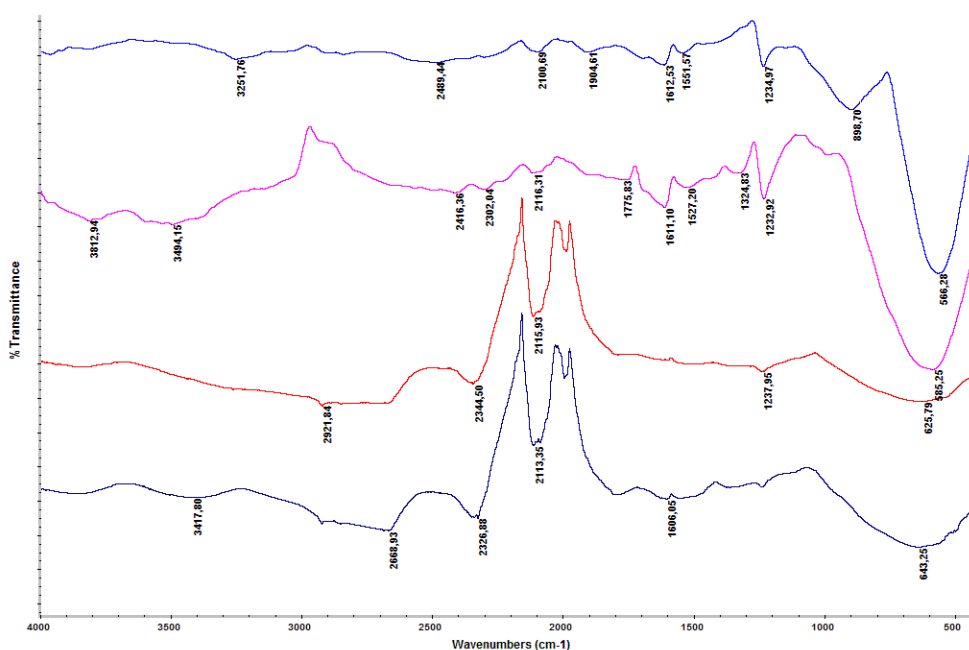
Figure 4.55. FT-IR spectra of the composites (from top to bottom: G, GDEA, GDEA-PEI, GDEA-VIM)

In Figure 4.55, the broad peak at around 3400 cm^{-1} was attributed to the N-H bond stretching vibration due to the increase in amino groups following the addition of DEA to graphene also PEI or VIM addition to DEA-modified graphene.

97

The sharp and strong absorption seen at 2921-2923 cm^{-1} caused by two diethyl groups of DEA which is not observed for graphene is due to lack of aliphatic C-H bond. In the case of graphene-DEA-VIM, this absorption indicates the addition of imidazole moiety. We can also notice that other C-H absorption band at 2840 cm^{-1} in graphene-DEA which can be defined as symmetrical C-H stretching vibration.

The absorption around 1612 cm^{-1} is characteristic for C=C double bond that was shown in graphene and its derivatives. The FT-IR spectrum of both graphene-DEA-VIM and graphene-DEA-PEI showed strong absorption at 2350 and 2112 cm^{-1} due to O=C=O , N=C=N bond which is evidence of composite formation .We did not observe these two absorption in the FT-IR spectra of graphene and graphene-DEA. It is important and remarkable that this band formed when DEA-modified graphene reacts with PEI and VIM [168, 169].

4.2.1.4. FT-IR analysis of EDA modified graphene-VIM and EDA modified graphene-PEI composites

Figure 4.56 indicates the FT-IR spectra of G, GEDA, GEDA-PEI and GEDA-VIM composites.
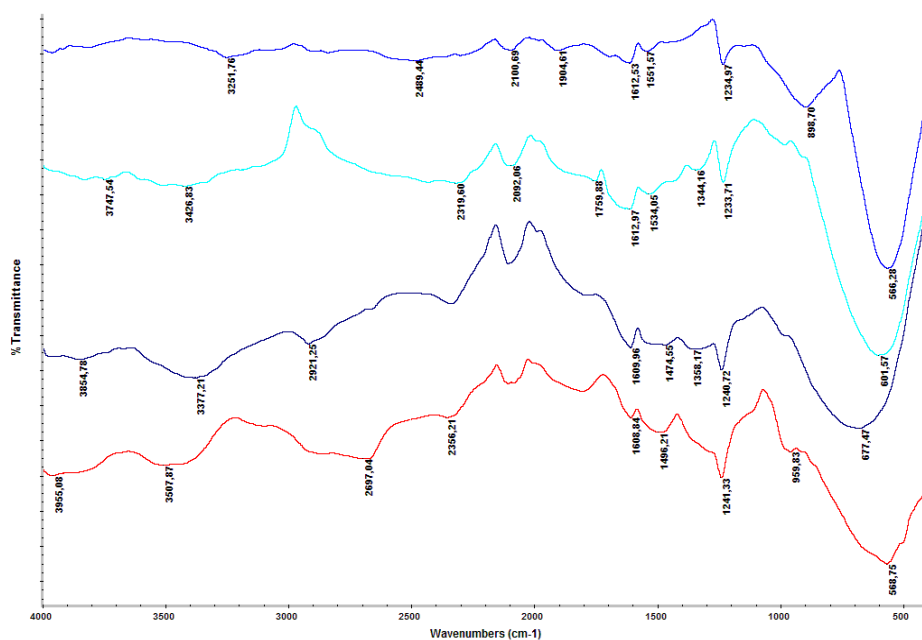
Figure 4.56. FT-IR spectra of the composites (from top to bottom: G, GEDA, GEDA-PEI, GEDA-VIM)

The absorption of N−H stretching vibrations was observed at range between around 3500-3600 cm^{-1} of graphene-EDA, graphene-EDA-PEI and graphene-EDA-VIM. All the amine derivatives of graphene showed strong and broad C-H stretching vibrations ranged between 2809 to 2916 cm^{-1}. The graphene EDA-VIM composite showed extra C-H of aromatic imidazole ring at 3150 cm^{-1}. The C=C was observed at around 1612 cm^{-1}, while the peak of C−N stretching vibrations was occurred at range between 1360-1400 cm^{-1} of all FT-IR spectra of amine derivatives of graphene. The main absorption of composite was appeared at around 2200-2300 cm^{-1} for N=C=N bond of carbodiimides and O=C=O [170].

4.2.2. XRD analysis of acid and base modified graphene composites

In this section, we present XRD patterns and related discussion for composites prepared with PEI and VIM of acid- and base- modified graphene. Results are given in Table 4.16 and Table 4.17.

Table 4.16. XRD analysis results for acid-modified graphene composites

Starting material	Polymer/ monomer	Composite code	XRD information		
			Pos. [°2 Th.] Θ	Height [cts]	D-spacing [Å]
GN	PEI	GN-PEI	26.5622	5114.59	3.3558
GN	VIM	GN-VIM	26.5196	9202.98	3.3612
GP	PEI	GP-PEI	26.5811	8167.67	3.3535
GP	VIM	GP-VIM	26.5419	6633.24	3.3583

Table 4.17. XRD analysis results for base-modified graphene composites

Starting material	Polymer/ monomer	Composite code	XRD information		
			Pos. [°2 Th.] Θ	Height [cts]	D-spacing [Å]
GDEA	PEI	GD-PEI	26.5139	4899.95	3.3617
GDEA	VIM	GD-VIM	26.5888	8172.50	3.3526
GEDA	PEI	GE-PEI	26.5510	8713.64	3.3573
GEDA	VIM	GE-VIM	26.5168	7264.21	3.3615

These tables reveal that the XRD pattern of the modified graphene composites exhibits a high intensity peak around 2θ 26.5° corresponding to the graphene structure (002) plane. They have difference in value of peak intensity coming from diffractions of beams of light [170] although the XRD patterns give almost same peak position. Single electron have different scattered energy [171] due to O-H and N-H group. The XRD data of graphene composites present crystalline peaks similar to those obtained from pristine and modified graphenes revealing that no additional crystalline order has been introduced into the composite and indicating that graphene and modified graphene are fully interacted with PEI and VIM [172].

4.2.3. SEM analysis of composites

4.2.3.1. SEM analysis of graphene and acid-modified graphene composites

The surface morphology of the acid- and base-modified graphene nanocomposites was investigated by using SEM. The morphology of our ''as prepared'' powder graphene composites was examined by SEM images and shown in Figures 4.57 - 4.61. The SEM demonstrate an agglomerated powder with a ''fluffy'' appearance [173], the view of obtained graphene composites reveals like rippled silk, further confirm the appearance of transparent with wrinkles and folds [174].
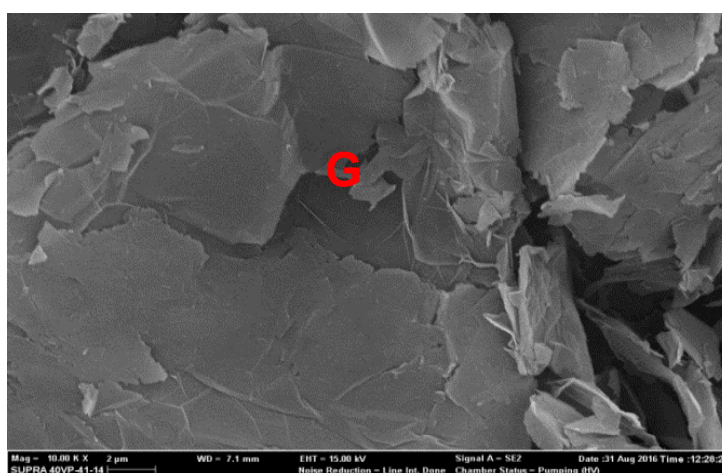
Figure 4.57. SEM images of graphene
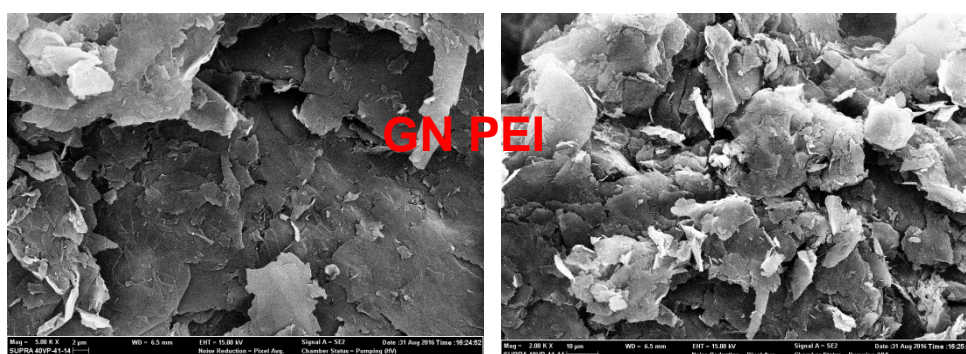
Figure 4.58. SEM images of HNO$_3$-modified graphene – PEI composites
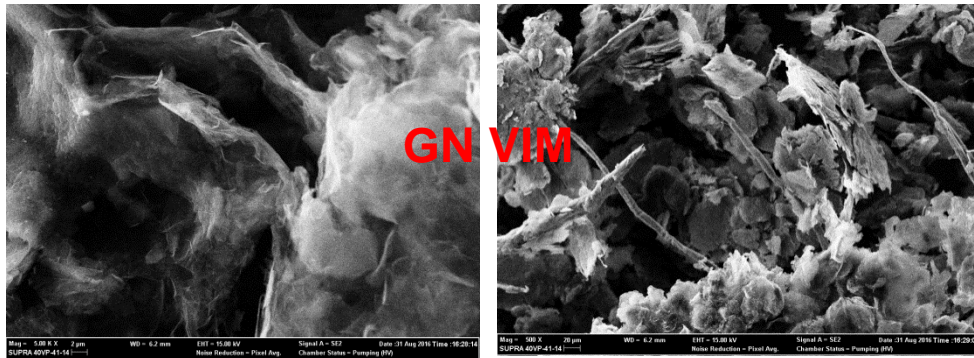
Figure 4.59. SEM images of HNO₃-modified graphene – VIM composites

The morphology of HNO$_3$-modified graphene composites was studied using SEM. Graphene particles are in the platelet-like crystalline form of carbon clearly seen from Figure 4.57. After PEI and VIM modification of HNO$_3$-modified graphene was carried out, as shown in Figure 4.58 – 4.59, surface sheets become smaller and transparent. The sheet is so thin that electron beam can be passed through sample [175].

Figure 4.60. SEM images of H$_3$PO$_4$-modified graphene – PEI composites
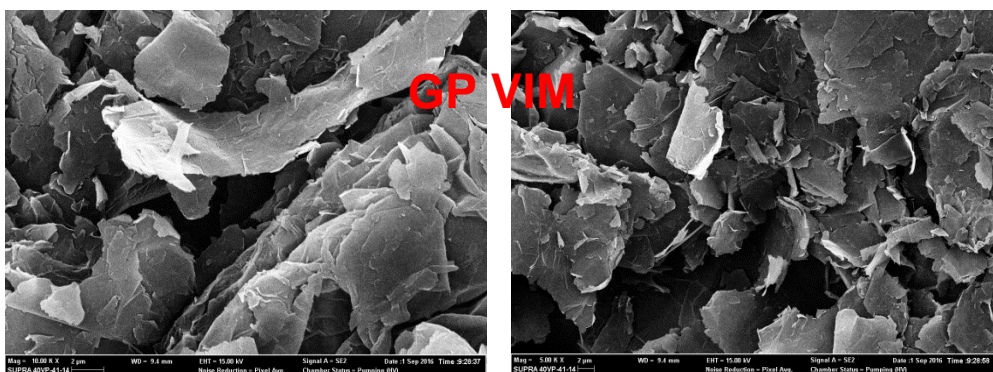
Figure 4.61. SEM images of H$_3$PO$_4$-modified graphene – VIM composites

Figure 4.60 and Figure 4.61 show the SEM images of GP-PEI and GP-VIM composites. Morphologies of graphene composites are observed as flaky texture reflecting its layered microstructure with bright color which may be due to PEI and VIM bonding to GP layers during reaction.

4.2.3.2. SEM analysis of base-modified graphene composites
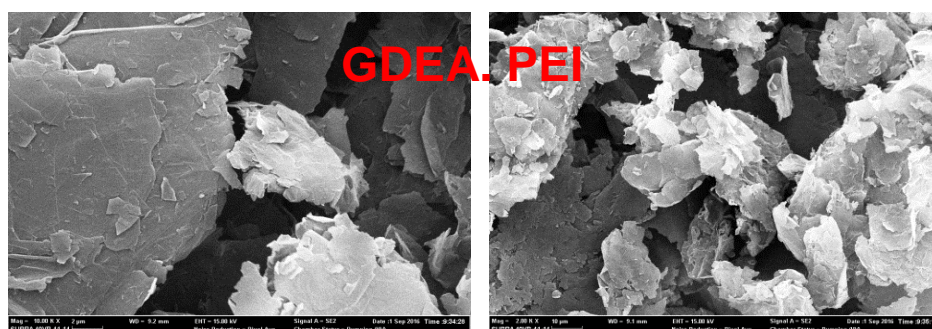
Figure 4.62. SEM images of DEA-modified graphene – PEI composites

Figure 4.63. SEM images of DEA-modified graphene – VIM composites

We further explore the structural features of graphene and modified graphene using SEM images. Some different types of morphological characteristics are shown in Figure 4.62 and 4.63 for GDEA-PEI, GDEA-VIM composites. The surface structure has a rough and rippled fracture due to incorporation of the PEI and VIM to GDEA.

Figure 4.64. SEM images of EDA-modified graphene – PEI composites

Figure 4.65. SEM images of EDA-modified graphene – VIM composites

Figure 4.64 and Figure 4.65 show the SEM images of GEDA composites to determine the morphological changes occurred in the surface feature. A remarkable aggregated particles were observed in several sizes, due to attachment of PEI or VIM to GEDA to obtain nanocomposite.

4.2.4. Elemental Mapping results for acid-modified graphene composites

4.2.4.1. Elemental mapping analysis of HNO₃-modified graphene PEI and VIM composites

Figure 4.66 and Figure 4.67 present the percentage of C, N, and O that associated with composites of HNO₃-modified graphene.
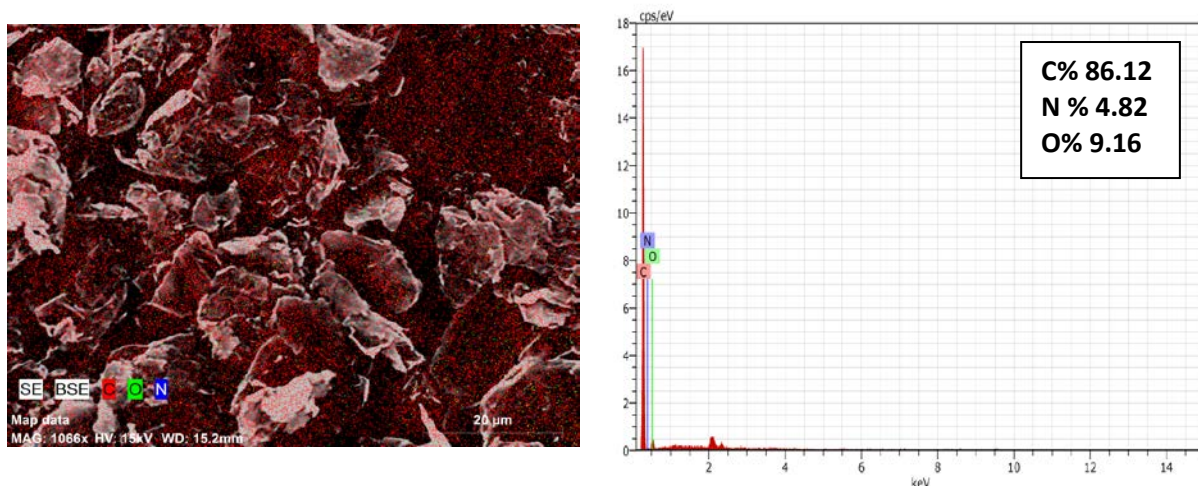
Figure 4.66. Elemental mapping results for HNO₃-modified graphene-PEI composites
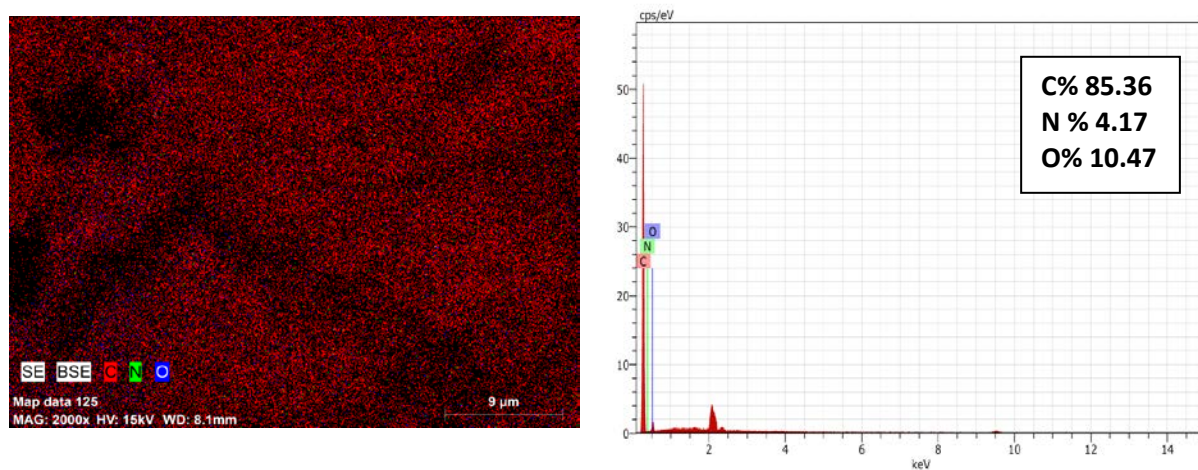
Figure 4.67. Elemental mapping results for HNO₃-modified graphene-VIM composites

An important issue is noteworthy here: Looking at the percentages of C, O, N given in Table 4.8, 4.12 and these figures, the elemental compositions obtained in the individual modification of the graphene with HNO_3 and VIM are lower than those obtained for the GN-VIM composite. This suggests that modifying the surface of the graphene with HNO_3 first creates new binding points for VIM, thus indicating increased π-π stacking interactions between the graphene layers and the VIM ring.

4.2.5. TEM analysis of acid-modified graphene composites
4.2.5.1. TEM analysis of HNO₃-modified graphene PEI and VIM composites
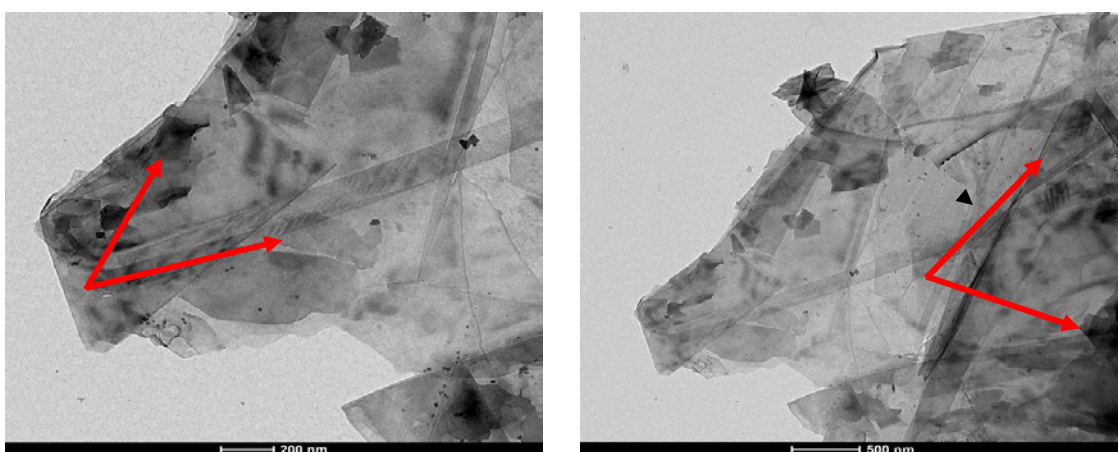
Figure 4.68. TEM image for HNO_3-modified graphene – PEI composites

The morphology and microstructure of GN-PEI nanocomposites were also characterized by TEM. It can be obviously seen from Figure 4.68 that the graphene forming thin-petal-like shape was crumpled and wrinkled [176], with a typical lamella structure in the presence of many PEI particles. The red arrows indicate the existence of PEI on the surface of GN, which further confirm that the modification was successfully carried out.
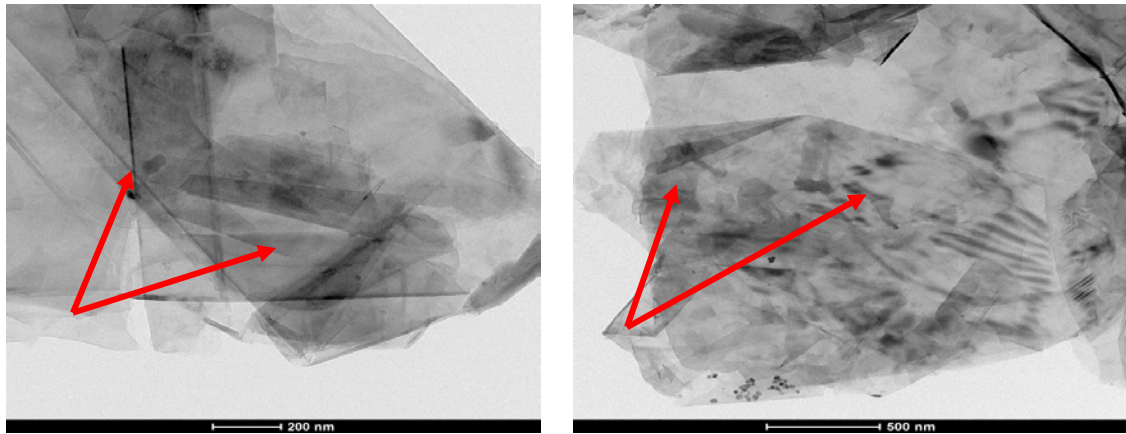
Figure 4.69. TEM image for HNO$_3$-modified graphene – VIM composites

TEM analysis was used to investigate the surface morphology of the GN-VIM composites, as shown in Figure 4.69. The micrographs of the composites clearly reveal a layered structure having dots by dark color, attributed to surface of the GN is well-coated by VIM.

4.2.6. Raman spectroscopic analysis results for composites

4.2.6.1. Raman spectroscopic analysis results for acid- and base- modified graphene composites

In the following Table 4.18 and Table 4.19, the information collected from Raman spectra of graphene and modified graphene were compared to data related to composites. Regardless of the thickness, the G peak reveals sp^2 bonds when the disorder of graphene structure (sp^3 bonds) is explained by D and 2D peaks [177]. The main features of the Raman spectrum of carbon are the peaks in the visible excitation called G (graphite as sp^2 form) and D (diamond as sp^3 form) [178].

Table 4.18. Raman analysis results for graphene and modified graphene

Sample	D Position (cm⁻¹)	G Position (cm⁻¹)	2D Position (cm⁻¹)	I_D/I_G	I_{2D}/I_G
G	1341	1576	2706	0.08	0.40
GN	1352	1583	2714	0.21	0.45
GPEI	1351	1580	2707	0.37	0.35
GVIM	1346	1575	2699	0.05	0.33
GDEA	1336	1574	2700	0.09	0.39

Table 4.19. Raman analysis results for acid- and base-modified graphene composites

Sample	D position (cm⁻¹)	G position (cm⁻¹)	2D position (cm⁻¹)	I_D/I_G	I_{2D}/I_G
GN-PEI	1371	1582	2716	0.21	0.65
GN-VIM	1341	1578	2710	0.15	0.39
GDEA-PEI	1353	1575	2702	0.20	0.35
GDEA-VIM	1349	1579	2705	0.26	0.39

Raman spectra showed that there is difference in D, G and 2D peaks of modified graphene and composites. In the spectral data of graphene, HNO_3- modified graphene and DEA-modified graphene we see a shift in D and G peak position; when we calculate the ratio of intensity of these peaks the results gave us the defect that happened in the structure. Graphene modified by VIM and DEA showed that there is no defect in structure that may be due to cyclization of VIM and DEA. Modification by HNO_3 followed by PEI create more defects in graphene structure. When we look at the spectra for PEI and VIM composites modified with the same acid and same amine, changes in the position and the ratio of I_D / I_G show that the reactions are successful and that new compounds are formed. These spectra are given in Figures 4.70 – 4.73.
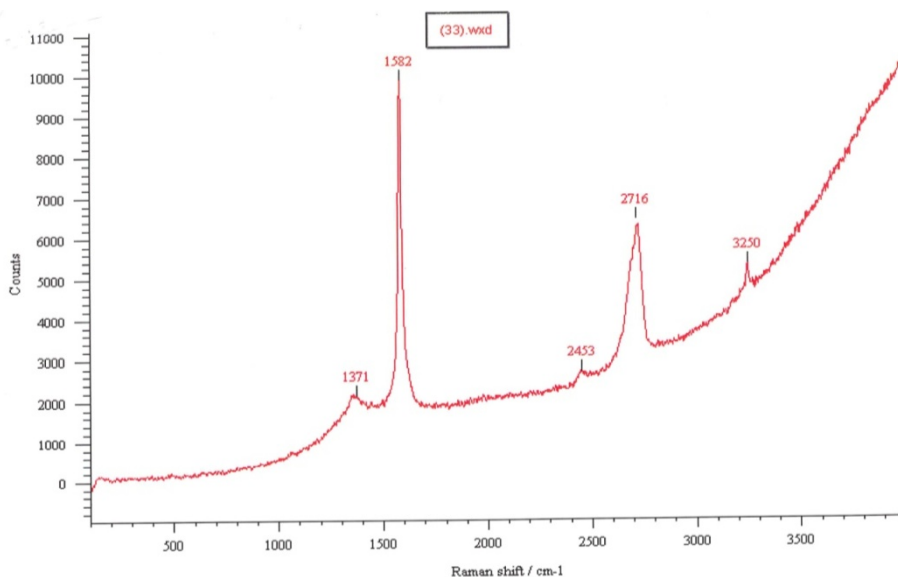
Figure 4.70. Raman spectrum of HNO$_3$-modified graphene-PEI composites

Figure 4.70 showing Raman spectrum of GN-PEI composite demonstrate D, G peaks at 1371, 1582 cm^{-1} with the ratio of I_D/I_G 0.21 and 2D peak position at 2716 cm^{-1}. All bands shifted compared with pristine graphene and other modified graphene that means for changing functional group in each case. See Table 4.18 and Table 4.19.
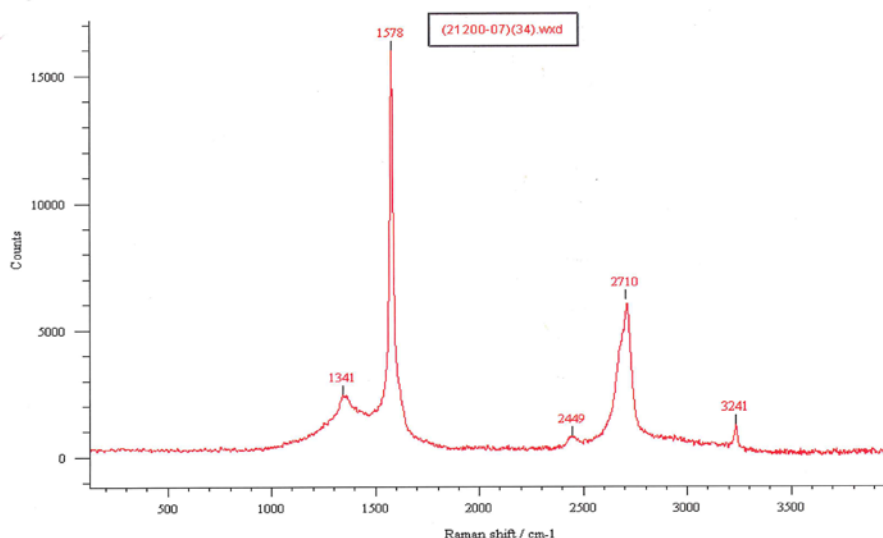
Figure 4.71. Raman spectrum of HNO$_3$-modified graphene-VIM composites

The Raman spectrum of HNO_3-modified graphene VIM composite given in Figure 4.71 reveal two prominent peaks for G and D peaks at 1341 cm^{-1} and 1578 cm^{-1}. The ratio of *ID/IG* is 0.15 due to chemical interactions of GN-VIM. See Table 4.18 and Table 4.19.
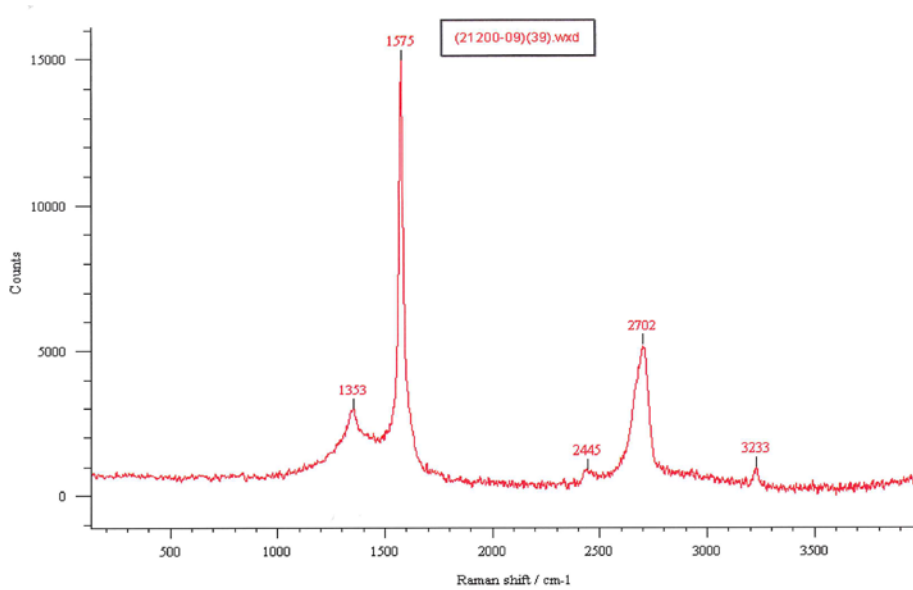
Figure 4.72. Raman spectrum of DEA-modified graphene-PEI composites

Figure 4.72 shows Raman spectrum for GDEA-PEI having the D peak at 1353 cm^{-1} and G peak at 1575 cm^{-1}. GDEA-PEI structure was more defected when calculated ratio for *ID/IG* 0.21 compared between with pristine graphene and DEA modified graphene. But this ratio was small regarding PEI modified graphene that indicates different binding mechanism available for composite.
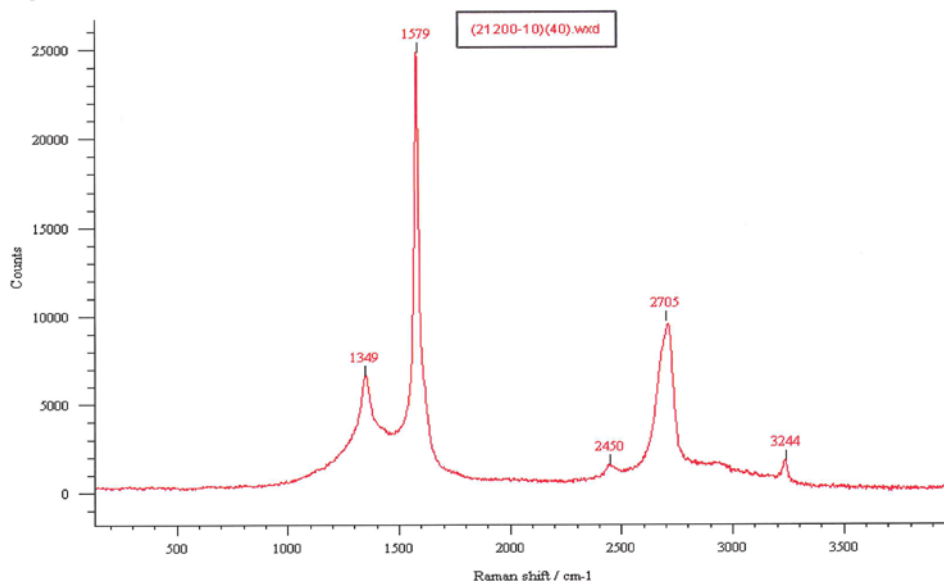
Figure 4.73. Raman spectrum of DEA-modified graphene-VIM composites

Figure 4-73 define the clearly peaks that appeared in D peak position at 1349 cm^{-1} with high intensity and G peak position at 1579 cm^{-1}. This was arised from the ratio of I_D/I_G 0.26 more than pristine graphene (0.08), DEA-modified graphene (0.09) and VIM-modified graphene (0.05). See Table 4.18 and 4.19.

Finally; the applications of Raman spectroscopy to characterizing graphene materials has become increasingly widespread. The sensitivity of the positions, widths and intensities of the D, G and 2D peaks has made it possible to probe a variety of attributes. The effects of edge states, strain, doping, temperature, thickness and disorder are all discernible in the Raman spectrum of graphene and other modified graphene materials given the proper conditions. This has given us a powerful, noninvasive tool for graphene characterization [179].

4.2.7. DSC analysis of composites

4.2.7.1. DSC analysis of acid- and base-modified graphene composites

DSC monitors heat effects associated with phase transitions and chemical reactions as a function of temperature. In a DSC the difference in heat flow to the sample and a reference at the same temperature, is recorded as a function of temperature [180].
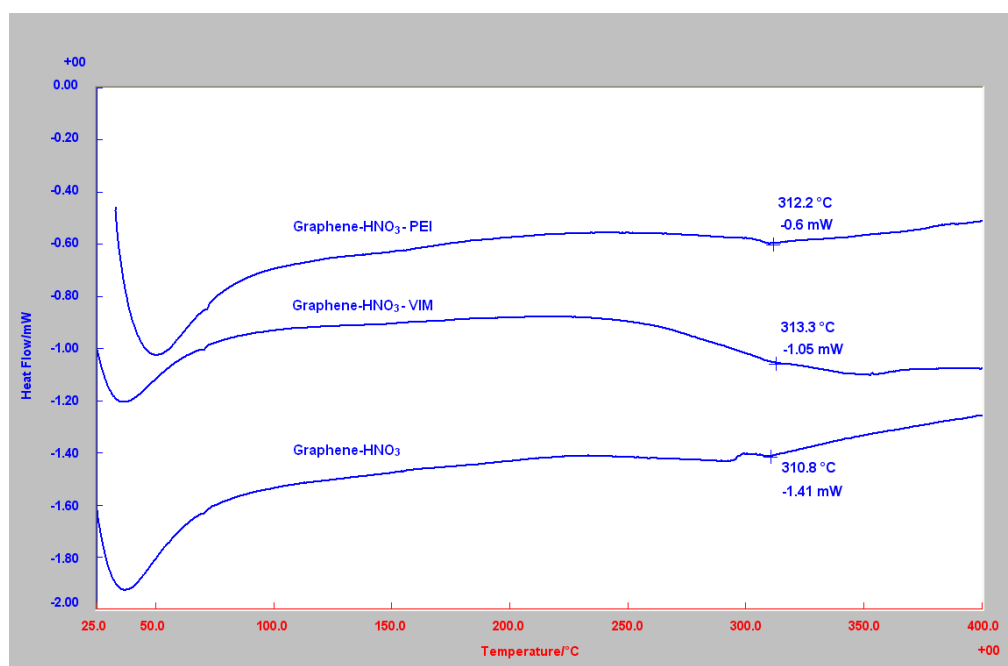
Figure 4.74. DSC thermogram for HNO$_3$-modified graphene and their composites

Figure. 4.74 shows the DSC curves of GN-VIM and GN-PEI composites. The results showed that there was noteworthy effect of the acid modified graphene addition on the transition temperature of the composites. The acid modified graphene had transition temperature of 310.8°C. The composites showed transition curves around 313.3°C and 312.2°C. Whereas composites have higher broad transition peak. There was 3-4% increases in degree of transition as GN-VIM, GN-PEI. Endothermic peak was changing by approximately with GN and GN-VIM by 35°C but the temperature of GNPEI increased that shows endotherm in 49°C due to crystallinity of this composite.
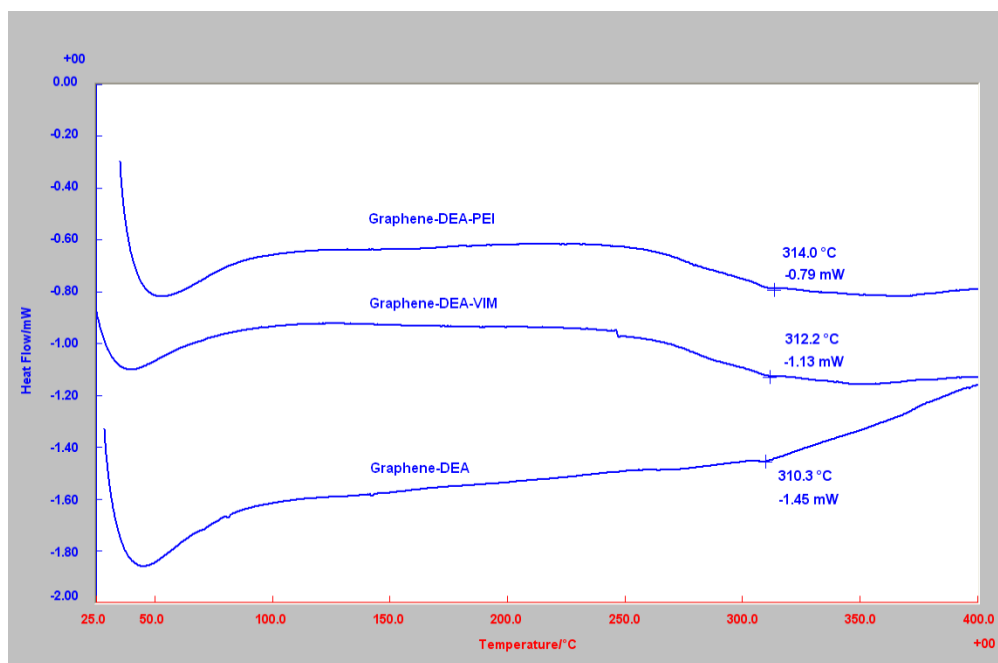
Figure 4.75. DSC thermogram for DEA-modified graphene and their composites

Figure 4.75 explain DSC measurements of DEA-modified graphene and its composites. A heating process have been performed in the temperature range between 25°C and 400°C. The peak showing endotherm of DEA-modified graphene was found as 40°C, 31°C and 49°C for GDEA, GDEA-VIM and GDEA-PEI, respectively. This situation is attributed to that there is different group attached on graphene surface that was changed the endothermic peak of molecule. The transition temperature (*T*) of GDEA, GDEA-VIM and GDEA-PEI were seen in 310.3°C, 312.2°C, 314°C, respectively. Increase in crystallinity means that the immobilization of polymer chains via H-bonding interactions with graphene [181].

Overall, the order of relative crystallinity in graphene and graphene composites is found to be greater than the pristine graphene. The transition peak of pristine graphene (at about 309°C) was slightly increased in the composites. This could be attributed crystal size of graphene composites due to the intercalation of VIM and PEI.

4.3. Results for graphene and modified graphene-doped 2-hydroxyethyl cellulose films

As mentioned in the experimental section we prepared 2-HEC films by selecting nine samples from the modified graphenes. These films were analyzed by FT-IR, XRD, SEM, elemental mapping, DSC and universal testing methods. The results of analyses are given below in separate sections.

4.3.1. The results of FT-IR characterization of 2-HEC/modified graphene films

The FT-IR analysis results for modified graphene-doped 2-HEC films are shown in Figure 4.76. Since the amount of modified graphene added to the 2-HEC films prepared on the basis of the mass ratio is very small, it is very difficult to observe the graphene-induced changes in the cellulose structure as a peak among the 2-HEC base peaks. Although there are no notable significant differences in the spectra, it is observed that there are very small differences in shape and intensity of the peaks in the range of 1500 cm^{-1} – 500 cm^{-1}. According to these differences, it can be said that the graphene and modified graphene were successfully distributed into the 2-HEC structure. From the FT-IR spectrum of 2-HEC (see inset figure), a broad band at 3456 cm^{-1} and 1358 cm^{-1} are due to the O-H stretching and O-H bending vibrations. The characteristic peak at 2876 cm^{-1} indicates the aliphatic C-H stretching. The C-O-C stretching vibrations are pointed out by bands at 1053 cm^{-1} and 1011 cm^{-1}, also band at 1134 cm^{-1} is attributed to C-O stretching vibrations. The characteristic vibrations in the FT-IR spectra of the 2-HEC-graphene nanocomposite films are approximately similar to those of 2-HEC, but with some subtle differences. Compared with 2-HEC, the C=O stretching vibration peak at 1712 cm^{-1} belonging to modified graphene was observed, indicating the existence of graphene in the composite films [182].
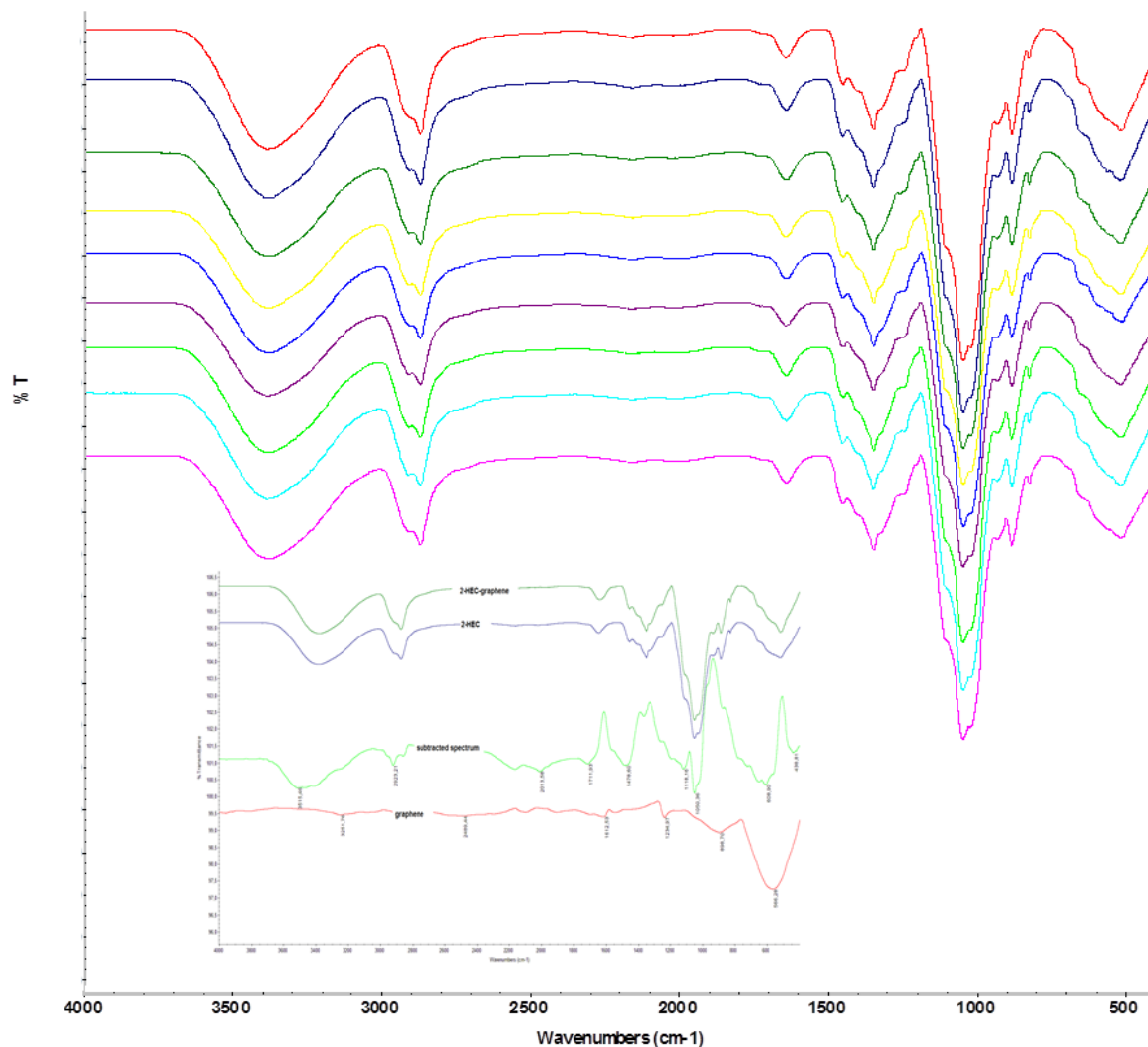
Figure 4.76. The FT-IR spectra of modified graphene-doped 2-HEC films.

(from top to bottom: G, GN, GPEI, GVIM, GDEA, GNPEI, GNVIM, GDEAPEI, GDEAVIM)

4.3.2 The results of XRD characterization of 2-HEC/modified graphene films

XRD structures of modified graphene-doped 2-HEC films are investigated as well. As it is depicted in Figure 4.77, a peak was seen at $2\theta = 21°$ which is characteristic peak of cellulose. Another broad and diffused peak was observed at $2\theta = 44.4°$. XRD spectrum of 2-HEC (see inset figure) showed typical semi-crystalline nature of the polymer. The characteristic 2θ peak of graphene was appeared at $26.5°$ which is correspond to graphene layers. For 2-HEC-graphene nanocomposites, the peaks observed at $2\theta = 26.5°$, $29°$ and $54°$ are due to graphene and modified graphene and their composites. The changes observed when compared to graphene and modified graphene peaks are evidence that

graphene and modified graphenes and their composites were successfully doped into 2-HEC structure [183,184].
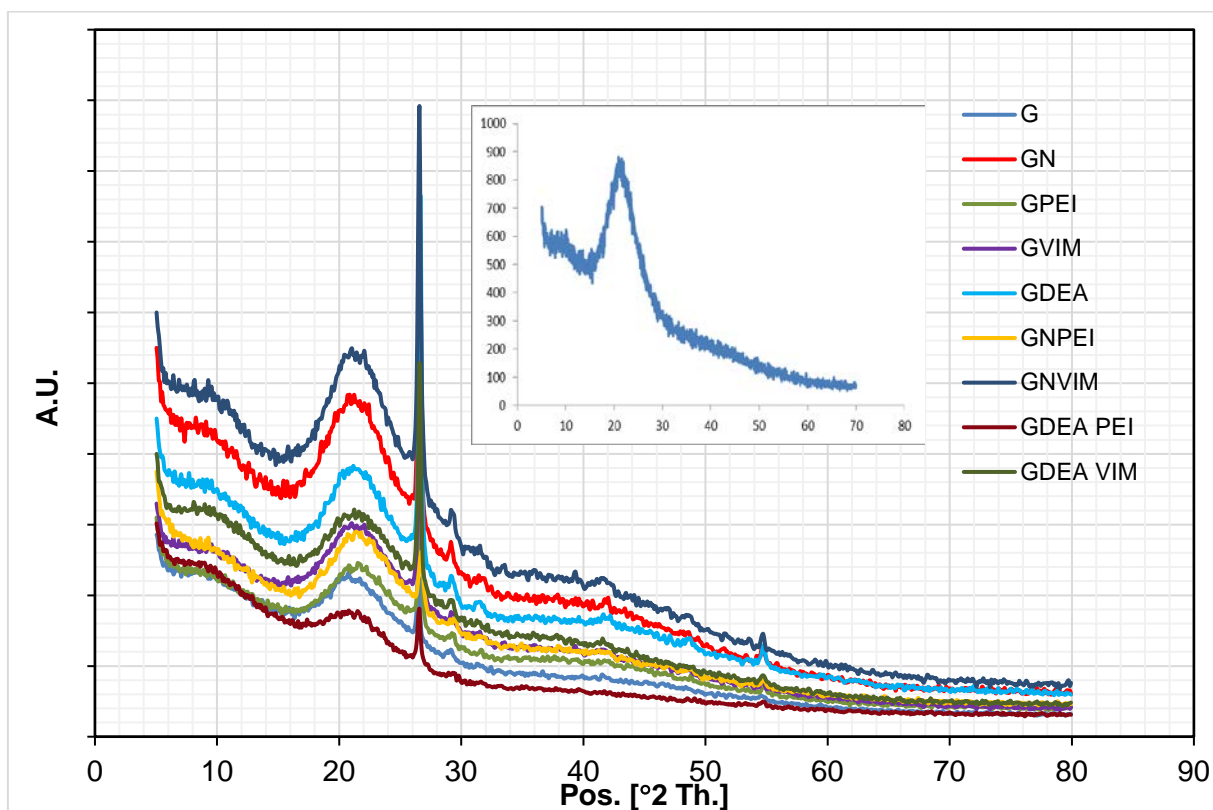
Figure 4.77. The XRD patterns of modified graphene-doped 2-HEC films.
(inset figure: XRD spectrum of 2-HEC)

To make a general assessment, the decrease in peak intensity of 2-HEC with the incorporation of modified graphene in the structure shows that the semi-crystalline structure changes with the presence of the graphene, that is, the graphene diffuses into the structure. On the other hand, the change in peak intensities of the graphene at 29° and 54° may be indicative of the homogeneous distribution of the graphene and modified graphenes into cellulose structures [183].

4.3.3 The results of SEM characterization of 2-HEC/modified graphene films

The surface morphology of 2-HEC film is shown in Figure 4.78. The SEM image showed that pure 2-HEC film has a uniform, smooth surface. This may be indicative of good film-forming properties of 2-HEC derived from renewable natural sources. The surface of the modified graphene-doped 2-HEC films (Figure 4.79) has not changed significantly since the incorporation of graphene sheets, but there have been major changes to the fractured surfaces. The homogeneous and smooth surfaces of the modified graphene-doped 2-HEC films have confirmed a fact: Graphene sheets were uniformly dispersed in the 2-HEC matrix, exhibiting films with high homogeneity without visible points of aggregation [183].
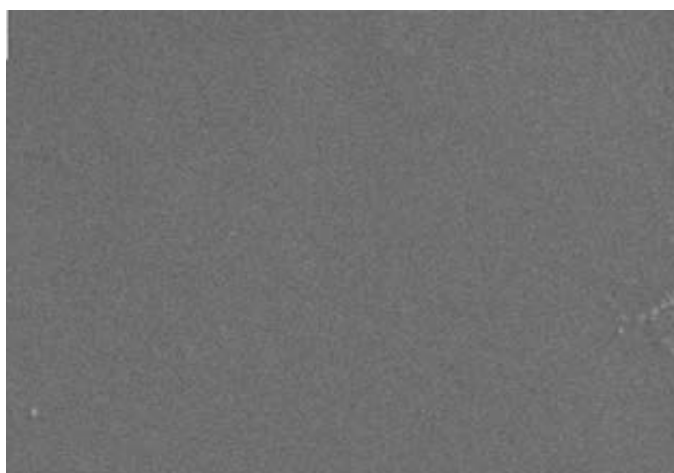
Figure 4.78. SEM image of 2-HEC
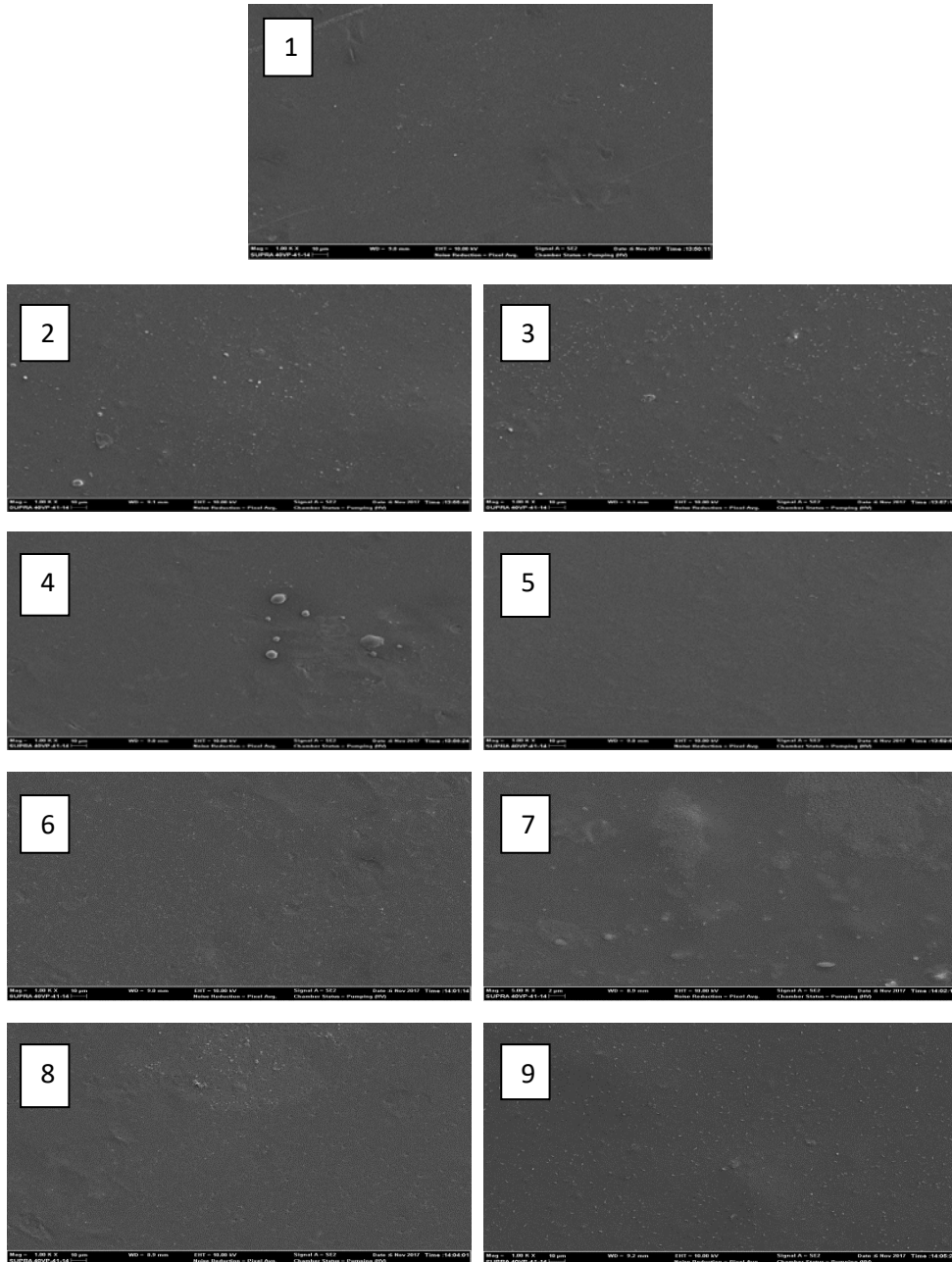
Figure 4.79. SEM images of modified graphene-doped 2-HEC films (1: G, 2:GN, 3: GPEI, 4: GVIM, 5: GDEA, 6: GN-PEI, 7: GN-VIM, 8: GDEA-PEI, 9: GDEA-VIM)

From the SEM images of fractured surfaces of 2-HEC/graphene and modified graphene composite films shown in Figure 4.79 (1 - 9) we can see fairly rough surface. This roughness due from functional groups exist on graphene could improve the uniform dispersion of graphene in the 2-HEC matrix and enhance the interfacial interaction with the 2-HEC chain that resulting to the formation of 2-HEC chains wrapped with graphene layers [183].

4.3.4. Elemental mapping results of SEM characterization of 2-HEC/modified graphene films

Figure 4.80 shows the EDS mapping images of modified graphene-doped 2-HEC films. From this figure, it can be said that C, N and O elements are uniformly distributed in 2-HEC structure. Elemental analysis revealed that the content of oxygen is increased in modified graphene-doped 2-HEC films. The percentages of C, N, and O in G, GN and GN-VIM powder samples are also given in Table 4.20 as an example. As can be seen from this table, C% in pristine graphene decreased depending on modification with HNO_3. Once treated with VIM, the amount of N in the modified graphene has increased.
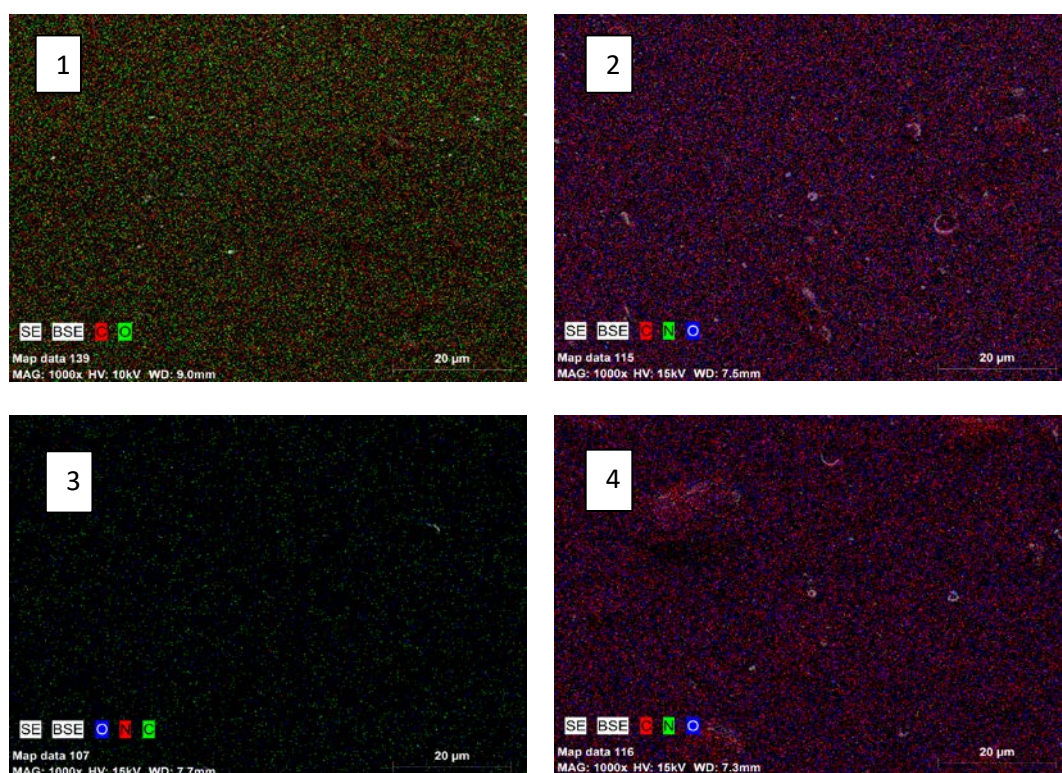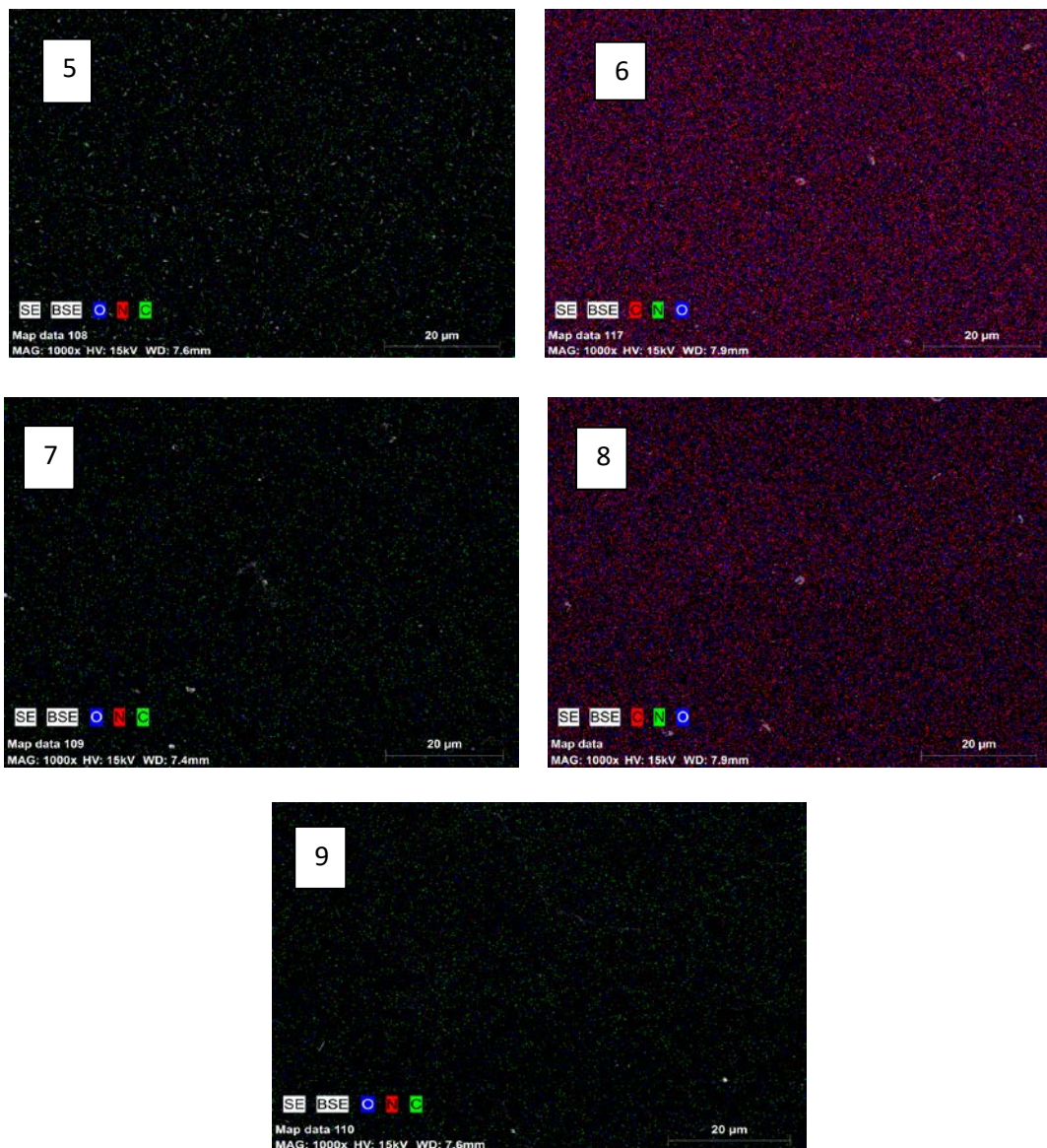
Figure 4.80. Elemental mapping of modified graphene-doped 2-HEC films. (1: G, 2:GN, 3: GPEI, 4: GVIM, 5: GDEA, 6: GN-PEI, 7: GN-VIM, 8: GDEA-PEI, 9: GDEA-VIM)

Table 4.20. Elemental mapping analysis results for modified graphene-doped 2-HEC films comparable with modified graphene composites

	Element %			Element % (with 2-HEC)		
	C	O	N	C	O	N
G	100	-	-	55.28	44.72	0.00
GN	86.36	9.62	4.02	53.25	46.45	0.30
GVIM	88.38	7.08	4.54	54.77	44.20	1.03
GN-VIM	85.36	10.47	4.17	54.79	43.94	1.27

4.3.5. The results of DSC analysis of modified graphene-doped 2-HEC films

Differential scanning calorimetry was used as an outstanding method to observe the glass transition and melting nature of the 2-HEC films. DSC curves for modified graphene-doped 2-HEC films are presented in Figure 4.81. In the DSC thermogram of pristine 2-HEC, an endothermic curling at 177°C due to a segmental motion of the polymer molecules reflecting the glass transition of 2-HEC. As a definition, the glass transition temperature is a thermal behavior of the amorphous regions present in the polymer. The DSC of 2-HEC displayed a broad and double-humped endothermic peak at 310°C and 339°C confirming the melting temperature of the different crystalline segments of polymer.

After incorporation of pristine graphene into the 2-HEC, the first and second melting peaks of the 2-HEC was seen as a single but complex peak and shifted to 335°C. Based on the results of this and previous analyzes, we can say that the graphene diffuses uniformly in the 2-HEC crystal structure and gives the structure stability. When the DSC curves of 2-HEC films prepared after the modification of the graphene with different agents are examined, it is possible to see the melting peak again at about 335°C. However, the curve is more symmetrical than complex. This result can be interpreted as follows: Graphene structure with hydrophobic character has acquired hydrophilic character after being modified. Since the graphene structure is now hydrophilic, it has better compatibility with the hydrophilic 2-HEC and interacted. This leads to a homogeneous distribution of the different segments of the 2-HEC structure.
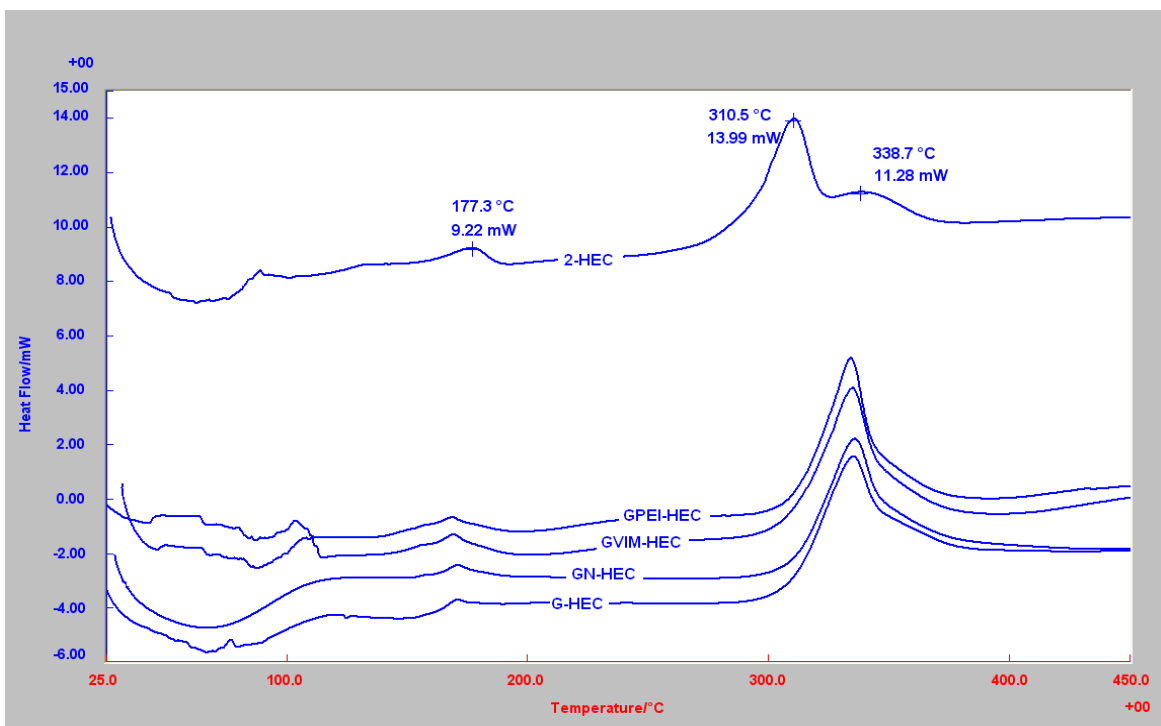
Figure 4.81. DSC thermogram of pristine and modified graphene-doped 2-HEC films.
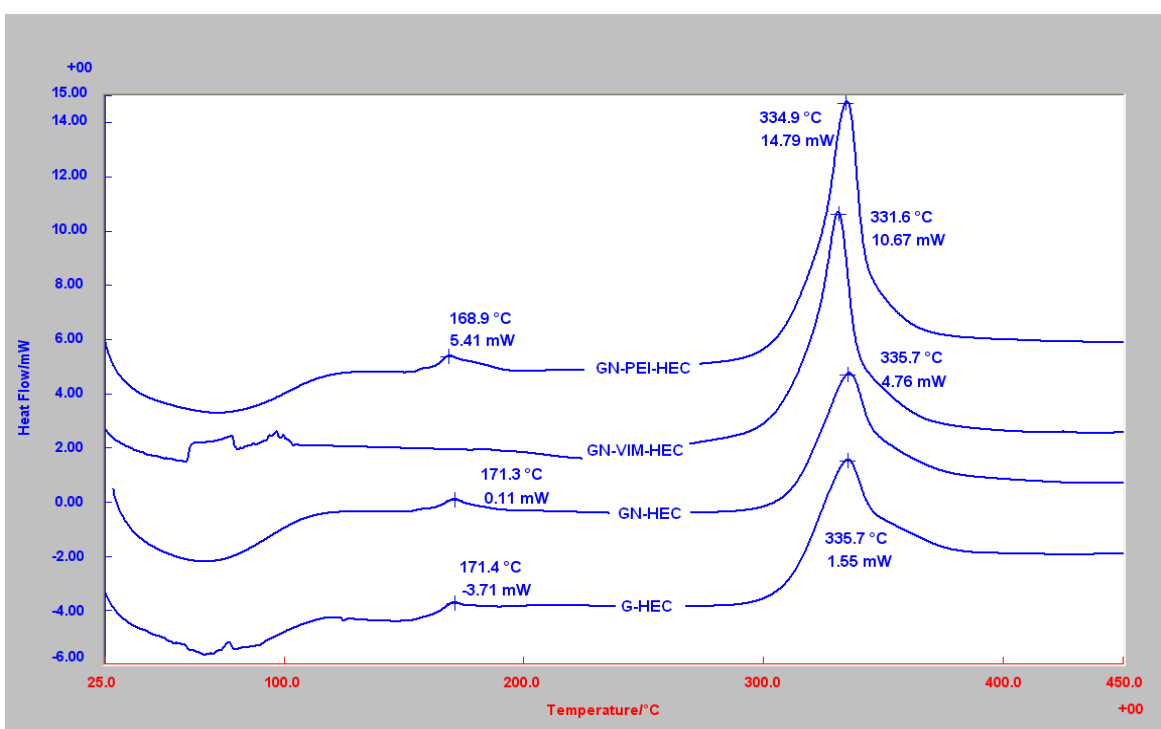
Figure 4.82. DSC thermogram of pristine and HNO$_3$-modified graphene-doped 2-HEC composite films.

Figure 4.82 shows the DSC curves of 2-HEC films doped with composites of HNO_3 modified graphene with VIM and PEI. A slight change was observed in the decreasing direction at the glass transition temperature observed at 177°C in the 2-HEC structure. We can say that this is due to the chain flexibility provided by two volume groups such as VIM and PEI that participate in the graphene structure. On the other hand, the melting peak of 2-HEC still has a symmetrical, smooth appearance, showing better segmental mixing due to the increased hydrophilic character of the modified graphene with VIM and PEI. A similar result was obtained in a study with biofield treatment of HEC and HPC [185]. When the thermal behavior of the 2-HEC structure designed as a drug delivery system was evaluated before and after the biofield treatment, the glass transition temperature and the melting point of the 2-HEC were observed at high temperatures due to the restriction of segmental motion in the amorphous regions due to the treatment.

Figure 4.83 shows the DSC curves of 2-HEC films doped with composites of DEA modified graphene with VIM and PEI. The interpretation of the incorporation of the DEA modified graphene composites prepared with VIM and PEI into the 2-HEC structure is similar to the comments made on the previous graphic. The glass transition temperature was again shifted to lower temperatures and the melting peak was observed at almost the same temperature. Melting peak is relatively symmetrical. The difference observed in PEI modified graphene-DEA-doped 2-HEC composite films can be explained by the presence of possible H-bonds between the NH and NH_2 groups in the DEA and PEI structure.
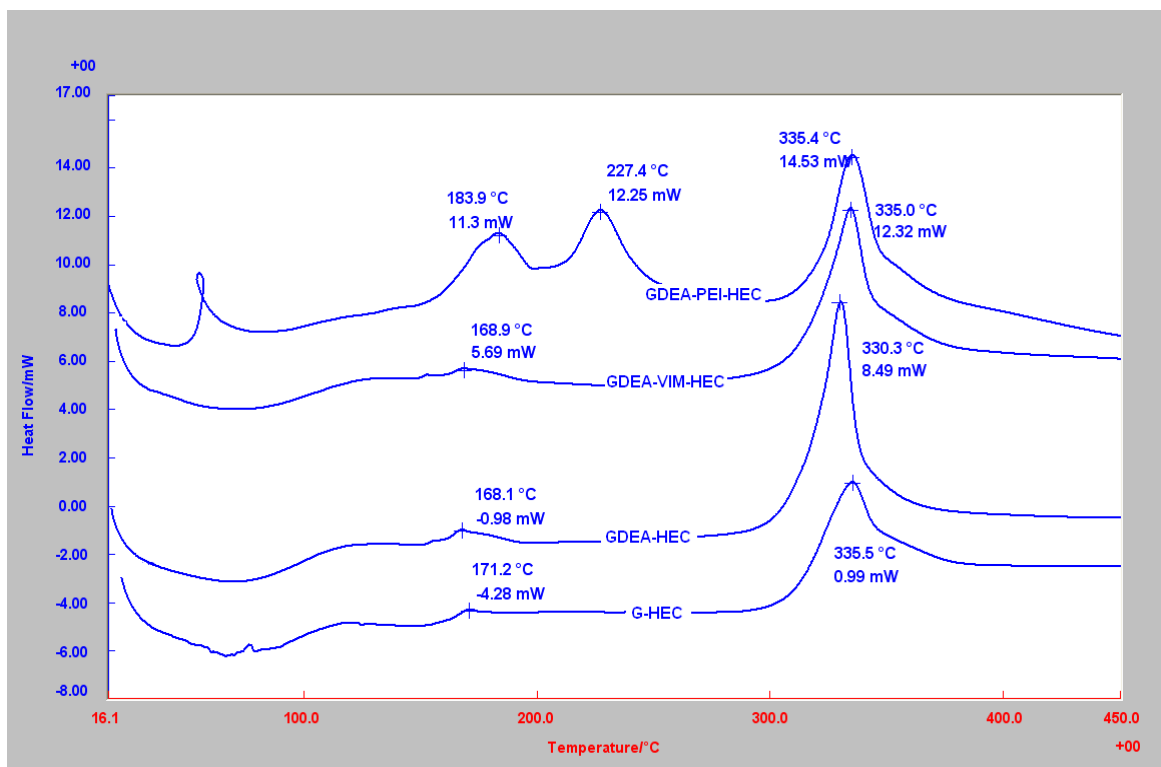
Figure 4.83. DSC thermogram of pristine and DEA modified graphene-doped 2-HEC composite films.

4.3.6. Mechanical behavior of modified graphene-doped 2-HEC films

Figure 4.84 shows the mechanical behavior of modified graphene-doped 2-HEC films. In the stress-strain curve obtained for pristine graphene-doped 2-HEC films, the tensile strength value obtained for 1.12% elongation was lower than the modified graphenes and found to be 16.5 MPa. This is a consequence of the fact that hydrophobic graphene sheets cannot interact with 2-HEC and therefore cannot be homogeneously dispersed. There was a significant increase in % elongation and stress values of all samples depending on the modification of the graphene with different agents. In general, this can be explained as a result of the presence of new functional groups formed in the graphene layers and the better and homogeneous distribution of the hydrophilic graphene layers to the 2-HEC structure. When all the modified graphenes are taken into consideration, the stress and strain values of 2-HEC films containing GN, GVIM, GPEI and GNVIM are found to be higher than those of other modified graphene-doped 2-HEC films. The reason for the high stress-strain values of GN-doped 2-HEC films can be explained as follows: The presence of O-functional groups formed on the

124

graphene with oxidizing agent increased the number of H-bonds on 2-HEC, thus interactively imparting elasticity to the structure. When evaluated from another perspective; the elasticity of the graphene with the O group in the regions containing the crystal phase in the semi-crystalline 2-HEC structure may also be an explanation of this observation. In a study in the literature [186], nanocomposites of polyurethane with functionalized graphene sheets were prepared and their structural, morphological, thermal and mechanical behaviors were investigated. Functional graphene sheets were prepared by exfoliating the graphite oxide chemically. When the mechanical behaviors of polyurethane nanocomposites with these graphene sheets were investigated, tensile strength and elongation at break were decreased due to increase of the amount of functional graphene sheets in the composites and tensile modulus was increased and this was explained by the inhibition of molecular rearrangement and orientation.

The situation in GPEI-doped 2-HEC films is may be due to the increased interactions due to the H-bonds formed in the 2-HEC structure through the abundant NH_2 groups on the PEI chains, thereby increasing the homogeneous distribution as well as the segmental mobility. On the other hand, the increase in stress and strain values of 2-HEC films prepared with first HNO_3 followed by VIM modified graphene may be arised from homogeneous distribution of graphene into the cellulose. H bonds formed between the N-H group of VIM and the O-H group of 2-HEC, as well as π-π stacking interactions, may have resulted in a homogeneous distribution of the graphene. The mechanical test results for all modified graphene-doped 2-HEC films are given in Figure 4.85. The interpretations made above can be reached from this figure.
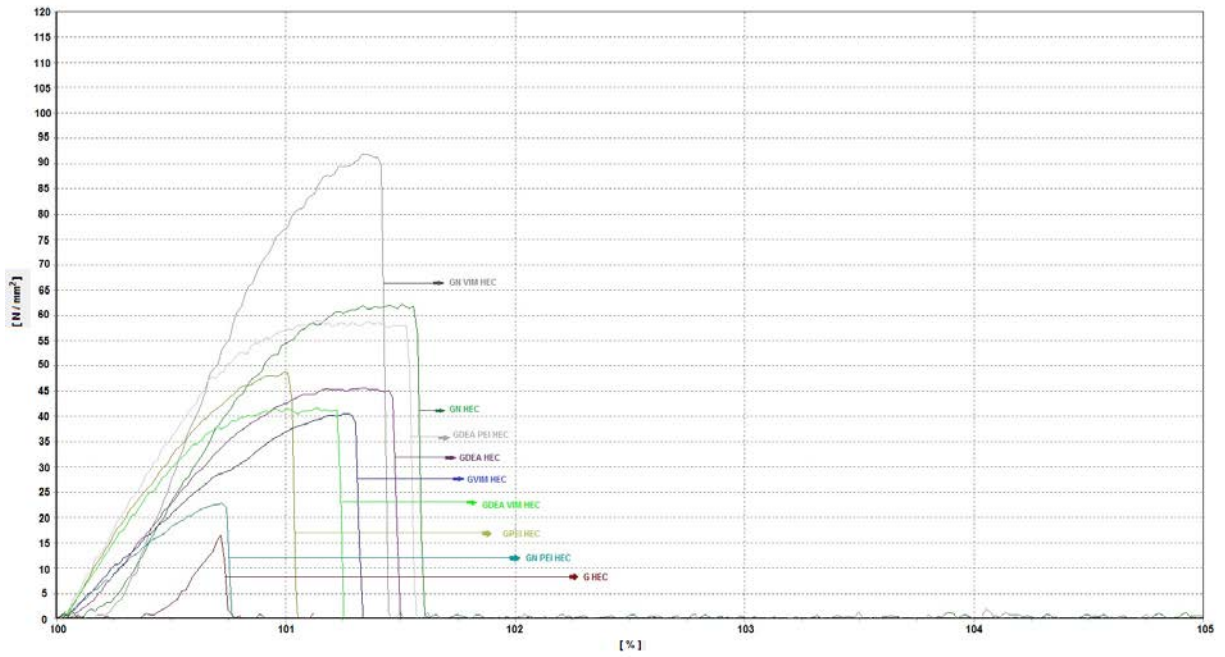
Figure 4.84. Mechanical behavior of modified graphene-doped 2-HEC films
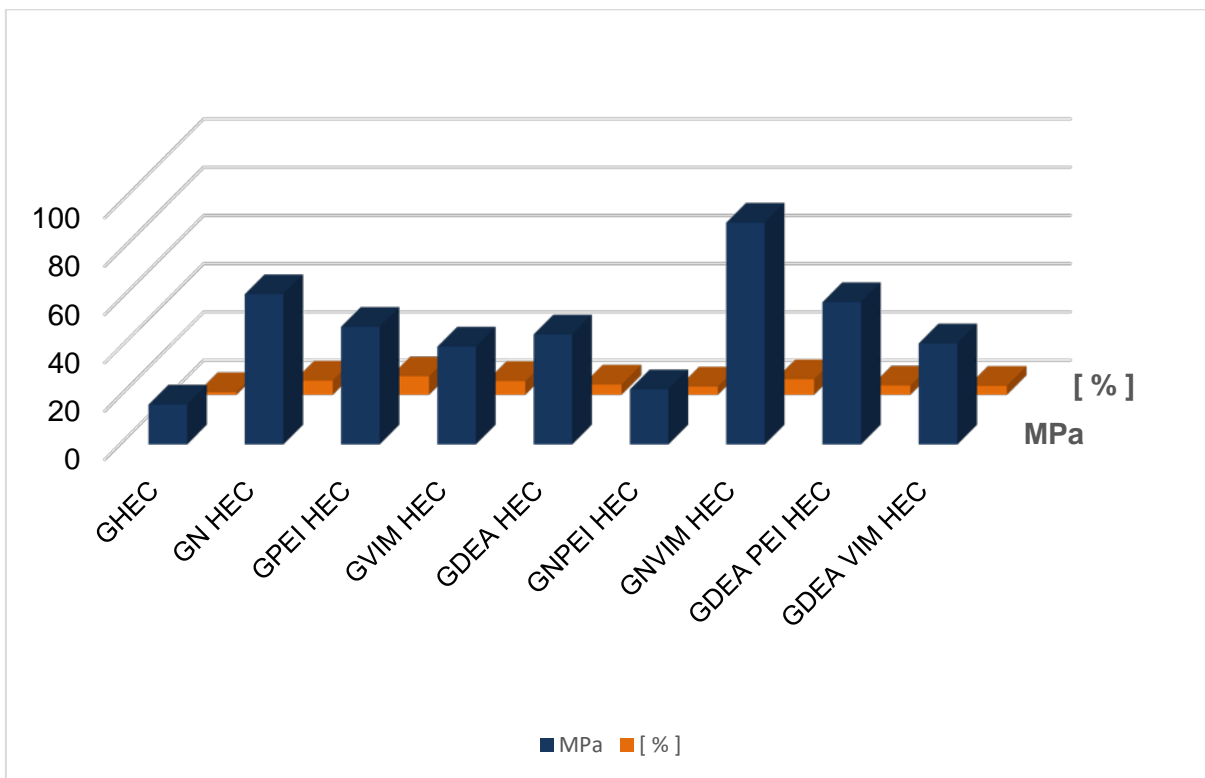
Figure 4.85. Stress-strain results of all modified graphene-doped 2-HEC films

4.4. Applications of graphene and prepared graphene derivatives

Graphene, as an amazing and wonderful material to each of nanocarbons family has drawn considerable interest in many fields. Its unique structure contributes to its fascinating chemical and physical properties, which lead to a broad range of applications in sensing. In this study, significant advances in functionalized graphene related to its electronic structure, biocompatibility and other things obtained through all characterizations indicate that graphene can successfully investigate by that procedure that we used. However, graphene, as a newly discovered material, faces several challenges including improving synthesis methods, extensive understanding of graphene surface and extending the applications in various practical fields.

4.4.1 Use of modified graphene-doped 2-HEC films for *doxorubicine* release

Another study intended in this thesis was to investigate the use of modified graphene and composite graphene samples in biological applications. For this reason, a certain amount of *doxorubicine* (DOXO), an anticancer drug, was mixed with 2-HEC, modified graphene and water to prepare drug-loaded films. Structural and morphological properties of the films were investigated by FT-IR, XRD, SEM, mapping analyzes and thermal properties by DSC. The results are compared to the same samples without DOXO. Figure 4.86 shows the FT-IR spectra of 2-HEC films containing DOXO. At first glance there may appear to be no difference between the spectra. However, in detail (Figure 4.87), there are significant peaks indicating the presence of DOXO.
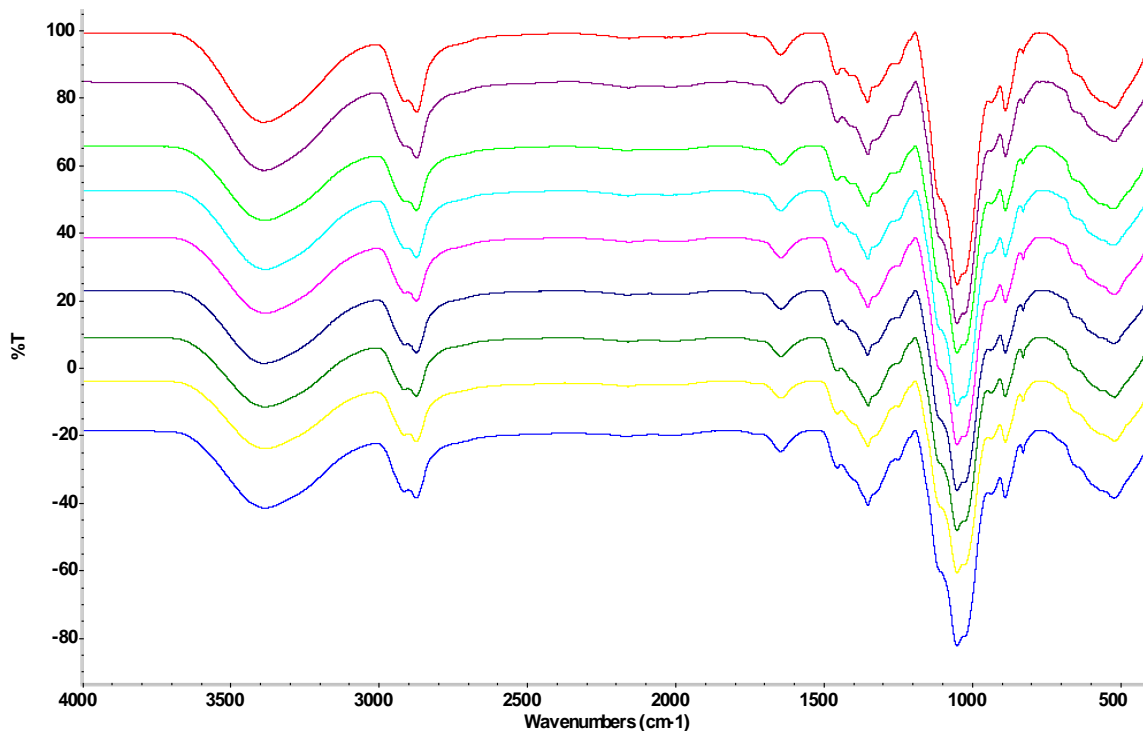
Figure 4.86. FT-IR spectra of DOXO loaded, modified graphene-doped 2-HEC films (from top to bottom: G, GN, GPEI, GVIM, GDEA, GN-PEI, GN-VIM, GDEA-PEI, GDEA-VIM)
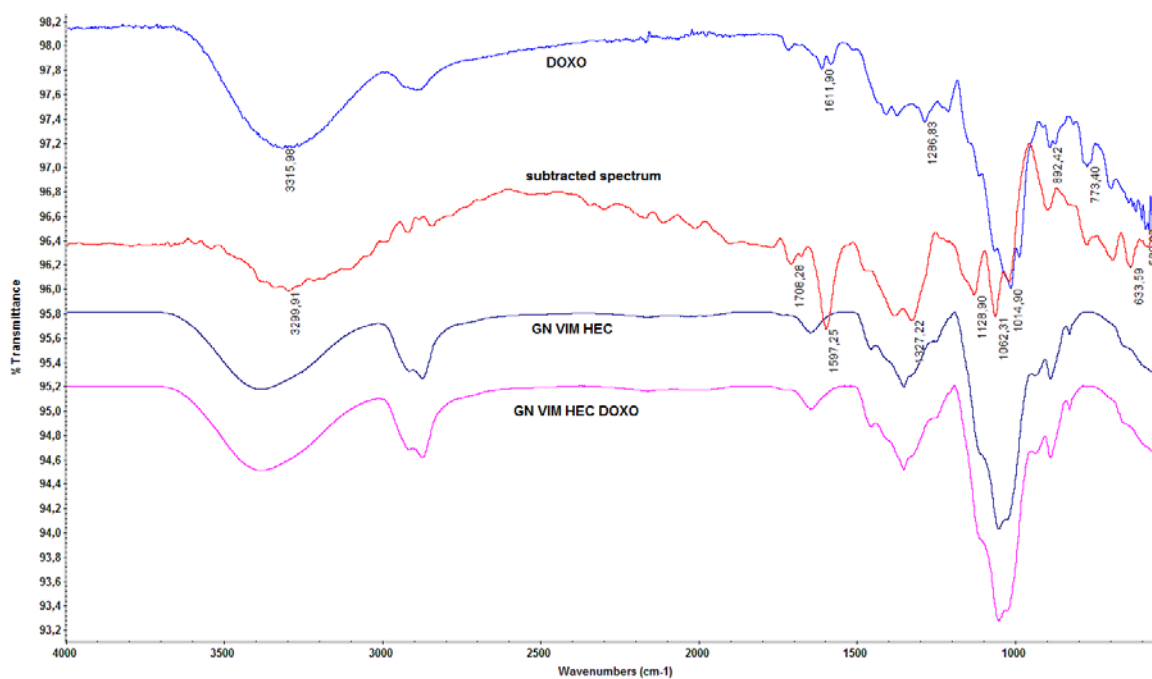
Figure 4.87. FT-IR spectra of DOXO loaded, GN-VIM- 2-HEC films

The peak of –OH groups at 3316 cm^{-1} observed for pure DOXO spectrum, has a small shift to the lower band and reaches a value of 3300 cm^{-1} due to possibly the interaction of DOXO with GNVIM-doped 2-HEC films. The characteristic peaks at 1725, 1612 and 1070 cm^{-1} are assigned to quinone and ketone carbonyl groups. The peak at 1725 cm^{-1} arised from the stretching bands of the C=O groups shifted to 1708 cm^{-1} indicating the interactions between DOXO and GNVIM-doped 2-HEC films. The peak at 1612 cm^{-1} is due to the stretching of the N-H groups. This band also shifted to 1597 cm^{-1}. The peak at 1070 cm^{-1} attributed to stretching bands of the C=O groups indicates shift to lower wavenumber (1062 cm^{-1}). The peaks at 892 and 773 cm^{-1} are due to the primary amine NH$_2$ wag and N-H deformation bonds, respectively [187]. All these observations prove the effective loading of DOXO on modified graphene-doped 2-HEC films.

In order to analyze in more detail the interaction between DOXO and GNVIM-doped 2-HEC films, the crystal characteristics of the DOXO/GNVIM-2-HEC complex were examined by XRD (Figure 4.88). For DOXO (inset figure), clear peaks at 2θ about 32° and 45° are visible in the diffractogram indicating the presence of crystalline phase in the native form. These peaks were not wholly present in the diffraction pattern of GNVIM-2-HEC films, suggesting that DOXO could be loaded by matrix material in molecular form. A similar result has also been found in oxidized carbon nanotubes modified with betulinic acid. Sharp peaks of betulinic acid have not been observed in the XRD spectrum after drug loading into the matrix material, and this has been described as loading of the betulinic acid into the carbon nanotubes in molecular form [188].
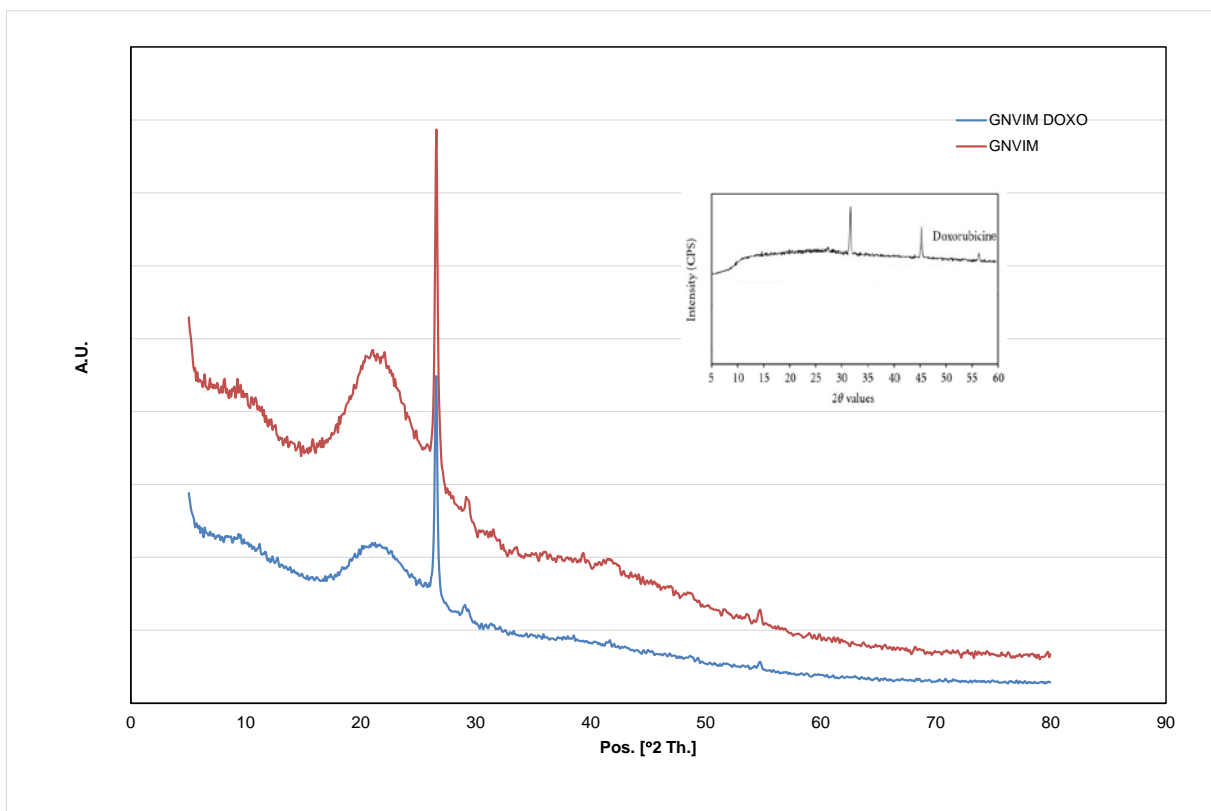
Figure 4.88. XRD spectra of DOXO loaded, GNVIM- 2-HEC films

The morphological characteristics of DOXO loaded, modified graphene 2-HEC films were analyzed by SEM and EDS mediated mapping analysis. Since the amount of DOXO in samples was very low, no difference was observed between the SEM images of samples with and without DOXO (see Figure 4.89). However, if we look at the mapping image given in Figure 4.90, only C and O elements are present for pristine graphene-2-HEC film (left hand-side), but, in DOXO loaded, pristine graphene-2-HEC film, N atoms arised from DOXO has been added to structure. Table 4.21 summarized all mapping results and as can be seen from this table, there has been an slight increase in N % of structure after DOXO is loaded.
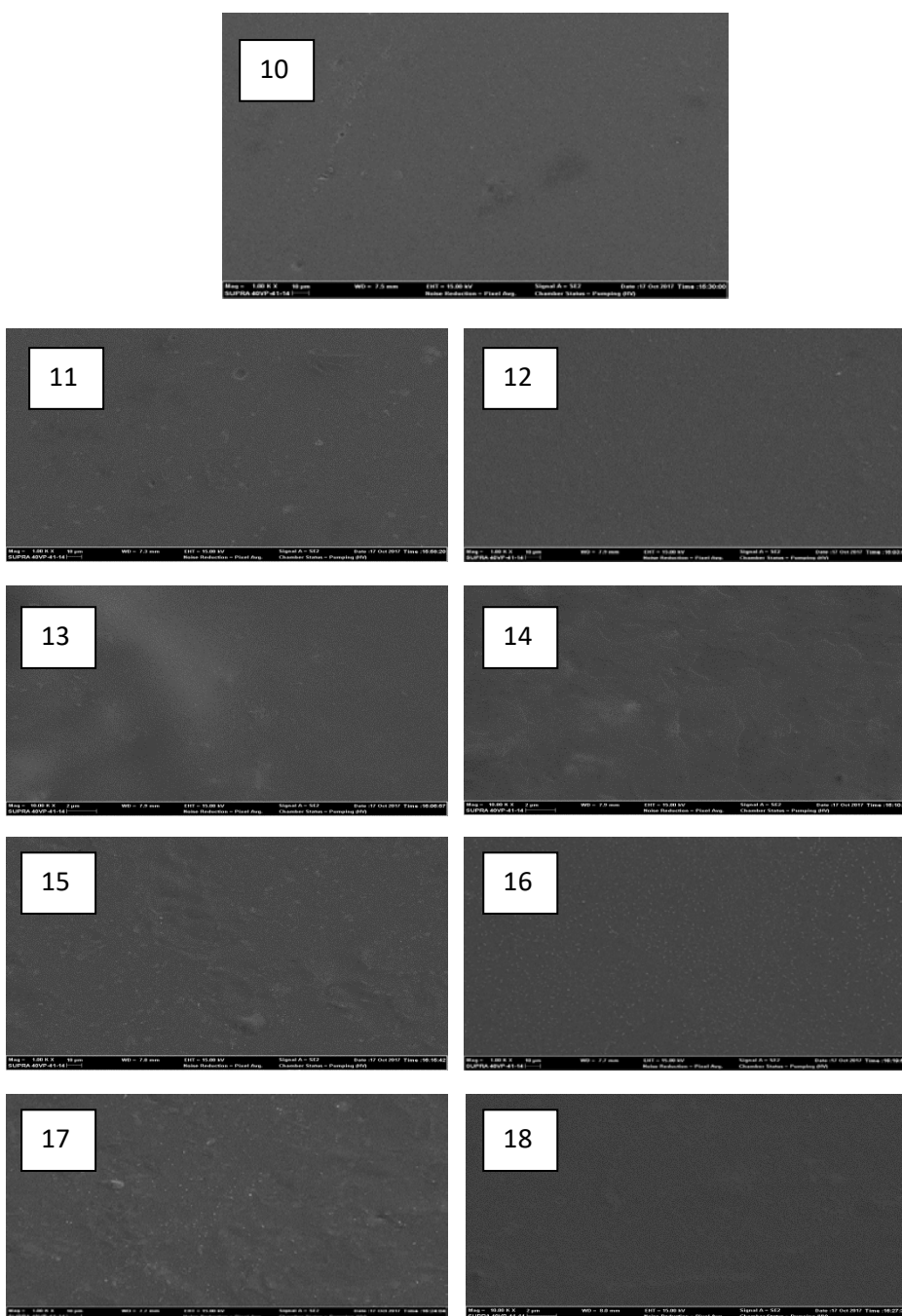
Figure 4.89. SEM images of DOXO loaded, modified graphene doped 2-HEC films (10:G, 11:GN, 12:GPEI, 13:GVIM, 14:GDEA, 15:GN-PEI, 16:GN-VIM, 17:GDEA-PEI, 18:GDEA-VIM)
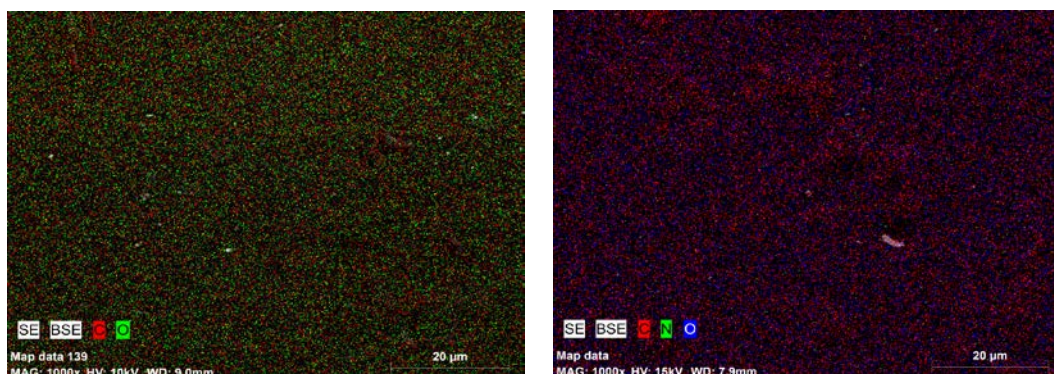
Figure 4.90. Elemental mapping of pristine graphene – 2-HEC (left) and DOXO loaded, pristine graphene - 2-HEC (right) films.

Table 4.21. Elemental mapping analysis results for DOXO loaded, modified graphene-doped 2-HEC films

| | Element % | | | Element % | | |
| | without DOXO | | | with DOXO | | |
	C	O	N	C	O	N
G	55.28	44.72	0.00	56.78	41.97	1.25
GN	53.25	46.45	0.30	56.68	42.12	1.20
GPEI	50.83	46.99	2.18	55.72	43.16	1.12
GVIM	54.77	44.20	1.03	55.95	42.71	1.34
GDEA	53.26	46.22	0.52	57.04	42.09	0.87
GNPEI	53.69	44.74	1.57	52.97	45.21	1.82
GNVIM	54.79	43.94	1.27	56.08	43.16	0.76
GDEAPEI	53.19	45.80	1.01	54.75	44.10	1.15
GDEAVIM	53.53	44.95	1.52	54.25	44.39	1.37

In addition to the characterizations given above, DSC thermograms of 2-HEC film samples containing DOXO were also taken (a) to learn how DOXO is dispersed into 2-HEC modified graphene films, (b) to understand whether pure DOXO precipitate or not during interaction, and (c) to prove that there is a specific interaction between DOXO and modified graphene-doped 2-HEC. Since the DSC thermograms taken after DOXO loading on modified graphene-doped 2-HEC films show similar characteristics, thermograms of HNO_3 modified graphene-doped 2-HEC with and without DOXO are given here, as an example (Figure 4.91). The glass transition temperature observed at 177°C and the melting peak observed at 335°C in the thermogram of HNO_3 modified graphene-doped 2-HEC film has been

shifted to lower temperatures after DOXO was loaded. In the DSC thermogram of pure DOXO, two characteristic peaks with behavior of crystalline regions were observed at 174°C and 189°C. DOXO peaks observed at 154°C and 174°C, when compared to the subtracted spectrum, are an indication that DOXO is in partially crystalline state in the 2-HEC film structure. In Figure 4.92, there is a different situation in the DSC thermogram from HNO$_3$ - PEI modified graphene-doped 2-HEC films. Here we can say that the DOXO crystals are relatively separated and enter the film structure, and that DOXO has not been precipitated during the interaction. In addition, the absence of shifts at the glass transition temperature observed at 177°C and also at the melting peak observed at 335°C of the main structure in the thermogram of HNO$_3$ - PEI modified graphene-doped 2-HEC films (with and without DOXO) indicates the interaction with DOXO is not too strong. The findings obtained in a study on DOXO release in the literature are interesting. DSC results of the interaction between DOXO and γ-polyglutamic acid [189] are very similar to the results that we have obtained in our study.

All information picked up from DSC thermograms are presented in Table 4.22. Maximum peak temperatures and area of endotherms are obviously seen from this table for all modified graphene-doped 2-HEC films.
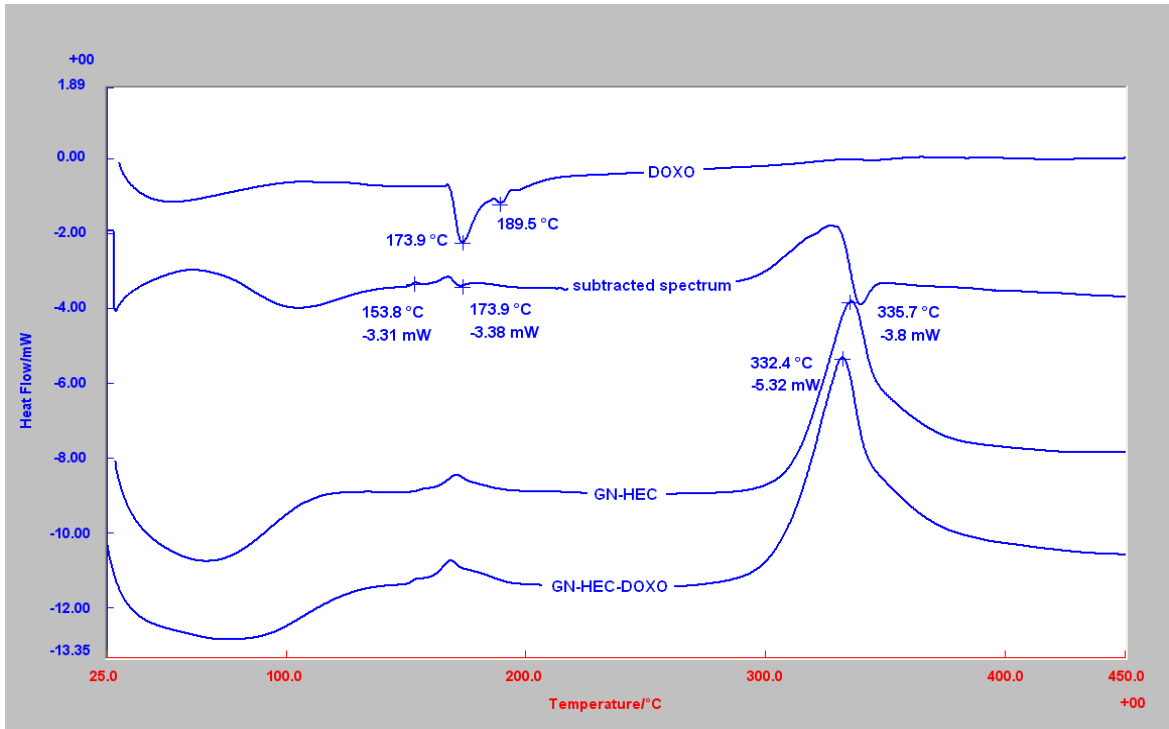
Figure 4.91. DSC thermograms of pure DOXO and DOXO loaded HNO_3 modified graphene-doped 2-HEC film.
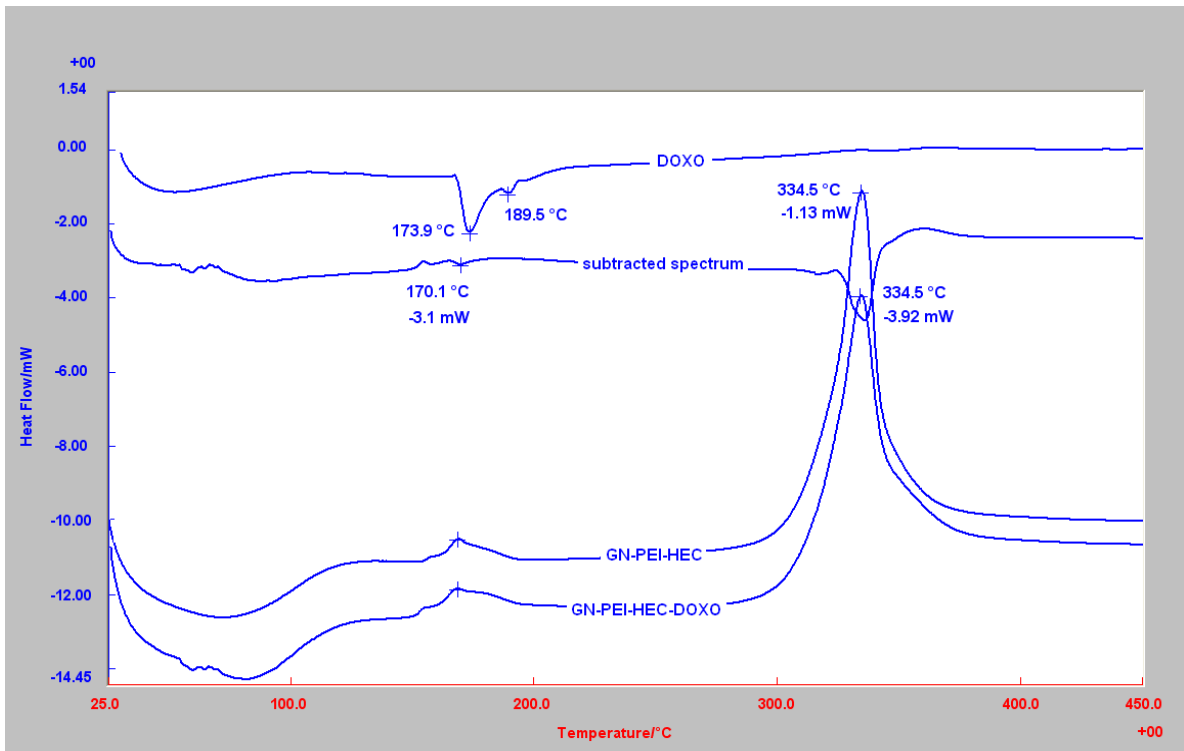
Figure 4.92. DSC thermograms of pure DOXO and DOXO loaded HNO_3 – PEI modified graphene-doped 2-HEC film.

Table 4.22. Maximum peak temperatures and peak area of endotherms in the DSC thermograms of modified graphene-doped 2-HEC film with and without DOXO.

Sample	without DOXO			with DOXO		
	T_{max1} (°C)	T_{max2} (°C)	Area (J/g)	T_{max1} (°C)	T_{max2} (°C)	Area (J/g)
G	170	335	195	175	339	213
GN	171	336	198	168	332	211
GPEI	168	334	198	169	336	181
GVIM	169	335	212	167	333	196
GDEA	167	330	261	169	331	256
GNPEI	169	335	287	168	334.5	216
GNVIM	167	331	249	182	335	213
GDEAPEI	186 - 227	335	216	168	336	209
GDEAVIM	168	335	251	168	335	194
2-HEC	177	310 - 339	181			

Doxorubicin, a representative anthracycline antibiotic, is one of the most widely used anticancer drugs in clinical applications; however, it is highly toxic in humans and can result in severe suppression of hematopoiesis, gastrointestinal and cardiac toxicity. The very high toxicity levels often involved in the use of these drugs prompted the recent research to generate selective carrier conjugates able to release the drug into cancerous cells or tumors, minimizing their distribution and toxicity in healthy tissues. DOXO association to nanoparticulate carriers such as liposomes, nanoparticles or micelles, dendrimers, nanoshell, carbon nanotubes have led to its controlled release over extended periods of time, thereby enhancing antitumor efficacy, improving safety profile and decreasing toxic side effects compared with free drug [190].

DOXO release profiles of all modified graphene-doped 2-HEC films were investigated under simulated physiological conditions (PBS, pH 7.4) and in an acidic medium (PBS, pH 4.5) at room temperature. The results were given in Figure 4.93 and 4.94. Generally speaking, the DOXO release is highly dependent on pH. As shown in Figure 4.93, except for the G, GN and GPEI-doped 2-HEC films, the release is fairly slow and only about 15-20% over the 1-day period, i.e. DOXO on modified graphene -doped 2-HEC films were stable in PBS buffer at pH 4.5. The percent release obtained from pristine graphene-doped 2-HEC films is

higher than that of all samples and is around 60%. This value was followed by GN and GPEI modified 2-HEC with 55% and 45% release values after 1 day period. Fast DOXO release from pristine graphene- doped 2-HEC films is expected result. Because the graphene is not modified here, there are no existing groups to interact with the acidic and basic groups of the DOXO structure in the hydrophobic graphene structure. Partially due to the DOXO trapped between the graphene layers and the DOXO interaction with the OH group of 2-HEC, the release value remained at about 60%.

As a model cancer drug, DOXO is known to have pH-dependent hydrophilicity. As the literature recognizes, doxorubicine is a natural anticancer agent and a basic (pK_a = 8.2), primary amine [191]. At acidic pH conditions, DOXO is protonated and quite water-soluble, which does not facilitate the hydrophobic $\pi-\pi$ stacking interaction with the pristine graphene, GN, and GPEI-doped 2-HEC films. In contrast, under basic condition, the deprotonated DOXO is quite hydrophobic, which is advantageous for its effective $\pi-\pi$ stacking interaction with the modified graphene-doped 2-HEC films. The lower DOXO release percentage of VIM and PEI modified graphene and composite-doped 2-HEC films than that of the pristine graphene, GN, and GPEI-doped 2-HEC films may be due to the fact that the modifications of branched PEI and VIM are quite effective in occupying the surface of graphene, thereby restricting the $\pi-\pi$ stacking interaction between DOXO and the graphene-doped 2-HEC films.
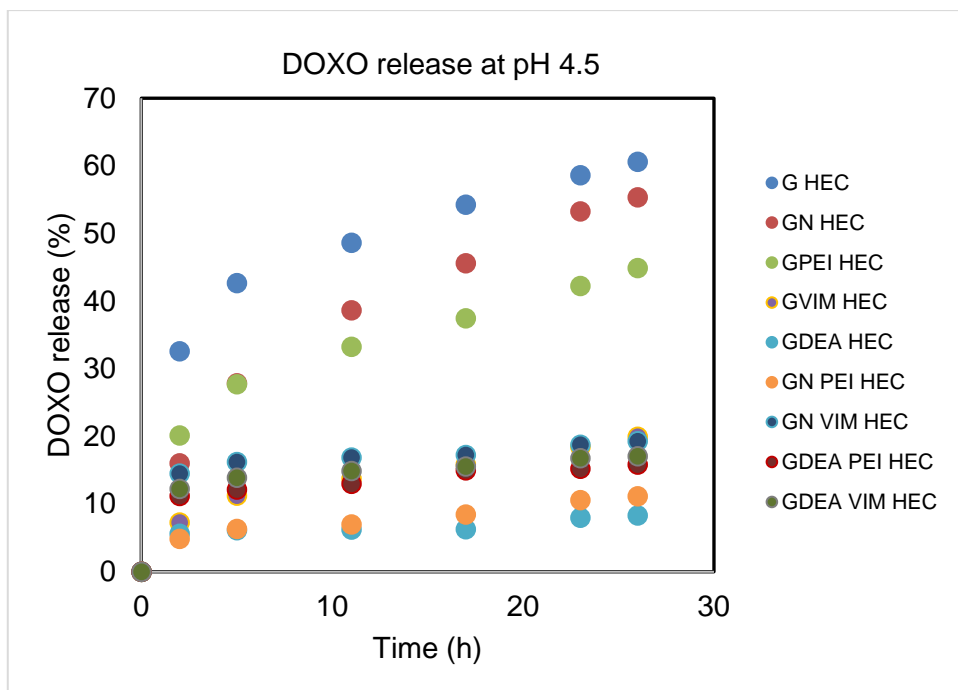
Figure 4.93. DOXO release from all types of graphene-doped 2-HEC films at pH 4.5

It can be seen from Figure 4.94, the DOXO release value is higher at pH 4.5 than at pH 7.4. After 1 day, 60 % of DOXO was released at the acidic pH (pH = 4.5), while only 40 % of DOXO was released at the physiological pH of 7.4. The pH-dependent DOXO release of modified graphene-doped 2-HEC films is useful for treating tumor site with slightly acidic pH microenvironment.
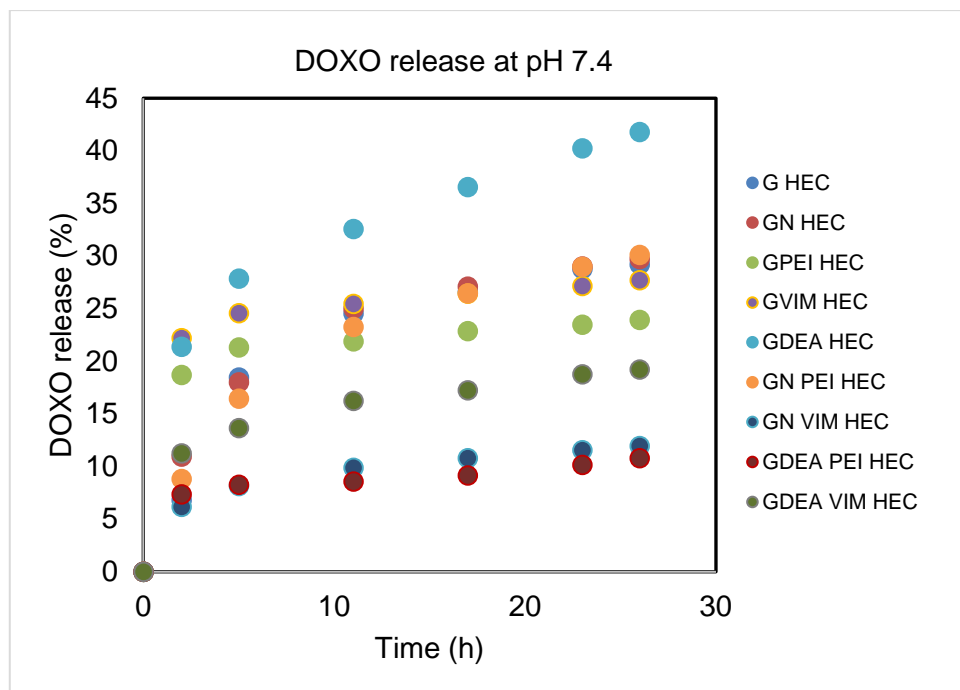
Figure 4.94. DOXO release from all types of graphene-doped 2-HEC films at pH 7.4

An interesting point in Figure 4.94 is that there is about 40% DOXO release from DEA modified graphene-doped 2-HEC films, while release from DEA-VIM and DEA-PEI modified graphene-doped 2-HEC films is only 10%. We can explain this observation as follows: Hydrophobic graphene layers are more sensitive to oxidizing agents. Modification is more successful with acidic agents than with amine-containing agents. Therefore, we can say that DOXO release at pH 7.4 is higher in GDEA-2-HEC films with the prediction that the amount of modification with DEA is kept low. Due to the N atoms formed by the modification of the DEA in the graphene layers, bulky groups such as PEI and VIM with potential amine groups for H-bonding are easier to attach. Therefore, due to increased N-H groups in the graphene, the release value is found to be low at this pH value as a result of increased interaction with the -OH, C = O and NH_2 groups on DOXO. Another special case for VIM is the interaction of π-π stacking with DOXO due to the π-bonds present in the imidazole with the five rings.

As a result, we can say that the binding between DOXO and modified graphene - doped 2-HEC films was due to electrostatic, π-π stacking and van der Waals interactions, also due to the pH dependent characteristics of both the modified graphene and DOXO, these interactions led to relatively different release curves.

4.4.2. Measurements for electrical conductivity of modified graphene doped 2-HEC films

The electrical conductivities of modified graphene doped 2-HEC films were investigated as well as their usability as a drug release system.

Table 4.23 Electrical information obtained for modified graphene 2-HEC films

Sample	Resonance frequency Hz	Impedance kΩ	Resistance mΩ
G	290	819	4
GN	290	557	3.2
GPEI	240	824	3.6
GVIM	240	575.6	3.0
GDEA	40	692	1.4
GN-PEI	250	582	3.0
GN-VIM	240	537	2.2
GDEA-PEI	530	199	0.5
GDEA-VIM	500	325	2.2

Table 4.23 and Figure 4.95 illustrate the electrical conductivity of graphene, modified graphene and their composites separately doped into 2-HEC.

Table 4.23 shows that all modified graphenes and their composite films has high impedance in resonance frequency while GDEA-PEI show up minimal impedance 199 kΩ by resonance frequency 500 Hz when compared to pristine graphene-2 - HEC that has 819 kΩ by resonance frequency 290 Hz. It means that this composite film has more conductivity than the other compounds that was prepared. In general, each modified product gave high effectiveness of conductivity, we conclude from this results that could confirm the properties of graphene and successfully modified happened.

For all modified specimens, the explanations we mentioned above can be seen more clearly when the direct current being passed is plotted against the measured resistance. The best result is obtained with GDEA-PEI giving a value of 0.5 mΩ, see Figure 4.95.
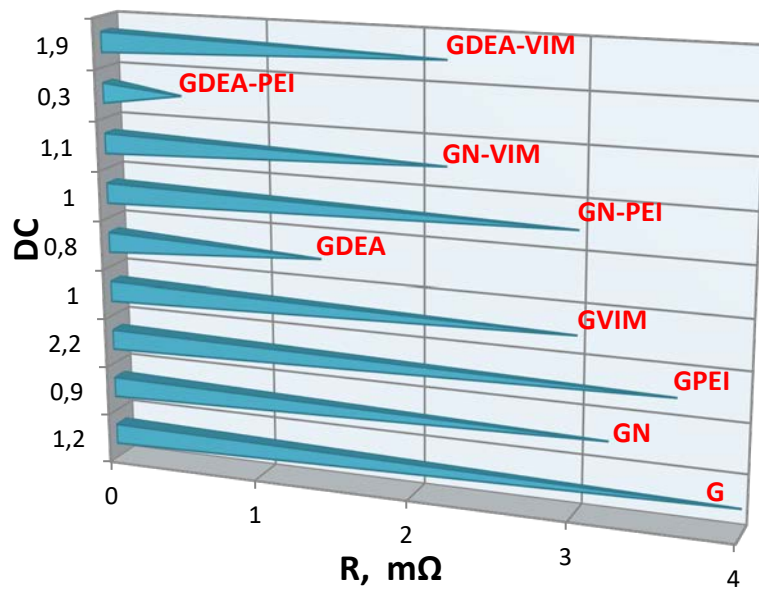
Figure 4.95. Relationship between direct current and resistance for all types of graphene doped 2-HEC films

5. OVERALL RESULTS

- Graphene has been chosen as the subject of this study because it possesses many distinctive properties. It is originally hydrocarbon product that prepared from graphite material that has been used since time immemorial in the manufacture of pencils. It is also cheap and available and has many properties that made it interesting and unique subject for the researchers.

- As a second step in this study, Composite was formed by selecting only two of acid modified graphene, all of which were satisfactory. The choice was based on the use of samples giving clear results by using low concentration and low time of stirring considering eco-friendly manner. The selected graphene samples are the GN21, GP21 where each of them was treated with PEI, VIM to obtained 4 new composite GN-PEI, GN-VIM, GP-PEI, and GP-VIM.

- GDEA and GEDA reacted with PEI, also VIM to produce 4 different composites GDEA-PEI, GDEA-VIM, GEDA-PEI, and GEDA-VIM. The total composite prepared from acid and base was 8.

- The third step in this study was to prepare a film to be applied in several fields. Nine different samples were selected including graphene, from we prepared, the film was prepared using 2-HEC with crosslinker in water.

- The properties of all the samples prepared in the different steps were characterized by using different techniques. All these techniques prove that results of each part were successfully obtained.

- The first characterization technique in which we identified the presence of added groups on the graphene is, FT-IR, which showed clear absorption of the groups expected to entering surface area of graphene and inter layer. Through acid modification, hydroxyl and carbonyl groups were observed, according to different concentrations of acids. As for the treatment with the different conditions, also the amino group was observed in the modification by amines. For different composites, new functional groups were observed indicating that the interactions were successfully happened. The FT-IR also indicated that graphene and modified graphene were doped into 2-HEC film.

- The XRD analysis, which depends on the reflections and diffraction of the incident beams on the crystal along, a specific wavelength according to the bonds and plane of crystal, confirmed that the pristine graphene having hexagonal plane of $2\theta = 26.5°$ did not change its form in modifications and interactions. But there were some changes in the intensity of peak height due to the presence of some adding different groups on graphene, XRD of the films also showed the incorporation of graphene and graphene derivatives into 2-HEC.

- The techniques of SEM, TEM, showed a significant change in the shape and appearance of the graphene surface after modification and the preparation of composites. We clearly saw wrinkles, gaps and bright color that was not observed in graphene which was semi-smooth, all of these signs indicate newly added groups depend on modification. As for the film, we note the homogeneous dispersion of graphene and its derivatives in the 2- HEC layer.

- The different proportions of the elements in the graphene were calculated using the new elemental mapping-EDX technique, which explained the differences in the ratios of C, O, N, depending on the reactant and the product.

- The Raman Spectroscopy had a significant role in clarifying and determining the defect in the basic morphology of the graphene before and after the modification. It was also used to determine the ratio of sp^2 sp^3 bonding, with the I_D/I_G ratio calculation. While in modification carried out with acids there was sp^3 bonding appeared, but the graphene modified with bases showed shifting peak position although the defect ratio was similar to pristine graphene. However, the percentage of change in the hybridization of the compound was not clear, indicating that the incoming amines were lead to no defect on the graphene structure.

- DSC was used to illustrate the evolution and change in the degree of transition of prepared samples. Graphene having a transition of 309.2°C gradually changed these transition by 1.6°C to 310.8° in the modification and increased to 314°C in some composites, reached up to 335°C in film.

- In the stress-strain experiments using 2-HEC films, we observed that the stress values of the modified graphene and composites films were higher than that of pristine graphene (the highest results were obtained from GN-VIM composite films) so that graphene samples were uniformly distributed to the 2-HEC structure after the modification process.

- For the drug delivery, 2-HEC films containing DOXO were prepared in the same manner with 2-HEC. Films were analyzed by FT-IR and XRD that clearly showed doped graphene into 2-HEC film, then applied to drug delivery in different pHs, which gave excellent results better than that pristine graphene.

- 2-HEC films without DOXO were also applied to electrical conductivity measurements, there were seen positive results, all different from pristine graphene.

- This study is being continued on the same subject, and further analysis will be done to calculate the proportion of functional group adding to graphene in the modifications process using other analysis methods such as XPS, AFM and Z potential measurements.

6. REFERENCES

[1]   Madhab Bera and Pradip K Maji, Graphene-Based Polymer Nanocomposites: Materials for Future Revolution, *Science*, 1 (3), 0013, **2017.**

[2]   Yanbin Cui, S. I. Kundalwal and S. Kumar, Gas Barrier Performance of Graphene/PolymerNanocomposites, https://arxiv.org/ftp/arxiv/papers/1509/1509.06256.pdf. **2015.**

[3]   Zorawar Singh and Rumina Singh, Recent Approaches in Use of Graphene Derivatives in Anticancer Drug Delivery Systems, *Journal of Drug Design and Research, J Drug Des Res.* 4(3):1041, **2017.**

[4]   Xiaoyun Qiu and Shuwen Hu, "Smart" Materials Based on Cellulose: A Review of the Preparations, Properties, and Applications*, Materials*, 6, 738-781, **2013.**

[5]   Chenghong Ao, Wei Yuan, Jiangqi Zhao, Xu He, Xiaofang Zhang, Qingye Li, Tian Xi, Wei Zhang, Canhui Lu, Superhydrophilic graphene oxide@electrospun cellulose nanofiber hybrid membrane for high-efficiency oil/water separation, *Carbohydrate Polymers*, 175, 216–222, **2017.**

[6]https://www.acs.org/content/dam/acsorg/education/whatischemistry/landmarks/lesson-plans/discovery-of-fullerenes.pdf

[7]   Adriano Ambrosi, Chun Kiang Chua, Alessandra Bonanni, and Martin Pumera**,** Electrochemistry of Graphene and Related Materials, *Chem. Rev.*, 114, 7150−7188, **2014.**

[8]   Jin-Yong Hong, Jeong Jae Wie, Yu Xu and Ho Seok Park, Chemical modification of graphene aerogels for electrochemical capacitor   applications, *Phys. Chem. Chem. Phys.*, vol. 17, issue 46, pp. 30946-30962, **2015.**

[9   ]https://www.reference.com/science/physical-properties-carbon-30e8ca2d5f7d68d8

[10]   J. Robertson, Diamound-like amphorus carbon, *Material Science and engineering*, R 37, 129-281, **2002.**

[11]   https://www.quora.com/What-is-the-molecular-structure-of-graphite

[12]   T. Pratheep Reddy, P. Charan Theja, B. Eswaraiah, P. Punna Rao**,** Preparation of Aluminium Reinforced with Granite and Graphite – A Hybrid Metal Matrix Composite*, International Journal of Engineering Research & Technology (IJERT)***,** Vol. 6 Issue 10, October **– 2017.**

[13]   https://www.transpacificminerals.com/copy-of-lithium-1

[14]   Edmond Lam and John H.T. Luong, Carbon Materials as Catalyst Supports and Catalysts in the Transformation of Biomass to Fuels and Chemicals, *ACS Catal., 4* (10), pp 3393–3410, **2014.**

[15]   Su-Juan Li, Ning Xia, Xia-Lei Lv, Meng-Meng Zhao, Bai-Qing Yuan, Huan Pang, A facile one-step electrochemical synthesis of graphene/NiO nanocomposites as efficient electrocatalyst for glucose and methanol, *Sensors and Actuators B*, 190, 809–817, **2014.**

[16]   Kuldeep Singh, Anil Ohlan and S.K. Dhawan, Polymer-Graphene Nanocomposites: Preparation, Characterization, Properties, and Applications, ons http://dx.doi.org/10.5772/50408, **2012.**

[17]   http://www.nanoscience.com/applications/education/overview/cnt-technology-overview/

[18]   Snehashis Paul, Twistron - Nano in size, Big on possibilities, https://www.linkedin.com/pulse/twistron-nano-size-big-possibilities-snehashis-paul, **2017.**

 [19]   N. Domun, H. Hadavinia, T. Zhang, T. Sainsbury, G. H. Liaghat and S. Vahid, Improving the fracture toughness and the strength of epoxy using nanomaterials – a review of the current status, *Nanoscale*, 7, 10294–10329, **2015.**

[20]   Ali Eatemadi, Hadis Daraee , Hamzeh Karimkhanloo , Mohammad Kouhi, Nosratollah Zarghami , Abolfazl Akbarzadeh, Mozhgan Abasi , Younes Hanifehpour and Sang Woo Joo, Carbon nanotubes: properties, synthesis, purification, and medical applications, *Nanoscale Research Letters*, , 9:393, **2014.**

[21]   http://www.bbc.co.uk/schools/gcsebitesize/science/add-ocr-gate way/chemical-economics/nanochemistryrev3.shtml

[22]   Science Daily, Fullerene, https://www.sciencedaily.com/terms/fullerene.htm

[23]   Lingling Ou, Bin Song, Huimin Liang, Jia Liu, Xiaoli Feng, Bin Deng, Ting Sun and Longquan Shao,Toxicity of graphene-family nanoparticles: a general review of the origins and mechanisms, *Particle and Fibre Toxicology*, 13:57, **2016.**

[24]   Sumit Goenka, Vinayak Sant, Shilp Sant, Graphene-based nanomaterials for drug delivery and tissue engineering, *Journal of Controlled Release*. 173, 75–88, **2014.**

[25]   Jumana Abdul Jaleel, S. Sruthi, K. Pramod, reinforcing nanomedicine using graphene family nanomaterials*, Journal of Controlled Release*, 255, 218–230, **2017.**

[26]   Rebecca S. Edwards and Karl S. Coleman, Graphene synthesis: relationship to applications, *Nanoscale*, 5,38-51, **2013.**

[27]   Chao Zhou, Sihao Chen, Jianzhong Lou, Jihu Wang, Qiujie Yang, Chuanrong Liu, Dapeng Huang and Tonghe Zhu, Graphene's cousin: the present and future of Graphene, *Nanoscale Research Letters*, 9:26, **2014.**

[28]   Ankita Dixit, Divya Dixit, Vidhi Vart Chandrodaya, Ashok kajla, Graphene: A new Era of Technology, *International Journal of Emerging Technology and Advanced Engineering*, Volume 3, Issue 3, **2013.**

[29]   https://www.materialstoday.com/carbon/articles/s1369702112701013

[30]   Phitsini Suvarnaphaet and Suejit Pechprasarn, Graphene-Based Materials for Biosensors: A Review, *Sensors*, 17, 2161, **2017.**

[31]   Rajni Garg, Naba K. Dutta and Namita Roy Choudhury, Work Function Engineering of Graphene, *Nanomaterials*, 4, 267-300, **2014.**

[32]   Yun-Jung Choi, Eunsu Kim, Jae Woong Han, Jin-Hoi Kim and Sangiliyandi Guru Nathan, A Novel Biomolecule-Mediated Reduction of Graphene Oxide: A Multifunctional Anti-Cancer Agent, *Molecules*, 21, 375, **2016.**

[33]   Sitansu Sekhar Nanda, Georgia C. Papaefthymiou, and Dong Kee Yi, Functionalization of Graphene Oxide AND Its Biomedical Applications- Critical Reviews in *Solid State and Materials Sciences*, 0:1–25, **2015.**

[34]   Chun Kiang Chua and Martin Pumera, Chemical reduction of graphene oxide: a synthetic chemistry viewpoint, *Chem. Soc. Rev.*, 43, 291—312, **2014.**

[35]   Fatimah Abdulbaqi Alussail, Synthesis and Characterization of Reduced Graphene Oxide Films**,** *Thesis of Master of Applied Science in Mechanical Engineering (Nanotechnology)*, University of Waterloo, Ontario, Canada, p.p. 3. **2015.**

[36]   Le Xin, Fan Yang, Somaye Rasouli, Yang Qiu, Zhe-Fei Li, ChengJun Sun, Yuzi Liu, Paulo Ferreira, Wenzhen Li, Yang Ren, and Jian Xie Understanding Pt nanoparticle anchoring on graphene supports through surface functionalization*, ACS Paragon Plus Environment*, **2016.**

[37]   Olena Ustavytska, Yaroslav Kurys, Vyacheslav Koshechko and Vitaly Pokhodenko, One-Step Electrochemical Preparation of Multilayer Graphene Functionalized with Nitrogen, *Nanoscale Research Letters*, 12:175, **2017.**

[38]   Sunil P Lonkar and Ahmed A Abdala , Applications of Graphene in Catalysis*, J Thermodyn Catal* , 5: 132, **2014.**

[39]https://www.acs.org/content/dam/acsorg/education/whatischemistry/landmarks/lesson-plans/discovery-of-fullerenes.pdf

[40]   http://www.nanoscience.com/applications/education/overview/cnt-technology-overview/

[41]   KH Basavaraj, Nanotechnology in medicine and relevance to dermatology: Present concepts, , *Indian J Dermatol*, 57:169-174, **2012.**

[42]   Yuxi Xu and Gaoquan Shi, Assembly of chemically modified graphene: methods and applications., *J. Mater. Chem.*, 21, 3311–3323, **2011.**

[43]   Bhaskar Garg, Tanuja Bisht and Yong-Chien Ling, Graphene-Based Nanomaterials as Heterogeneous Acid Catalysts: A Comprehensive Perspective Molecules 19, 14582-14614, **2014.**

[44]   Bich Ha Nguyen, and Van Hieu Nguyen, Promising applications of graphene and graphene-based nanostructures, *Adv. Nat. Sci.: Nanosci. Nanotechnol.* 7, 023002 (15pp) **2016.**

[45]   Prashant Tripathi, Ch. Ravi Prakash Patel, M. A. Shaz and O. N. Srivastava, Synthesis of High-Quality Graphene through Electrochemical Exfoliation   of   Graphite   in   Alkaline   Electrolyte, https://arxiv.org/ftp/arxiv/papers/1310/1310.7371.pdf, **2013.**

[46]   Q. Ashton Acton, Issues in Chemistry and General Chemical Research: **2013**.

[47]   Jesus   de   La   Fuente,   Graphene   Applications   &   Uses, **https://www.graphenea.com/pages/graphene** properties#.WIKzr66WbIV

[48]   https://www.revolvy.com/main/index.php?s=Graphite&item_type=topic

[49]   T. Pratheep Reddy , P. Charan Theja , B. Eswaraiah , P. Punna Rao**,**Preparation of Aluminium Reinforced with Granite and Graphite – A Hybrid Metal Matrix Composite International Journal of Engineering Research & Technology (IJERT), Vol. 6 Issue 10, October – **2017.**

[50] http://www.nanoscience.com/applications/education/overview/cnt-technology-overview/

[51] Hiroki Hibino, Graphene Research at NTT, NTT Technical Review, Vol. 11 No. 8 Aug. **2013.**

[52]   Vanesa C. Sanchez, Ashish Jachak, Robert H. Hurt, and Agnes B. Kane, Biological Interactions of Graphene-Family Nanomaterials: An Interdisciplinary Review, *Chem. Res. Toxicol.*, *25* (1), pp 15–34, **2012.**

[53]   Changuan Hu, Tiewen Lu, Fei Chen and Rongbin Zhang, A brief review of graphene-metal oxide composites synthesis and applications in photocatalysis, *Journal of the chinese Advanced Materials Society*, Vol. 1, No. 1, 21-39, **2013.**

[54]   QiZhang, ZhuonaWu, NingLi, YiqiongPu, BingWang,TongZhang, JianshengTao, Advanced review of graphene-based nanomaterials in drug delivery systems: Synthesis, modification, toxicity and application*, Materials Science and Engineering: C.* Volume 77, Pages 1363-1375, 1 August **2017.**

[55]   Xiluan Wang and Gaoquan Shi, An introduction to the chemistry of graphene, *Phys. Chem. Chem. Phys.*, 17, 28484, **2015.**

[56]   Kunal S. Mali, John Greenwood, Jinne Adisoejoso, Roald Phillipson and Steven De Feyter, Nanostructuring graphene for controlled and reproducible functionalization, *Nanoscale*, 7, 1566, **2015.**

[57]   SHEN Bao-Shou, FENG Wang-Jun1, LANG Jun-Wei, WANG Ru-Tao, TAI Zhi-Xin, YAN Xing-Bin, Nitric Acid Modification of Graphene Nanosheets Prepared by Arc Discharge Method and Their Enhanced Electrochemical Properties, *Acta Phys. -Chim. Sin.* 28 (7), 1726-1732, **2012.**

[58]   Sunil P. Lonkar , Yogesh S. Deshmukh and Ahmed A. Abdala, Recent Advances in Chemical Modifications of Graphene, *Nano Research*, © Tsinghua University Press and Springer-Verlag Berlin Heidelberg, 4, **2014.**

[59]   Xuqiang Ji, Liang Cui, Yuanhong Xu, Jingquan Liu, Non-covalent Interactions for Synthesis of New Graphene Based Composites, *Composites Science and Technology*, **2014.**

[60]   Tanwistha Ghosh, Jayanthy S. Panicker and Vijayakumar C. N, Self-Assembled Organic Materials for Photovoltaic Application, *Polymers* , *9*(3), 112**2017.**

[61]   Ning Wang, Likun Wang, Qinggang Tan, Yun-Xiang Pan, Effects of hydroxyl group on H_2dissociation on graphene: A density functional theory study, *Journal of Energy Chemistry*, Vol. 22 No. 3, 493–497, **2013.**

[62]   Guiyin Xu, Ping Nie, Hui Dou, Bing Ding, Laiyang Li, Xiaogang Zhang, Exploring metal organic frameworks for energy storage in batteries and supercapacitors, *Materials Today,* Volume 20,Number 4, May **2017.**

[63]   Mukarram Zubair, Jobin Jose, Abdul-Hamid Emwas and Mamdouh A. Al-Harthi, Effect of modified graphene and microwave irradiation on the mechanical and thermal properties of poly (styrene-co-methyl methacrylate)/graphene nanocomposites, *Surf. Interface Anal.*, 46, 630–639. **2014.**

[64]   Martin J. Sweetman, Steve May, Nick Mebberson , Phillip Pendleton, Krasimir Vasilev, Sally E. Plush, and John. Hayball, Activated Carbon, Carbon

Nanotubes and Graphene: Materials and Composites for Advanced Water Purification, *Carbon*, 3, 18. **2017.**

[65]   Ahmed Najem, Abd Abdulwahhab H., Al-Agha Mustafa.A.Alheety, Addition of Some Primary and Secondary Amines to Graphene Oxide, and Studying Their Effect on Increasing its Electrical Properties, *Baghdad Science Journal*, Vol.13(1), 0097-0111, **2016.**

[66]   Dimitrios Bitounis , Hanene Ali-Boucetta , Byung Hee Hong , Dal-Hee Min , and Kostas Kostarelos, Prospects and Challenges of Graphene in Biomedical Applications, *Adv. Mater.* 25, 2258–2268, **2013.**

[67]   Phitsini Suvarnaphaet and Suejit Pechprasarn, Graphene-Based Materials for Biosensors: A Review, *Sensors*, 17, 216, **2017.**

[68]   Ivan Buckley, Graphene introduction and overview, Manchester university, National Graphene Institute (NGI). WWW.graphene.manchester.ac.uk, **2015.**

[69]   Yuhai Hu and Xueliang Sun, Chemically Functionalized Graphene and Their Applications in Electrochemical Energy Conversion and Storage, Advances in Graphene Science, Chapter 7, **2013.**

[70]   Hale BERBER, Ezgi UÇAR , Utkan ŞAHİNTÜRK, Synthesis and Properties of Waterborne Few-layer Graphene Oxide/Poly(MMAco-BuA) Nanocomposites by in situ Emulsion Polymerization Colloids and Surfaces A: *Physicochem. Eng. Aspects,* vol.531, pp.56-66, **2017.**

[71]   Fen Lia , Xue Jianga , Jijun Zhaoa,b,n , Shengbai Zhang, Graphene oxide: A promising nanomaterial for energy and environmental applications*, Nano Energy*, 16, 488–515, **2015.**

[72]   Yunfeng Shi, Zhipeng Xiong, Xuefei Lu, Xin Yan, Xiang Cai, Wei Xue, Novel carboxymethyl chitosan-graphene oxide hybrid particles for drug delivery, *J Mater Sci: Mater Med.* 27:169, **2016.**

[73]   J. I. Paredes, S. Villar-Rodil, A. Martınez-Alonso, and J. M. D. Tascon, Graphene Oxide Dispersions in Organic Solvents, *Langmuir*, 24, 10560-10564, **2008.**

[74]   Jingquan Liu,*a Jianguo Tanga and J. Justin Gooding,Strategies for chemical modification of graphene and applications of chemically modified graphene, *J. Mater. Chem.*, **2012.**

[75]   Cristina Buzea, Ivan I. Pacheco, Kevin Robbie, Nanomaterials and nanoparticles: Sources and toxicity , Biointerphases 2, December **2007.**

 [76]   http://www.nanobusiness.org/, Nanotechnology as a Science

[77]   Md. Nahid Hossain and Masud H Chowdhury, Graphene Nanotechnology for the Next Generation Nonvolatile Memory,https://arxiv.org/pdf/1308.6782,**2013.**

[78]   Tapan K. Das and Smita Prusty, Graphene-Based Polymer Composites and Their Applications, Polymer-Plastics Technology and Engineering, 52: 319–331, **2013.**

[79]   http://www.nanobusiness.org/, Nanotechnology as a Science

[80]https://ipfs.io/ipfs/QmXoypizjW3WknFiJnKLwHCnL72vedxjQkDDP1mXWo6uco/wiki/Nanotechnology.html, Nanotechnology.

[81] Olgun Guven, Abel Maharramov, Mohammad Ali Ramazanov and Mohammad Reza Saboktakin, Book- Nanotechnology Science and Technology, Advanced Nanocomposites: Types, Properties and Applications, **2013.**

[82]   D.R.Paul, L.M.Robeson, Polymer nanotechnology: Nanocomposites Polymer , 49, 3187–3204, **2008.**

[83]   Obassi Ettu, The Role/Importance of Engineering Materials Utilization in Present Day World, *International Journal of Engineering Development and Research*, Volume 3, Issue 1, **2014**.

[84]   https://sciencing.com/types-composite-materials-5868282.html

[85]   http://compositeslab.com/composites-101/what-are-composites/

[86]   http://www.explainthatstuff.com/composites.html

[87]   http://nptel.ac.in/courses/Webcourse-contents/IISc-BANG/Composite%20Materials/pdf/Lecture_Notes/LNm1.pdf

[88]   Introduction of Composites, http://nptel.ac.in/courses/Webcourse-contents/IISc-BANG/Composite%20Materials/pdf/Lecture_Notes/LNm1.pdf

[89]   Pedro Henrique Cury Camargo; Kestur Gundappa Satyanarayana ,Fernando Wypych, Nanocomposites: synthesis, structure, properties and new application opportunities, *Mat. Res.* vol.12 no.1 -39, **2009.**

[90]   Puneet Sharma, Vijay Kumar Bhanot, Dharminder Singh, Harmanjit Singh Hundal and Meenakshi Sharma, RESEARCH WORK ON FIBER GLASS WOOL REINFORCED AND EPOXY MATRIX COMPOSITE MATERIAL, Int. *J. Mech.*

Eng. & Rob. Res. Vol. 2, No. 2, **2013.**

[91]   Jeffrey R. Potts , Daniel R. Dreyer , Christopher W. Bielawski , Rodney S. Ruoff , Graphene-based polymer nanocomposites, *Polymer* 52 ,5-25,**2011.**

[92]   Perry T. Yin, Shreyas Shah, Manish Chhowalla, and Ki-Bum Lee, Design, Synthesis, and Characterization of Graphene−Nanoparticle Hybrid Materials for Bioapplications*, Chem. Rev.* XXXX, XXX, XXX−XXX
American Chemical Society

[93]   Hun Wook Ha, Arup Choudhury, Tahseen Kamal, Dong-Hun Kim, and Soo-Young Park, S, Effect of Chemical Modification of Graphene on Mechanical, Electrical, and Thermal Properties of Polyimide/Graphene Nanocomposites, *Appl. Mater. Interfaces* XXXX, XXX, XXX−XXX, 2012.

[94]   Chun Kiang Chua and Martin Pumera, Chemical reduction of graphene oxide: a synthetic chemistry viewpoint, *Chem. Soc. Rev.*, 43, 291—312, 2014.

[95]   Uses of graphene Oxide, https://www.google.com.tr/search?q=uses+of+graphene+oxide&source=lnms&tbm=isch&sa=X&ved=0ahUKEwj6yceRk8fYAhWCZlAKHY2-DmYQ_AUICigB&biw=1366&bih=613#imgrc=1IEx-7D8SHMc9M.

[96]   Evgeniy Tkalya, Graphene-based polymer nanocomposites, http://citeseerx.ist.psu.edu/viewdoc/download?doi=10.1.1.922.9158&rep=rep1&type=pdf

[97]   Jeddah Marie G. Vasquez , Terence P. Tumolva, Synthesis and Characterization of a Self-Assembling Hydrogel from Water-Soluble Cellulose Derivatives and Sodium Hydroxide/Thiourea Solution,
American Journal of Chemistry, 5(2): 60-65, **2015.**

[98]   Cellulose. http://www.pslc.ws/macrog/cell.htm

[99]   Sachiko Kaihara Nitta and Keiji Numata. Biopolymer-Based Nanoparticles for Drug/Gene Delivery and Tissue Engineering, *Int. J. Mol. Sci.*, 14, 1629-1654, **2013.**

[100]   Sugandha Chahal, Fathima Shahitha Jahir Hussain, Anuj Kumar, Mashitah M. Yusoff and Mohammad Syaiful Bahari Abdull Rasad, Electrospun hydroxyethyl cellulose nanofibers functionalized with calcium phosphate coating for bone tissue engineering, *RSC Adv.*, 5, 29497, **2015.**

[101]   Hanieh Mianehrow, Ronak Afshari, Saeedeh Mazinani,Farhad Sharif,Majid Abdouss; Introducing a highly dispersed reduced graphene oxide nano-biohybrid employing/hydroxyethyl cellulose for controlled drug delivery; International Journal of Pharmaceutics,vol.509,issues 1-2,400-407,**2016.**

[102]   Sitansu Sekhar Nanda, Georgia C. Papaefthymiou, and Dong Kee Yi, Functionalization Of Graphene Oxide AND Its Biomedical Applications, Critical Reviews in *Solid State and Materials Sciences*, 0:1–25, **2015.**

[103]   Tapan Kumar Das, Smita Prusty , Graphene: A Revolution in Nanobiotechnology, , *Journal of Research in Nanobiotechnology*, 1(1), 19-30, **2012.**

[104]   Yanwu Zhu , Shanthi Murali , Weiwei Cai , Xuesong Li , Ji Won Suk , Jeffrey R. Potts , and Rodney S. Ruoff, Graphene and Graphene Oxide: Synthesis, Properties, and Applications, *Adv. Mater.*, 22, 3906–3924, **2010.**

[105]   A.K. Bajpai, Jaya Bajpai, Rajesh Kumar Saini, Smart Biomaterial Devices: *Polymers in Biomedical Sciences*, CRC Press,**2016.**

[106]   Yuqi Yang, Abdullah Mohamed Asiri , Zhiwen Tang , Dan Du and Yuehe Lin,Graphene based materials for biomedical applications, *Materials Today* Volume 16, Number 10 October **2013.**

[107]   Dr. Zhen Gu, Matt Shipman, 'Flying Carpet' Technique Uses Graphene to Deliver One-Two Punch of Anticancer Drugs, **2015.**

[108]   Kshitij Chaudhary, Graphene, Its Synthesis and Its Application in AntiCancer Drug Delivery, *International Journal of Science and Research (IJSR)*, Volume 4 Issue 8, August **2015.**

[109]   Nguyen TH, Lin M, Mustapha A, Toxicity of graphene oxide on intestinal bacteria and Caco-2 cells, *J Food Prot.*, 78(5):996-1002, **2015.**

[110]   Junmin Zhu and Roger E Marchant, Design properties of hydrogel tissue-engineering scaffolds, *Expert Rev Med Devices*, 8(5): 607–626, **2011.**

[111] Sangiliyandi Gurunathan Jin-Hoi Kim, Synthesis, toxicity, biocompatibility, and biomedical applications of graphene and graphene-related materials, *International Journal of Nanomedicine,*11 1927–1945, **2016.**

[112] Tapan K.Das and Smita Prusty, RECENT ADVANCES IN APPLICATIONS OF GRAPHENE*, International Journal of Chemical Sciences and Applications*, Vol 4, Issue 1, pp 39-55, **2013.**

[113] Padmakar D. Kichambare and Alexander Star, Biosensing using Carbon Nanotube Field-effect Transistors, *Nanotechnologies for the Life Sciences*, Vol. 8, **2007.**

[114]   Sumit Goenka' Vinayak Sant Shilpa Sant, Graphene-based nanomaterials for drug delivery and tissue engineering, *Journal of Controlled Release*, Volume 173, , Pages 75-88, 10 January **2014.**

[115] Feifei Zhang, Lin Lu, Min Yang, Cuili Gao, Zonghua Wang, Electrochemistry of Graphene Flake Electrodes: Edge and Basal Plane Effect for Biosensing *Int. J. Electrochem. Sci.*, 11, 10172 – 10184, **2016.**

[116] Bich Ha Nguyen, and Van Hieu Nguyen, Promising applications of graphene and graphene-based nanostructures, *Adv. Nat. Sci.: Nanosci. Nanotechnol.* 7,023002, **2016.**

[117] Hang Zhang, Mechanical and Electrical Properties of Modified Graphene Devices, A Dissertation submitted in partial satisfaction of the requirements for the degree of Doctor of Philosophy in Physics, UNIVERSITY OF CALIFORNIA RIVERSIDE, p.p. 29, **2012.**

[118] Somnath Bharech and Richa Kumar, A Review on the Properties and Applications of Graphene *Journal of Material Science and Mechanical Engineering (JMSME)*, Volume 2, Number 10; pp. 70-73, April-June, **2015.**

[119] K. Christian Kemp, Humaira Seema, Muhammad Saleh, Nhien H. Le, Kandula Mahesh, Vimlesh Chandra and Kwang S. Kim, Environmental applications using graphene composites: water remediation and gas adsorption: *Nanoscale*, 5, 3149- 3171, 2013**.**

[120] Yi Shen, Qile Fang, and Baoliang Chen, Environmental Applications of Three-Dimensional Graphene Based Macrostructures: Adsorption, Transformation, and Detection, *Environ. Sci. Technol*, ACS Paragon Plus Environment, p.p.1-55, **2014.**

[121] Valentinas Snitka, Graphene Based Materials: Opportunities and Challenges in Nanomedicine, *Journal of Nanomedicine Research*, Volume 2 issue 4, 00035, **2015.**

[122] Wenbing Hu, Cheng Peng, Min Lv, Xiaoming Li, Yujie Zhang, Nan Chen, Chunhai Fan, and Qing Huang, Protein Corona-Mediated Mitigation of Cytotoxicity of Graphene Oxide, ACS Nano, VOL. 5' NO. 5' 3693–3700' **2011.**

[123] Introduction to FTIR spectroscopy, Thermo Fisher Scientific

https://www.thermofisher.com/tr/en/home/industrial/spectroscopy-elemental-isotope-analysis/spectroscopy-elemental-isotope-analysis-learning-center/molecular-spectroscopy-information/ftir-information/ftir-basics.html

[124] Paulchamy B, Arthi G and Lignesh BD, A Simple Approach to Stepwise Synthesis of Graphene Oxide Nanomaterial, *J. Nano med Nano technol*, 6:1, **2015.**

[125] Min Yan, Qionglin Liang, Wei Wan, Qiang Han, Siyuan Tan and Mingyu Ding, Amino acid-modified graphene oxide magnetic nanocomposite for the magnetic separation of proteins, *RSC Adv.* 7, 30109, **2017.**

[126] Weilie Zhou, Robert P. Apkarian, Zhong Lin Wang, and David Joy, Fundamentals of Scanning Electron Microscopy, http://homes.ufam.edu.br/berti/nanomateriais/aulas%20pptx%20e%20livros/livro/S

canning%20Microscopy%20for%20Nanotechnology/Fundamentals%20of%20Sca
nning%20Electron%20Microscopy%20(SEM).pdf

[127]   CicarboTM, Graphene Characterization and Analysis, *Carbon*, vol. 65, p. 1,
http://www.celtig.com/wp-content/uploads/2016/07/CicarboTM-Graphene-
Characterization-and-Analysis.pdf, **2013.**

[128]   John Goodge, Element Mapping,
https://serc.carleton.edu/research_education/geochemsheets/elementmapping.ht
ml

[129]   John Goodge, Energy-Dispersive X-Ray Spectroscopy (EDS)
https://serc.carleton.edu/research_education/geochemsheets/eds.html

[130]   Michael Mowry, Dennis Palaniuk, Claudia C. Luhrs and Sebastian Osswald,
In situ Raman spectroscopy and thermal analysis of the formation of nitrogen-doped
graphene from urea and graphite oxide, *RSC Adv.*,3, 21763-21775, **2013**.

[131]   Zhen hua Ni, Ying ying Wang, Ting Yu, and Ze xiang Shen, Raman
spectroscopy and imaging of graphene,
https://arxiv.org/ftp/arxiv/papers/0810/0810.2836.pdf, **2008.**

[132]   Siegfried Eigler and Andreas Hirsch, Chemistry with Graphene and
Graphene Oxide—Challenges for Synthetic Chemists,
Angew. Chem. Int. Ed., 53, 7720 – 7738, **2014.**

[133]   Muhammad Ali, RAMAN CHARACTERIZATION OF STRUCTURAL
PROPERTIES OF THERMALLY MODIFIED NANOGRAPHITE, Master's Thesis in
Physics, **2015.**
https://www.diva-portal.org/smash/get/diva2:852894/FULLTEXT01.pdf

[134]   Pooria Gill, Tahereh Tohidi Moghadam, and Bijan Ranjbar, Differential
Scanning Calorimetry Techniques: Applications in Biology and Nanoscience,
J Biomol Tech. 21(4): 167–193, **2010.**

[135]   DSC, https://www.perkinelmer.com/CMSResources/Images/44-
74542GDE_DSCBeginnersGuide.pdf

[136]   Vikas Patil, Robert V. Dennis, Tapan K. Rout, Sarbajit Banerjee
and Ganapati D. Yadav, Graphene oxide and functionalized multi walled carbon
nanotubes as epoxy curing agents: a novel synthetic approach to nanocomposites
containing active nanostructured fillers, *RSC Adv.,***4**, 49264-49272, **2014.**

[137]   I. A. Ovidko, MECHANICAL PROPERTIES OF GRAPHENE, Mechanical
properties of graphene, *Rev.Adv. Mater. Sci.* 34, 1-11, **2013.**

[138]   Dimitrios G. Papageorgiou, Ian A. Kinloch, Robert J. Young, Mechanical
properties of graphene and graphene-based nanocomposites,
Progress in Materials Science 90, 75–127, **2017.**

[139]   Anne Marie Helmenstine, Electrical Conductivity Definition, https://www.thoughtco.com/definition-of-electrical-conductivity-605064

[140]   Ion Ion, Alina Catrinel Ion, Alina Culetu , Application of an exfoliated graphite nanoplatelet-modified electrode for the determination of quintozen, *Materials Science and Engineering* ,1553–1557, **2011.**

[141]   Williams,Dudley,Howard,Spectroscopic methods in organic chemistry ,3rd ed,Biritish Library Cataloguing in Publication Data , copyright Mc Graw-Hill Book Company,**1980.**

[142]   Ziyin Lin, Yan Liu, and Ching-ping Wong, Facile Fabrication of Superhydrophobic Octadecylamine-Functionalized Graphite Oxide Film, *Langmuir*, 26(20), 16110–16114, **2010.**

[143]   Viet Hung Pham, Tran Viet Cuong, Eun Woo Shin and Jin Suk Chung; Chemical functionalization of graphene sheet by solvothermal reduction of a graphene oxide suspension in N-methyl-2-pyrrolidone; *J. of Mater. Chem*, 21; 3371, **2011.**

[144]   Ion Ion, Alina Catrine Ion, Differential puls voltammetric analysis of lead in vegetables using a surface amino-functionalized exfoliated graphite nanoplatedelet chemically modified electrode; *Sensors and Actuators B,* 166-167, 842-847, **2012.**

[145]   Shanshan Wang, Jun Wang, Wenfeng Zhang, Junyi Ji, Yang Li, Guoliang Zhang, Fengbao Zhang, and Xiaobin Fan, Ethylenediamine Modified Graphene and Its Chemically Responsive Supramolecular Hydrogels,
American Chemical Society, *Ind. Eng. Chem. Res.*,**2014.**

[146]   Niranjanmurthi Lingappan, Do Hoon Kim,Jong Myung Park, and Kwon Taek Lim, Water Soluble Graphene Oxide/Poly(1-vinylimidazole) Composites: Synthesis and Characterization, *Journal ofNanoscience and Nanotechnology,*
Vol. 14, 5713–5717, **2014.**

[147]   Shanshan Wang, Jun Wang, Fengbao Zhang and Xiaobin Fan, Ethylenediamine modified graphene and its chemically responsive supramolecular hydrogels, *Ind. Eng. Chem. Res.* 53, 13205-13209, **2015.**

[148]   Huating Hu, Xianbao Wang, Jingchao Wang, Fangming Liu, Min Zhang, Chunhui Xu, Microwave-assisted covalent modification of graphene nanosheets with chitosan and its electrorheological characteristics, *Applied Surface Science* 257 ,2637–2642,**2011.**

[149] Seung Hun Huh,Thermal Reduction of Graphene Oxide, Physics and Applications of Graphene -Experiments, Dr. Sergey Mikhailov (Ed.), InTech, Available   from: http://www.intechopen.com/books/physics-and-applications-of-graphene-experiments/thermal-reduction-ofgraphene-oxideISBN: 978-953-307-217-3, **2011.**

[150] Burcu Saner, Fatma Dinç, Yuda Yürüm , Utilization of multiple graphene nanosheets in fuel cells: 2. The effect of oxidation process on the characteristics of graphene nanosheets, *Fuel* ,90 2609–2616**, 2011.**

[151] SHEN Bao-Shou, FENG Wang-Jun, LANG Jun-Wei WANG Ru-Tao, TAI Zhi-Xin YAN Xing-Bin, Nitric Acid Modification of Graphene Nanosheets Prepared by Arc- Discharge Method and Their Enhanced Electrochemical Properties; *Acta Phys. -Chim. Sin.***,** *28* (7), 1726-1732,**2012.**

[152] Sudesh, N Kumar, S Das, C Bernhard and G D Varma, Effect of graphene oxide doping on superconducting properties of bulk MgB2, Supercond. *Sci. Technol.* 26 ,095008, **2013.**

[153]   Jashiela Wani Jusin, Madzlan Aziz, Goh Pei Sean, Juhana Jaafar, PREPARATION AND CHARACTERIZATION OF GRAPHENE-BASED MAGNETIC HYBRID NANOCOMPOSITE; *Malaysian Journal of Analytical Sciences,* Vol 20 No 1, 149 – 156, **2016.**

[154]   Shu-Peng Zhang, and Hai-Ou Songb, Supramolecular graphene oxide-alkylamine hybrid materials: variation of dispersibility and improvement of thermal stability, *New J. Chem.,* **36**, 1733–1738 1733, **2012.**

[155]   S. Suresh Balaji and M. Sathish, Supercritical fluid processing of nitric acid treated nitrogen doped graphene with enhanced electrochemical supercapacitance, The Royal Society of Chemistry , *RSC Adv.*, 4, 52256–52262, **2014.**

[156] Assist. Prof. Dr. F. Mindivan, THE SYNTHESIS AND CHARECTERIZATION OF GRAPHENE OXIDE (GO) AND REDUCED GRAPHENE OXIDE (RGO), YEAR XXIV, VOLUME 2, P.P. 51-54, **2016.**

[157]   Pedro Montes-Navajas, Natalia G. Asenjo, Ricardo Santamaría,Rosa Menéndez, Avelino Corma, and Hermenegildo García, Surface Area Measurement of Graphene Oxide in Aqueous Solutions, American Chemical *Society,Langmuir* XXXX, XXX, XXX−XXX,**2013.**

[158]   Enamul Haque,a Md. Monirul Islam,b Ehsan Pourazadi,c Mahbub Hassan,a Shaikh Nayeem Faisal,c Anup Kumar Roy,c Konstantin Konstantinov,b Andrew T. Harris,c Andrew Minettc and Vincent G. Gomes, Nitrogen doped graphene via thermal treatment of composite solid precursors as a high performance supercapacitor, *RSC Adv.*, 5, 30679, **2015.**

[159]   Vijay Bhooshan Kumara , Jakkid Sanetuntikulb , Pandian Ganesanb , Ze'ev Poratc,d , Sangaraju Shanmugamb, Aharon Gedanken, Sonochemical Formation of Ga-Pt Intermetallic Nanoparticles Embedded in Graphene and its Potential Use as an Electrocatalyst, *Electrochimica Acta* 190, 659–667, **2016.**

[160] Niranjanmurthi Lingappan, Do Hoon Kim, Jong Myung Park, and Kwon Taek Lim;Water Soluble Graphene Oxide/Poly(1-vinylimidazole) Composites:

Synthesis and Characterization; Journal *of Nanoscience and Nanotechnology* Vol. 14, 5713–5717, **2014.**

[161]   Huating Hu, Xianbao Wanga, Jingchao Wanga, Fangming Liu, Min Zhanga, Chunhui Xua; Microwave-assisted covalent modification of graphene nanosheets with chitosan and its electrorheological characteristics; *Applied Surface Science*, 257, 2637–2642,**2011.**

[162]   Ching-Chang Lai, Meng-Yin Chung and Chieh-Tsung Lo, Nitric acid oxidation of electrospun carbon nanofibers as supercapacitor electrodes, *Textile Research Journal*, 0(00) 1–12, **2016.**

[163]   Mark Wall, Ph.D., Thermo Fisher Scientific, Madison, WI, USA, The Raman Spectroscopy of Graphene and the Determination of Layer Thickness, Fisher Scientific Inc. All rights reserved. ISO is a trademark of the International Standards Organization. All other trademarks are the property of Thermo Fisher Scientific Inc, **2011.**
www.thermoscientific.com

[164]   Robert J. Young ,Ian A. Kinloch, Lei Gong, Kostya S. Novoselov, The mechanics of graphene nanocomposites: A review,*Composites Science and Technology* 72 ,1459–1476,**2012.**

[165]   Yejing Weng,*ab* Bo Jiang,*a* Kaiguang Yang,*a* Zhigang Sui,*a* Lihua Zhang,*a* and Yukui Zhang*a ;* Polyethyleneimine-Modified Graphene Oxide Nanocomposites for Effective Protein Functionalization; *J. Name.*, 00, 1-31, **2013.**

[166]   Niranjanmurthi Lingappan, Do Hoon Kim, Jong Myung Park, and Kwon Taek Lim,Water Soluble Graphene Oxide/Poly(1-vinylimidazole) Composites: Synthesis and Characterization; *J. Nanosci. Nanotechno*, Vol. 14, No. 8, **2014.**

[167]   Manoj Kumar Pati, Puspalata Pattojoshi,and Gouri Sankar Roy, Synthesis of Graphene-Based Nanocomposite and Investigations of Its Thermal and Electrical Properties,*Journal of Nanotechnology,* Volume, 9, **2016.**

[168] Shengli Wu Tiejun Shi and Liyuan Zhang, Preparation and properties of amine-functionalized reduced graphene oxide/waterborne polyurethane nanocomposites ; New York University on August 5, **2015.**

[169] Alireza Ashori, Hossein Rahmani, Reza Bahrami ; Preparation and characterization of functionalized graphene oxide/carbon fiber/epoxy nanocomposites *; Polymer Testing*, 48 82e88, **2015.**

[170] Debasis Ghosh, Soumen Giri, Sumanta Sahoo,and C.K.Das ; Insitu Synthesis of Graphene/Amine-Modified Graphene , Polypyrrole Composites in Presence of SrTiO₃ forSupercapacitor Applications; *Polymer-Plastics Technology and Engineering* , 52:213-220, **2013.**

[171]   James R. Connolly; Diffraction Basics, Part, Introduction to X-Ray Powder Diffraction; Material in this document is borrowed from many sources; all original material is ,by James R. Connolly, **2012.**

[172] Deepshikha Saini T. Basu; Synthesis and characterization of nanocomposites based on polyaniline-gold/graphene nanosheets *; Appl Nanosci* 2:467–479, **2012.**

[173] G. Srinivas, Yanwu Zhu, Richard Piner, Neal Skipper, Mark Ellerby, Rod Ruoff; Synthesis of graphene-like nanosheets and their hydrogen adsorption capacity ; *C A R B ON x x -x x x –x x x,* **2009.**

[174] Shabnam Sheshmani and Marzieh Arab Fashapoyeh ;SuitableChemical Methods for Preparation of GGraphene Oxide , Graphene and Surface Functionalized Graphene Nanosheets ;*Acta. Chim.Slov.*,60,813-825, **2013.**

[175] Vorrada Loryuenyong, Krit Totepvimarn, Passakorn Eimburanapravat, Wanchai Boonchompoo, and Achanai Buasri, Preparation and Characterization of Reduced Graphene Oxide Sheets via Water-Based Exfoliation and Reduction Methods; Hindawi Publishing Corporation *Advances in Materials Science and Engineering*, Article ID 923403, 5 pages, **2013.**

[176] H. Yang , Y. Hernandez , A. Schlierf , A. Felten , A. Eckmann , S. Johal , P. Louette , J.-J. Pireaux , X. Feng , K. Mu ellen , V. Palermo , C. Casiraghi,
 A simple method for graphene production based on exfoliation of graphite in water using 1-pyrenesulfonic acid sodium salt, *C A R B O N* ,5 3 ,3 5 7 –3 6 5, **2013.**

[177] Andrea C. Ferrari, Raman spectroscopy of graphene and graphite: Disorder, electron–phonon coupling, doping and nonadiabatic effects, Solid *State Communications* ,47–57,**2007.**

[178] HEE JIN JEONG, Synthesis and Dispersion of Chemically Exfoliated Graphene Nanosheets, *FEATURE ARTICIES*, VOL. 25 NO. 5,**2015.**

[179]   Isaac Childres, Luis A. Jaureguib, Wonjun Parkb, Helin Caoa, and Yong P. Chena, Raman Spectroscopy of Graphene and Related Materials **,**chpter19, E-mail address: ichildre@purdue.edu , **2013.**

[180]   Chufeng Sun, Yanbin Wang and Qiong Su**;** The impacts of graphene concentration and thickness on the photocatalytic performance of Bi12TiO20/graphene composite thin films**;** *Mater. Res. Express* **4** ,085003, **2017.**

[181] Vikas Patil,ab Robert V. Dennis,b Tapan K. Rout,c Sarbajit Banerjeeb and Ganapati D. Yadav, Graphene oxide and functionalized multi walled carbon nanotubes as epoxy curing agents: a novel synthetic approach to nanocomposites containing active nanostructured fillers, *RSC Adv.,* 4, 49264, **2014.**

[182] Zhili Zhang and Rendang Yang; Novel Nanocomposites Based on Hydroxyethyl Cellulose and Graphene Oxide; *Fibers and Polymers*,Vol.18, No.2, 334-341, **2017.**

[183] Che Zhang, Run Z. Zhang, Yong Q. Ma, Wen B. Guan, Xiao L. Wu, Xue Liu, Hong Li, Yan L. Du, and Can P. Pan; Preparation of Cellulose/Graphene Composite and Its Applications for Triazine Pesticides Adsorption from Water; ACS, *Sustainable Chem. Eng. XXXX, XXX, XXX−XXX;***2014.**

[184] Trivedi MK, Nayak G, Patil S, Tallapragada RM, Mishra R Influence of Biofield Treatment on Physicochemical Properties of Hydroxyethyl Cellulose and Hydroxypropyl Cellulose. *J Mol Pharm Org Process Res* 3, (2): 126. 1-7, doi:10.4172/2329-9053.1000126, **2015.**

[185] Shaoling Wu Xindong Zhao, Yanhui Li , Qiuju Du, Jiankun Sun, Yonghao Wang , Xin Wang , Yanzhi Xia, Zonghua Wang and Linhua Xia Adsorption Properties of Doxorubicin Hydrochloride onto Graphene Oxide: Equilibrium, *Kinetic and Thermodynamic Materials*, 6, 2026-2042, **2013.**

[186] Dr. Sergey Mikhailov, Hyung-il Lee and Han Mo Jeong – Experiments Functionalized Graphene Sheet / Polyurethane Nanocomposites , *Physics and Applications of Graphene* ,193-208 p., 10, **2011.**

[187] D. Depan, J. Shah , R.D.K. Misra, Controlled release of drug from folate-decorated and graphene mediated drug delivery system: Synthesis, loading efficiency, and drug release response*, Materials Science and Engineering C*, 31,1305–1312, **2011.**

[188] Julia M Tan, Govindarajan Karthivashan,Palanisamy Arulselvan ,Sharida Fakurazi, Mohd Zobir Hussein, *Drug Design, Development and* Characterization and in vitro studies of the anticancer effect of oxidized carbon nanotubes functionalized with betulinic acid, *Therapy*,8 2333–2343, **2014.**

[189] Controlled Release of Doxorubicin from Doxorubicin/γ-Polyglutamic Acid Ionic Complex BhavikManocha and ArgyriosMargaritis Hindawi Publishing Corporation Journal of Nanomaterials Volume 2010, Article ID 780171, 9 pages doi:10.1155/780171,**2010.**

[190] Alessandro Pistonea, Daniela Iannazzoa, Shabana Ansaria, Candida Milonea, Marina Salamòa, Signorino Galvagnoa, Santa Cirmib, Michele Navarrab Tunable doxorubicin release from polymer-gated multiwalled carbon nanotubes *International Journal of Pharmaceutics* 515 ,30–36, **2015.**

[191] Esra Kiliç, Arzu Yakar, Nursel Pekel Bayramgil, Preparation of electrospun polyurethane nanofiber mats for the,release of doxorubicine, *J Mater Sci: Mater Med*, 29:8 , DOI 10.1007/s10856-017-6013-5, **2018.**

CURRICULUM VITAE

Identification Information

Name &Surname   : Hiba Salih Hussein Salih

Place of birth   : Oxford – England

Marital Status   : Married with children

E-Mail   : hamsara7@hotmail.com

Adress   : Omdurman Islamic University, Khartoum, Sudan

Education

BSc   : 1997-2000 , Omdurman Islamic University, Faculty of science ,Department of Chemistry

MSc   : 2003-2008 , Sudan University for Science and Technology, ,Department of Chemistry

Ph D   : 2011-2018 , Hacettepe University, School of Science and Engineering , Department of Chemistry

Foreign Language

English

Turkish

Work Experience

2001 – 2008   : Teaching Assistant, Omdurman Islamic University, Faculty of science ,Department of Chemistry, Khartoum, Sudan

2008 – Present   : Lecturer Omdurman Islamic University, Faculty of science ,Department of Chemistry, Khartoum, Sudan

Area of Experiences

Physical Chemistry and Organic Chemistry

Project and Budgets from Thesis :   -

Publications :   -

Oral and Poster Presentation : Preparation and characterization of acid-modified graphene,Hiba Salih Hussein, Nursel Pekel Bayramgil,3rd EMERGING 2D MATERIALS & GRAPHENE CONFERENCE, (Poster) , Istanbul, **2016.**

Preparation and characterization of amine-modified graphene , Hiba Salih Hussein, Nursel Pekel Bayramgil, 29th NATIONAL CONFERENCE OF CHEMISTRY , (Poster), Ankara, **2017.**

HACETTEPE UNIVERSITY
GRADUATE SCHOOL OF SCIENCE AND ENGINEERING
THESIS/DISSERTATION ORIGINALITY REPORT

HACETTEPE UNIVERSITY
GRADUATE SCHOOL OF SCIENCE AND ENGINEERING
TO THE DEPARTMENT OF ....CHEMISTRY...........

Date: 05/02./2018

Thesis Title / Topic: Modified Graphene-Polymer Nanocomposites and Their Utilization in Various Applications
....

According to the originality report obtained by myself/my thesis advisor by using the *Turnitin* plagiarism detection software and by applying the filtering options stated below on **05/02/2018** for the total of **190** pages including the a) Title Page, b) Introduction, c) Main Chapters, d) Conclusion sections of my thesis entitled as above, the similarity index of my thesis is **10 %**.

Filtering options applied:
1. Bibliography/Works Cited excluded
2. Quotes excluded / ~~included~~
3. Match size up to 5 words excluded

I declare that I have carefully read Hacettepe University Graduate School of Sciene and Engineering Guidelines for Obtaining and Using Thesis Originality Reports; that according to the maximum similarity index values specified in the Guidelines, my thesis does not include any form of plagiarism; that in any future detection of possible infringement of the regulations I accept all legal responsibility; and that all the information I have provided is correct to the best of my knowledge.

I respectfully submit this for approval.

February 5, 2018
Date and Signature

Name Surname:	HIBA SALIH HUSSEIN SALIH
Student No:	N11144269
Department:	CHEMISTRY
Program:	
Status:	☐ Masters ☒ Ph.D. ☐ Integrated Ph.D.

ADVISOR APPROVAL

APPROVED.

Prof.Dr. NURSEL PEKEL BAYRAMGİL

(Title, Name Surname, Signature)

HACETTEPE ÜNİVERSİTESİ
FEN BİLİMLERİ ENSTİTÜSÜ
YÜKSEK LİSANS/DOKTORA TEZ ÇALIŞMASI ORJİNALLİK RAPORU

HACETTEPE ÜNİVERSİTESİ
FEN BİLİMLER ENSTİTÜSÜ
...................KİMYA.............. ANABİLİM DALI BAŞKANLIĞI'NA

Tarih: 05/02./2018

Tez Başlığı / Konusu: ....Modifiye Grafen – Polimer Nanokompozitler ve Çeşitli Uygulamalarda Kullanılması.........................

Yukarıda başlığı/konusu gösterilen tez çalışmamın a) Kapak sayfası, b) Giriş, c) Ana bölümler d) Sonuç kısımlarından oluşan toplam **190** sayfalık kısmına ilişkin, **05/02/2018** tarihinde şahsım/tez danışmanım tarafından *Turnitin* adlı intihal tespit programından aşağıda belirtilen filtrelemeler uygulanarak alınmış olan orijinallik raporuna göre, tezimin benzerlik oranı % **10** 'dur.

Uygulanan filtrelemeler:
1- Kaynakça hariç
2- Alıntılar hariç/~~dâhil~~
3- 5 kelimeden daha az örtüşme içeren metin kısımları hariç

Hacettepe Üniversitesi Fen Bilimleri Enstitüsü Tez Çalışması Orjinallik Raporu Alınması ve Kullanılması Uygulama Esasları'nı inceledim ve bu Uygulama Esasları'nda belirtilen azami benzerlik oranlarına göre tez çalışmamın herhangi bir intihal içermediğini; aksinin tespit edileceği muhtemel durumda doğabilecek her türlü hukuki sorumluluğu kabul ettiğimi ve yukarıda vermiş olduğum bilgilerin doğru olduğunu beyan ederim.

Gereğini saygılarımla arz ederim.

05 Şubat 2018
Tarih ve İmza

Adı Soyadı:	HIBA SALIH HUSSEIN SALIH
Öğrenci No:	N11144269
Anabilim Dalı:	KIMYA
Programı:	
Statüsü:	☐ Y.Lisans ☒ Doktora ☐ Bütünleşik Dr.

DANIŞMAN ONAYI

UYGUNDUR.

Prof.Dr. NURSEL PEKEL BAYRAMGİL

(Unvan, Ad Soyad, İmza)